Mathematical modelling and optimization of biocatalytic synthesis of fluorinated chiral building blocks

Milčić, Nevena

University of Zagreb

FACULTY OF CHEMICAL ENGINEERING AND TECHNOLOGY

Nevena Milčić

MATHEMATICAL MODELLING AND OPTIMIZATION OF BIOCATALYTIC SYNTHESIS OF FLUORINATED CHIRAL BUILDING BLOCKS

DOCTORAL THESIS

Zagreb, 2023.

Sveučilište u Zagrebu

FAKULTET KEMIJSKOG INŽENJERSTVA I TEHNOLOGIJE

Nevena Milčić

MATEMATIČKO MODELIRANJE I OPTIMIZACIJA BIOKATALITIČKE SINTEZE FLUORIRANIH KIRALNIH GRAĐEVNIH BLOKOVA

DOKTORSKI RAD

Zagreb, 2023.

University of Zagreb

FACULTY OF CHEMICAL ENGINEERING AND TECHNOLOGY

NEVENA MILČIĆ

MATHEMATICAL MODELLING AND OPTIMIZATION OF BIOCATALYTIC SYNTHESIS OF FLUORINATED CHIRAL BUILDING BLOCKS

DOCTORAL THESIS

Supervisors:
Prof. Zvjezdana Findrik Blažević, PhD
Maja Majerić Elenkov, PhD

Zagreb, 2023.

University of Zagreb

FAKULTET KEMIJSKOG INŽENJERSTVA I TEHNOLOGIJE

NEVENA MILČIĆ

MATEMATIČKO MODELIRANJE I OPTIMIZACIJA BIOKATALITIČKE SINTEZE FLUORIRANIH KIRALNIH GRAĐEVNIH BLOKOVA

DOKTORSKI RAD

Mentori:
Prof. dr. sc. Zvjezdana Findrik Blažević
Dr. sc. Maja Majerić Elenkov

Zagreb, 2023.

Bibliographic facts

UDC: 66.011:544.473:577.15(043.3)=111

Scientific area: Technical Sciences

Scientific field: Chemical Engineering

Scientific branch: Reaction Engineering

Institution: University of Zagreb, Faculty of Chemical Engineering and Technology, Department of Reaction Engineering and Catalysis

Supervisors:

- Prof. Zvjezdana Findrik Blažević, Ph.D.
- Maja Majerić Elenkov, Ph.D.

Number of pages: 215

Number of figures: 70

Number of tables: 19

Number of supplements: 54

Number of references: 165

Date of defense: May 9th 2023

Members of the Committee for defense of the thesis:

1. Assist. Prof. Martina Sudar, Ph.D., University of Zagreb, Faculty of Chemical Engineering and Technology
2. Prof. Pere Clapés, Ph.D., Institute for Advanced Chemistry of Catalonia, CSIC, Barcelona, Spain
3. Prof. Marija Vuković Domanovac, Ph.D., University for Zagreb, Faculty of Chemical Engineering and Technology, Croatia

Dissertation is stored at:

- National and University Library Zagreb, Hrvatske bratske zajednice bb, Zagreb;
- Library of University of Zagreb, Faculty of Chemical Engineering and Technology, Trg Marka Marulića 20, Zagreb

Dissertation topic was accepted on regular session of Council of the Faculty of Chemical Engineering and Technology, University of Zagreb, held on July 13th 2020, and approved at 1st session of the Senat of the University of Zagreb in 352th academic year (2020/2021) held on October 13th 2020.

Information about supervisors

Prof. Zvjezdana Findrik Blažević, PhD

Zvjezdana Findrik Blažević [redacted] She graduated from the Faculty of Chemical Engineering and Technology, University of Zagreb in 2002. After graduation she was employed as a junior researcher – younger assistant in the Department of Reaction Engineering and Catalysis of the same Faculty. She obtained her PhD in 2006 as part of the project "Biocatalysis and biotransformations" under supervision of prof. Đurđa Vasić-Rački, PhD, in the field of technical sciences with the topic *Study of reactions catalyzed by amino acid oxidases*. She was appointed as an assistant professor in 2009, associate professor in 2012, and full professor in 2018. She spent some time at several foreign institutions: Department of Technical Chemistry, University of Rostock (Germany), Institute of Biotechnology of the Research Center Jülich (Germany) and Institute for the Advanced Chemistry, CSIC (Spain). She won several awards, such as Rector's award (2002), the Award of the Society of University Teachers, Scholars and other Scientists (2005), National Science Award – Annual Award for Junior Researchers (2006), and the Award of the Academy of Engineering of Croatia – award to the young scientist "Vera Johanides" (2009). Her scientific research is focused on the application of biocatalysis and optimization of biocatalytic processes using reaction engineering approach, especially complex multi-enzyme cascade reaction systems. She managed one past (Carbazymes) and two current Horizon 2020 (RadicalZ and C-C Top) and one Horizon Europe project (Biodeccodinng) where the Faculty is a beneficiary. She is also a collaborator on several national projects, such as Croatian Science Foundation funded project EnzyFluor and Catpharma funded by the EU structural and investment funds. She is the author and co-author of more than 50 scientific publications, she was invited lecturer at national and international conferences, and was the supervisor of more than 60 BSc, MSc and PhD theses. She is an active member of the Croatian Society of Chemical Engineers and the Society of University Teachers, Scholars and other Scientists. She is also a member of the Editorial Board of *Hungarian Journal of Industry and Chemistry* and *Biocatalysis and Biotransformation*.

Maja Majerić Elenkov, PhD

Maja Majerić Elenkov [redacted] She studied chemistry at the Faculty of Science, University of Zagreb. She obtained her PhD in 2003 under the mentorship of prof. Vitomir Šunjić, PhD, in the field of natural sciences with the topic *Biocatalytically generated chiral ligands used for homogeneous catalysts based on 1, 4-benzodiazepines*. After her PhD, she joined the group of prof. Dick B. Janssen, PhD (University of Groningen, the Netherlands) as a postdoctoral researcher for two years, where she worked on stereoselective transformations catalyzed by halohydrin dehalogenases. She is currently employed as a senior research associate at the Ruđer Bošković Institute in the Laboratory for Stereoselective Synthesis and Biocatalysis, Department of Organic Chemistry and Biochemistry. Her scientific activity is focused on biocatalytic research, specifically, the application of halohydrin dehalogenases in organic chemistry for the preparation of synthetically valuable molecules. She is the author and co-author of numerous scientific publications, direct supervisor of several graduate and doctoral theses, and supervisor of numerous projects including *Enzymatic Synthesis of Fluorinated Chiral Building Blocks – EnzyFluor* (HrZZ IP-2018-01-4493) funded by Croatian Science Foundation (2018 – 2023). In addition, in the period from 2007 to 2015, she led the courses *Stereochemistry of drugs and asymmetric synthesis* and *Special methods in organic synthesis* at the doctoral studies of the Faculty of Medicine in Rijeka, and since 2011 she is leading the course *Stereoselective reactions catalyzed by enzymes* at the doctoral studies of the Faculty of Chemistry and Technology in Split.

This PhD thesis was financially supported by the project *Enzymatic synthesis of fluorinated chiral building blocks* (Croatian Science Foundation, IP-2018-01-4493). PhD scholarship was provided through the program Career Development Project for Young Researchers (Croatian Science Foundation).

Acknowledgments

I am truly grateful to my supervisors, Zvjezdana and Maja, for their unprecedented diligence and dedication to our scientific work. You were great inspiration by example and created incredible balance between offering me help and providing me the freedom I needed to unleash my scientific creativity. Zvjezdana, thank you for huge support and care invested in every aspect of my life as a PhD student. It was a pleasure working with you every step of the way.

Thanks to the members of the Department for Reaction Engineering and Catalysis, especially Martina who facilitated and accelerated my onboarding, and continued to provide helpful guidance to this day. Ivana B., Ivana Ć., Dino, Mervan, Emerik, Lorena, and Goran – thank you for the lovely microenvironment and all the pleasant moments we spent together.

Thanks to Petra, brilliant young scientist and caring friend – you were the best possible companion on this journey. Thanks to my dear and always helpful Emina, together with the rest of the IRB team who contributed to this thesis.

Special acknowledgement goes to Silvia and Dino, genuine friends with huge hearts and unfailing sense of humor, who also happen to be some of the smartest people I have ever encountered. Thank you for all the hilarious moments, sincere conversations, invaluable advices, and infinite support. What a privilege it was to work with wonderful friends every day!

My wholehearted thank goes to the rest of my incredible and extraordinary friends who have stuck by me from the moment we met to this day. The whole list would be too long – which makes me the luckiest person in the world – but I would like to especially thank Anja, Klara, Otto, Kristina & Iva – caring, supportive, loving individuals who mean a world to me. I would also like to acknowledge truly brilliant friends Nikoletta & Camilo – I am so glad our paths have crossed. You have contributed a huge part to my happiness during last 4 years.

Finally, this journey would not have been possible without my family. Thanks to the members of this unique, loving, humorous, peculiar group – my parents, Ela, Iva, and especially Marko. Thank you for your full-time support, splendid and treasured moments, and shifting my work/life balance when needed. Without your unconditional love and selfless help in every way and situation, none of this would be possible ♥

Abstract

Biocatalysis is an emerging and important scientific filed for the asymmetric synthesis of pharmaceuticals and fine chemicals that has accomplished astonishing growth in industrial sector in recent years. For individual biocatalytic synthesis to reach its full potential, the process must be explored from the aspect of various scientific fields, including protein engineering, organic chemistry, reaction engineering, and more. The focus of this PhD thesis are halohydrin dehalogenases (HHDHs), promising and yet quite unexplored group of enzymes, and their potential for industrial-scale synthesis. Through extensive research of the existing literature, a serious lack of kinetic data in biotransformations with enzymes from HHDH group was determined. Therefore, one of the objectives of the thesis was to gain insight into kinetic characteristics of HHDH from *Agrobacterium radiobacter* AD1 (HheC) and develop a mathematical model in synthesis of important building blocks, since this approach may lead to the discovery of enzyme kinetic limitations and process bottlenecks, and, more importantly, enable the enhancement of process outcome through model-based simulations.

The investigated reactions were kinetic resolutions for the synthesis of optically pure, fluorinated β-substituted alcohols and epoxides that represent valuable building blocks in pharmaceutical and fine chemicals industries. Ring-opening reactions of fluorinated styrene oxide derivatives, catalyzed by wild-type HheC and its variants W249P and ISM-4, were explored. Fluorinated derivatives of styrene oxide with substituents in *para*-position were found to be most convenient substrates for HheC based on the activity, enantioselectivity and hydrolytic stability, whereby 2-[4-(trifluoromethyl)phenyl]oxirane stood out as the best option. Enzyme variant W249P, with exchanged Trp and Pro amino acids on position 249, displayed higher substrate affinity in comparison to the wild type. Hence, it was selected for further kinetic investigation. The synthesis of (*R*)-2-azido-1-[4-(trifluoromethyl)phenyl]ethanol was described by double substrate Michaelis-Menten kinetics, with the presence of enzyme inhibitions with reacting substrate (*R*)-2-[4-(trifluoromethyl)phenyl]oxirane, opposite enantiomer (*S*)-2-[4-(trifluoromethyl)phenyl]oxirane, product (*R*)-2-azido-1-[4-(trifluoromethyl)phenyl]ethanol, by-product *rac*-2-[4-(trifluoromethyl)phenyl]-1,2-ethanediol, and co-solvent DMSO. Apart from numerous inhibitions and substantial hydrolysis effect, operational stability decay was found to contribute greatly to the synthesis outcome on higher concentration scale, since deactivation constant is directly correlated to the initial concentration of the substrate, 2-[4-(trifluoromethyl)phenyl]oxirane. The mathematical model was developed,

and process simulations were employed in process optimization. Significant improvements in process metrics were achieved by modifying reactor set-up and selecting suitable initial conditions. The optimized biocatalytic system in repetitive batch reactor led to high reaction yield and optical purity (Y = 95%, ee > 99 %). However, process should be optimized further in order to increase reaction productivity that meets the target for industrial synthesis.

The existence of various enzyme inhibitions and concentration-dependent enzyme deactivation, as well as low solubility and hydrolytic instability of the substrate, makes the system convenient for the switch from aqueous to alternative media. In the second part of the thesis, the focus was on the investigation of the influences of organic solvents (OSs) on HheC catalytic and structural performances. The stability of HheC in presence of dimethyl sulfoxide (DMSO), the most used co-solvent in HHDH-catalyzed biotransformations, was found to be preserved in cases when DMSO volume ratio does not exceed 30% (*v*/*v*). In higher DMSO content, HheC is not able to retain native structure and is completely and rapidly inactivated at 50% (*v*/*v*) co-solvent. This was confirmed by the combination of experimental studies, including monitoring enzyme stability and protein size distributions during incubation with different DMSO content, together with molecular dynamic studies (MD). DMSO also proved to be a mixed-type inhibitor of HheC in the reactions of *para*-nitro-2-bromo-1-phenylethanol (PNSHH) dehalogenation and *para*-nitro styrene oxide (PNSO) ring-opening with bromide ions. The inhibitory behavior was detected by kinetic Lineweaver-Burk analysis and confirmed by MD. Likewise, DMSO was found to be inhibitor of W249P variant in (*R*)-2-[4-(trifluoromethyl)phenyl]oxirane azidolysis during kinetic investigation. Wild-type HheC also displayed inadequate catalytic properties in presence of other tested water-miscible co-solvents, specifically dimethylformamide, methanol, isopropanol, acetonitrile, and tetrahydrofuran. In case of hydrophobic solvents, a direct correlation between HheC activity and logP value was found in PNSHH ring-closure reaction. Knowledge of such a relationship makes biocatalysis with organic solvents more predictable, which may reduce the need to experiment with a variety of solvents in the future. However, this trend was not reported for PNSO ring-opening reaction. From hydrophobic OSs, tested alkanes (cyclohexane, *n*-hexane, *n*-heptane) were found to be compatible with HheC activity and stability during incubation, indicating the preservation of high enzyme structural integrity in these biphasic systems. Chloroform and toluene displayed inhibitory properties, especially in ring-opening reaction, which is more valuable from the synthetic point of view. In comparison to the wild type HheC, thermostable variant ISM-4 performed better in presence of OSs in terms of activity, stability, and enantioselectivity. In

other words, the link between thermal stability and resistance to the action of OSs was established. These results revealed that ISM-4 has excellent potential for biotransformations in organic media, and as such should be explored for future implementations.

Keywords: biocatalysis, chiral building blocks, dimethyl sulfoxide, enzyme kinetics, fluorinated building blocks, halohydrin dehalogenases, mathematical modeling, organic solvents, reaction engineering

Sažetak

Biokataliza je važno znanstveno područje u razvoju za asimetričnu sintezu lijekova i finih kemikalija koje je postiglo zapanjujući rast u industrijskom sektoru posljednjih godina. Kako bi pojedinačna biokatalitička sinteza dosegla svoj puni potencijal, proces se mora istražiti s aspekta različitih znanstvenih područja, uključujući proteinsko inženjerstvo, organsku kemiju, reakcijsko inženjerstvo itd. U fokusu ovog doktorskog rada su halogenhidrin-dehalogenaze (HHDH), obećavajuća ali još nedovoljno istražena skupina enzima, te njihov potencijal za industrijsku sintezu. Opsežnim istraživanjem postojeće literature utvrđen je ozbiljan nedostatak kinetičkih podataka u biotransformacijama s enzimima iz skupine HHDH. Stoga je jedan od ciljeva doktorskog rada bio dobiti uvid u kinetičke karakteristike HHDH iz *Agrobacterium radiobacter* AD1 (HheC) i razviti matematički model za sintezu važnih građevnih blokova, budući da ovaj pristup može dovesti do otkrića kinetičkih ograničenja enzima i uskih grla procesa te, što je još važnije, omogućiti poboljšanje ishoda procesa kroz simulacije temeljene na modelu.

Istraživane reakcije bile su kinetičke rezolucije za sintezu optički čistih, fluoriranih β-supstituiranih alkohola i epoksida koji predstavljaju vrijedne gradivne elemente u farmaceutskoj industriji i industriji finih kemikalija. Istražene su reakcije otvaranja prstena fluoriranih derivata stiren-oksida, katalizirane divljim tipom HheC i njegovim mutantima W249P i ISM-4. Utvrđeno je da su fluorirani derivati stiren-oksida sa supstituentima u *para*-položaju najprikladniji supstrati za HheC na temelju aktivnosti, enantioselektivnosti i hidrolitičke stabilnosti, pri čemu se 2-[4-(trifluormetil)fenil]oksiran istaknuo kao najbolja opcija. Enzim W249P, sa zamijenjenim Trp i Pro aminokiselinama na poziciji 249, pokazao je veći afinitet prema supstratu u usporedbi s divljim tipom, stoga je odabran za daljnje kinetičko istraživanje. Sinteza (*R*)-2-azido-1-[4-(trifluorometil)fenil]etanola opisana je dvosupstratnom Michaelis-Menteničinom kinetikom, uz prisutnost inhibicija enzima sa supstratom (*R*)-2-[4-(trifluormetil)fenil]oksiranom, suprotnim enantiomerom (*S*)-2-[4-(trifluormetil)fenil]oksiranom, produktom (*R*)-2-azido-1-[4-(trifluormetil)fenil]etanolom, nusproduktom *rac*-2-[4-(trifluorometil)fenil]-l,2-etandiolom, i ko-otapalom DMSO. Osim brojnih inhibicija i značajnog učinka hidrolize, utvrđeno je da pad operacijske stabilnosti enzima uvelike pridonosi ishodu sinteze pri višim koncentracijama, budući da je konstanta deaktivacije enzima izravno ovisna o početnoj koncentraciji supstrata, 2-[4-(trifluorometil)fenil]oksirana. Razvijen je matematički model, a pri optimizaciji procesa

korištene su simulacije procesa. Značajna poboljšanja u ishodu sinteze postignuta su modificiranjem tipa reaktora i odabirom odgovarajućih početnih uvjeta. Optimizirani biokatalitički sustav u repetitivnom šaržnom reaktoru doveo je do visokog iskorištenja na produktu i optičke čistoće (Y = 95%, ee > 99 %). Međutim, proces treba dodatno optimizirati kako bi se povećala produktivnost reakcije koja ispunjava ciljeve za industrijsku sintezu.

Postojanje različitih inhibicija i deaktivacije enzima ovisne o koncentraciji, kao i niska topljivost i hidrolitička nestabilnost supstrata, čine sustav pogodnim za prelazak s vodenog na alternativni medij. U drugom dijelu doktorskog rada fokus je bio na istraživanju utjecaja organskih otapala (engl. *organic solvent* – OS) na katalitička i strukturna svojstva HheC. Utvrđeno je da je stabilnost HheC u prisutnosti dimetil-sulfoksida (DMSO), najčešće korištenog ko-otapala u HHDH-biotransformacijama, očuvana u slučajevima kada volumni udio DMSO ne prelazi 30% (*v*/*v*). Pri većem udjelu DMSO, HheC nije u stanju zadržati prirodnu strukturu te se potpuno i brzo inaktivira pri 50% (*v*/*v*) ko-otapala. To je potvrđeno kombinacijom eksperimentalnih istraživanja, uključujući praćenje stabilnosti enzima i raspodjele veličine proteina tijekom inkubacije s različitim sadržajem DMSO, zajedno s molekulsko-dinamičkim studijama (engl. *molecular dynamics* – MD). Prema HheC, DMSO se također pokazao kao inhibitor miješanog tipa u reakcijama dehalogenacije *para*-nitro-2-bromo-1-feniletanola (PNSHH) i otvaranja prstena *para*-nitro stiren oksida (PNSO) s bromidnim ionima. Inhibicijsko ponašanje otkriveno je kinetičkom Lineweaver-Burk analizom i potvrđeno MD analizom. Isto tako, tijekom kinetičkih ispitivanja, otkriveno je da je DMSO inhibitor W249P mutanta tijekom azidolize (*R*)-2-[4-(trifluorometil)fenil]oksirana. Divlji tip HheC također je pokazao neadekvatna katalitička svojstva u prisutnosti drugih testiranih ko-otapala koja se miješaju s vodom, a posebice dimetilformamida, metanola, izopropanola, acetonitrila i tetrahidrofurana. U slučaju hidrofobnih otapala, izravna korelacija između aktivnosti HheC enzima i logP vrijednosti pronađena je u reakciji zatvaranja prstena PNSHH. Saznanje o takvoj ovisnosti čini biokatalizu s organskim otapalima predvidljivijom, što može smanjiti potrebu za eksperimentiranjem s različitim otapalima u budućnosti. Međutim, ovaj trend nije pronađen u reakciji otvaranja PNSO prstena. Od hidrofobnih OS, utvrđeno je da su alkani (cikloheksan, *n*-heksan, *n*-heptan) kompatibilni s HheC aktivnošću i stabilnošću tijekom inkubacije, što ukazuje na očuvanje visokog strukturnog integriteta enzima u ovim dvofaznim sustavima. Kloroform i toluen pokazali su inhibicijska svojstva, posebno u reakciji otvaranja prstena koja je vrjednija sa sintetičkog gledišta. U usporedbi s divljim tipom HheC, termostabilni mutant ISM-4 demonstrirao je bolje rezultate u prisutnosti OS u smislu aktivnosti, stabilnosti i

enantioselektivnosti. Drugim riječima, za slučaj ovog enzima utvrđena je poveznica između termičke stabilnosti i otpornosti na djelovanje otapala. Ova istraživanja otkrila su da ISM-4 mutant enzima ima izvrstan potencijal za biotransformacije u organskim medijima, te bi ga kao takvog trebalo istražiti za buduće primjene.

Ključne riječi: biokataliza, dimetil-sulfoksid, enzimska kinetika, fluorirani građevni blokovi, halogenhidrin-dehalogenaze, kiralni građevni blokovi, matematičko modeliranje, organska otapala, reakcijsko inženjerstvo

Table of contents

1. Introduction

Enzymes are macromolecular, biological catalysts exploited in industrial processes for decades [1]. Since enzymes operate at mild reaction conditions with high activity, specificity and selectivity, biocatalysis is often imposed as an environmentally acceptable and economically more profitable alternative to the traditional synthetic procedures in organic chemistry [2]. Although it was long perceived as green promising tool, biocatalysis is nowadays recognized and accepted as a mature technology in asymmetric synthesis [3]. In the focus of this thesis is quite unexplored but promising group of enzymes under the name halohydrin dehalogenases (HHDHs). In their natural environment, HHDHs are involved in degradation of halogenated organic compounds as they are able to cleave carbon-halogen bond in vicinal halohydrins and form corresponding epoxides [4]. Synthetic value of the HHDH group lies in their ability to employ a broad range of unnatural nucleophiles in ring-opening reaction, thus enabling formation of novel C-C, C-S, C-N, and C-O bonds. In addition, HHDH-catalysis is often highly regioselective and enantioselective; therefore, products of high optical purity can be obtained. Optical purity represents an important requirement in the pharmaceutical and fine chemical industries. The importance of HHDHs is best illustrated by industrial application of C-type variant in the industrial production of atorvastatin, active ingredient of cholesterol-lowering drug sold under the brand name Lipitor (Pfizer) [5]. HHDHs are also employed in the synthesis of a key intermediate for the (*S*)-cidofovir, antiviral drug for treating cytomegalovirus retinitis sold under the brand name Vistide (Gilead Sciences) [6].

This dissertation, conceived as research on the C-type HHDH from *Agrobacterium radiobacter* AD1 (HheC), is divided into two main parts. The focus of the first part is biocatalytic synthesis of optically pure, fluorinated, organic compounds employing HheC and its variants. Starting point of the synthesis are racemic fluorinated derivatives of styrene oxide. These F-substituted aromatic epoxides undergo asymmetric ring-opening with HHDH enzyme mediated by azide ions. The reaction products are (*R*)-1,2-azido alcohols, and unreacted enantiomers of (*S*)-epoxides. These reactions were selected based on the value of resulting products as intermediates for synthetic purposes, as described below. Fluorinated organic compounds have been extensively studied in pharmaceutical research and medicinal chemistry based on their exquisite and unique properties. In general, organofluorine compounds are scarce in nature. Natural organic compounds containing F-moiety are practically non-existent, with

only a few structurally similar exceptions. This means that the availability and diversity of fluorinated building blocks is purely a responsibility of synthetic chemistry. On the current global market, more than 20% of drugs contain fluorine, and about a half of them contain a mono- or multifluorinated aromatic ring [7,8]. Moreover, the number of F-containing drugs on global market is in a trend of constant growth.

Epoxides are highly valuable starting materials in organic chemistry based on their reactivity and synthetic potential [9]. Likewise, organic azides are strategically valuable building blocks as azido group is highly reactive and enables the adjunction of building blocks to other molecules, thus simplifying the process of designing complex APIs. They are often employed in pharmaceutical industry for the synthesis of various N-containing building blocks, e.g. amines and heterocycles such as triazole [10,11]. Moreover, organic azides are often reactive and unstable, which makes their handling more demanding, and are often omitted from industrial processes. However, new studies have showed that the incorporation of fluorine atoms into the organic azides results in stabilization of molecules, making the large-scale synthesis by far safer, and thus more desirable from the process engineering point of view [12]. Although their potential is great, available methods for the synthesis of fluorinated organic azides are rare and delicate [13]. In this dissertation, the HHDH-catalyzed synthesis of fluorinated optically pure 1,2-azido alcohols and epoxides was studied from the viewpoint of enzyme reaction engineering. In the first part of the study, main objectives are determination of the kinetics in HHDH-catalyzed biotransformations and development of detailed mathematical models. Hypothesis of the research is that kinetic models will point out to the weak points of the synthesis, thus enabling the choice of the most efficient reactor types, and that mathematical model and process simulations will facilitate the optimization of the process conditions. Since the modelling approach has not yet been used for the reactions catalyzed by HHDHs, this research will bring valuable insight in the kinetic characteristics of the enzyme, its operational stability, as well as potential bottlenecks in HHDH application.

The second part of the dissertation is focused on characterization of suitable media for the HHDH-catalyzed biotransformations. Since substrates are often poorly soluble in water on account of their synthetic, hydrophobic and aromatic nature, biotransformations are usually carried out in concentrations in the millimolar range. This can be suitable for laboratory-scale research; however, scale-up reactions on the millimolar system is not economically profitable [14,15]. Thus, the possibility of performing HHDH-biotransformations in presence of organic solvents (OSs) is of great interest. In addition to improving substrate solubility, the introduction

of OSs can also minimize other limitations and offer some additional advantages. For example, transfer to water-organic systems can reduce the influence of hydrolytic side reactions that take place in the aqueous medium, shift the thermodynamic equilibrium, simplify the product isolation and enzyme recovery, etc. [16]. Enzymes usually function best in the aqueous media due to their biological origin. However, there are various successful examples of biocatalysis in non-aqueous and alternative reaction media. The most common approach is the introduction of certain amount of an OS into the buffer medium. Depending on the polarity and miscibility of an OS with water, a monophasic or biphasic water-solvent system is formed. At the expense of listed advantages, OSs can negatively influence catalytic and structural properties of the enzymes [16–18]. Main objective in the second part of the research is determination of reaction medium and solvent content for carrying out HHDH-biotransformations, with the hypothesis that the introduction of the organic phase in the reaction media will have a positive effect on the substrate solubility, thus increasing its bioavailability and leading to higher volume productivity. Although HHDH-catalysis has been tested in different solvents, systematic study on their influence on the properties of HHDH has not been performed up to date. Comprehensive study on this topic may serve as a guide for the future selection of the most suitable solvent system for HHDH-catalyzed biotransformations.

2. State of the art

2.1 Compounds of interest

2.1.1 Organofluorinated compounds and organic azides

On the scale of the most abundant chemical elements in the Earth's crust, fluorine ranks high in the 13th place, but it is almost exclusively found in form of mineral salts, such as fluorite, cryolite, fluoroapatite, topaz etc. [19,20]. Despite of its high presence in rock-forming salts, naturally occurring fluorinated organic compounds are exceptionally rare. So far, only around dozen F-bearing organic molecules of natural origin have been discovered, which makes them below approximately 0.5% of all known natural organohalogens. These mostly include monofluorinated derivatives of fluoroacetate and ω-fluorinated fatty acids that are seldom found in southern hemisphere plants and some actinomycete species [21–23]. Such scarce presence is suspected to be a result of poor aqueous solubility of fluorine that led to its low bioavailability during evolution. In contrast to 19350 ppm of chlorine in seawater, fluorine concentration is only 1.3 ppm [24,25]. In addition, aqueous fluoride is very hydrated, and as a consequence nucleophilic reactions are highly hindered [23]. Although extremely rare in nature reservoir, synthetic fluorinated organic compounds have been extensively studied in pharmaceutical and medicinal chemistry, materials science, agrochemicals etc. There are numerous studies reporting novel F-containing liquid crystals, polymers, active pharmaceutical ingredients (APIs), membranes and pesticides with vastly enhanced properties [26]. When fluorine is introduced into small synthetic molecules, as pharmaceuticals and agrochemicals, their properties could change drastically [27]. The novel characteristics, exhibited by fluorinated molecules, derive from small F-atom size, greatest electronegativity of all elements and low polarizability [28]. Moreover, C-F bond is the strongest single covalent bond between carbon and any common atom [29]. Organic fluorinated molecules came onto the scene in medicinal chemistry in the 1950s when Fried and Sabo [30] developed the first fluorinated pharmaceutical. Fludrocortisone (9α-fluoro-11β,17α,21-trihydroxypregn-4-en-3,20-dione) was found to exhibit enhanced biological activity in comparison with non-fluorinated structural analogue, thus paving the way to the development of field of fluoroorganic chemistry [21]. From then until today the application of fluorine in pharmaceutical industry has expanded astonishingly. Fluorinated APIs are typically superior over their non-fluorinated structural analogues since presence of fluorine atoms or fluorine-containing substituents can substantially

change biochemical reactivity of molecules and cause or intensify a broad spectrum of properties, often the ones of critical importance in drug design and development. Introduction of F-atoms in organic molecules can provide greater stability during metabolism, increase biological half-life, target effectiveness, intrinsic activity and drug lipophilicity, i.e., membrane permeability leading to enhanced bioabsorption etc. [31–33]. To this point, more than 300 fluorinated pharmaceuticals have been approved worldwide [8]. From the novel small-molecule pharmaceuticals approved by the Food and Drug Administration (FDA), 45% were fluorinated in 2018, 41% in 2019, 35% in 2020, and 24% in 2021 [34]. The FDA statistics for the last few years dictates that the inclusion of F-atoms during the stage of drug research and development reduces the chance of failure in the approval process [8]. Based on the listed properties, fluorinated molecules are rising-stars in agrochemical industry as well. In comparison to 2003 when 16% of agrochemicals on global market were fluorinated, in 2020 this number was as high as 53% [35].

Classic methods for flourine incorporation include direct and Swartz fluorination, Halex and Simons process, and Balz–Schiemann reaction, all of which demand highly corrosive and explosive agents, such as hydrogen fluoride, difluorine, antimony trifluoride and cobalt trifluoride. These methods are cost-effective, but in the same time hazardous, conducted under harsh conditions and applicable only to a limited scope of substrates. Through years, various reagents for fluorination of second generation (e.g. *N*-fluorobenzenesulfonimide and Selecfluor) and third generation (e.g. *N*-fluoro-*N*-arylsulfonamides) were developed [36–38]. Novel fluorination approaches are performed under milder conditions, thus lessening environmental impact. However, these processes are expensive and sometimes unprofitable, which is especially true when final products are agrochemical, rather than drugs, judging by the difference in the prices they achieve on the market. Along with invention of cost-effective and environmentally acceptable fluorinating agents, another focus in fluoroorganic chemistry is the development of novel methods of modifying simple, commercially available F-bearing molecules. Since the late-stage fluorination of complex molecules is often not an option, the availability of a wide range of small, fluorinated building blocks is crucial in development of new APIs and agrochemicals [39].

Azido group is strategically valuable part of the fluorinated building block since it facilitates the incorporation of C-F moiety into another structure. Azido group is highly reactive and it enables the adjunction of fluorinated building blocks to other molecules, thus simplifying the process of designing complex APIs [10,40]. Organic azides are extensively employed in

click chemistry reactions, enabling access to various valuable compounds, such as extensively studied triazoles, highly important class of compounds in medicinal chemistry [13]. Organic azides are often reactive and unstable, which makes their handling more demanding and are often omitted from industrial processes. However, new studies have shown that the incorporation of fluorine atoms into the organic azides results in stabilization of molecules, making the large-scale synthesis by far safer, and thus more desirable from an process engineering point of view [12]. Although their potential is great, available methods for the synthesis of fluorinated organic azides are rare and delicate [13]. In this thesis, biocatalytic synthesis of fluorinated 1,2-azido alcohols is assessed. Optically pure 1,2-azido ethanols are highly important building blocks in pharmaceutical industry since they represent starting points for synthesis of various 1,2-amino alcohols, tailor-made amino acids and triazole derivatives [41]. In the global market, more than 30% of small synthetic drugs contain residues of amino acids or corresponding amino alcohols and diamines. Such a trend is still in rise, e.g. out of 24 novel molecules approved by the FDA in 2019, 13 contain residues or derivatives of amino acids [42].

2.1.2 Chiral organic compounds

Together with expanding assortment of organofluorine compounds, another focus of the pharmaceutical industry is broadening the possibilities for synthesis of enantiopure drugs. When it comes to *in vivo* systems, chirality is everywhere. Nucleic acids, proteins, polysaccharides and lipids are chiral, and the property extends from these fundamental macromolecular components of cellular life all the way to the layout of the human body. On that account, biological receptors frequently distinguish pair of enantiomers as different compounds [43]. Enantiomers display unchanged physicochemical characteristics when placed to achiral surroundings; however, in chiral environment, they may exhibit completely different behavior [44,45]. One conformation causes the desired result, while the other is inactive or weakly active in the best scenario. As learned the hard way after Thalidomide scandal that occurred during late 1950s and early 1960s, the opposite enantiomer of the API even can cause serious side effects or be toxic [46]. Enantiopure drugs, relative to racemic ones, lead to dose reduction, i.e., better therapeutic properties, reduced variability in drug metabolism, simplification of dose-response relationships and improved tolerance [44,47]. Modern pharmaceutical practice includes chiral switch, a strategy of substituting racemic drugs on the market with single enantiomeric forms [48]. Consequently, optically pure substances are valuable precursors in the pharmaceutical and fine chemical industries. The approaches for

obtaining pure enantiomers include separation methods, better known as chiral resolution methods, and asymmetric syntheses. Separation methods include crystallization, kinetic and dynamic resolution methods [49].

2.2 Biocatalysis

Biocatalysis was long perceived just as a green promising tool reserved for scientific experimentations. Since adequate thermal and operational stability is one of main prerequisites for implementation of biocatalytic process in industrial sector [50], the omission of large-scale biocatalysis was mostly based on generalizations that enzymes, as molecules of biological origin, do not meet these requirements. However, the situation has dramatically changed over the years on the account of enormous progress in biocatalysis. In recent years, biocatalysis has experienced astonishing growth due to application of interdisciplinary approach and implementation of knowledge from various scientific fields such as microbiology, molecular biology, protein engineering, enzymology, biochemistry, organic chemistry, process chemistry, transport phenomena and reaction engineering [51,52]. Until recently, only a handful of enzymes from common (micro)organisms were available for biocatalysis. Nowadays, methods such as metagenomic and *in silico* screening, optimization of wild-type enzymes by the directed evolution, and even *de novo* computational enzyme design, are available. Biocatalysis is today accepted as established method for industrial synthesis of pharmaceuticals, as evidenced by numerous biocatalytic syntheses implemented on an industrial scale, such as Merck's nine-enzyme cascade production of Islatravir for treatment of HIV patients [1]. Except high stereo-, regio- and chemoselectivity, the main driving forces in biocatalytic development are the environmental aspect and cost-effectiveness. Enzymes are very modest catalysts when it comes to reaction conditions, i.e., they work best in buffer media under ambient temperature and atmospheric pressure, thus reducing energy consumption and greenhouse gas emissions, and are completely biodegradable. Due to the high specificity of enzymes, the protection and subsequent deprotection of functional groups are not usual as in chemocatalysis [53,54].

2.2.1 Halohydrin dehalogenases (HHDHs)

Halohydrin dehalogenases (HHDHs), also called haloalcohol dehalogenases and halohydrin hydrogen-halide lyases, belong to E.C. 4.5.1.- and are seldomly found in microorganisms where they are naturally involved in a degradation of halogenated contaminants which they use as a sole energy source [4,55]. Halogenated organic compounds are persistent, toxic, and widespread xenobiotics, hence HHDHs are interesting allies in

bioremediation of polluted environment. On that account, dehalogenation of 1,3-dichloro-2-propanol (1,3-DCP) and synthesis of epichlorohydrin (ECH), the corresponding epoxide, is one of the best studied reactions catalyzed by HHDH [56]. As the reaction of dehalogenation is reversible, HHDHs are not only known for their ability to remove chlorine, bromine, and iodine atoms from contaminants, but also for the incorporation of halogen ions into molecules. The fact that HHDHs catalyze the conversion of dibromopropanol to epibromohydrin was observed in 1968 by Castro and Bartnicki [57], but it was only in early 1990s discovered that HHDHs have the ability of catalyzing *in vitro* ring-opening reactions with different nucleophiles [58]. From their discovery until today, in addition to halogens, a whole series of nucleophiles was found to be accepted by HHDH in the epoxide ring-opening reactions (Scheme 1). These unnatural nucleophiles are small, negatively charged ions such as azide, cyanide, cyanate, thiocyanate, nitrite, and formate [59]. This property has proven to be extremely useful from synthetic chemistry point of view, since it leads to the formation of novel C-C, C-O, C-S, and C-N bonds, and enables the access to the corresponding unnatural alcohols like β-nitro– and β-azido alcohols, as well as β-hydroxynitriles and generally 1,2-difunctionalized organic compounds [60,61]. Except for their remarkable nucleophile acceptance, HHDH members do not require cofactors and display high regio- and enantioselectivity, which makes them attractive candidates for different synthetic applications [62]. HHDHs can be used for the synthesis of important building blocks and precursors in the pharmaceutical, agrochemical and fine chemicals industries. The most prominent industrial example is the use of C-type HHDH variant for the production of ethyl (*R*)-4-cyano-3-hydroxybutanoate, the key intermediate in atorvastatin synthetic route [5].

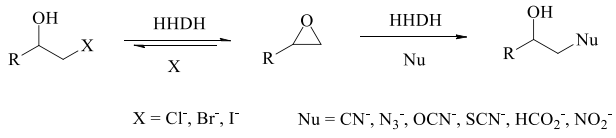

Scheme 1. Scope of nucleophiles accepted in reactions catalyzed by halohydrin dehalogenases. Scheme adapted from [59,63]

According to the sequence identities, substrate acceptance and affinities, HHDHs are divided into seven distinct phylogenetic subtypes ascribed with letters A-G [62,64]. Until recently, only enzymes from subclasses A, B, and C were known. Among them, the HheC enzyme from *Agrobacterium radiobacter* AD1 is by far the most studied member, since it exhibits high β-regioselectivity and (*R*)-enantioselectivity in nucleophilic ring-opening

reactions [65]. From the enzymes that belong to newly discovered subclasses, HheG from *Ilumatobacter coccineus* received a lot of attention on account of substantial differences in scope of accepting substrates [66,67]. Crystallization studies revealed that all known HHDHs are homotetramers in their active form, i.e., dimers of dimers composed of identical subunits of approximately 28 kDa (Figure 1). Studies have revealed that HHDHs are structurally related to short-chain dehydrogenases/reductases (SDRs) [4] whereby one of the main differences is cofactor independency of HHDHs [62]. Instead of cofactor binding site, HHDHs possess quite spacious nucleophile pocket that accepts monovalent nucleophiles of linear geometry. All known HHDHs own catalytic triad Ser-Tyr-Arg responsible for reversible dehalogenation reaction occurring according to S_N2-nucleophilic mechanism [55]. More about HHDHs, their classification, and industrial applications, can be found in the paper joined in this doctoral dissertation (Appendix II).

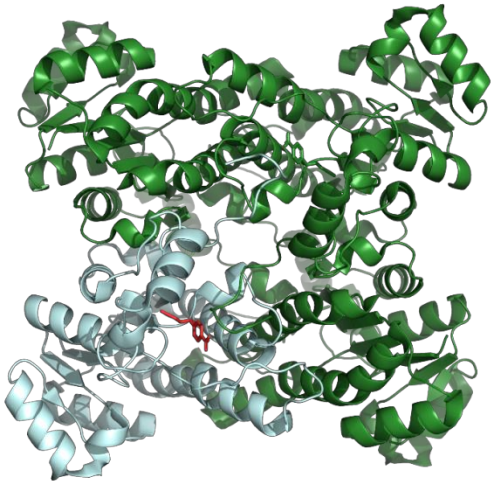

Figure 1. Tertiary structure of HheC enzyme from *Agrobacterium radiobacter* AD1 complexed with (*R*)-1-para-nitro-phenyl-2-azido-ethanol at Ser132/Try145/Arg149 catalytic triad. Figure adapted from [68]

2.2.1.1 HHDHs in the synthesis of compounds of interest

As introduced earlier, HHDHs can accept azido group as nucleophile in ring-opening reactions. This ability was demonstrated previously in various reaction systems, such as azidolysis of *p*-substituted styrene oxide derivatives [69], enantioselective synthesis of 1,2-azidoalcohols and their further transformation to chiral hydroxytriazoles [70], azidolysis of aromatic epoxides with (*S*)-selective variant HheA-N178A [65], azidolysis of spiroepoxides [71], etc. A detailed overview of the previous research with azide ions is included in the review

paper (Appendix II) republished as an integral part of this dissertation, and therefore will not be repeated.

The first paper concerning fluorinated organic compounds and HHDHs was presented by Majerić et al. in 2018 [63]. Authors showed that HheB2 from *Mycobacterium* sp. GP1 can catalyze azidolysis of epifluorohydrin in non-selective fashion. Final product is 1-azido-3-fluoro-2-propanol, which contrasts with other investigated epihalohydrins (X = Cl, Br, I), where 1,3-diazido-2-propanol was produced. In this way, authors have demonstrated that fluoro alcohols are not accepted by HHDHs as substrates in ring-closure reaction since enzymes are incapable of carbon-fluorine bond cleavage [63]. Subsequently, azidolysis and cyanolysis of a series of fluorine-substituted styrene oxide derivatives were investigated in the same research group [40]. Enantioselective ring-opening reactions catalyzed by HHDHs were performed with the goal of producing β-azido alcohols and hydroxynitriles of high optical purity. Kinetic resolutions were started from five styrene oxide derivatives bearing different fluorinated groups in *para*-position (F, CF_3, OCF_3, $OCHF_2$, SCF_3). Azidolysis reactions proceeded with high β-regioselectivity and enantioselectivity, with $E > 100$ for *p*-fluoro-styrene oxide, and $E > 200$ for other derivatives. This research, first of its kind, demonstrated that HHDH enzymes can be used in the synthesis of useful, optically pure, fluorinated building block. However, some shortcomings were pointed out in the research, especially evident during the transition from analytical to preparative scale. The primary concerns are the presence of hydrolytic reactions and chemical azidolysis, both of which reduce yield of the final products. One of the conclusions of the study is that scaled-up biotransformations should be optimized in order to reduce losses in the system and improve process metrics.

2.2.2 Biocatalysis in organic solvents

Enzymes for research and commercial use are obtained by overexpression and isolation from living organisms, whereby microorganisms are most often used as enzyme-production factories due to simplicity, high growth rate and cost effectiveness. Given their biological origin, enzymes usually function best in their natural environment, which generally includes aqueous media with diluted salts at neutral pH and room temperature [72]. Nonetheless, when enzymes are used as natural catalysts in synthetic processes, the required and expected output is often far from the one encountered in biological processes. Although highly selective, specific, and rapid in their action, enzymes in living cells often catalyze the formation of products in millimolar quantities, which does not represent a profitable transfer to an industrial

scale. The most interesting organic compounds from the synthetic point of view are often hydrophobic and consequently only sparingly soluble in aqueous media. Poor solubility is often disregarded in initial research on laboratory scale, since screening of possible substrates and synthetic routes is usually performed at low concentrations [73]. On the industrial scale, the isolation of the product of interest from the diluted aqueous solutions is often unprofitable due to high boiling point and low vapor pressure of water [74]. In order to increase the solubility of organic substrates, and thus enhance the enzyme productivity, aqueous medium is often modified by introduction of a non-aqueous solvent, or completely replaced by an alternative medium [16]. Some of the additional advantages of biocatalysis with solvents are shift of thermodynamic equilibrium, easier recovery of the enzyme from the reaction mixture, simpler isolation of final products, and avoidance of unwanted reactions such as substrate hydrolysis, racemization and polymerization, as well as microbial contaminations in the system. However, the introduction of alternative media can often come at a price in the form of a decrease in enzyme activity and stability, coupled with severe mass-transfer limitations [16,74-76]. As field of biocatalysis in OSs began to develop in the 1970s, certain conclusions about effects of individual solvents and the system types can be drawn from a vast number of research published since then. Interactions between an enzyme and OS can result in molecular changes in the enzyme structure, such as loss of structural water, changes in flexibility and conformational alterations [77–79]. Moreover, OS molecules may act as enzyme inhibitors [80]. Enzyme activity and stability are usually preserved better in hydrophobic OSs rather than hydrophilic ones, since the later can eliminate water molecules from hydration shell around protein, which is essential for structure and activity conservation, and penetrate the structure more easily [16,17]. Understanding complex enzyme-solvent interactions is of primary concern in the rational design of OS resistant enzymes. A combination of experimental and computational methods is a particularly useful and efficient pathway to provide insight into these complex interrelations [81]. Studies have shown that the effects of OSs on enzyme properties depend on the chemical and physicochemical properties of the solvent and the type of enzyme [16]. Hence, generalizations cannot be made and detailed solvent tolerance study should be conducted for each enzyme of interest.

2.2.2.1 HHDH-catalyzed reactions with organic solvents

In this dissertation, the emphasis is on the research of OSs suitable for HHDH-catalysis. Laboratory scale HHDH-catalyzed reactions are usually performed in aqueous media with

addition of dimethyl sulfoxide (DMSO) in concentrations 2-5% (*v*/*v*), while in certain research this number goes up to a maximum of 10% [65,71,90,91,82–89]. DMSO is a suitable co-solvent in biocatalysis due to its amphipathic nature [92], property which allows it to dissolve a wide range of hydrophilic and hydrophobic compounds of interest. Systems containing small amounts of DMSO allow synthetic substrates to be dissolved in higher concentrations, thus increasing bioavailability to HHDH [17,93]. Although it is known that OSs can have a negative effect on enzyme catalytic and structural properties, even when present in small quantities, the effect of 2-5% (*v*/*v*) DMSO on HHDH has never been investigated in detail. In addition, at such low co-solvent amounts, the substrate solubility is still too low for industrial purposes. Also, even more important, the effects of higher DMSO concentrations on HHDH-catalysis were not presented up to date.

Except for DMSO, other enzyme-solvent systems were reported in the existing literature. Jin et al. tested the effect of several OSs on immobilized *Escherichia coli* cells harboring HHDH and epoxide hydrolase. Cells were used for the synthesis of (*R*)-ECH from 1,3-DCP. Organic solvents were introduced in the system with the aim of reducing substrate racemization, thus increasing the product yield [94]. When present, isobutyl alcohol, dichloromethane, acetone and toluene decreased both product yield and optical purity to some extent. In presence of *n*-hexane, cyclohexane, *n*-heptane and isooctane, optical purity was high (*ee* > 99%) and the yield was somewhat higher that in buffer medium. The highest yield of 25.1% was achieved in presence of cyclohexane, compared to 19.2% in buffer medium. Although slight increase in yield represents a certain improvement over aqueous biocatalysis, the results leave a lot of room for optimization, i.e., wider screening of solvents and their corresponding concentrations. Zou et al. employed different solvents in order to minimize product inhibition in (*S*)-2,3-dichloro-1-propanol synthesis catalyzed by *E. coli* cells expressing HHDH [95]. Candidates in solvent screening were toluene, cyclohexane, dichloromethane, *n*-hexane, *n*-heptane and isooctane, whereby *n*-heptane performed the best. Authors found that the solvent ratio, pH and temperature have decisive effect on the product yield and the optical purity, thus indicating the need for their optimization. Biphasic system, containing volume ratio of *n*-heptane to buffer 1:4, resulted in 2.5 fold higher biocatalyst productivity. Dong et al. employed HheC variant in biphasic bioelectrocatalytic cascade for production of (*R*)-ethyl-4-cyano-3-hydroxybutyrate [96]. Originally, activity of HHDH was assessed in biphasic system with 30% *n*-hexane, ethyl acetate, dichloromethane and MTBE. Authors stated that first three tested solvents decreased the activity of HHDH, while the later had slight positive impact on

enzyme activity. Roiban et al. screened the activity of immobilized HHDH towards *rac*-2-butyl-2-ethyloxirane in set of solvents, namely toluene, methyl *tert*-butyl ether (MTBE), 2-methyltetrahydrofuran, isopropyl acetate, cyclohexane, and ethyl acetate [97]. Although they were able to obtain satisfactory conversion and product purity on small-scale with 20% (*v*/*v*) ethyl acetate, authors reported that increase in reaction volume to 30 mL resulted in dramatic drop of conversion and *ee*. This was attributed with high probability to mass-transfer limitations but was not inspected further. Zhang et al. performed water-free HHDH biotransformations [98]. Authors examined 10 water-saturated solvents in HHDH-catalyzed synthesis of (*S*)-ECH from 1,3-DCP. Compared to the biotransformation in aqueous medium, the optical purity in almost all tested solvents was lower, except in ethyl acetate, where increase in *ee* from 88% to 99% was obtained. However, the relative activities of the free enzyme in solvents were fairly low, up to 10% of the value in buffer medium. By immobilizing enzyme on A502Ps resin, authors were able to perform synthesis in water-saturated ethyl acetate with high yield (52%) and *ee* (> 98%). In case of immobilized enzymes, lower initial activity can be compensated by good process reusability, which was demonstrated by 24 consecutive batch cycles in this research [98].

Previously listed studies [94–98] were examples of some of the HHDH-catalyzed biotransformations in the presence of OSs. Although there are several reports of HHDH-catalyzed transformations in aqueous-organic media, no systematic study of solvent effects on the properties of the HHDH enzyme has been carried out to date. Previous studies generally agree on the fact that polar OSs have a stronger negative effect on HHDH performance compared to non-polar ones, but the mechanism of OSs action on activity, stability, enantioselectivity and overall productivity is unknown. The severity of these effects will depend on the solvent properties and the enzyme nature, as well as the type of catalyzed reaction. Lower productivity with OSs, especially in biphasic systems, is not always a consequence of a decrease in enzymatic activity, but mass-transfer limitations should be taken into account as well. Likewise, the apparent improvement in the enzymatic productivity in presence of OS does not necessarily point out on a better enzyme performance *per se*, but could be a result of more efficient and complete product extraction.

2.3 Enzyme reaction engineering and mathematical modelling

In recent years, the scientific field of biocatalysis occupies an important place in the pharmaceutical industry and the industry of fine chemicals as it provides economically and

environmentally acceptable ways towards synthesis of a wide range of novel, highly pure compounds. Biocatalysis is relatively young field in the industrial sector of the production of drugs and fine chemicals, but has been the subject of research for decades in scientific and academic communities. In modern times, science and industry are aiming towards symbiotic relationship, while research towards reducing the gap between them is highly encouraged. Key towards the convergence of these two spheres and establishment of novel processes is application of engineering science approach and principles. Comprehensive engineering approach in the field of biocatalysis includes:

i. substrate engineering,
ii. protein engineering,
iii. medium engineering,
iv. biocatalyst engineering,
v. reaction engineering.[99]

Chemical reaction engineering is a scientific branch that unites chemistry, physics and mathematics as fundamental sciences into modelling of processes and optimization of their performances [100]. Biochemical engineering studies biocatalytic processes with the aim of their improvement by applying the rules of chemical engineering but respecting the limitations and special conditions concerning catalysts with biological origin. Enzyme reaction engineering takes into account thermodynamics and kinetics of catalyzed process with the goal of process intensification by solving reaction bottlenecks and choosing the best biocatalyst formulations, process conditions, and reactor types [101–103]. Main assignment when employing enzyme reaction engineering approach is obtaining great space–time yield in highly selective fashion with minimization of waste generation and rational distribution of resources [104].

The enzyme reaction engineering research begins with the characterization of the suitable enzyme microenvironment, which includes selection of buffer medium, ionic strength, pH and temperature [105]. The reaction scheme of the system, as well as the system thermodynamics, must be known, and the existence of reverse reactions must be identified, so that the kinetics of all reaction paths and directions can be investigated. Kinetic measurements must be performed starting from the individual substrates of all existing reactions, and the influence of all present compounds on the enzymatic activity must be examined [104,106]. Kinetic measurements are often performed by rapid data collection using the initial reaction rates method, within 10% of substrate conversion, in the period where the influence of reverse

reactions, product inhibitions and enzyme deactivation are excluded. Based on reaction schemes, experimental data trends and known interdependencies, a kinetic model of the process is developed and the corresponding kinetic parameters are estimated [102]. It is preferable to use non-linear regression methods since linearized methods can misrepresent experimental data by introducing great errors, especially at high and low concentrations of examined compound. After the fitting of kinetic models and finding a satisfactory dependence, mathematical models must be developed and validated in different types of reactors [102,104,107]. The choice of reactor type in the validation phase, and in particular the phase of process optimization, will depend on the kinetic equations and specific features of the observed reaction system [108]. For example, in the presence of strong inhibitions by substrates, reactors with a continuous inflow of substrate or its repetitive addition in portions should be considered. Likewise, in case of inhibition by the product, its continuous removal from the system can be applied [109,110]. More about enzyme reaction engineering as a tool in exploration of biocatalytic systems for detection and resolution of reaction bottlenecks, together with facilitation of transfer to industrial scale, can be found in the first review paper (Appendix I) integrated into this doctoral thesis, thus it will not be discussed here in more detail [111].

Until this research, mathematical modelling methodology has not been used yet to analyze HHDH-catalyzed biotransformations. In the second review paper (Appendix II) included in this dissertation, literature-derived kinetic data about HHDH enzymes were analyzed and discussed. The research is conceived as a review of previous studies with special reference to kinetic characterization, process considerations and challenges in HHDH-catalyzed reactions from the viewpoint of enzyme reaction engineering. Therefore, an overview of previously known research on the kinetics of HHDH enzyme group can be found in Appendix II and will not be repeated here.

3. Discussion

3.1 Reaction engineering in biocatalytic synthesis of fluorinated building blocks

As already demonstrated in the state of the art, the HHDH group of enzymes is still largely unexplored, and is continuously and extensively studied not just in academic research groups, but industrial as well [5,6,61]. Great advances have been achieved in recent years regarding HHDH enzymes in different aspects, from discovering hitherto unknown subgroups with novel substrate specificities and activities [66,112], through unknown preferences of long-known enzymes [113], to the construction of new variants with improved properties [114]. In 2020, in our research group, we have collected and processed data from all published studies on the topic of HHDHs, approximately 100 at the time (Appendix II). Despite numerous quality studies dealing with HHDH enzymes published recently, we have encountered a serious shortage of the data on the kinetic behavior of HHDH enzymes in existing literature. Through data evaluation we have found that 34 papers reported some or all of fundamental kinetic parameters (V_m, K_m, k_{cat}) for specific reactions, but none of the studies conducted a more thorough kinetic analysis that would point to anything more than simple enzyme-substrate relationship. Fundamental kinetic parameters represent valuable data when evaluating different wild-types or variants of HHDHs, and can serve as a solid ground for the initial screening of enzyme activities towards various natural and unnatural substrates. Nevertheless, a wider set of kinetic data is needed to truly assess the applicability of individual enzymes. For example, only 7 of the studies addressed the existence of enzyme inhibition by some compounds present in the reaction system and numerically expressed them as inhibition constants (K_i). Enzyme inhibitions by substrates, products and by-products represent an important part of metabolism for the maintenance of cell homeostasis; hence, they are widely spread phenomena in enzyme kinetics and are often encountered during *in vitro* experiments with all forms of biocatalysts. Of course, compounds present in biocatalytic reactions from natural metabolic pathways are not the only the ones that cause inhibitions. There are also OSs added for solubility, various stabilizers, as well as other compounds that participate in different enzymatic reactions if the syntheses are carried out in a cascade fashion, which is often the case with HHDH enzymes. Therefore, it is not expected that inhibitions are not present in any of the other investigated HHDH-reaction systems, approximately 70 of them, rather that they were not addressed and evaluated at the time. The existence of inhibitions, i.e., the detection of the actual cause of a

drop in enzyme specific activity, is difficult to determine from the output reaction profiles when all reaction compounds are present in the system. For instance, during the case study of HHDH-catalysis and bottlenecks of their industrial implementation (Appendix II), we have pointed out an example where An et al. [115] assumed the existence of product inhibition, because they did not obtain satisfactory yields with increasing substrate concentration, whereas their data actually indicated an misinterpreted inhibition by azide ions as nucleophiles in the styrene oxide ring-opening reaction. Hence, detailed kinetic measurements, starting from individual reaction compounds, are required for obtaining deeper knowledge about enzyme and reaction limitations.

The drop in the reaction productivity at elevated concentrations of reaction compounds is very often the result of inhibitions. However, such an interpretation should always be taken with caution, since the decrease in product yield at different substrate concentrations could also occur on the account of concentration-dependent drop in enzyme operational stability [116,117]. A handful of enzymes are stable when exposed to small organic molecules only in millimolar scale that corresponds to the concentrations found in physiological environment. Higher substrate loadings, usually required for economically profitable synthesis, may lead to irreversible changes in protein native structure, and consequently, enzyme deactivation. Thus, enzyme tolerance towards higher substrate concentrations is an important parameter when evaluating enzymes as catalysts for synthetic procedures. However, there are very limited data in the existing literature about HHDHs operational stability, and none of the studies reported about influences of different process parameters on the operational stability decay.

In most studies with HHDHs reported up to now, enzyme inhibitions may have gone unnoticed because the concentrations of substrates were too low for such phenomena to be observed or determined with certainty. Similarly, potential problems with the operational stability of the enzyme have not been reported, perhaps because they are negligible, or, more likely, because they were not detected during activity screening at substrate concentrations of 1-5 mM without repeating experiments with same enzyme loading. In addition, some other drawbacks, such as low substrate solubility and bioavailability, intensification of the unwanted chemical reactions or the conversion of the opposite enantiomer of the substrate in reactions that were considered completely enantioselective, are as well often only noticeable when conducting experiments at elevated substrate concentrations. In order to identify the stated problems on the specific system of interest, a detailed kinetic analysis of HHDH-

biotransformation was carried out and presented in Appendix III and is explained and discussed below in more detail.

As reactions of interest in this dissertation, biotransformations using HHDH enzymes were selected with the aim of increasing the availability of optically pure, small, fluorinated building blocks. When azide and cyanide ions are utilized in ring-opening reactions, enantiopure or enantioenriched 1,2-azido alcohols and hydroxynitriles are produced via biocatalytic reactions, while optically pure unreacted (*S*)-enantiomers of the substrate lag behind in the mixture [40]. This kind of kinetic resolution, carried out by biocatalytic means, is in theory very attractive from the environmental and economic aspect, since direct fluorination with toxic chemicals is avoided. In our research group [40], we have shown that the wild-type HheC and its W249P variant can be used in the modification of small, fluorinated organic molecules employing azides and cyanides as unnatural nucleophiles, whereby products of interest are formed; however, certain limitations were discovered. In the respective study, kinetic resolution of *rac*-2-(4-(trifluoromethyl)phenyl)oxirane with NaCN catalyzed by W249P variant was conducted on preparative scale. To obtain product (*S*)-3-hydroxy-3-(4-(trifluoromethyl)phenyl)propanenitrile in 30% yield and 98% *ee*, high enzyme loadings (40% wt) and quite low substrate concentrations (20 mM) were used through prolonged period (15 h). High consumption of the enzyme and resulting unsatisfactory product concentrations, together with the total duration of the reaction, leave a lot of room for the improvement.

The lack of knowledge of the kinetic behavior of the HHDH enzymes, as well as insufficient biocatalytic productivities in some cases, all presented at the beginning of the discussion and in Appendix II [61], together with above explained limitations on preparative scale encountered in our group [40], led to the systematic characterization of HheC and variant W249P from reaction engineering point of view (Appendix III). In the respective study, preliminary kinetic characterization was performed on a set of 11 fluorinated styrene oxide derivatives with wild-type HheC, as well as detailed kinetic characterization and development of a mathematical model of the selected system with W249P. The processes of screening and modelling will not be repeated here since all the results can be found in the main paper, but the key findings and their context in respective with results existing in the literature are discussed. By applying enzyme reaction engineering approach, we have learned about the bottlenecks of the biocatalytic system, but what is more important, how to reduce their impact by taking their existence into account during the setup of the reactor and selection of the initial conditions for the biocatalytic synthesis.

System limitations include low solubility of the substrate in the aqueous medium, the substantial influence of hydrolysis, the presence of numerous inhibitions by the reaction compounds, as well as the concentration-dependent drop in operational stability. A brief overview of each of the listed limitations is given below.

3.1.1 Screening of fluorinated styrene oxide derivatives as HheC substrates

Fluorinated derivatives of styrene oxide are poorly soluble in aqueous media, with an example of *para*-fluorostyrene oxide having the solubility of 0.26 g/L, that is, 1.88 mM. This in practice means that, during individual kinetic assays, the substrate concentration could only be varied below 2 mM. Such low concentrations are in many cases too low for obtaining information about the fundamental kinetic parameters. Apart from the laboratory kinetic studies, the substrate should also be well solubilized to increase its bioavailability to the enzyme during large-scale synthesis. Since most HHDH biotransformations in the literature are carried out with the addition of small amount of DMSO [65,71,90,91,82–89], the concentration of 10% (*v*/*v*) of this solvent was found to provide sufficient solubility (experimentally tested up to 150 mM of 2-[4-(trifluoromethyl)phenyl]oxirane), while avoiding structural degradations [18], which is elaborated in detail in chapter 3.2.1 of this discussion.

Another encountered weak point concerns the chemical stability of the fluorinated styrene oxide derivatives. Epoxides as HHDH substrates, in addition to being poorly soluble in water, are often very hydrolytically unstable. Hydrolysis of epoxide implies relieving the strain by ring-opening and formation of corresponding 1,2-diol (Appendix III, Scheme 2). During investigation of chemical stability on the set of 11 substrates (Appendix III, Table 2), it was found that hydrolysis impact cannot be neglected. Although all the selected substrates are structurally similar, differing only in the number and position of substituents, their hydrolytic stability differs greatly (Appendix III, Supplementary information S-7), with hydrolytic constants (k_h) ranging from 0.0012 to 0.0078 min^{-1}. Clearer depiction of epoxide instabilities is obtained by the comparison of half-life times (Figure 2). Hydrolysis of the substrate is an undesirable characteristic when setting up a new biotransformation, since it leads to the loss of the substrate, and thus to a lower final yield. Also, if the biotransformation starts from a racemic mixture of the epoxide, the useful products of the reaction would be an optically pure product, but also an unreacted enantiomer of the substrate. The presence of the hydrolytic reaction, however, not only reduces the final yield of β-azido alcohol, but also leads to the consumption of valuable, unreacted (*S*)-epoxide, since the chemical hydrolysis is completely nonselective

and consumes both substrate enantiomers. Moreover, hydrolysis leads to the accumulation of byproduct 1,2-diol in the system, which may have an unknown, possibly inhibitory, effect on the enzyme. Finally, hydrolysis effect becomes more prominent as substrate concentrations in the reactor get higher. As reported in Appendix III, hydrolysis is described by pseudo-first-order kinetics, which means that the rate of the hydrolytic reaction is directly proportional to the concentration of the substrate. Although there are reactor designs by which it is possible to maintain low concentrations of the substrate and still achieve high product yield, which will be discussed later, biotransformations with substrates of higher hydrolytic stability are favored in terms of simplicity and profitability. At this point, hydrolytic characterization served only for preliminary screening of the substrates for further research, whereby the most stable substrate 2-[4-(trifluoromethyl)phenyl]oxirane (referred as **1k** from this point on, whereby the designation is retained from Appendix III) was chosen for further kinetic characterization. Some authors have previously also pointed out reduced productivity due to hydrolysis of substrates [69,71,94,118]. For example, Haak et al. [118] performed kinetic resolutions on 10 mM scale and synthesized optically pure chloroalcohols in moderate to high yields; however, authors were not able to isolate remaining epoxides at all due to the rapid in *situ* hydrolysis to corresponding diols. HHDHs can also be used in cascades with other enzymes, such as epoxide hydrolase, to reduce the impact of unwanted chemical transformations in a non-enantioselective fashion [119].

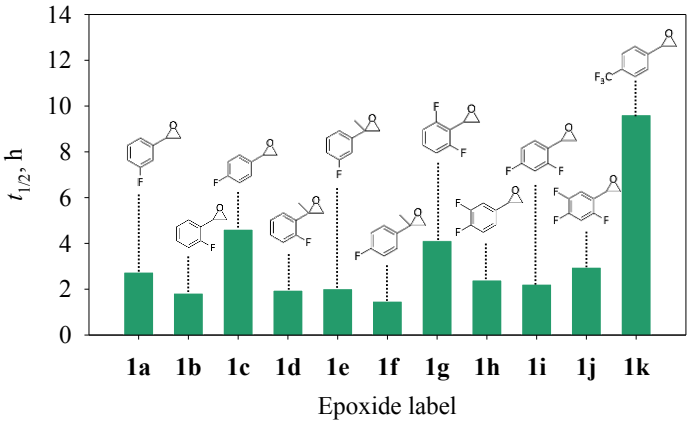

Figure 2. Half-life times for fluorinated derivatives of styrene oxide evaluated as substrates in HheC-catalyzed azidolysis. Internal epoxide labels are consistent with those presented in the Appendix III.

In addition to the significant influence of hydrolysis, preliminary characterization indicated preferences of wild-type HheC towards some types of substrates. Most of the

investigated substrates follow Michaelis-Menten kinetics, while more sterically demanding disubstituted styrene oxide derivatives 2-(2-fluorophenyl)-2-methyloxirane (**1d**) and 2-(2,6-difluorophenyl)oxirane (**1g**) follow first-order kinetics (Appendix III, Table 2). Linear response, to which chemical azidolysis may also contribute in this case, means that the reaction can be accelerated only by increasing the concentration of the substrate, which is very impractical due to the presence of a hydrolytic reaction. Similarly, Dokli et al. [120] observed no activity with the same substrates at 2 mM scale. Regarding the remaining substrates, we have found that *ortho*- and *meta*-substituted derivatives of styrene oxide are accepted by HheC, but that *para*-substituted compounds are the most suitable substrates in terms of both hydrolytic stability and enzymatic activity towards them (Appendix III, Table 2). In parallel, Dokli et al. [120] also found that F-substituent position plays an important role in enantioselectivity of the reaction, whereby biotransformations with *para*-F-substituted substrates result with the highest *E* values. As probable explanation to such enantiopreference, authors offered different charge distributions that affect ligand orientation and activation energy.

During the preliminary screening, W249P variant proved to have better affinity towards **1k** than the wild-type ($K_m^{\text{HheC-WT}}$ = 14.32 mM; K_m^{W249P} = 1.10 mM), which explains its better performance in azidolysis and cyanolysis reactions of fluorinated styrene oxide derivatives obtained previously [40]. Tryptophan (Trp, W) on the position 249 is placed close to the active site of HheC, and was earlier proved to play important role in enzyme activity. Tang et al. [121] found that replacement of Trp with Phenylalanine (Phe, F) changed the K_m values with all tested substrates and assumed that W249 could be part of the halide release path. Since this was found to be rate limiting step, the authors hypothesized that replacement of amino acid on 249 position lead to more rapid bromide release, thus lowering Michaelis constants. Later, Wang et al. constructed W249P variant by changing Trp to proline (Pro, P). Authors found that variant exhibited 4.3 fold improvement in k_{cat} value in comparison to the wild-type [122]. On account of our results and findings from the literature, W249P variant was chosen for further kinetic investigation.

3.1.2 Kinetic features of the investigated biocatalytic system

From the substrate screening, knowledge about the solubility and hydrolysis of the substrates was obtained, together with the preferences of the HheC enzyme in terms of activity and enantioselectivity. In further research, i.e., kinetic characterization of the W249P variant in the enantioselective synthesis of (*R*)-2-azido-1-[4-(trifluoromethyl)phenyl]ethanol (referred as

(*R*)-**2k** in the respective manuscript and following discussion), some other process bottlenecks were addressed as well.

To begin with, it was shown that W249P variant displays higher affinity towards the substrate (*R*)-**1k** by an order of magnitude compared to the wild-type enzyme (Appendix III, Tables 2 and 4). This is consistent with the previous studies by our group where W249P showed superior catalytic properties with a range of fluorinated styrene oxide derivatives [40]. Furthermore, enzyme kinetics was described with double substrate Michaelis-Menten kinetics (V_m = 0.40 U/mg; K_m^{azide} = 2.02 mM; $K_m^{(R)\text{-}\mathbf{1k}}$ = 1.10 mM), whereby enzyme is inhibited by the substrate (*R*)-**1k** ($K_i^{(R)\text{-}\mathbf{1k}}$ = 32.86 mM), opposite enantiomer of the substrate (*S*)-**1k** ($K_i^{(S)\text{-}\mathbf{1k}}$ = 2.26 mM), biocatalytic product (*R*)-**2k** ($K_i^{(R)\text{-}\mathbf{2k}}$ = 6.14 mM), hydrolytic product *rac*-**4k** ($K_i^{rac\text{-}\mathbf{4k}}$ = 6.53 mM), and co-solvent DMSO (K_i^{DMSO} = 373.01 mM) (Appendix III, Fig. 1 and Table 4). In other words, biocatalytic formation of (*R*)-**2k** is a demanding task due to presence of inhibitions by all of the reaction compounds except for azide ions. As stated earlier in the discussion, the reports of the inhibitions of HHDH enzymes are scarce, with only 7 studies reporting inhibition constants (K_i) of any kind. According to our findings, it is highly improbable that inhibitions are not present in other HHDH-catalyzed syntheses in the literature, but it is more likely that they were simply not observed due to the narrow concentration ranges in which previous studies were conducted. In this research (Appendix III, Fig 1.), the concentration of (*R*)-**1k** was varied in the range from 0 to 150 mM, whereby the inhibition by the substrate is only apparent at concentrations above 10 mM. For comparison, when screening enzyme activities towards specific substrates, concentrations between 2 and 5 mM are most commonly used in existing literature [65,123–126]. According to the same logic, inhibitions by products or by-products were never observed in other studies, because the concentrations of the forming compounds were too low to cause a significant drop in enzyme activity. Moreover, when kinetic measurements with initial reaction rates at several different concentrations are not carried out, but only the amount of product formed after a certain amount of time is being observed, it is impossible to conclude whether the lower product yield in some cases is the result of a reduced affinity of the enzyme towards the substrate, or a result of the presence of inhibitions by substrate, product or by-product, or even rapid enzyme deactivation under the tested conditions. Lower enzyme affinity and activity towards the selected substrate cannot be distinguished from the negative effects of inhibitions and deactivations based on single experiment for each enzyme-substrate set. Although the presence of inhibitions discovered in our study cannot be generalized without adaptations to the other HHDH-catalyzed reactions, or

even W249P reactions, our findings should raise awareness of the possible significant influences of inhibitions in these types of biotransformations.

In earlier studies, HHDHs were shown to be inhibited by ethyl 4-chloroacetoacetate (COBE), which is not a compound related to HHDH-catalysis, rather the substrate for ketoreductase in the cascade synthesis of atorvastatin precursor, ethyl (*R*)-4-cyano-3-hydroxybutyrate [5]. Later, the inhibition proved to be of competitive nature [127], whereby COBE binds to the active site of HheC. The inhibition constant was approximated to 0.249 μM, which is extensively lower than K_m value of the substrate (3.5451 mM), indicating severe inhibition. Since the respective cascade represents the most important industrial application of the HHDH enzyme so far, study by Chen et al. was further orientated towards the discovery of enzyme variants with a reduced inhibition effect while retaining good catalytic properties [127]. Schallmey et al. [128] found that HheC variant T134A displayed substrate inhibition in dehalogenation reaction with 1,3-dichloro-2-propanol (K_i^{DCP} = 8.9 mM), 1,3-dibromo-2-propanol (K_i^{DBP} = 1.7 mM), 1-bromo-2,3-propanediol (K_i^{BPP} = 33.3 mM), 1-chloro-2-propanol (K_i^{CCP} = 32.8 mM), 1-chloro-2-methyl-2-propanol (K_i^{CMP} = 4.9 mM) and 2-chloro-1-phenylethanol (K_i^{CPE} = 8.5 mM) [128]. Zou et al. found that ECH, product in the dehalogenation of 1,3-DCP, act as competitive inhibitor (K_i^{ECH} = 9 mM) and thereby reduces the productivity of the reaction [91]. Authors offered the *in situ* product removal as potential solution to product inhibition. Tang et al. showed that in the *para*-nitro-2-bromo-1-phenylethanol (PNSHH) synthesis, enzymes are inhibited by substrate (K_i^{PNSHH} = 1 mM) and products *para*-nitro styrene oxide (PNSO) and bromide ions (K_i^{PNSO} = 0.01 mM; K_i^{HBr} = 1.2 mM) [121,129]. Lutje Spelbeg et al. [87] investigated the same reaction and explored the inhibition of various nucleophiles in the dehalogenation of (*R*)-PNSHH catalyzed by wild-type HheC. Authors found that the enzyme is inhibited by I^- (K_i^{iodide} = 1 mM), Br^- ($K_i^{bromide}$ = 4.3 mM), Cl^- ($K_i^{chloride}$ = 13 mM), F^- ($K_i^{fluoride}$ = 29 mM), N_3^- (K_i^{azide} = 2.7 mM), NO_2^- ($K_i^{nitrite}$ = 20 mM), OCN^- ($K_i^{cyanate}$ = 4.5 mM), SCN^- ($K_i^{thiocyanate}$ = 30 mM), NO_3^- ($K_i^{nitrate}$ = 44 mM), and CH_3COO^- ($K_i^{acetate}$ = 33 mM). Unfortunately, in none of the studies reviewed, kinetic investigations of inhibitions were not performed in the epoxide ring-opening reactions, which are far more valuable synthetic pathways from the industrial point of view, since they lead to formation of new C-C, C-S, C-N, and C-O bonds. Nevertheless, even with deficiency of the kinetic data, certain parallels can be drawn with existing cases from literature, as for example with the HheG-catalyzed synthesis of 4-aryloxazolidinones from styrene oxide derivatives with different substituents in *meta*- and *para*-position [130]. Authors performed the screening of the initial conditions on the

biocatalytic reaction outcome (*Y*, *ee*) with styrene oxide as a representative of the investigated substrates. They found that employing substrate concentrations of 5-30 mM results in stable yields above 75%, but at higher concentrations the yield drops significantly, whereby the resulting yield amounts only about 50% with 50 mM styrene oxide. The authors did not offer a possible explanation for such a drop in reaction yield, but only accepted the fact that synthesis has a good outcome when moderate substrate concentrations are used. Although substrate inhibition was not confirmed by independent concentration-activity kinetic measurements, it is the most possible explanation in given case, based on the presented results from Wan et al. [130]. Substrate inhibition in this case is not surprising, especially taking into account structural similarity of styrene oxide and **1c**, **1e** and **1k** (Appendix III, Table 2), all of which displayed inhibitory properties towards HheC or W249P in investigated concentration range.

3.1.3 Enzyme operational stability limitations

In addition to affecting specific enzyme activity in the reactor, the reaction components could also have a negative impact on the stability of the enzyme, leading to structural degradation of the protein and, consequently, loss of enzymatic activity [116,117]. On that account, information about lower activity with higher substrate loadings, like the above described case in HheG-catalyzed synthesis of 4-aryloxazolidinones from styrene oxide derivatives [130], should be interpreted with caution.

A decrease in operational stability can be distinguished from an inhibitory effect by performing independent measurements [111,116]. In our research (Appendix III), we found that enzyme loses the activity when being incubated with substrate **1k** at higher concentrations, whereas incubation with nucleophile did not have any measurable effect on enzyme stability (Appendix III, Fig. 2). Incubation studies, when enzyme is in resting state, have shown in some cases to be a good indicator regarding enzyme operational stability, when enzyme is employed in catalytic process [116]. By monitoring the enzyme activity in the independent measurements during the biocatalytic syntheses in the batch reactor, stability profiles were constructed and values of operational stability decay (k_d) were estimated (Appendix III, Fig. S-11 and Table S-12). As anticipated from incubation studies, by correlating the estimated k_d values with the initial concentrations of the epoxide in the reactor, a hyperbolic dependence of the operational stability decrease with increasing substrate concentration was found (Appendix III, Fig. 5). That in fact means that substrate concentration plays a decisive role in operational stability of the enzyme. Knowledge about the dependence of the operational stability decay rate constant on

the initial conditions in the reactor represents especially useful information because it enables the selection of the conditions and reactor types where enzyme deactivation can be minimized.

Similar dependencies were also observed with other enzyme types [116,117], but never HHDHs. Rare studies that mention the operational stability of HHDH enzymes refer to immobilized enzymes in the synthesis of ECH from 1,3-DCP. For example, Zou et al. [131] reported high operational stability of the immobilized wild-type HheC in the respective synthesis. They reported maintaining high conversion and yield even after 50 consecutive reaction cycles, stating the enzyme retained impressively high operational stability. In mentioned case enzyme operational stability decay seems to be negligible; however, if only the final productivity of the reaction after a certain reaction time is compared, possible enzyme deactivation also may not be observed. Zhang et al. [98] also studied ECH synthesis from 1,3-DCP with immobilized HheC variant P175S/W249P. The authors reported almost no decrease in the yield at the last cycle compared to the first one, stating excellent operational stability. However, they also measured the remaining enzyme activity after 45 consecutive batches, which amounted around 80% of the initial value. That means that, even though reaction productivity remained practically the same, operational stability decrease occurred anyway, but was not reflected on the reaction yield in the observed reaction time.

3.1.4 Considerations based on developed mathematical model

Mathematical model for the synthesis of optically pure fluorinated building blocks (Appendix III, Table 1) represents the first of its kind for any of the HHDH-catalyzed biotransformations. The utility of the kinetic mathematical models was already proven for other types of enzymes and reactions in terms of discovering and understanding process bottlenecks, together with optimization of process conditions for enhanced reaction outcomes [116,132–134]. Thus, developed mathematical model and model-based process simulations offer valuable insight into HHDH-catalyzed process limitations and possible solutions for some of them. It was found that the hydrolysis of the substrate has a substantial influence on the final outcome of the reaction. Since the enzyme is completely enantioselective in investigated kinetic resolution, the theoretical maximum conversion of the substrate is 50%, whereby two valuable building blocks are obtained – optically pure azido alcohol, (*R*)-**2k**, and the unreacted enantiomer of the substrate, (*S*)-**1k**. However, if the compounds are not separated from the reaction mixture after the complete conversion of (*R*)-**1k**, the consumption of (*S*)-**1k** in the hydrolytic reaction will be continued, leading to the decrease in the final productivity of the

kinetic resolution. With process simulations based on the mathematical model, it is possible to predict the optimal moment to terminate the reaction by extracting the obtained products, without the need for expensive on-line monitoring (Appendix III, Fig. 6C). Apart from hydrolysis, two more unrelated negative effects occur at elevated **1k** concentrations in the batch reactor, namely enzyme inhibition by both (*R*)-**1k** and (*S*)-**1k**, together with concentration-dependent enzyme deactivation. Naturally, by lowering the *rac*-**1k** concentration in the batch reactor, higher yields could be obtained (Appendix III, Fig. 6A), but overall product concentrations would not meet the process demands from the economical aspect [15,135,136]. Instead of lowering the overall substrate concentration, these drawbacks could be successfully overcome by conducting reactions in a repetitive batch and fed-batch reactors (Appendix III, Fig. 4 and 7). With substrate inflow or repetitive addition, (*R*)-**1k** concentration is kept inside the concentration range where enzyme displays maximal activity. In the optimized reaction (Appendix III, Fig. 8), by distributing 160 mM of *rac*-**1k** into 8 portions instead of just one, a reaction yield of 95% could be obtained, together with the increase in reaction selectivity from 0.7 to 1.4. It is worth emphasizing that the achieved concentration scale is comparable or higher than the one commonly encountered in HHDH biocatalysis, especially in cases when poorly soluble aromatic compounds are investigated (Appendix II, Table 2).

Although repetitive and fed-batch reactors represent an improvement in comparison with the batch reactor, their use does not solve all the stated problems. After certain amount of time, accumulation of (*S*)-**1k** starts to represent a problem since it inhibits the biocatalytic reaction and leads to higher rates of hydrolytic reaction and, consequently, formation and accumulation of inhibiting diol. Even though the optimized system met some of the criteria for the successful scale-up on a level of industrial biotransformations in the fine chemicals production and pharmaceutical industry, there is still room for improvement. The optimized biocatalytic system for the synthesis of fluorinated building blocks offered a high reaction yield and optical purity (Y = 95%, *ee* > 99 %), both of which are fulfilling the requirements for the industrial implementation; however, product concentration of 20 g/L is below the required threshold of 50 g/L [135]. Enzyme concentration could be increased to meet the process targets, but biocatalyst loading makes for a big part of the overall process cost and should be considered as well [15,135,136]. Since hydrolysis and inhibitions are mostly responsible for the reduced productivity of the biocatalytic reaction, one of the approaches towards the minimization of their impact is by conducting biocatalytic reactions in alternative media, as discussed below in section 3.2.

3.2 The effects of organic solvents on HHDH-biocatalysis

During the investigation of biocatalytic synthesis of optically pure fluorinated building blocks from enzyme reaction engineering perspective, several system limitations were detected and explained. First of all, fluorinated styrene oxide derivatives proved to be only sparingly soluble in aqueous media, which is often the case with HHDH substrates (Table 1). Epichlorohydrin as natural substrate of HHDHs is very soluble in water (Table 1), so it is no wonder that most scaled-up biotransformations at higher substrate loadings have been demonstrated on reactions of the reversible reactions of ECH ring-opening and 1,3-DCP dehalogenation [56,91,94,98]. However, more complex substrates, especially aromatic epoxides such as substituted styrene oxide derivatives [69,113], or cyclic epoxides such as limonene oxide or cyclohexene oxide [66], are difficult to dissolve in water [137–139] (Table 1).

Table 1. Examples of HHDH substrates and their solubility in water at 25 °C

Compound	Structure	Examples of studies employing compound of interest as HHDH substrate	Solubility in water at 25 °C		
			mM	g/L	Reference
epichlorohydrin	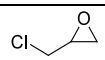	Zhang et al. 2019 [140]	712	65.9	[137]
2-(phenoxymethyl)oxirane	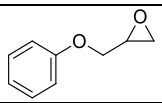	Xue et al. 2020 [141]	16	2.4	[142]
p-nitrostyrene oxide	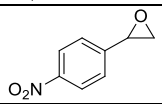	Lutje Spelberg et al. 2001 [69]	< 2	< 0.33	[139]
p-fluorostyrene oxide	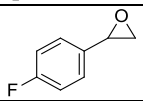	Dokli et al. 2021 [40]	1.88	0.26	[143]
limonene oxide	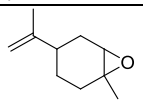	Koopermeiners et al. 2017 [66]	0.65	0.1	[137]
cyclohexene oxide			insoluble		[138]

Other unfavorable properties of the investigated biocatalytic system include significant contribution of unwanted hydrolytic reaction (Appendix III, Table 2) in the microenvironment that proved to be ideal for HHDH-catalysis in terms of activity and stability, together with the presence of numerous inhibitions and concentration-dependent enzyme deactivation. These limitations were detected in Appendix III and discussed more in depth in chapter 3.1. Since not all the requirements for profitable synthetic procedure for industrial biotransformations could

be met by optimizing the process conditions based on the kinetic mathematical model (Appendix III, Chapter 3.8), further research was focused on switching from aqueous to an alternative medium. Since the aqueous medium is responsible for the low solubility and hydrolysis, reducing the ratio of water or its complete replacement could help to reduce these problems [50,93]. Moreover, inhibitions are more pronounced at the higher concentrations of the inhibitor in the solution, therefore biphasic water-solvent systems could serve to separate enzymes from inhibitors, lowering the inhibition influence. In this case, aqueous medium serves as a shield for enzyme, protecting it from inhibitions and deactivations, while organic phase serves as substrate pool and product extraction phase [144,145]. However, the introduction of alternative media into biocatalytic system can cause unknown, often negative effects on the enzyme structure and its catalytic properties, as explained in Chapter 2.2.2. of this dissertation. Hence, the second phase of the research was orientated to the investigation of the relationship between HheC and commonly used OSs with the aim of finding appropriate medium for synthetic purposes. A detailed study of the influence of DMSO, the most commonly used co-solvent in HHDH-biocatalysis, as well as a wide range of other common OSs, is given in papers Appendix IV and Appendix V and discussed in detail in chapters 3.2.1 and 3.2.2, respectively.

3.2.1 DMSO as a co-solvent for HheC-catalyzed biotransformations

The most commonly used OS in HHDH-catalyzed biotransformations is DMSO, usually added in volume ratios up to 5% to increase the solubility of hydrophobic synthetic molecules. The utilization of DMSO as a co-solvent in HHDH biocatalysis seems to be established practice that extends through a large number of studies with unnatural substrates [65,71,90,91,82–89], as already presented in Chapter 2.2.2.1. Despite its extensive use in HHDH biocatalysis, the influence of DMSO on catalytic performance of this enzyme group has never been investigated. However, since DMSO is widely used as cells cryoprotectant, pharmaceuticals transporter and solvent in high-throughput screening biochemical assays [146–148], its effect on the functional and structural properties of other proteins has been explored. These studies are mostly performed on model proteins, especially hen lysozyme [146,148–154]. From the previous studies, it is well known that DMSO can disrupt protein structure as well as exhibit inhibitory properties [155–157]; on the other hand, DMSO-induced activity increase and protein stabilization were also reported in some cases [158]. Since co-solvents in general can affect catalytic and structural properties of enzymes even when present in small amounts, like 2-5% which is added to the most HHDH-catalyzed biotransformations, a thorough analysis of the DMSO-HheC interactions was performed. Detailed report of the procedure and the obtained

results is given in Appendix IV and will not be repeated here, but the main outcomes from the study and their contribution in relation to findings from existing literature are discussed below.

To begin with, the dehalogenation ability of the HheC enzyme in the PNSHH ring-closure activity assay (Appendix IV, Scheme S1) was tested in the presence of different ratios of DMSO (Appendix IV, Fig. 5). It was found that the activity profile changes abruptly with an increase in the co-solvent ratio. The severity of DMSO impact can be demonstrated by the fact that already at 10% (*v*/*v*) the specific enzyme activity is reduced to 50% of the initial value. A decrease in activity measured by the initial reaction rates method usually indicates an inhibitory effect of the compound which concentration is being varied, but due to the multiple possible influences of co-solvents on the structural and catalytic properties of the enzyme, the underlying mechanism of the loss of activity was investigated through several complementary experimental and computational techniques (Appendix IV).

3.2.1.1 Stability of HheC in presence of DMSO

Measurements of the kinetic stability of the enzyme during incubation with different co-solvent concentrations (Appendix IV, Fig. S7) revealed that HheC is highly stable when exposed to DMSO in amounts up to 30% (*v*/*v*). At 40% DMSO enzyme starts losing its activity over the time (with a half-life of 41 h, compared to 520 h for pure aqueous media), with DMSO being fully detrimental to the enzyme stability at a concentration of 50% ($t_{1/2}$ = 40 min) (Appendix IV, Table 2, Fig. S7). Protein size distributions, obtained under similar conditions (Appendix IV, Figs. 4, S9 and S10), displayed no change in distribution over 7 days in buffer medium and 48 h in 30% (*v*/*v*) DMSO. In 40% DMSO, complete shift in size occurred after 5 h, while in 50% DMSO almost instant structural changes were detected. In other words, clear correlation between the HheC stability during incubation (Appendix IV, Table 2) and the extent of aggregation (Appendix IV, Fig. 4) was established. Until now, such tolerance of the rather high DMSO ratios has not been reported for any wild-type HHDH. When comparing the structural stability of HheC in the presence of co-solvent with the tolerance of other proteins towards DMSO, the superior stability and robustness of HheC is evident. In many cases, structural degradation occurs at substantially lower DMSO amounts [148,154]. For example, Tjernberg et al. [148] examined the influence of DMSO on aggregation of BPase and found that, without DMSO, 80% of protein is in monomeric state, while already at 0.5% (*v*/*v*) DMSO, protein monomer peak is not detectable and share of large-size aggregates is increased. Nemzer et al. [159] demonstrated with dynamic light scattering technique that hen lysozyme

aggregation greatly depends on ethanol concentration, whereby aggregation occurred at ethanol volume ratios above 15% in acidic conditions.

High structural tolerance of HheC towards DMSO action is also manifested in thermodynamic stability (Appendix IV, Fig. 3 and Table 3). By increasing DMSO content from 0 to 20% (*v*/*v*), T_m values lower just from 60.0 to 54.1 °C, while unfolding process enthalpy remains unchanged to 30% (*v*/*v*) of DMSO. Relatively high ΔH values (up to 30% DMSO) may occur due to enzyme conformational alterations and/or changes in protein solvation [151]. Despite the high tolerance towards DMSO in thermally induced denaturation, progressive thermal destabilization with DMSO concentration increase is manifested through the linear decrease in $\Delta T_{1/2}$ values. At 40 and 50% (*v*/*v*) DMSO, all the unfolding characteristics (T_m, ΔH, $\Delta T_{1/2}$) decline abruptly (Appendix IV, Fig. 3 and Table 3). This is a unique proof of the correlation between kinetic and thermal stability in the investigated HheC-DMSO system. In comparison with other proteins, HheC also displays high stability when exposed to the joint effect of co-solvent and elevated temperatures. For example, Tjernberg et al. showed that thermodynamic stability of phosphatase domain of PFKFB1 (BPase) protein depends on the co-solvent amount, while it unfolded and aggregated at room temperature at DMSO content as low as 1% (v/v) [148]. Kamiyama et al. assessed the thermal stability of hen lysozyme in binary water-DMSO solutions and found that co-solvent presence reduces protein thermostability [160]. Its T_m shifted to lower values with an increase in DMSO amount, while around 70% (*v*/*v*) DMSO denaturation occurred already at room temperature.

3.2.1.2 Inhibitory effect of DMSO

The presented results revealed that HheC is kinetically and thermodynamically quite stable if the content of DMSO does not exceed 30% (*v*/*v*). These experimental findings, supported by computational analysis (Appendix IV, Figs. 2A, S2, S3), implied that observed specific activity decline (Appendix IV, Figure 5), could be attributed solely to the inhibitory effect of DMSO up to 30% volume content. Further decline of the reaction rate at higher shares is the joint result of co-acting inhibition and protein structural degradation. Inhibitory effect was subsequently confirmed by kinetic analyses (Appendix IV, Figs. S14 and 8) and molecular dynamics studies (Appendix IV, Table 4, Figs. 6 and 7). By Lineweaver-Burk analysis, DMSO proved to be a mixed-type inhibitor, whereby lower value of the competitive inhibition constant (Appendix IV, Table 5) indicates that its share in the activity reduction is predominant (K_{i1}^{c} = 3.9 mM, K_{i1}^{u} = 998.9 mM). Although not the rule, competitive inhibitors more often bind to the

active site of the enzyme, which agrees with molecular dynamic simulations that demonstrated DMSO tendency to accumulate close to Ser-Tyr catalytic residues (Appendix IV, Figs. 6 and 7). DMSO binds to the active site of the enzyme and interferes with the course of the PNSHH dehalogenation reaction. Further studies confirmed that DMSO acts as potent mixed-type inhibitor (K_{i2}^{c} = 10.4 mM, K_{i2}^{u} = 104.5 mM) in reversible reaction of PNSO ring-opening as well (Appendix IV, Fig S16 and Table 5).

The inhibitory effect of DMSO towards different enzymes has also been observed in other studies. Based on NMR studies, Bhattacharjya et al. suggested that overall lysozyme structure is conserved in DMSO ratios up to 8-10%, wherein DMSO binds to the protein, inclusive of the active site [150]. Kumar et al. found that DMSO is a powerful mixed-type inhibitor of human acetylcholinesterase (AChE) with $K_i^{\text{DMSO-AChE}}$ = 88.70 mM, inhibiting 98% enzyme activity at only 16.6% (*v*/*v*). Furthermore, DMSO proved to be irreversible inhibitor, permanently inactivating AChE [155]. In another research, Misuri et al. found that DMSO acts as differential inhibitor in reactions catalyzed by human aldose reductase (AR), i.e., DMSO exhibits competitive nature in AR-catalyzed L-idose reduction, as well as mixed-type inhibition behavior towards the same enzyme in reduction of trans-4-hydroxy-2,3-nonenal [156]. Kwak et al. found that DMSO acts as competitive and non-competitive reversible inhibitor with mouse methionine sulfoxide reductase MsrA and MsrB2, respectively [157]. On the contrary, DMSO has an activating effect on glyceraldehyde-3-phosphate dehydrogenase from *Trypanosoma cruzi*, which is manifested in 10 fold K_m decrease and 2.5 times k_{cat} increase at 7.5% (*v*/*v*) DMSO [161].

From the comparison of the presented inhibitory effect of DMSO on HheC-catalyzed reactions (Appendix III and Appendix IV) and various scenarios extracted from the literature (e.g. lysozyme, AChE, AR, MsrA, MsrB2 [150,155–157]), it can be concluded that the inhibitory effect of DMSO towards different types of enzymes cannot be generalized; moreover, same enzyme can be inhibited by DMSO to a different extent in two reactions. When considering that DMSO is always the first choice for a co-solvent in screening of HHDH activity towards synthetic, hydrophobic substrates, the question of the severity of its inhibitory effect arises. It was shown that in the dehalogenation of PNSHH and ring-opening of PNSO with bromide ions, only a few volume percentages of DMSO can cause a drastic drop in the specific activity. Moreover, the inhibition by DMSO does not seem to be equally potent in all studied reactions (Appendix IV, Fig. S16; Appendix III, Fig. 1f), which means that it is sometimes possible to misinterpret the strong inhibition by DMSO for a weak activity towards

the hypothetical substrate. If we move up on the scale from substrate screening to HHDH-catalyzed biotransformations on preparative scale, the impact of inhibition by DMSO on the overall outcome can be even more problematic. When enzyme activity is suppressed by the action of inhibitor in high concentrations, the conversion of the substrate in biocatalytic reaction will take significantly longer. In that case, hydrolysis and other unwanted spontaneous or biocatalytic reactions will have more time in a competition for conversion of valuable compounds into by-products. Moreover, prolonged operating time can also lead to enzyme deactivation. Hence, if DMSO is to be utilized in biotransformation on a larger scale, detailed kinetic studies on its effect on respective enzyme-substrate system should be examined.

3.2.2 Search for compatible solvents for HheC-catalyzed biotransformations

In chapter 3.2.1 and Appendix IV, detailed study of the influence of DMSO on HheC activity was presented, whereby mixed-type inhibition with prevalent competitive contribution proved to be the main cause of the decrease in enzyme activity. Inhibition behavior is related not only to the enzyme, but also to the nature of OS, as diverse solvent molecules may have different binding affinities to the active site of the enzyme, or even demonstrate other inhibition modes. DMSO proved to display inhibitory effect in all tested HHDH-catalyzed reactions (Appendix IV, Fig. S16.; Appendix III, Fig. 1f) even when present in small amounts, thus proving that it is not completely harmless in the volume ratios of 2-5% (*v*/*v*) that are usually used for screening of enzyme activities or small-scale biocatalytic synthesis. In addition, biocatalysis with OSs is often carried out with mixtures of buffers and OSs present in much higher amounts, or even in neat OSs only saturated with water. However, above 30% (*v*/*v*) DMSO, irreversible structural changes and loss of catalytic features occur. The results presented in 3.2.1 aroused the need to screen other candidates in the search of other HheC-compatible solvents. Therefore, in the next phase of the research, the screening of fundamental catalytic properties of HheC was performed in the presence of 15 common OSs, namely: dimethyl sulfoxide (DMSO), dimethylformamide (DMF), methanol (MeOH), acetone, acetonitrile (MeCN), isopropyl alcohol (*i*-PrOH), tetrahydrofuran (THF), ethyl acetate (EtOAc), methyl *tert*-butyl ether (MTBE), diisopropyl ether (DIPE), chloroform, toluene, cyclohexane, *n*-hexane and *n*-heptane (Table 2). The set of solvents was chosen to cover the entire range of LogP values, as well as solvent types according to the classification by functional groups – alcohols, ethers, alkanes etc. Enzyme properties in water-solvent systems are known to be dependent on hydrophilicity/hydrophobicity of the alternative solvent, and are usually conserved to a higher extent in presence of hydrophobic OSs. Hydrophilic solvents have a stronger tendency of

altering the microenvironment suitable for the enzyme, whereby they eliminate the catalytically necessary water and enter the native structure of the protein more easily [16,17]. Functional groups of used OSs can also play an essential role in affecting enzyme properties [16]. In order to select a suitable solvent, screening should be focused on the type of the reaction, the stability of the biocatalyst, the solubility of the compounds of interest and the possibility of enzyme recovery, together with the environmental and economical aspect [75].

Table 2. Properties and classifications of organic solvents tested in HHDH-biocatalysis [162]

Solvent	LogP value	Miscibility with water	Classification by the functional group	Structure
DMSO	-1.35	Miscible	Sulfoxide	
DMF	-1.01		Amide	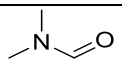
MeOH	-0.77		Alcohol	
Acetone	-0.34		Ketone	
MeCN	-0.24		Nitrile	
i-PrOH	0.05		Alcohol	
THF	0.46		Ether (cyclic)	
EtOAc	0.73	Partially miscible	Ester	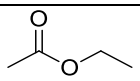
MTBE	0.94		Ether	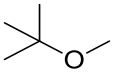
DIPE	1.52		Ether	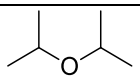
chloroform	1.97		Kaloalkane	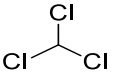
toluene	2.73		Arene	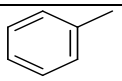
cyclohexane	3.44	Immiscible	Alkane (cyclic)	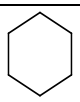
n-hexane	3.9		Alkane	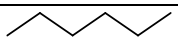
n-heptane	4.66		Alkane	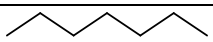

3.2.2.1 Hydrophilic vs. hydrophobic solvents for HheC-catalysis

The investigation of the specific enzyme activity in PNSHH ring-closure reaction in dependence of the volume ratio of solvents (Appendix V, Fig. S2) demonstrated low HheC

activity in presence of co-solvents, i.e. monophasic systems (DMSO, DMF, MeOH, *i*-PrOH, acetone, MeCN, THF). Instant degradation of enzyme structure was ruled out by monitoring the protein size distribution in the presence of 1% THF, the volume ratio at which HheC loses about 70% of its activity. These findings, together with insights obtained from study of DMSO influence, point to the existence of inhibitions by co-solvents, which seem to be the predominant cause of the decrease in the activity. In the presence of MeCN and DMF (Appendix V, Fig. 2), non-uniform activity profiles were obtained, where the initial plateau is followed by steeper activity drop. Such a trend indicates the probable existence of more than one mechanism of enzyme activity reduction, whereby the enzyme becomes less resistant to the action of solvents at 20 and 30% (*v*/*v*). The plateau is very likely attributed to the presence of inhibitions as well, but further decrease could be a consequence of dehydration and rapid structural changes. Apart from the enzyme activity, the stability during incubation with selected co-solvents was monitored. The enzyme half-life in 30% *i*-PrOH was below 12 h, and in 20% DMF only 1 hour (Appendix V, Table 1), while in pure Tris-SO_4 buffer it amounts to 520 h. Poor stability during incubation with DMF supports the hypothesis of the already destabilized structure in the activity test at higher proportions. The slow progress in the azidolysis of 2-(benzyl)oxirane (BNO) in the presence of 30% *i*-PrOH and MeOH (Appendix V, Fig. 4), as well as the decline in the enantioselectivity of the reaction (Appendix V, Table S3; $E_{\text{buffer}} = 6$, $E_{i\text{-PrOH}} = 4$, $E_{\text{MeOH}} = 3$) served as the final confirmation of the unsuitability of hydrophilic solvents for HheC-catalysis. Although it could not be assumed without an initial screening, the unsatisfactory enzyme performance in hydrophilic co-solvents is not surprising. Hydrophilic solvents are usually more potent in altering the patent of hydrogen bonds on the protein surface and penetrating into the native enzyme structure, leading to dehydration, irreversible structural changes and, consequently, partial or complete deactivation [16,17,76]. Apart from this being a common case for a vast amount of other enzymes, the inadequate catalytic and structural properties of HHDH enzymes among hydrophilic solvents has also been observed by Jin et al. [94], who found that product yield and optical purity were reduced in the presence of acetone and isobutyl alcohol, compared to reactions in buffer medium.

On the other hand, HheC enzyme displayed a considerably better performance with hydrophobic OSs in all tested aspects. The stability experiments revealed that HheC remains highly stable when incubated in biphasic media containing *n*-heptane, cyclohexane, toluene, chloroform and DIPE in a ratios of 30%, whereby the remaining relative activity after 24 h amounts to 80% or more (Appendix V, Table 1 and Figure 3). Moreover, HheC stability is not

dependent of *n*-heptane content in investigated volume ratios, retaining same deactivation constant in presence of 30, 50 and 80% solvent as in buffer medium. High structural stability of HHDH in presence of hydrophobic solvents is also supported by results from literature. Liao et al. showed that HHDH retained 90, 80, and 72% of the initial activity after incubation with 50% (*v*/*v*) *n*-heptane, n-hexane, and cyclohexane, respectively [163]. Zou et al. [95] also found that *E. coli* cells retained high specific activity after incubation with *n*-heptane, toluene, and cyclohexane. It is known that alkane-protein interactions are merely hydrophobic; therefore, alkanes can conserve the native protein structure and sometimes even prolong enzyme stability [16].

Stability during incubation may or may not be related to catalytic performance; therefore, activity in specific reactions needs to be assessed as well. Since HHDH enzymes have the ability of catalyzing both dehalogenation of β-substituted alcohols and epoxide ring-opening reactions with nucleophiles, the activity of HheC enzyme with hydrophobic solvents was tested in both directions, i.e., ring-closure of PNSHH and ring-opening of PNSO with bromide ions. The parameter c_{50} was defined as the volume concentration of OS which reduces enzyme activity by half in each assay (Appendix V, Fig. 1a). The parameter incorporates the total impact of the OS on the enzyme during individual activity assay, including inhibition by solvent, rapid deactivation, and mass transfer limitations. In the PNSHH ring-closure reaction, a direct correlation between c_{50} and logP values was discovered. This in practice means that the more hydrophobic solvent is, the higher HheC activity will be in PNSHH dehalogenation. However, in the PNSO test, the activities generally turned out to be somewhat lower, whereby c_{50} values of approximately 50% were obtained for the most suitable solvents (cyclohexane, *n*-hexane, *n*-heptane), compared to the PNSHH-closure reaction where they were above 70%. Lower apparent activities in PNSO ring-opening reaction could also be due to mass-transfer limitations, as in this type of reactions two substrates need to establish a contact with enzyme instead of one. The major difference between the two reaction directions is manifested in the catalytic performance in presence of toluene and chloroform (Appendix V, Fig. 2a and b), whereby c_{50} values are 4 and 12 fold lower in ring-opening reaction, respectively. These findings are consistent with the results of BNO azidolysis, which proceeded faster in biphasic systems containing *n*-heptane, DIPE, cyclohexane and MTBE, while far slower and not at all with toluene and chloroform, respectively (Appendix V, Fig. 4). Since the enzyme is very stable with both solvents, in which the opening reaction does not proceed, and proceeds with difficulties, the results indicate the existence of inhibitions. Toluene might be engaged in π–π

interactions with aromatic amino acids in the active site, thus hindering the substrate entry and inhibiting its productive binding. Our results can also correlate to the ones from the literature, even when obtained with different forms of biocatalysts. Jin et al. tested several OSs in the (*R*)-ECH synthesis with immobilized *E. coli* cells co-expressing HHDH and epoxide hydrolase. Authors have found that introduction of *n*-hexane, cyclohexane and *n*-heptane has positive or neutral effect on the process outcome. Toluene, although hydrophobic, also decreased product yield and optical purity, but to a lesser extent [94]. Inhibitions are plausible explanation in the case of chloroform as well. As HHDHs are, in their primary natural function, involved in the metabolism of halogenated molecules, which occur on millimolar scale during catalysis, it is likely that polychlorinated molecules of chloroform, present in molar scale, will present strong inhibitory action towards HheC. A parallel can be drawn with our results and those presented for dichloromethane (DCM) in the literature. Liao et al. reported that DCM, although having a similar logP value to *n*-hexane, reduced the HheC-CLEA activity to a much greater extent [163]. Similarly, Zou et al. [95] observed that whole cells showed no activity with 50% DCM, while under the same conditions they remained fully active with *n*-hexane. As DCM was not part of our study, disruption of structure and stability cannot be ruled out; however, we could presume that inhibition is one of the mechanisms by which DCM reduces enzyme activity.

Taking into account the activity, stability and enantioselectivity in the investigated reactions, hydrophobic solvents, and especially alkanes, proved to be the best media for the implementation of HHDH-catalyzed reactions in biphasic systems, with *n*-heptane as the most preferred option. Although widely used, *n*-heptane as solvent is problematic from an environmental perspective based on its eco-toxicity and origin from petroleum-based sources, i.e. crude oil. The "green" solvent alternatives include ethanol ($logP_{EtOH}$ = -0.18), which can be obtained by fermentation, Cyrene obtained by pyrolysis and hydrolysis of cellulose ($logP_{Cyrene}$ = -1.52), 2-methyl tetrahydrofuran (2-MeTHF) and cyclopentyl-methyl ether (CPME) obtained by dehydration of sugars ($logP_{2\text{-}MeTHF}$ = 1.1; $logP_{CPME}$ = 1.6). However, all of these solvents have relatively low log P values. Since we have shown that reactions with HHDH proceed very poorly in more polar OSs, it is to be expected that most of these alternatives will not be suitable. This assumption was confirmed by the PNSO ring-opening activity assays (Fig. 3), where less than 10% relative activity was obtained at 50% volume ratio of 2-MeTHF, CPME and Cyrene (Table 3). Hydrophobic "green" solvents are also still rare, and with the current offer it is still often impossible to find alternatives to the traditional solvents derived from petroleum sources. The activity assay with 50% (*v*/*v*) 1-octanol, hydrophobic aliphatic alcohol ($logP_{1\text{-}otcanol}$ = 3.5)

that can be obtained from sugars, displayed none of the activity retained, indicating that hydrophobicity/hydrophilicity is not the only factor affecting enzyme activity. It is evident that solvent functional groups play a role as well, since HheC enzyme performed very poorly in the presence of all tested alcohols (methanol, isopropanol, 1-octanol).

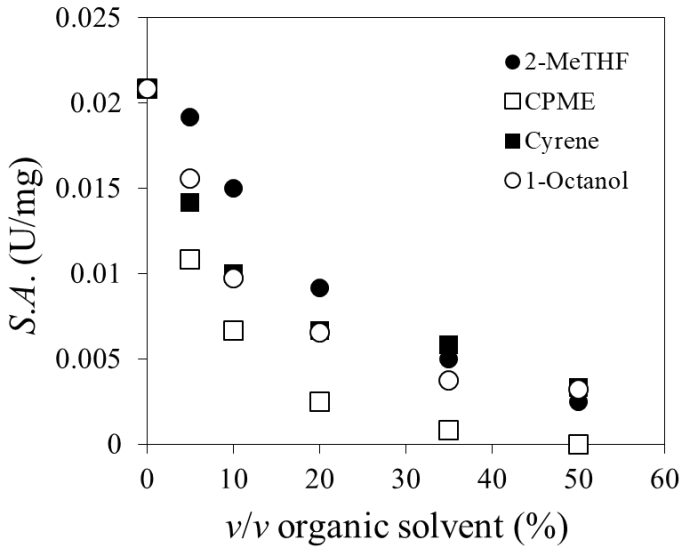

Fig. 3. Activity profiles in PNSO ring-opening reaction with "green" OSs obtained by independent activity assays using methodology and conditions described in Appendix V.

Table 3. Comparison of half maximum effective concentration (c_{50}) and partition coefficient between octanol and water (log P) for different "green" OSs.

Solvent	**log P**	**c_{50}, %**
Cyrene	-1.52	9.8
2-MeTHF	1.1	18.0
CPME	1.6	5.1
1-Octanol	3.5	9.7

3.2.2.2 Enhanced solvent resistance of thermostable variant

In Appendix V, in addition to a detailed study of the effect of solvents on the performance of the wild-type HheC, the enhanced solvent resistance of the variant ISM-4 was also reported. This enzyme was earlier constructed by Wu et al. [164] when authors conducted the evolution of HheC by the combinatorial directed evolution strategy in search for more thermostable variants. ISM-4 was obtained by error-prone polymerase chain reaction (PCR)

with low frequency of mutation and subsequent 4 rounds of iterative saturation mutagenesis. The variant demonstrated 3400-fold higher half-life time at 65 °C compared to the wild-type, 18 °C increase in apparent T_m value, and 20 °C increase in optimal temperature [164]. Our studies revealed that mutations present in ISM-4 were valuable not only for the thermal resistance, but also for the catalytic properties and stability in the presence of OSs (Appendix V, Table 2, Fig. S8). The link between thermostability and resistance to OSs is not a general rule, but a correlation between thermostability and resilience towards various harsh conditions often exists for enzymes from various groups [93,165]. Arabnejad et al. [84] also reported that thermostable HheC-H12, obtained by computational library design "FRESCO", displayed outstanding resistance in monophasic co-solvent systems. Variant retained high activities with 50% DMSO, MeOH, MeCN, and DMF, while THF was detrimental to its activity in ratios above 25% (*v*/*v*).

The improved stability of ISM-4 variant is best observed with the solvents that had the detrimental effect on HheC (*i*-PrOH, MTBE), as well as with the combinatorial effect of elevated temperature and most of the tested solvents (Appendix V, Table 2, Fig. S9). Moreover, mutations also lead to the increase of enantioselectivity, which was manifested through higher *E* values in BNO azidolysis both in buffer medium and tested solvents (Appendix V, Table 3). Since the variant showed superior longevity in both polar organic co-solvents and biphasic systems, future research should be orientated towards exploration of synthetic ISM-4 catalyzed reactions with "green" solvents, in terms of reduction of hydrolysis and possible inhibitions by reaction compounds.

4. Conclusion

Biocatalysis is an emerging field in modern organic synthesis for production of pharmaceuticals and fine chemicals. It is experiencing groundbreaking progress in large-scale implementations on account of various contributions from interdisciplinary approach. HHDHs, although already applied in industry due to their high regio- and enantioselectivity in the synthesis of valuable building blocks, have not yet been investigated by the enzymatic reaction engineering approach. In the case study analysis (Appendix II), the lack of knowledge about the kinetic behavior of the HHDH enzyme family was demonstrated, as well as the consequent lower yields, conversions, and optical purities, that is, poorer overall biocatalysis outcome in certain cases. Therefore, in depth characterization by employing reaction engineering methodology was carried out in the HheC-catalyzed synthesis of small, fluorinated, chiral building blocks (Appendix III). The study revealed that fluorinated derivatives of styrene oxide are hydrolytically unstable under optimal microenvironment for the enzyme; moreover, they are only sparingly soluble in aqueous medium, which makes their bioavailability to enzyme rather poor. Hydrolysis reactions are described by pseudo-first order kinetics, which indicates more rapid substrate degradation at its higher concentrations. From the tested substrate set, *para*-substituted derivatives proved to be the best choice for biotransformation based on the activity and enantioselectivity in HheC-catalyzed reactions, coupled with their hydrolytic stability. The synthesis of (*R*)-2-azido-1-[4-(trifluoromethyl)phenyl]ethanol (**2k**) in azidolysis of 2-[4-(trifluoromethyl)phenyl]oxirane (**1k**) with HheC-W249P variant was selected for further kinetic characterization. The reaction was described by double substrate Michaelis-Menten kinetics, whereby enzyme is inhibited by reacting enantiomer of the substrate (*R*)-2-[4-(trifluoromethyl)phenyl]oxirane ((*R*)-**1k**), opposite enantiomer (*S*)-2-[4-(trifluoromethyl)phenyl]oxirane ((*S*)-**1k**), biocatalytic product (*R*)-2-azido-1-[4-(trifluoromethyl)phenyl]ethanol ((*R*)-**2k**), hydrolytic product *rac*-2-[4-(trifluoromethyl)phenyl]-1,2-ethanediol (*rac*-**4k**), and co-solvent DMSO. The inhibitions with the greatest negative impact are those by epoxides, both the substrate (*R*)-**1k**, and the opposite, non-reacting enantiomer, (*S*)-**1k**. Besides significant hydrolysis and numerous inhibitions, enzyme deactivation was found to be substantial when reactions were performed at increased substrate concentrations; moreover, operational stability was found to be directly correlated to the initial concentration of 2-[4-(trifluoromethyl)phenyl]oxirane in the reactor. The developed mathematical model provided valuable insight into the kinetic behavior of the enzyme in this

type of reactions and, as such, provided guidance for addressing the stated limitations and reducing their effect. The synthesis of optically pure (*R*)-**2k** on a higher concentration scale, which is a prerequisite for industrial implementation, is difficult to perform due to the presence of plentiful inhibitions and concentration-dependent enzyme deactivation, which give advance to hydrolysis in the competition for substrate conversion. By performing process simulations, a considerable enhancement of reaction outcome was achieved by gradually feeding/repetitively adding *rac*-**1k** in portions into the reactor, which kept the concentration of the substrate in area where maximal enzyme activity is obtained, and hydrolysis and enzyme deactivation are minimized. The optimized biocatalytic system in repetitive batch reactor lead to high reaction yield and optical purity (Y = 95%, ee > 99 %). Nevertheless, productivity of the reaction should be enhanced to meet the requirements for the industrial implementation, as obtained product concentration of 20 g/L is less than threshold of 50 g/L. Since switching the biocatalysis from aqueous to alternative media may be beneficial in reducing hydrolysis and inhibitions impacts, the second part of the dissertation was directed towards exploring HheC performance with OSs. The tolerance of the HheC enzyme to action of DMSO, the most commonly used co-solvent in HHDH-biocatalysis, was evaluated first (Appendix IV). It was found that DMSO does not pose a problem for HheC structural integrity when present in amounts up to 30% (*v*/*v*). In higher DMSO amounts, HheC losses its native structure, being fully inactivated and aggregated almost instantly in 50% co-solvent. Such high tolerance to the action of elevated amounts of DMSO has not been reported for any natural HHDH to date; moreover, it is very high compared to wild-type enzymes from other families as well. Despite the ability to preserve structural integrity in rather high amounts of DMSO, HheC catalytic function is inhibited to a great extent already in low co-solvent content. By applying a combined experimental and computational approach, it was found that DMSO behaves as a mixed-type inhibitor towards the HheC enzyme in the reactions of *para*-nitro-2-bromo-1-phenylethanol (PNSHH) dehalogenation and *para*-nitro styrene oxide (PNSO) ring-opening with bromide ions. Similar behavior was found in (*R*)-2-[4-(trifluoromethyl)phenyl]oxirane azidolysis by W249P (Appendix III). These results awakened the need to explore the catalytic and structural properties of HheC with other OSs (Appendix V). Satisfactory enzyme activity is an elementary prerequisite for establishing a biocatalytic reaction. In monophasic systems in presence of dimethylformamide, methanol, isopropanol, acetonitrile, and tetrahydrofuran, HheC performed poorly in terms of activity. In case of hydrophobic solvents, a direct correlation between HheC activity and logP value was found in PNSHH ring-closure reaction. However, this trend was not reported for PNSO ring-opening reaction. Inhibitions are present in all monophasic systems;

however, the ability to inhibit HheC catalytic function is not limited to polar co-solvents, but also characteristic for chloroform and toluene. Their inhibitory effect on HheC activity is more severe in reactions of epoxide ring-opening, which are more valuable from the synthetic point of view compared to ring-closure. The best enzyme activities were obtained in the presence of hydrophobic OSs, specifically alkanes; *n*-heptane, *n*-hexane, and cyclohexane. With these solvents, HheC and variant ISM-4 also displayed great stability and enantioselectivity. In comparison to the wild-type, ISM-4 variant stands out for its resistance towards the action of OSs. The link between thermostability and resistance to denaturing solvents of ISM-4 was established, whereby the improvements in stability are accompanied by superior enantioselectivity and retained activity. Therefore, this variant has great potential for biocatalysis in alternative media. Further research should be focused on screening of HHDH performance in biphasic systems were enzyme could be sheltered to a certain degree from inhibitory effect by reaction compounds, while hydrolysis of epoxides could also be diminished. Emphasis in future research should be in screening "green" solvent alternatives, together with enzyme immobilization methods which enable catalyst recycling, leading not only to economically profitable, but also environmentally acceptable processes.

5. Bibliography

[1] E. L. Bell, W. Finnigan, S. P. France, A. P. Green, M. A. Hayes, L. J. Hepworth, S. L. Lovelock, H. Niikura, S. Osuna, E. Romero, K. S. Ryan, N. J. Turner, S. L. Flitsch, Biocatalysis, Nat. Rev. Methods Prim. 1 (2021) 46, 1-21.

[2] R. A. Sheldon, D. Brady, Broadening the Scope of Biocatalysis in Sustainable Organic Synthesis, ChemSusChem 12 (2019) 2859-2881.

[3] P. María, G. Gonzalo, A. Alcántara, Biocatalysis as Useful Tool in Asymmetric Synthesis: An Assessment of Recently Granted Patents (2014-2019), Catalysts 9 (2019) 802.

[4] J. van Hylckama Vlieg, L. Tang, J. H. Lutje Spelberg, T. Smilda, G. J. Poelarends, T. Bosma, A. E. J. van Merode, M. Fraaije, D. B. Janssen, Halohydrin Dehalogenases Are Structurally and Mechanistically Related to Short-Chain Dehydrogenases/Reductases, J. Bacteriol. 183 (17) (2001) 5058-5066.

[5] S. K. Ma, J. Gruber, C. Davis, L. Newman, D. Gray, A. Wang, J. Grate, G.W. Huisman, R.A. Sheldon, A green-by-design biocatalytic process for atorvastatin intermediate, Green Chem. 12 (2010) 81-86.

[6] S. Simić, E. Zukić, L. Schmermund, K. Faber, C. K. Winkler, W. Kroutil, Shortening Synthetic Routes to Small Molecule Active Pharmaceutical Ingredients Employing Biocatalytic Methods, Chem. Rev. 122 (2022) 1052-1126.

[7] D. O'Hagan, Fluorine in health care: Organofluorine containing blockbuster drugs, J. Fluor. Chem. 131 (2010) 1071-1081.

[8] M. Inoue, Y. Sumii, N. Shibata, Contribution of Organofluorine Compounds to Pharmaceuticals, ACS Omega 5 (2020) 10633-10640.

[9] S. Matsunaga, Desymmetrization of meso Epoxide, in E. M. Carreira, H. Yamamoto (Eds.), Comprehensive Chirality, Elsevier, Amsterdam, 2012, p. 534-580.

[10] H. Tanimoto, K. Kakiuchi, Recent applications and developments of organic azides in total synthesis of natural products., Nat. Prod. Commun. 8 (2013) 1021-1034.

[11] S. Bräse, C. Gil, K. Knepper, V. Zimmermann, Organic Azides: An Exploding Diversity of a Unique Class of Compounds, Angew. Chem. 44 (2005) 5188-5240.

[12] O. Bakhanovich, P. Beier, Synthesis, Stability and Reactivity of α-Fluorinated Azidoalkanes, Chem. Eur. J. 6 (2020) 773-782.

[13] J. Tomaszewska, K. Koroniak, H. Koroniak, Fluorinated organic azides – their preparation and synthetic application, Ark. Arch. Org. Chem. 2017 (2017) 421-432.

[14] A. Pellis, S. Cantone, C. Ebert, L. Gardossi, Evolving biocatalysis to meet bioeconomy challenges and opportunities, N. Biotechnol. 40 (2018) 154-169.

[15] P. Tufvesson, J. Lima-Ramos, M. Nordblad, J. M. Woodley, Guidelines and Cost Analysis for Catalyst Production in Biocatalytic Processes, Org. Process Res. Dev. 15 (2011) 266-274.

[16] S. Wang, X. Meng, H. Zhou, Y. Liu, F. Secundo, Y. Liu, Enzyme Stability and Activity in Non-Aqueous Reaction Systems: A Mini Review, Catal. 6 (2016) 1-16.

[17] V. Stepankova, S. Nevolova, T. Koudelakova, Z. Prokop, R. Chaloupkova, J. Damborský, Strategies for Stabilization of Enzymes in Organic Solvents, ACS Catal. 3 (2013) 2823-2836.

[18] N. Milčić, V. Stepanić, I. Crnolatac, Z. Findrik Blažević, Z. Brkljača, M. Majerić Elenkov, Experimental and Computational Insights on the Influence of Organic Co-solvent on Structural and Catalytic Properties of a Biocatalyst: Inhibitory Effect of DMSO on Halohydrin Dehalogenase, Chem. Eur. J. 28 (2022) 1-11.

[19] M. G. García, L. Borgnino, Fluoride in the Context of the Environment, in V. R. Preedy (Ed.) Fluorine: Chemistry, Analysis, Functions and Effects, The Royal Society of Chemistry, London, 2015, p. 3-21.

[20] M. Doble, A. Kumar, Fluoride Removal, in M. Doble, A. Kumar (Eds.), Biotreatment of Industrial Effluents, Butterworth-Heinemann, Burlington, 2005, p. 83-88.

[21] A. Harsanyi, G. Sandford, Organofluorine chemistry: applications, sources and sustainability, Green Chem. 17 (2015) 2081-2086.

[22] G. Gribble, Naturally Occurring Organofluorines, in A. H. Neilson (Ed.),

Organofluorines, Springer Berlin, Heidelberg, 2005, p. 121-136.

[23] M. F. Carvalho, R. S. Oliveira, Natural production of fluorinated compounds and biotechnological prospects of the fluorinase enzyme, Crit. Rev. Biotechnol. 37 (2017) 880-897.

[24] M. Kendrick, Halogens in Seawater, Marine Sediments and the Altered Oceanic Lithosphere, in A. Buettner (Ed.), Springer Geochemistry, Springer, Heidelberg, 2018, p. 591-648.

[25] D. O'Hagan, C. Schaffrath, S. L. Cobb, J. T. G. Hamilton, C. D. Murphy, Biosynthesis of an organofluorine molecule, Nature 416 (2002) 279.

[26] R. Berger, G. Resnati, P. Metrangolo, E. Weber, J. Hulliger, Organic fluorine compounds: a great opportunity for enhanced materials properties, Chem. Soc. Rev. 40 (2011) 3496-3508.

[27] H. W. Roesky, A flourish of fluorine, Nat. Chem. 2 (2010) 240.

[28] K. Reichenbächer, H. I. Süss, J. Hulliger, Fluorine in crystal engineering—"the little atom that could," Chem. Soc. Rev. 34 (2005) 22-30.

[29] B. M. Johnson, Y.-Z. Shu, X. Zhuo, N. A. Meanwell, Metabolic and Pharmaceutical Aspects of Fluorinated Compounds, J. Med. Chem. 63 (2020) 6315-6386.

[30] J. Fried, E. F. Sabo, Synthesis of 17α-hydroxycorticosterone and its 9α-halo derivatives from 11-epi-17α-hydroxycorticosterone, J. Am. Chem. Soc. 75 (1953) 2273-2274.

[31] J. Wang, M. Sánchez-Roselló, J. L. Aceña, C. del Pozo, A. E. Sorochinsky, S. Fustero, V. A. Soloshonok, H. Liu, Fluorine in Pharmaceutical Industry: Fluorine-Containing Drugs Introduced to the Market in the Last Decade (2001–2011), Chem. Rev. 114 (2014) 2432-2506.

[32] M. G. Perrone, P. Vitale, A. Panella, A. Tolomeo, A. Scilimati, Current and emerging applications of fluorine in medicinal chemistry, in A. D. Westwell, Fluorinated Pharmaceuticals: Advances in Medicinal Chemistry, Future Science, London, 2015, p. 126-139.

[33] E. P. Gillis, K. J. Eastman, M. D. Hill, D. J. Donnelly, N. A. Meanwell, Applications of

Fluorine in Medicinal Chemistry, J. Med. Chem. 58 (2015) 8315-8359.

[34] URL: https://www.fda.gov/ (accessed January 10th 2023).

[35] Y. Ogawa, E. Tokunaga, O. Kobayashi, K. Hirai, N. Shibata, Current Contributions of Organofluorine Compounds to the Agrochemical Industry, IScience 23 (2020) 101467.

[36] M.G. Campbell, T. Ritter, Late-Stage Fluorination: From Fundamentals to Application, Org. Process Res. Dev. 18 (2014) 474-480.

[37] D. Meyer, H. Jangra, F. Walther, H. Zipse, P. Renaud, A third generation of radical fluorinating agents based on N-fluoro-N-arylsulfonamides, Nat. Commun. 9 (2018) 4888.

[38] R. Britton, V. Gouverneur, J. H. Lin, M. Meanwell, C. Ni, G. Pupo, J. C. Xiao, J. Hu, Contemporary synthetic strategies in organofluorine chemistry, Nat. Rev. Methods Prim. 1 (2021) 47.

[39] A. Konev, A. Khlebnikov, A Building Block Approach to Monofluorinated Organic Compounds, Collect. Czechoslov. Chem. Commun. 73 (2008) 1553-1611.

[40] I. Dokli, N. Milčić, P. Marin, M. Svetec Miklenić, M. Sudar, L. Tang, Z. Findrik Blažević, M. Majerić Elenkov, Halohydrin dehalogenase-catalysed synthesis of fluorinated aromatic chiral building blocks, Catal. Commun. 152 (2021) 106285.

[41] H.-Y. Wang, K. Huang, M. de Jesús, S. Espinosa, L. E. Piñero-Santiago, C. L. Barnes, M. Ortiz-Marciales, Synthesis of enantiopure 1,2-azido and 1,2-amino alcohols via regio- and stereoselective ring-opening of enantiopure epoxides by sodium azide in hot water, Tetrahedron. Asymmetry. 27 (2016) 91-100.

[42] A. Liu, J. Han, A. Nakano, H. Konno, H. Moriwaki, H. Abe, K. Izawa, V. A. Soloshonok, New pharmaceuticals approved by FDA in 2020: Small-molecule drugs derived from amino acids and related compounds, Chirality 34 (2022) 86-103.

[43] W. H. Brooks, W. C. Guida, K. G. Daniel, The significance of chirality in drug design and development., Curr. Top. Med. Chem. 11 (2011) 760-770.

[44] J. McConathy, M. J. Owens, Stereochemistry in Drug Action, Prim. Care Companion J. Clin. Psychiatry. 5 (2003) 70-73.

[45] J. D. Marth, A unified vision of the building blocks of life, Nat. Cell Biol. 10 (2008) 1015.

[46] T. W. Graham Solomons, Craig B. Fryhle, S. A. Snyder, Solomons' Organic Chemistry, Wiley, USA, 2017, p. 202.

[47] L. A. Nguyen, H. He, C. Pham-Huy, Chiral drugs: an overview, Int. J. Biomed. Sci. 2 (2006) 85-100.

[48] M. Abram, M. Jakubiec, K. Kamiński, Chirality as an Important Factor for the Development of New Antiepileptic Drugs, ChemMedChem. 14 (2019) 1744-1761.

[49] M. M. M. Pinto, C. Fernandes, M. E. Tiritan, Chiral Separations in Preparative Scale: A Medicinal Chemistry Point of View, Molecules 25 (2020).

[50] C. Silva, M. Martins, S. Jing, J. Fu, A. Cavaco-Paulo, Practical insights on enzyme stabilization, Crit. Rev. Biotechnol. 38 (2018) 335-350.

[51] J. M. Woodley, Biocatalysis for future sustainable manufacturing, Biochem. (Lond). 44 (2022) 6-8.

[52] P. Grunwald, Introduction, in P. Grunwald (Ed.), Biocatalysis - Biochemical Fundamentals and Appliactions, World Scientific, Singapore, 2015, p. 1-9.

[53] R. N. Patel, Biocatalysis for synthesis of pharmaceuticals., Bioorg. Med. Chem. 26 (2018) 1252-1274.

[54] A. S. Bommarius, Biocatalysis: A Status Report., Annu. Rev. Chem. Biomol. Eng. 6 (2015) 319-345.

[55] M. Estévez-Gay, J. Iglesias-Fernández, S. Osuna, Conformational Landscapes of Halohydrin Dehalogenases and Their Accessible Active Site Tunnels, Catal. 10 (2020).

[56] Q. Jiang, R. Fang, I. Gul, L. Aer, Y. Zhao, J. Guo, L. Tang, Halohydrin dehalogenase immobilization in magnetic biochar for sustainable halocarbon biodegradation and biotransformation, Environ. Technol. Innov. 27 (2022) 102759.

[57] C. E. Castro, E. W. Bartnicki, Biodehalogenation. Epoxidation of halohydrins, epoxide opening, and transhalogenation by a *Flavobacterium* species, Biochemistry 7 (1968) 3213-3218.

[58] T. Nakamura, T. Nagasawa, F. Yu, I. Watanabe, H. Yamada, A new catalytic function of halohydrin hydrogen-halide-lyase, synthesis of beta-hydroxynitriles from epoxides and cyanide, Biochem. Biophys. Res. Commun. 180 (1991) 124-130.

[59] A. Schallmey, M. Schallmey, Recent advances on halohydrin dehalogenases - from enzyme identification to novel biocatalytic applications, Appl. Microbiol. Biotechnol. 100 (2016) 7827–7839.

[60] K. Faber, W. Kroutil, New enzymes for biotransformations, Curr. Opin. Chem. Biol. 9 (2005) 181-187.

[61] Z. Findrik Blažević, N. Milčić, M. Sudar, M. Majerić Elenkov, Halohydrin Dehalogenases and Their Potential in Industrial Application - A Viewpoint of Enzyme Reaction Engineering, Adv. Synth. Catal. 363 (2021) 388-410.

[62] M. Schallmey, J. Koopmeiners, E. Wells, R. Wardenga, A. Schallmey, Expanding the Halohydrin Dehalogenase Enzyme Family: Identification of Novel Enzymes by Database Mining, Appl. Environ. Microbiol. 80 (2014) 7303-7315.

[63] M. Majerić Elenkov, M. Čičak, A. Smolko, A. Knežević, Halohydrin dehalogenase-catalysed transformations of epifluorohydrin, Tetrahedron. Lett. 59 (2018) 406-408.

[64] J. Koopmeiners, B. Halmschlag, M. Schallmey, A. Schallmey, Biochemical and biocatalytic characterization of 17 novel halohydrin dehalogenases, Appl. Microbiol. Biotechnol. 100 (17) (2016) 7517-7527.

[65] A. Mikleušević, I. Primožič, T. Hrenar, B. Salopek-Sondi, L. Tang, M. Majerić Elenkov, Azidolysis of epoxides catalysed by the halohydrin dehalogenase from *Arthrobacter* sp. AD2 and a mutant with enhanced enantioselectivity: an (*S*)-selective HHDH, Tetrahedron. Asymmetry. 27 (2016) 930-935.

[66] J. Koopmeiners, C. Diederich, J. Solarczek, H. Voß, J. Mayer, W. Blankenfeldt, A. Schallmey, HheG, a Halohydrin Dehalogenase with Activity on Cyclic Epoxides, ACS Catal. 7 (10) (2017), 6877-6886.

[67] J. Solarczek, T. Klünemann, F. Brandt, P. Schrepfer, M. Wolter, C. Jacob, W. Blankenfeldt, A. Schallmey, Position 123 of halohydrin dehalogenase HheG plays an important role in stability, activity, and enantioselectivity, Sci. Rep. 9 (2019) 5106.

[68] R. M. de Jong, J. J. W. Tiesinga, H. J. Rozeboom, K. H. Kalk, L. Tang, D. B. Janssen, B. W. Dijkstra, Structure and mechanism of a bacterial haloalcohol dehalogenase: a new variation of the short-chain dehydrogenase/reductase fold without an NAD(P)H binding site, EMBO J. 22 (2003) 4933–4944.

[69] J. H. Lutje Spelberg, J. E. T. van Hylckama Vlieg, L. Tang, D. B. Janssen, R. M. Kellogg, Highly Enantioselective and Regioselective Biocatalytic Azidolysis of Aromatic Epoxides, Org. Lett. 3 (2001) 41-43.

[70] L. S. Campbell-Verduyn, W. Szymański, C. P. Postema, R. A. Dierckx, P. H. Elsinga, D. B. Janssen, B. L. Feringa, One pot 'click' reactions: tandem enantioselective biocatalytic epoxide ring opening and [3+2] azide alkyne cycloaddition, Chem. Commun. 46 (2010) 898-900.

[71] M. Majerić Elenkov, I. Primožič, T. Hrenar, A. Smolko, I. Dokli, B. Salopek-Sondi, L. Tang, Catalytic activity of halohydrin dehalogenases towards spiroepoxides, Org. Biomol. Chem. 10 (2012) 5063–5072.

[72] H. Bisswanger, pH and Temperature Dependence of Enzymes, in H. Bisswanger (Ed.), Enzyme Kinetics: Principles and Methods, Wiley-VCH, Germany, 2017, p. 145-152.

[73] P. Domínguez de María, F. Hollmann, On the (Un)greenness of Biocatalysis: Some Challenging Figures and Some Promising Options, Front. Microbiol. 6 (2015) 1257.

[74] A. Nadda, K. Dhar, S. Kanwar, P. Arora, Lipase catalysis in organic solvents: Advantages and applications, Biol. Proced. Online 18 (2) (2016) 1-11.

[75] C. Cao, T. Matsuda, Biocatalysis in Organic Solvents, Supercritical Fluids and Ionic Liquids, in A. Goswami and J. D. Stewart (Eds.), Organic Synthesis Using Biocatalysis, Cambridge, Elsevier, 2016, p. 67-97.

[76] D. Holtmann, F. Hollmann, Is water the best solvent for biocatalysis?, Mol. Catal. 517 (2022) 1-4.

[77] M. Khabiri, B. Minofar, J. Brezovský, J. Damborský, R. Ettrich, Interaction of organic solvents with protein structures at protein-solvent interface, J. Mol. Model. 19 (2013) 4701-4711.

[78] H. Cui, T. H. J. Stadtmüller, Q. Jiang, K.-E. Jaeger, U. Schwaneberg, M. D. Davari, How

to Engineer Organic Solvent Resistant Enzymes: Insights from Combined Molecular Dynamics and Directed Evolution Study, ChemCatChem. 12 (2020) 4073-4083.

[79] M. Dirkmann, J. Iglesias-Fernández, V. Muñoz, P. Sokkar, C. Rumancev, A. von Gundlach, O. Krenczyk, T. Vöpel, J. Nowack, M.A. Schroer, S. Ebbinghaus, C. Herrmann, A. Rosenhahn, E. Sanchez-Garcia, F. Schulz, A Multiperspective Approach to Solvent Regulation of Enzymatic Activity: HMG-CoA Reductase, ChemBioChem. 19 (2018) 153-158.

[80] S. Dutta Banik, M. Nordblad, J. M. Woodley, G. H. Peters, A Correlation between the Activity of *Candida antarctica* Lipase B and Differences in Binding Free Energies of Organic Solvent and Substrate, ACS Catal. 6 (2016) 6350-6361.

[81] M. Nachiappan, G. R. Rao, R. Mariadasse, P. Saritha, M. Amala, D. Prabhu, R. Sundarraj, C. Pandian, J. Jeyaraman, Experimental and Computational Methods to Determine Protein Structure and Stability, in D. B. Singh, T. Tripathi (Eds.), Frontiers in Protein Structure, Function, and Dynamics, Springer, Singapore, 2020, p. 23-55.

[82] G. Hasnaoui-Dijoux, M. Majerić Elenkov, J. H. Lutje Spelberg, B. Hauer, D. B. Janssen, Catalytic Promiscuity of Halohydrin Dehalogenase and its Application in Enantioselective Epoxide Ring Opening, ChemBioChem. 9 (2008) 1048-1051.

[83] M. Majerić Elenkov, H. W. Hoeffken, L. Tang, B. Hauer, D. B. Janssen, Enzyme-Catalyzed Nucleophilic Ring Opening of Epoxides for the Preparation of Enantiopure Tertiary Alcohols, Adv. Synth. Catal. 349 (2007) 2279-2285.

[84] H. Arabnejad, M. Dal Lago, P. A Jekel, R. Floor, A.-M. Thunnissen, A. Terwisscha van Scheltinga, H. Wijma, D. B Janssen, A robust cosolvent-compatible halohydrin dehalogenase by computational library design, 30 (2017) 173-187.

[85] R. M. Haak, F. Berthiol, T. Jerphagnon, A. J. A. Gayet, C. Tarabiono, C. P. Postema, V. Ritleng, M. Pfeffer, D. B. Janssen, A. J. Minnaard, B. L. Feringa, J. G. de Vries, Dynamic Kinetic Resolution of Racemic β-Haloalcohols: Direct Access to Enantioenriched Epoxides, J. Am. Chem. Soc. 130 (2008) 13508-13509.

[86] G. Hasnaoui, J. H. Lutje Spelberg, E. de Vries, L. Tang, B. Hauer, D. B. Janssen, Nitrite-mediated hydrolysis of epoxides catalyzed by halohydrin dehalogenase from *Agrobacterium radiobacter* AD1: a new tool for the kinetic resolution of epoxides,

Tetrahedron: Asymmetry 16 (2005) 1685-1692.

[87] J. H. Lutje Spelberg, L. Tang, M. van Gelder, R. M. Kellogg, D. B. Janssen, Exploration of the biocatalytic potential of a halohydrin dehalogenase using chromogenic substrates, Tetrahedron: Asymmetry 13 (2002) 1083-1089.

[88] A. Mikleušević, Z. Hameršak, B. Salopek-Sondi, L. Tang, D. B. Janssen, M. Majerić Elenkov, Oxazolidinone Synthesis through Halohydrin Dehalogenase-Catalyzed Dynamic Kinetic Resolution, Adv. Synth. Catal. 357 (2015) 1709-1714.

[89] C. Molinaro, A.-A. Guilbault, B. Kosjek, Resolution of 2,2-Disubstituted Epoxides via Biocatalytic Azidolysis, Org. Lett. 12 (2010) 3772-3775.

[90] L. Tang, X. Zhu, H. Zheng, R. Jiang, M. Majerić Elenkov, Key residues for controlling enantioselectivity of Halohydrin dehalogenase from *Arthrobacter* sp. strain AD2, revealed by structure-guided directed evolution, Appl. Environ. Microbiol. 78 (2012) 2631-2637.

[91] S. P. Zou, Z. C. Wang, C. Qin, Y. G. Zheng, Covalent immobilization of *Agrobacterium radiobacter* epoxide hydrolase on ethylenediamine functionalised epoxy supports for biocatalytical synthesis of (*R*)-epichlorohydrin., Biotechnol. Lett. 38 (2016) 1579-1585.

[92] S. Tunçer, R. Gurbanov, I. Sheraj, E. Solel, O. Esenturk, S. Banerjee, Low dose dimethyl sulfoxide driven gross molecular changes have the potential to interfere with various cellular processes, Sci. Rep. 8 (2018) 14828.

[93] M. M. C. H. van Schie, J.-D. Spöring, M. Bocola, P. Domínguez de María, D. Rother, Applied biocatalysis beyond just buffers – from aqueous to unconventional media. Options and guidelines, Green Chem. 23 (2021) 3191-3206.

[94] H.-X. Jin, Z.-Q. Liu, Z.-C. Hu, Y.-G. Zheng, Production of (*R*)-epichlorohydrin from 1,3-dichloro-2-propanol by two-step biocatalysis using haloalcohol dehalogenase and epoxide hydrolase in two-phase system, Biochem. Eng. J. 74 (2013) 1-7.

[95] S.-P. Zou, Y.-G. Zheng, E.-H. Du, Z.-C. Hu, Enhancement of (*S*)-2,3-dichloro-1-propanol production by recombinant whole-cell biocatalyst in *n*-heptane-aqueous biphasic system., J. Biotechnol. 188 (2014) 42-47.

[96] F. Dong, H. Chen, C. A. Malapit, M. B. Prater, M. Li, M. Yuan, K. Lim, S.D. Minteer,

Biphasic Bioelectrocatalytic Synthesis of Chiral β-Hydroxy Nitriles, J. Am. Chem. Soc. 142 (2020) 8374-8382.

[97] D. Roiban, P. Sutton, R. Splain, C. Morgan, A. Fosberry, K. Honicker, P. Homes, C. Boudet, A. Dann, J. Guo, K. Brown, L. Ihnken, D. Fuerst, Development of an Enzymatic Process for the Production of (*R*)-2-Butyl-2-ethyloxirane, Org. Process Res. Dev. 21 (2017) 1302-1310.

[98] X.-J. Zhang, P.-X. Shi, H.-Z. Deng, X.-X. Wang, Z.-Q. Liu, Y.-G. Zheng, Biosynthesis of chiral epichlorohydrin using an immobilized halohydrin dehalogenase in aqueous and non-aqueous phase, Bioresour. Technol. 263 (2018) 483-490.

[99] R. A. Sheldon, P. C. Pereira, Biocatalysis engineering: the big picture, Chem. Soc. Rev. 46 (2017) 2678-2691.

[100] M. Di Serio, Chemical Reaction Engineering as a Bridge Between Nano and Macro World, Front. Chem. Eng. 1 (2019) 1-3.

[101] A. Lorente-Arevalo, A. Garcia-Martin, M. Ladero, J. M. Bolivar, Chemical Reaction Engineering to Understand Applied Kinetics in Free Enzyme Homogeneous Reactors in F. Magnani, C. Marabelli, F. Paradisi (Eds.), Enzyme Engineering: Methods and Protocols, Humana, New York, 2022, p. 277-320.

[102] M. Sudar, Z. Findrik Blažević, Enzyme Cascade Kinetic Modelling, in S. Kara, F. Rudroff (Eds.), Enzyme Cascade Design and Modelling, Springer International Publishing, Cham, 2021, p. 91-108.

[103] Đ. Vasić-Rački, U. Kragl, A. Liese, Benefits of Enzyme Kinetics Modelling, Chem. Biochem. Eng. Q. 17 (1) (2003) 7-18.

[104] A. Bommarius, B. Riebel, Enzyme Reaction Engineering, in A. S. Bommarius, B. R. Riebel (Eds.), Biocatalysis, Wiley-VCH, Germany, 2005, p. 91-134.

[105] N. Milčić, M. Česnik, M. Sudar, Z. Findrik Blažević, Primjena matematičkog modeliranja u razvoju enzimskih kaskadnih reakcija, Kem. Ind. 68 (2019) 427-436.

[106] Đ. Vasić-Rački, Z. Findrik, A. Presečki, Modeling as a tool of enzyme reaction engineering for enzyme reactor development, Appl. Microbiol. Biotechnol. 91 (2011) 845-856.

[107] M. Sudar, Z. Findrik Blažević, A. Szekrenyi, P. Clapés, Đ. Vasić-Rački, Reactor and microreactor performance and kinetics of the aldol addition of dihydroxyacetone to benzyloxycarbonyl-N-3-aminopropanal catalyzed by D-fructose-6-phosphate aldolase variant A129G, Chem. Eng. Commun. 206 (2019) 927-939.

[108] L. Mazzeo, V. Piemonte, Fermentation and biochemical engineering: principles and applications, in A. Basile, G. Centi, M. De Falco, G.B.T.-S. in S.S. and C. Iaquaniello (Eds.), Studies in Surface Science and Catalysis, Elsevier, Netherlands, 2020, p. 261-285.

[109] R. M. Lindeque, J. M. Woodley, Reactor Selection for Effective Continuous Biocatalytic Production of Pharmaceuticals, Catal. 9 (2019) 1-17.

[110] A. Illanes, C. Altamirano, Enzyme Reactors, in A. Illanes (Ed.), Enzyme Biocatalysis Principles and Applications, Springer Netherlands, Dordrecht, 2008, p. 205-251.

[111] N. Milčić, I. Ćevid, M. M. Çakar, M. Sudar, Z. Findrik Blažević, Enzyme Reaction Engineering as a Tool to Investigate the Potential Application of Enzyme Reaction Systems, Hung. J. Ind. Chem. 50 (2022) 45-55.

[112] H.-H. Wang, N.-W. Wan, R.-P. Miao, C.-L. He, Y.-Z. Chen, Z.-Q. Liu, Y.-G. Zheng, Identification and Structure Analysis of an Unusual Halohydrin Dehalogenase for Highly Chemo-, Regio- and Enantioselective Bio-Nitration of Epoxides, Angew. Chem. 61 (2022) 1-9.

[113] E. Mehić, L. Hok, Q. Wang, I. Dokli, M. Svetec Miklenić, Z. Findrik Blažević, L. Tang, R. Vianello, M. Majerić Elenkov, Expanding the Scope of Enantioselective Halohydrin Dehalogenases – Group B, Adv. Synth. Catal. 364 (2022) 2576-2588.

[114] R. Ma, X. Hua, C.-L. He, H.-H. Wang, Z.-X. Wang, B.-D. Cui, W.-Y. Han, Y.-Z. Chen, N.-W. Wan, Biocatalytic Thionation of Epoxides for Enantioselective Synthesis of Thiiranes, Angew. Chem. 61 (2022) 1-9.

[115] M. An, W. Liu, X. Zhou, R. Ma, H. Wang, B. Cui, W. Han, N. Wan, Y. Chen, Highly α-position regioselective ring-opening of epoxides catalyzed by halohydrin dehalogenase from *Ilumatobacter coccineus*: a biocatalytic approach to 2-azido-2-aryl-1-ols, RSC Adv. 9 (2019) 16418-16422.

[116] M. Česnik, M. Sudar, R. Roldan, K. Hernandez, T. Parella, P. Clapés, S. Charnock, Đ. Vasić-Rački, Z. Findrik Blažević, Model-based optimization of the enzymatic aldol addition of propanal to formaldehyde: A first step towards enzymatic synthesis of 3-hydroxybutyric acid, Chem. Eng. Res. Des. 150 (2019) 140-152.

[117] Đ. Vasić-Rački, J. Bongs, U. Schörken, G. Sprenger, A. Liese, Modeling of reaction kinetics for reactor selection in the case of L-erythrulose synthesis, Bioprocess Biosyst. Eng. 25 (2003) 285-290.

[118] R. M. Haak, C. Tarabiono, D. B. Janssen, A. J. Minnaard, J. G. de Vries, B. L. Feringa, Synthesis of enantiopure chloroalcohols by enzymatic kinetic resolution, Org. Biomol. Chem. 5 (2007) 318-323.

[119] J. H. Lutje Spelberg, J. E. T. van Hylckama Vlieg, T. Bosma, R. M. Kellogg, D. B. Janssen, A tandem enzyme reaction to produce optically active halohydrins, epoxides and diols, Tetrahedron: Asymmetry 10 (1999) 2863-2870.

[120] I. Dokli, Z. Brkljača, P. Švaco, L. Tang, V. Stepanić, M. Majerić Elenkov, Biocatalytic approach to chiral fluoroaromatic scaffolds, Org. Biomol. Chem. 20 (2022) 9734-9741.

[121] L. Tang, A. E. J. van Merode, J. H. Lutje Spelberg, M. W. Fraaije, D. B. Janssen, Steady-State Kinetics and Tryptophan Fluorescence Properties of Halohydrin Dehalogenase from *Agrobacterium radiobacter*. Roles of W139 and W249 in the Active Site and Halide-Induced Conformational Change, Biochemistry 42 (2003) 14057-14065.

[122] X. Wang, S. Han, Z. Yang, L. Tang, Improvement of the thermostability and activity of halohydrin dehalogenase from *Agrobacterium radiobacter* AD1 by engineering C-terminal amino acids, J. Biotechnol. 212 (2015) 92-98.

[123] C. Guo, Y. Chen, Y. Zheng, W. Zhang, Y. Tao, J. Feng, L. Tang, Exploring the Enantioselective Mechanism of Halohydrin Dehalogenase from *Agrobacterium radiobacter* AD1 by Iterative Saturation Mutagenesis, Appl. Environ. Microbiol. 81 (2015) 2919-2926.

[124] X. Wang, Z. Xie, J. Yan, X. He, W. Liu, Y. Sun, Enhancement of the thermostability of halohydrin dehalogenase from *Agrobacterium radiobacter* AD1 by constructing a combinatorial smart library, Int. J. Biol. Macromol. 130 (2019) 19-23.

[125] N. Wan, J. Tian, H. Wang, M. Tian, Q. He, R. Ma, B. Cui, W. Han, Y. Chen, Identification and characterization of a highly *S*-enantioselective halohydrin dehalogenase from *Tsukamurella* sp. 1534 for kinetic resolution of halohydrins, Bioorg. Chem. 81 (2018) 529-535.

[126] H.-B. Cui, L.-Z. Xie, N.-W. Wan, Q. He, Z. Li, Y.-Z. Chen, Cascade bio-hydroxylation and dehalogenation for one-pot enantioselective synthesis of optically active β-halohydrins from halohydrocarbons, Green Chem. 21 (2019) 4324-4328.

[127] S.-Y. Chen, X.-J. He, J.-P. Wu, G. Xu, L.-R. Yang, Identification of halohydrin dehalogenase mutants that resist COBE inhibition, Biotechnol. Bioprocess Eng. 19 (2014) 26-32.

[128] M. Schallmey, P. Jekel, L. Tang, M. Majerić Elenkov, H. W. Höffken, B. Hauer, D. B. Janssen, A single point mutation enhances hydroxynitrile synthesis by halohydrin dehalogenase, Enzyme Microb. Technol. 70 (2015) 50-57.

[129] L. Tang, J. H. Lutje Spelberg, M. W. Fraaije, D. B. Janssen, Kinetic Mechanism and Enantioselectivity of Halohydrin Dehalogenase from *Agrobacterium radiobacter*, Biochemistry 42 (2003) 5378-5386.

[130] N. Wan, J. Tian, X. Zhou, H. Wang, B. Cui, W. Han, Y. Chen, Regioselective Ring-Opening of Styrene Oxide Derivatives Using Halohydrin Dehalogenase for Synthesis of 4-Aryloxazolidinones, Adv. Synth. Catal. 361 (2019) 4651-4655.

[131] S.-P. Zou, K. Gu, Y.-G. Zheng, Covalent immobilization of halohydrin dehalogenase for efficient synthesis of epichlorohydrin in an integrated bioreactor, Biotechnol. Prog. 34 (2018) 784-792.

[132] G. Masdeu, Z. Findrik Blažević, S. Kralj, D. Makovec, J. López-Santín, G. Álvaro, Multi-reaction kinetic modeling for the peroxidase–aldolase cascade synthesis of a D-fagomine precursor, Chem. Eng. Sci. 239 (2021) 116602.

[133] M. Sudar, M. Česnik, P. Clapés, M. Pohl, Đ. Vasić-Rački, Z. Findrik Blažević, A cascade reaction for the synthesis of D-fagomine precursor revisited: Kinetic insight and understanding of the system, N. Biotechnol. 63 (2021) 19-28.

[134] M. Česnik, M. Sudar, K. Hernández, S. Charnock, Đ. Vasić-Rački, P. Clapés, Z. Findrik

Blažević, Cascade enzymatic synthesis of L-homoserine – mathematical modelling as a tool for process optimisation and design, React. Chem. Eng. 5 (2020) 747-759.

[135] P. Tufvesson, J. Lima-Ramos, N. Al Haque, K. V. Gernaey, J. M. Woodley, Advances in the Process Development of Biocatalytic Processes, Org. Process Res. Dev. 17 (2013) 1233-1238.

[136] P. Tufvesson, M. Nordblad, U. Krühne, M. Schürmann, A. Vogel, R. Wohlgemuth, J. M. Woodley, Economic Considerations for Selecting an Amine Donor in Biocatalytic Transamination, Org. Process Res. Dev. 19 (2015) 652-660.

[137] URL: https://hmdb.ca/ (accessed January 10th 2023).

[138] URL: https://www.chemblink.com (accessed January 10th 2023).

[139] R. M. de Jong, J. J. W. Tiesinga, A. Villa, L. Tang, D. B. Janssen, B. W. Dijkstra, Structural Basis for the Enantioselectivity of an Epoxide Ring Opening Reaction Catalyzed by Halo Alcohol Dehalogenase HheC, J. Am. Chem. Soc. 127 (2005) 13338-13343.

[140] X.-J. Zhang, H.-Z. Deng, N. Liu, Y.-C. Gong, Z.-Q. Liu, Y.-G. Zheng, Molecular modification of a halohydrin dehalogenase for kinetic regulation to synthesize optically pure (*S*)-epichlorohydrin, Bioresour. Technol. 276 (2019) 154-160.

[141] F. Xue, X. Yu, Y. Shang, C. Peng, L. Zhang, Q. Xu, A. Li, Heterologous overexpression of a novel halohydrin dehalogenase from *Pseudomonas pohangensis* and modification of its enantioselectivity by semi-rational protein engineering, Int. J. Biol. Macromol. 146 (2019) 80-88.

[142] URL: https://www.ilo.org/ (accessed January 10th 2023).

[143] URL: https://www.fishersci.at (accessed January 10th 2023).

[144] G. Castro, T. Knubovets, Homogeneous Biocatalysis in Organic Solvents and Water-Organic Mixtures, Crit. Rev. Biotechnol. 23 (2003) 195-231.

[145] P. Fernandes, J. Cabral, Biocatalysis in Biphasic Systems: General, in G. Carrea, S. Riva (Eds.), Organic Synthesis with Enzymes in Non-Aqueous Media, Wiley-VCH, Germany, 2008, p. 191-210.

[146] I. K. Voets, W. A. Cruz, C. Moitzi, P. Lindner, E. P. G. Arêas, P. Schurtenberger, DMSO-induced denaturation of hen egg white lysozyme, J. Phys. Chem. B. 114 (2010) 11875-11883.

[147] M. Verheijen, M. Lienhard, Y. Schrooders, O. Clayton, R. Nudischer, S. Boerno, B. Timmermann, N. Selevsek, R. Schlapbach, H. Gmuender, S. Gotta, J. Geraedts, R. Herwig, J. Kleinjans, F. Caiment, DMSO induces drastic changes in human cellular processes and epigenetic landscape in vitro, Sci. Rep. 9 (2019) 4641.

[148] A. Tjernberg, N. Markova, W. J. Griffiths, D. Hallén, DMSO-related effects in protein characterization, J. Biomol. Screen. 11 (2006) 131-137.

[149] Z. W. Yang, S. W. Tendian, W. M. Carson, W. J. Brouillette, L. J. Delucas, C. G. Brouillette, Dimethyl sulfoxide at 2.5% (*v*/*v*) alters the structural cooperativity and unfolding mechanism of dimeric bacterial NAD+ synthetase, Protein Sci. 13 (2004) 830-841.

[150] S. Bhattacharjya, P. Balaram, Effects of organic solvents on protein structures: Observation of a structured helical core in hen egg-white lysozyme in aqueous dimethylsulfoxide, Proteins: Struct. Funct. Bioinf. 29 (1997) 492-507.

[151] T. Magsumov, A. Fatkhutdinova, T. Mukhametzyanov, I. Sedov, The Effect of Dimethyl Sulfoxide on the Lysozyme Unfolding Kinetics, Thermodynamics, and Mechanism, Biomolecules 9 (2019) 1-16.

[152] E. L. Kovrigin, S. A. Potekhin, Preferential Solvation Changes upon Lysozyme Heat Denaturation in Mixed Solvents, Biochemistry 36 (1997) 9195-9199.

[153] A. Torreggiani, M. Di Foggia, I. Manco, A. De Maio, S. A. Markarian, S. Bonora, Effect of sulfoxides on the thermal denaturation of hen lysozyme: A calorimetric and Raman study, J. Mol. Struct. 891 (2008) 115-122.

[154] D. Sate, M. H. A. Janssen, G. Stephens, R. A. Sheldon, K. R. Seddon, J. R. Lu, Enzyme aggregation in ionic liquids studied by dynamic light scattering and small angle neutron scattering, Green Chem. 9 (2007) 859-867.

[155] A. Kumar, T. Darreh-Shori, DMSO: A Mixed-Competitive Inhibitor of Human Acetylcholinesterase, ACS Chem. Neurosci. 8 (2017) 2618-2625.

[156] L. Misuri, M. Cappiello, F. Balestri, R. Moschini, V. Barracco, U. Mura, A. Del-Corso, The use of dimethylsulfoxide as a solvent in enzyme inhibition studies: the case of aldose reductase, J. Enzyme Inhib. Med. Chem. 32 (2017) 1152-1158.

[157] G.-H. Kwak, S. H. Choi, J.-R. Kim, H.-Y. Kim, Inhibition of methionine sulfoxide reduction by dimethyl sulfoxide., BMB Rep. 42 (2009) 580-585.

[158] D. S.-H. Chan, M. E. Kavanagh, K. J. McLean, A. W. Munro, D. Matak-Vinković, A. G. Coyne, C. Abell, Effect of DMSO on Protein Structure and Interactions Assessed by Collision-Induced Dissociation and Unfolding, Anal. Chem. 89 (2017) 9976-9983.

[159] L. R. Nemzer, B. N. Flanders, J. D. Schmit, A. Chakrabarti, C. M. Sorensen, Ethanol shock and lysozyme aggregation, Soft Matter 9 (2013) 2187-2196.

[160] T. Kamiyama, H. L. Liu, T. Kimura, Preferential solvation of lysozyme by dimethyl sulfoxide in binary solutions of water and dimethyl sulfoxide, J. Therm. Anal. Calorim. 95 (2009) 353-359.

[161] H. J. Wiggers, J. Cheleski, A. Zottis, G. Oliva, A. D. Andricopulo, C. A. Montanari, Effects of organic solvents on the enzyme activity of *Trypanosoma cruzi* glyceraldehyde-3-phosphate dehydrogenase in calorimetric assays, Anal. Biochem. 370 (2007) 107-114.

[162] URL: https://pubchem.ncbi.nlm.nih.gov (accessed January 10th 2023).

[163] Q. Liao, X. Du, W. Jiang, Y. Tong, Z. Zhao, R. Fang, J. Feng, L. Tang, Cross-linked enzyme aggregates (CLEAs) of halohydrin dehalogenase from *Agrobacterium radiobacter* AD1: Preparation, characterization and application as a biocatalyst, J. Biotechnol. 272-273 (2018) 48-55.

[164] Z. Wu, W. Deng, Y. Tong, Q. Liao, D. Xin, H. Yu, J. Feng, L. Tang, Exploring the thermostable properties of halohydrin dehalogenase from *Agrobacterium radiobacter* AD1 by a combinatorial directed evolution strategy, Appl. Microbiol. Biotechnol. 101 (2017) 3201-3211.

[165] N. Doukyu, H. Ogino, Organic solvent-tolerant enzymes, Biochem. Eng. J. 48 (2010) 270-282.

6. Thesis Supplements

Appendix I

N. Milčić, I. Ćevid, M. M. Çakar, M. Sudar, Z. Findrik Blažević, Enzyme reaction engineering as a tool in investigation of the application potential of enzyme reaction systems, Hung. J. Ind. Chem. (2021)

Nevena Milčić: investigation, formal analysis, writing – review & editing

Ivana Ćevid: investigation, formal analysis

Mehmet Mervan Çakar: investigation, formal analysis

Martina Sudar: investigation, formal analysis, writing – review & editing

Zvjezdana Findrik Blažević: conceptualization, funding acquisition, writing – original draft, writing – review & editing

This publication was republished as an integral part of PhD thesis with the permission of Hungarian Journal of Industry and Chemistry.

HUNGARIAN JOURNAL OF INDUSTRY AND CHEMISTRY
HJIC

Editorial Office
University of Pannonia

To

Nevena Milčić
Faculty of Chemical Engineering and Technology
University of Zagreb

Veszprém, 7/11/2022

PERMISSION

Dear Ms Milčić,

Your paper entitled

"Enzyme Reaction Engineering as a Tool to Investigate the Potential Application of Enzyme Reaction Systems"

was published in the HUNGARIAN JOURNAL OF INDUSTRY AND CHEMISTRY 50, pp. 45–55 (2022), with an open access status.

Upon your request the permission is officially given to you: the paper is allowed to be included into your doctoral thesis, hence it is permitted to republish the paper in this way.

Kind regards

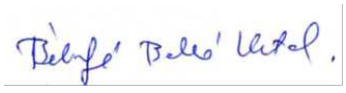

Prof Katalin Bélafi-Bakó

Editor-in-Chief

Egyetem str. 10.
Veszprém, H-8201, Hungary

E-mail: hjic@almos.uni-pannon.hu
http://hjic.mk.uni-pannon.hu

HUNGARIAN JOURNAL OF
INDUSTRY AND CHEMISTRY
Vol. 50 pp. 45–55 (2022)
hjic.mk.uni-pannon.hu
DOI: 10.33927/hjic-2022-08

HUNGARIAN JOURNAL OF INDUSTRY AND CHEMISTRY
HJIC

ENZYME REACTION ENGINEERING AS A TOOL TO INVESTIGATE THE POTENTIAL APPLICATION OF ENZYME REACTION SYSTEMS

NEVENA MILČIĆ [1], IVANA ĆEVID[1], MEHMET MERVAN ÇAKAR[1], MARTINA SUDAR[1], AND ZVJEZDANA FINDRIK BLAŽEVIĆ [*1]

[1]Faculty of Chemical Engineering and Technology, University of Zagreb, Marulićev trg 19, Zagreb, HR-10000, CROATIA

It is widely recognized and accepted that although biocatalysis is an exquisite tool to synthesize natural and unnatural compounds under mild process conditions, much can be done to better understand these processes as well as detect resulting bottlenecks and help to resolve them. This is the precise purpose of enzyme reaction engineering, a scientific discipline that focuses on investigating enzyme reactions with the goal of facilitating their implementation on an industrial scale. Even though reaction schemes of enzyme reactions often seem simple, in practice, the interdependence of different variables is unknown, very complex and may prevent further applications. Therefore, in this work, important aspects of the implementation of enzyme reactions are discussed using simple and complex examples, along with principles of mathematical modelling that provide explanations for why some reactions do not proceed as planned.

Keywords: enzyme kinetics, modelling, reaction optimisation

1. Setting up the reaction conditions for an enzyme reaction

In each reaction system, first a proper buffer must be selected and the pH dependence of the enzyme activity determined in order to identify the optimal working conditions [1]. Although the impact of temperature on enzyme activity is also important, it should be remembered that the temperature at which the enzyme exhibits the highest level of activity is not necessarily that at which the enzyme stability is optimal. At higher temperatures, the enzyme activity is often increased but at the cost of progressive and irreversible denaturation due to poor thermal stability [2, 3]. When multiple enzymes are present in the reaction system and are supposed to operate in the same reactor, as is the case in cascade reactions, the optimal conditions can seldom be chosen for all of them. Usually, a compromise must be reached whereby the selection of the reaction conditions depends on the enzyme activity required to catalyse the reaction [4, 5]. After selecting the buffer, temperature and pH for the studied reaction system, it must be analysed in detail, starting from the reaction scheme. Even though the reaction scheme usually clearly depicts the reaction, it should be noted that issues beyond the reaction scheme of the enzymatic reaction need to be discussed and analysed.

In many cases, unwanted but insignificant side reactions may take place that sometimes also have a detrimental effect on the outcome of the reaction. Although this may not be so important on the laboratory scale as far as screening for enzyme activities is concerned, given that the concentrations applied on that scale fall within the range of a few mM, it must be noted that the rate of chemical reactions increases as the concentration of reactants increases, e.g. first- and second-order reactions. Therefore, further analyses to determine the effect of increasing the scale of the reaction by hundreds of mM are required. The same applies to the chemical stability of compounds present in the reactor. In this case, engineering methodology is priceless for the purpose of exploring the possibility of slowly feeding the reactive compound into the reactor. Alternatively, if an intermediate is reactive, the reaction rate in the reactor may be tuned to ensure its concentration is always minimal. For example, in the case of epoxides that are substrates of halohydrin dehalogenases [6], it is known that their stability is poor [7, 8]. As a result, in these reactions, a prochiral substrate is often used to start the reaction [9, 10]. The same is true in this case whereby an epoxide intermediate is formed in situ and immediately spent in the subsequent reaction with the same or a different enzyme such as the one presented in Scheme 1.

Additionally, since both epoxides and their corre-

Recieved: 4 April 2022; Revised: 10 April 2022; Accepted: 11 April 2022
*Correspondence: zfindrik@fkit.hr

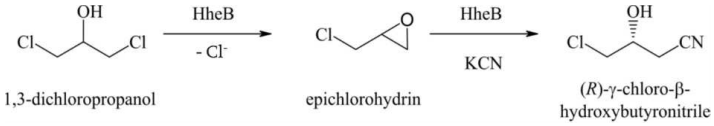

Scheme 1: Synthesis of (*R*)-γ-chloro-β-hydroxybutyronitrile from an achiral substrate

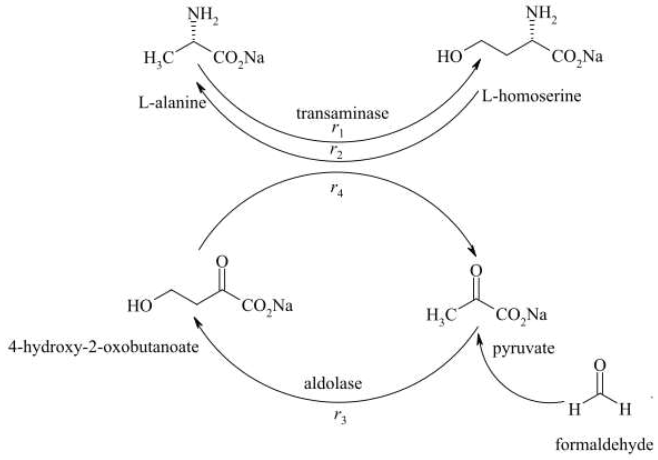

Scheme 2: Synthesis of L-homoserine in a cascade reaction

sponding nucleophiles can inhibit the catalytic activity of an enzyme [11], the selection of their concentrations in the reactor is crucial in facilitating a successful reaction [12]. Clearly, these are very complex reaction systems and the suitable set up of a reactor as well as reaction conditions determined by the model-aided approach can be vital [13].

Multi-step reactions cannot always be performed simultaneously in one pot due to complex relationships between the process variables [14, 18]. In a study of an innovative reaction scheme for the preparation of the atorvastatin side-chain precursor, it was found that the two reaction steps consisting of aldol addition and the oxidation of the corresponding product amino lactol could not be performed simultaneously [14]. This was mostly due to the fact that acetaldehyde as the substrate in the first reaction step interferes with the oxidoreduction and coenzyme regeneration by acting as a substrate for the oxidoreductase or as an inhibitor as well as deactivator of both oxidoreductase and NADH oxidase. It is important to determine if all the reaction steps are compatible with each other before deciding how to develop the reaction. Although this might suggest a significant amount of experimental work, this can be considerably reduced by evaluating the enzyme kinetics [13, 19, 20].

Forming the reaction model enables a vast variable space to be explored in silico. Apart from that, combining the kinetic model with mass balances in different reactors enables different types of reactors to be explored in each system. This was found to be crucial with regard to improving the process metrics in the synthesis of L-homoserine [21], a system governed by the unfavourable equilibrium of the transaminase-catalysed reaction and aided by the pyruvate recycling system catalysed by aldolase (Scheme 2).

The application of model-based optimization techniques led to a doubling of the product concentration (up to 80 gL^{-1}) and an 18% increase in the volumetric productivity (up to 3.2 $gL^{-1}h^{-1}$) in comparison with a previously published work [22]. In this system, it was crucial that both reactions were carried out simultaneously to improve the position of the equilibrium. Formaldehyde was gradually added to the system by using a pump due to its reactivity and inhibiting effect on enzyme activity. Additionally, pyruvate and L-alanine were added sequentially once the pyruvate had been consumed in several doses, which, according to calculations, was found to work in silico experiments (Fig. 1 A-B) and subsequently proved experimentally (Fig. 1 C-D).

2. Side reactions and their effect on the reaction scheme.

When studying a complex reaction system, possible side reactions must be taken into account. These can be caused by the instability of reactants, products or intermediates; by chemical reactions between the compounds present in the reaction mixture; as well as by the side reactions

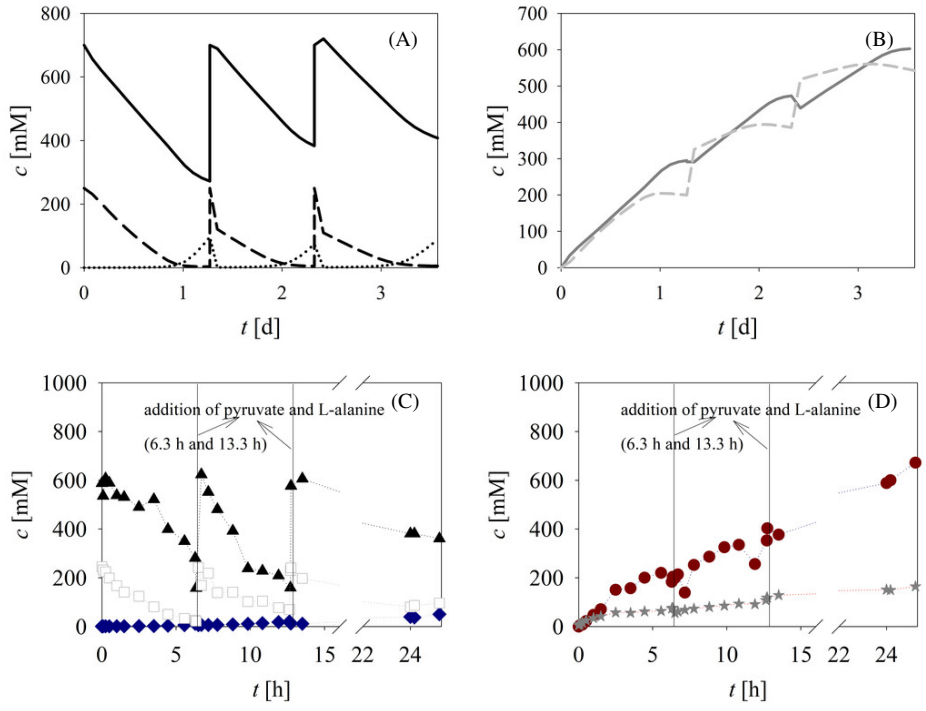

Figure 1: Cascade synthesis of L-homoserine [20] in a fed-batch bioreactor by gradually adding formaldehyde via a pump as well as sequentially adding pyruvate and L-alanine incrementally once the pyruvate had been consumed. (A) (black line – L-alanine, dashed line – pyruvate, dotted line – formaldehyde), (B) (grey line – L-homoserine, grey dashed line – aldol intermediate). In silico experiments, (C) experimental validation (black triangles – L-alanine, white squares – pyruvate, blue diamonds – formaldehyde), and (D) experimental validation (red circles – L-homoserine, grey stars – aldol intermediate).

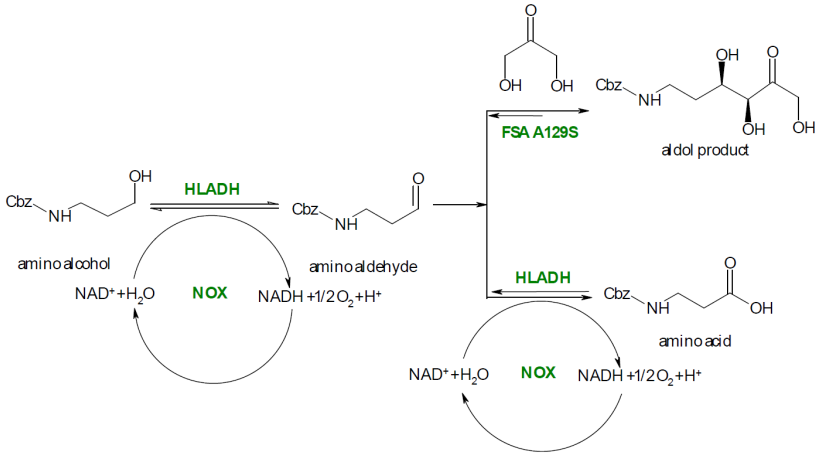

Scheme 3: Synthesis of the aldol product (3*S*,4*R*)-6-[(benzyloxycarbonyl)amino]-5,6-dideoxyhex-2-ulose in a cascade reaction

caused by the catalytic enzymes due to their low purity or ability to catalyse more than one reaction [8, 23, 24]. Reactions are often carried out with a crude enzyme extract or whole cells in order to reduce the costs of synthesising the protein by avoiding the necessity for purification. Although such systems often offer an additional advantage in terms of enhancing the operational stability of the desired enzyme within the protein mixture or cell compartment, other enzymes in these systems can also catalyse undesirable enzymatic reactions [23].

All of these aforementioned reactions can lower the concentration of the target product as well as decrease the reaction yield, moreover, in some cases, even prevent the formation of the target product. One example of such an event is the oxidation of an alcohol to form an aldehyde catalysed by horse liver alcohol dehydrogenase that reacts further by oxidizing the aldehyde to form the corresponding acid as a side product. In the cascade synthesis of (3*S*,4*R*)-6-[(benzyloxycarbonyl)amino]-5,6-dideoxyhex-2-ulose (Scheme 3), *N*-Cbz-3-aminopropanoic acid was the dominant main product following our first attempt, with only 2% of the target product being formed [25, 26]. Considering the complexity of the system, reaction engineering methodology was applied to determine the reason behind this. A statistical model implied the occurrence of this side reaction [25] which was later confirmed by kinetic studies [26].

Not only did the aforementioned studies reveal the reasons for the poor yield but also determined how to improve it to between 79 and 92%, respectively. In many cases, although commercial compounds that contain small quantities of certain additives are purchased for research purposes, these additives can also frequently act as enzyme inhibitors, such as in the case of 4-methoxyphenol as a stabilizer of acrylonitrile that was used as a substrate in one of the reactions studied by us [27]. In fact, this was one of the crucial reasons why it was not possible to obtain significant amounts of product in any reactor.

3. Investigation of the kinetics of the enzyme-catalysed reaction

To formally identify the system, the effect of all the compounds present in the reaction mixture on the enzyme activity / reaction rate can be evaluated. During these measurements, the effects of all the compounds on the enzyme activity can be measured and, in many cases, substrate, intermediate and product inhibition can be detected, which subsequently help with regard to decision-making and selection of the reactor mode to be used for the reaction. Some examples of reactor designs that can be applied, according to the properties of the studied reaction and desired outcome, are given in Fig. 2. In theory, it is known that the fed-batch bioreactor is a favourable choice for reactions subjected to substrate inhibition to increase the concentration of the obtained product [31].

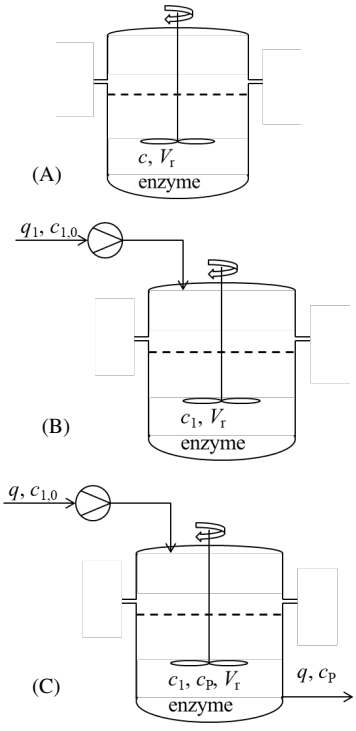

Figure 2: Schemes of different reactors applied in biocatalysis: (A) batch reactor, (B) fed-batch bioreactor, (C) continuous stirred tank reactor

For product-inhibited reactions, a continuous stirred tank reactor operating at the maximum concentration of the product is not recommended and, therefore, the resultant enzyme activity is unsatisfactory [32, 33]. In practice, reactions are rarely inhibited by a single compound, moreover, in many cases, several important inhibitions and/or side reactions take place. Therefore, the reactor mode cannot be easily set by viewing the results of the effect of substrates on the reaction rate. In these cases, kinetic models help simulate different scenarios and enable the best choice for the studied reaction system to be made [13].

The simulations of a relatively simple double-substrate reaction in which the kinetics can be described by double Michaelis-Menten kinetics with both substrate and product inhibition are presented in Fig. 3. The impact of reaction conditions on substrate conversion and volumetric productivity in the batch reactor is presented in Figs. 3A and 3B, while 3C and 3D show the same for the continuous stirred tank reactor (CSTR). Substrate conversion is governed by the enzyme concentration as well as the reaction time and residence time in the batch reactor and CSTR, respectively. The main difference that can be

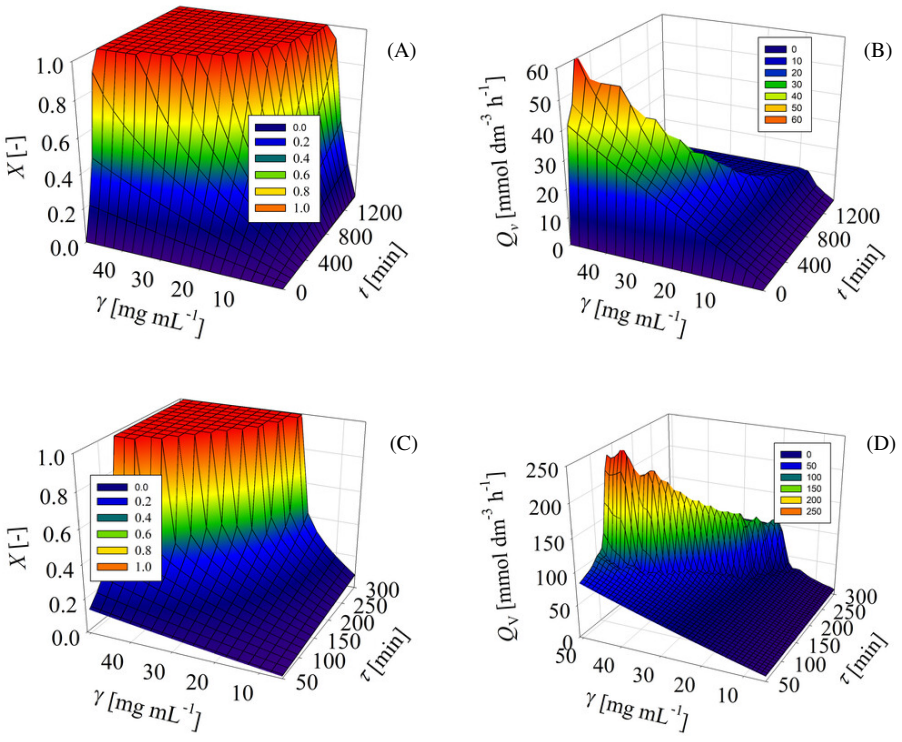

Figure 3: Model simulations demonstrating the impact of the reaction conditions on the conversion and volumetric productivity in the batch and continuous stirred tank reactors

observed is in terms of volumetric productivity, which explains why continuous processes are currently in the spotlight. In this simulation, the maximum volumetric productivity of the CSTR is fourfold greater than that of the batch reactor. Nevertheless, it must be noted that the operational stability of the enzyme is important and that the enzyme activity was assumed to be constant. In practice, since the enzyme activity inevitably drops over time and, therefore, enzymes must be stabilized by a form of immobilization, ensuring the continuous process functions is not a straightforward task.

The first step to investigate enzyme kinetics is to find an appropriate method that will result in the rapid collection of enzyme kinetic data. This can be done by applying a spectrophotometric enzyme assay and microtiter plate reader, however, should these methods be unavailable, this can also be achieved in a traditional manner by determining the initial reaction rates from HPLC or GC data with regard to the concentrations of substrates and products [13]. Given that data collection must be accurate and reliable, analytics is the foundation of the research. Data must be reproducible and trustworthy to be used for modelling. An example of kinetic data is presented in Fig. 4 where the grey line denotes the experiment where the enzyme concentration was too high. Furthermore, even though the linear dependence of absorbance over time is obvious in the initial part of the curve, the error of such measurements can be high and depends on the individual measuring. On the other hand, the black line clearly

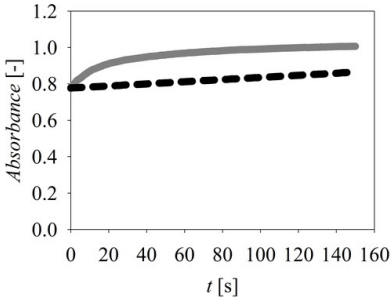

Figure 4: The impact of enzyme concentration on the quality of the experimental data

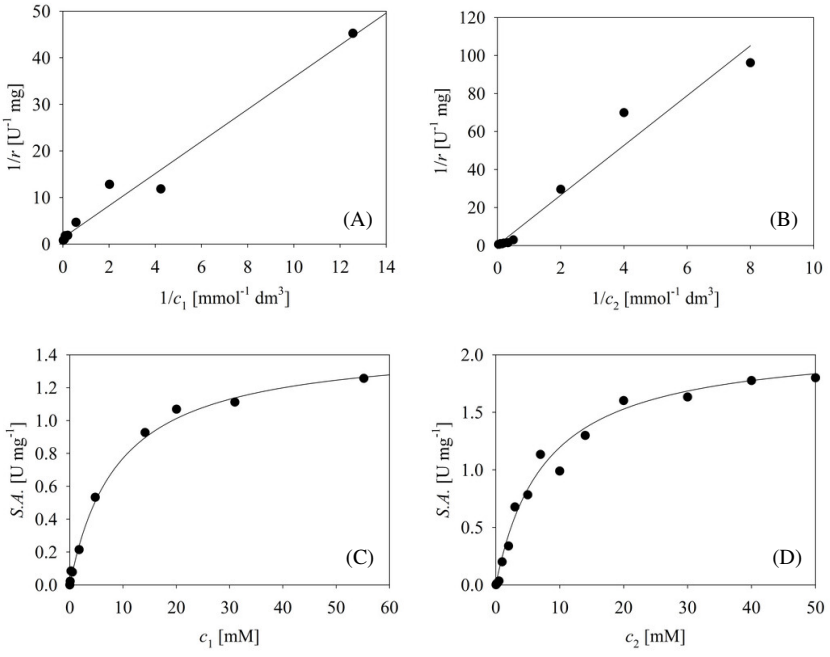

Figure 5: Estimation of kinetic parameters for a two-substrate reaction by applying linear (A and B) and nonlinear regression (C and D) analyses

represents linear data with a relatively small gradient, indicating that the measurements were made properly and the dependence is undoubtedly linear within that range. A series of such experiments performed at different concentrations of substrates, products and intermediates is required to obtain one set of experimental data to be subsequently used for the estimation of kinetic parameters.

Based on the kinetic data, the kinetic parameters can be estimated by using nonlinear regression analysis, which is far better than the still commonly used linear regression analysis [34]. This can be illustrated by the example presented in Fig. 5 whereby a double-substrate reaction was considered and the kinetic data concerning the dependence of the specific enzyme activity on the concentration of the reactants measured. By measuring the initial reaction rate (conversion less than 10%), the effect of product inhibition or enzyme deactivation could be minimized [35]. This example will be used to illustrate the differences between the values of the estimated kinetic parameters when various methods of estimation are applied. In the first case, linear regression analysis was applied by using a Lineweaver-Burk plot (Figs. 5A-5B). The data show discrepancies and, in the case of 5B, two points needed to be removed from the analysis as they were outliers. The estimated kinetic parameters are presented in Table 1. In the second case, the kinetic parameters were estimated by using single-substrate Michaelis-Menten kinetics, which in all likelihood is frequently used in practice. The estimated kinetic parameters presented in Table 1 are very different from the ones obtained following linear regression analysis. Furthermore, since the maximum reaction rates differ for each substrate, the measurements in all probability were not made in the area of substrate saturation. Michaelis constants estimated by using double-substrate Michaelis-Menten kinetics strongly resemble the values estimated by using single-substrate Michaelis-Menten kinetics. However, when the maximum reaction rates are compared, a significant discrepancy between them can still be observed. Estimating the maximum reaction rate by using double-substrate Michaelis-Menten kinetics is the optimum solution offering a unique value of V_m and taking into consideration the case when the non-varying substrate was not saturated. Therefore, in the case when both substrates are saturated, single-substrate Michaelis-Menten kinetics and nonlinear regression analysis offer a suitable solution to estimate the kinetic parameters.

4. Investigation of the operational stability of the enzyme

Enzyme activity inevitably decreases in the reactor over time, which means that the operational stability reduces as well [28–30]. This also needs to be quantified from the

Parameter	Linear regression analysis $\frac{1}{r} = \frac{1}{V_m} + \frac{K_m}{V_m}\frac{1}{c}$	Nonlinear regression analysis – single-substrate kinetics $r = \frac{V_m c}{K_m + c}$	Nonlinear regression analysis – double-substrate kinetics $r = \frac{V_m c_1 c_2}{(K_{m1} + c_1)(K_{m2} + c_2)}$
V_m [U/mg]	0.743 (3.539)	1.448 (2.119)	4.177
K_{m1} [mmol/dm^3]	2.56	8.2	9.09
K_{m2} [mmol/dm^3]	46.366	7.726	9.191

Table 1: Comparison between different methods to estimate the values of kinetic parameters in an enzymatic reaction

experimental data [29] and incorporated into the kinetic model. In many cases, the enzyme activity can be followed by an independent enzyme assay. In other cases, it can be estimated by using the kinetic model and other experiments. The operational stability of enzymes is an important topic not only in terms of research but also with regard to their applications. Understanding and describing quantitatively as well as qualitatively how enzyme function and structure change during conversion in a bioreactor is of crucial importance [28, 36].

In their work, Börner et al. investigated the mechanistic reasons for the poor operational stability of amine transaminases along with the influence of quaternary structure, cofactors and substrates. Through their kinetic and thermodynamic experiments, they were able to identify the structural domain that appears to confer stability. The study revealed that the enzyme is significantly more stable when at rest than in its operational state, moreover, its operational stability was lower and experiments suggested a mechanism that brought about substrate-induced deactivation [28]. In many reports to date, it has been stated that the presence of substrates and their concentrations can have both positive [37] and negative [30] effects on enzyme stability. In a study by Česnik et al. [30], formaldehyde as a substrate was found to have a negative effect on enzyme activity during experiments (Fig. 6A). Subsequently, it was found that this could be correlated with the operational stability of the enzyme (Fig. 6B). Considering the reactivity of formaldehyde and the size of this molecule, chemical damage to the protein may occur in its presence, as reported in other studies. In a study involving the dehalogenation of 1,3-dichloro-2-propanol (1,3-DCP) catalysed by halohydrin dehalogenases (HHDHs), it was found that the substrate 1,3-DCP causes enzyme deactivation during incubation, moreover, as observed in the previously described case, the substrate concentration has a significant effect on enzyme activity (unpublished data, Fig. 6C). Experiments conducted in batch reactors corroborated that the operational stability decay rate constant can be directly correlated to the substrate concentration (unpublished data, Fig. 6D). These are not the only examples of this behaviour. In a study by Vasić-Rački et al., it was also shown that glycolaldehyde caused operational stability decay in the reactor, the rate of which was dependent on its concentration [38]. In all of these cases, the quantification of the operational stability decay rate constant and the modelling approach improved the outcome of the reaction and increased process metrics values.

Another example of the effect of a substrate on enzyme activity can be demonstrated by different oxidases. In one study, the operational stability of D-amino acid oxidase was investigated in the presence and absence of aeration [40]. The enzyme operational stability decay rate of D-amino acid oxidase from porcine kidneys was reduced by increasing the oxygen concentration in the reaction solution and the enzyme activity decreased more rapidly. Similar conclusions were drawn in a later study on glucose oxidase [40]. This can be related to the oxidation of protein residues in the presence of oxygen and requires some sort of quantification to enable development of the reaction by focusing on resolving bottlenecks.

If operational stability is considered in a very simple reaction with only a basic Michaelis-Menten model, its effect during dynamic simulations can be observed (Fig. 7A). When the enzyme activity reduces in the batch reactor, the shape of the curve changes slightly. To the untrained eye, this can also resemble the result of reaching equilibrium or product inhibition. Therefore, if the kinetics of the reaction are completely unknown, it is very difficult to draw the right conclusion. The situation is quite different if the continuous stirred tank reactor is used, since this reactor ideally works at a stationary state and, therefore, no changes in enzyme activity nor in stationary concentrations of reactants and products occur. Hence, enzyme operational stability decay in CSTRs results in the stationary state being lost and the clearly visible shape of the curve caused by the reduction in enzyme activity (Fig. 7B). A third type of reactor often applied in biocatalysis due to substrate inhibition are fed-batch bioreactors. Although enzyme operational stability decay can be observed from the shape of the curve (Fig. 7C), here, like in the case of the batch reactor, it is more difficult to clearly define the reason for this trend. The answer that is suggested here concerns quantification of enzyme activity during the reaction.

5. Choosing the best enzyme variant for the reaction

Techniques for genetically modifying enzymes have advanced greatly over recent years and can be applied to produce industrially suitable catalysts more quickly and

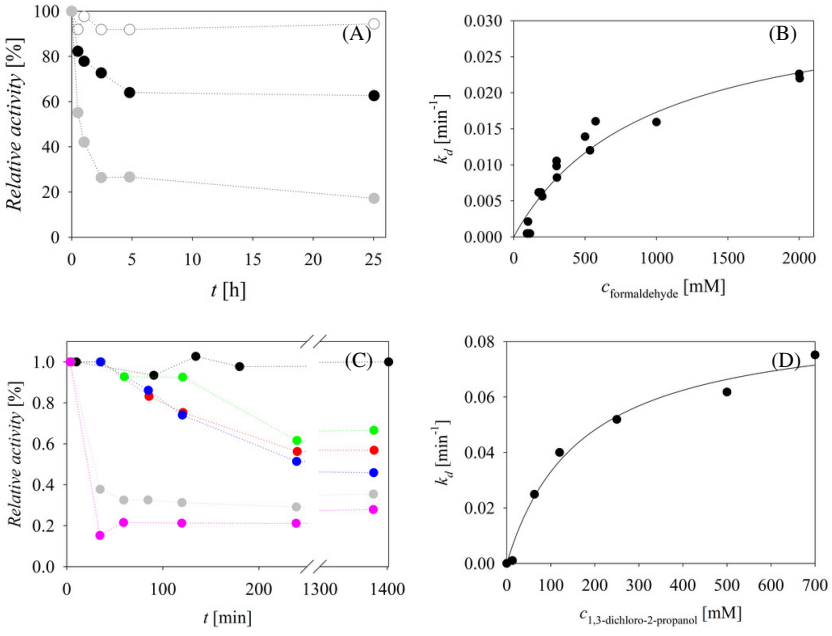

Figure 6: (A)The influence of the initial concentration of formaldehyde on the enzyme activity of FSAD6Q during incubation; (B) Dependence of the operational stability decay rate constants of FSAD6Q on the initial concentration of formaldehyde; (C) The influence of the initial concentration of 1,3-DCP on the enzyme activity of HHDH during incubation; (D) Dependence of the operational stability decay rate constants of HHDH on the initial concentration of 1,3-DCP

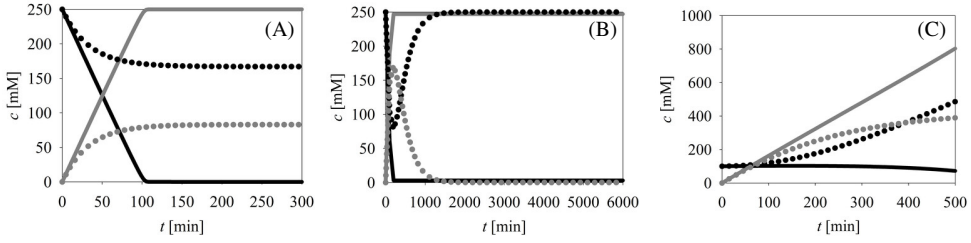

Figure 7: The effect of operational stability decay on model curves in different types of reactors: (A) batch reactor, (B) continuous stirred tank reactor, (C) fed-batch bioreactor

Parameter	Unit	Enzyme 1	Enzyme 2	Enzyme 3
V_{m}	U/mg	3.42 ± 0.05	1.74 ± 0.11	0.74 ± 0.03
K_{m}	mM	102.24 ± 4.01	67.52 ± 7.22	36.33 ± 8.82
K_{i}	mM	679.94 ± 38.81	183.19 ± 29.25	377.28 ± 68.70

Table 2: Estimated kinetic parameters for the three enzyme variants

cost-effectively. However, in order for new biocatalysts to be worthy of industrial large-scale production, reliable and comprehensive methods for the initial kinetic characterization of possible enzyme variants are necessary. In search of an optimal enzyme variant, the enzyme with the highest activity (highest V_m value) or highest affinity for the substrate (lowest K_m value) is often sought [41]. This is only valid when Michaelis-Menten kinetics are applied, however, in practice, the situation is rarely that simple. For example, this is not so in the case

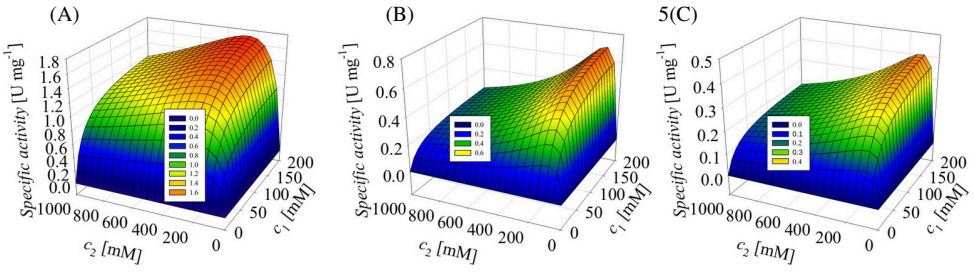

Figure 8: Comparison between the three enzyme variants which exhibit substrate inhibition at different levels

of Michaelis-Menten kinetics with substrate inhibition, when the substrate concentration used during screening is critical. Given that screening seems to only be conducted at one concentration, accurate data of enzyme activity is not provided, considering that the shape of the Michaelis-Menten curve is unknown. Since variants of the same enzyme differ with regard to the estimated values of their kinetic constants, combinations of the relevant kinetic parameters (V_m, K_m, K_i) were obtained for each variant (Table 2). Although it may be assumed that the enzyme with the minimum Michaelis constant and highest activity is most suitable, in practice, this enzyme may exhibit a higher level of substrate inhibition as a result. Three enzyme variants were kinetically characterized and the dependence of their specific enzyme activities on the substrate concentration is presented in Fig. 8, while the kinetic parameters are shown in Table 2. The best applied variant was found to be Enzyme 1, written in bold, in Table 2 because the level of substrate inhibition it is subjected to is by far the least pronounced. In practice, this means a broader substrate concentration area in which the highest enzyme activities can be obtained in the reactor (Fig. 8A) and enhanced stability of the reactor's operating conditions. Simulations presented in Fig. 8 also show that when screening the enzyme variants, it is important to not only evaluate their activities but also estimate all their kinetic parameters.

In further stages of process development, the application of reaction engineering to identify process bottlenecks is required to exploit the full potential of novel enzymes. To develop novel green routes in biocatalysis and scale them up, it is crucial to adopt a multidisciplinary approach by combining the fields of chemistry, biology and chemical engineering.

6. Conclusions

Enzyme reaction engineering can provide explanations for and give answers to different phenomena that occur in bioreactors. This is of particular importance when it comes to multienzyme systems which are very important in terms of sustainable development and green synthesis. Many obstacles to their development must be overcome, for example, adjusting enzyme activities, choosing suitable enzyme variants, selecting the best reactor and determining the optimal reaction conditions while considering the side reactions that may occur. Therefore, a combined effort and multidisciplinary approach are required to prepare complex enzyme reaction systems for industrial applications.

Acknowledgement

Authors would like to thank the Croatian Science Foundation for the PhD scholarship of N. Milčić. This work was partly supported by the project CAT PHARMA (KK.01.1.1.04.0013) co-financed by the Croatian Government and the European Union through the European Regional Development Fund - the Competitiveness and Cohesion Operational Programme (I. Ćevid). We acknowledge the funding from EU H2020-MSCA-ITN-2020 project C-C Top under the grant agreement no. 956631 (M. M. Çakar).

REFERENCES

[1] Burgess, R.R.; Deutscher, M.P.: Guide to protein purification (Academic Press, Cambridge, UK), 2nd edition, 2009, ISBN: 978-008-092-317-8

[2] Robinson, P.K.: Enzymes: Principles and biotechnological applications, *Essays Biochem*, 2015, **59**, 1–41. DOI: 10.1042/bse0590001

[3] Bisswanger, H.: Enzyme kinetics: Principles and methods (Wiley, New York, USA), 3rd edition, 2017 ISBN: 978-352-780-646-1

[4] Siedentop, R.; Claaßen, C.; Rother, D.; Lütz, S.; Rosenthal, K.: Getting the most out of enzyme cascades: Strategies to optimize in vitro multienzymatic reactions, *Catalysts*, 2021, **11**(10), 1183 DOI: 10.3390/catal11101183

[5] Komáromy, P.; Bélafi-Bakó, K.; Hülber-Beyer, É.; Nemestóthy, N.: Enhancement of oxygen transfer through membranes in bioprocesses, *Hung. J. Ind. Chem.*, 2020, **48**(2), 5–8 DOI: 10.33927/hjic-2020-21

[6] Schallmey, A.; Schallmey, M.: Recent advances on halohydrin dehalogenases–from enzyme identification to novel biocatalytic applications, *Appl. Microbiol. Biotechnol.*, 2016, **100**(18), 7827–7839 DOI: 10.1007/s00253-016-7750-y

[7] González-Pérez, M.; Gómez-Bombarelli, R.; Arenas-Valgañón, J.; Pérez-Prior, M.T.; García-Santos, M.P.; Calle, E.; Casado, J.: Connecting the chemical and biological reactivity of epoxides, *Chem. Res. Toxicol.*, 2012, **25**(12), 2755–2762 DOI: 10.1021/tx300389z

[8] Lee, E.Y.: Enantioselective hydrolysis of epichlorohydrin in organic solvents using recombinant epoxide hydrolase, *J. Ind. Eng. Chem.*, 2007, **13**(1), 159–162 https://www.cheric.org

[9] Jin, H.X.; Liu, Z.Q.; Hu, Z.C.; Zheng, Y.G.: Production of (*R*)-epichlorohydrin from 1,3-dichloro-2-propanol by two-step biocatalysis using haloalcohol dehalogenase and epoxide hydrolase in two-phase system, *Biochem. Eng. J.*, 2013, **74**, 1–7 DOI: 10.1016/j.bej.2013.02.005

[10] Watanabe, F.; Yu, F.; Ohtaki, A.; Yamanaka, Y.; Noguchi, K.; Odaka, M.; Yohda, M.: Improvement of enantioselectivity of the B-type halohydrin hydrogen-halide-lyase from Corynebacterium sp. N-1074, *J. Biosci. Bioeng.*, 2016, **122**(3), 270–275 DOI: 10.1016/j.jbiosc.2016.02.003

[11] Yao, P.; Wang, L.; Yuan, J.; Cheng, L.; Jia, R.; Xie, M.; Feng, J.; Wang, M.; Wu, Q.; Zhu, D.: Efficient biosynthesis of ethyl (*R*)-3-Hydroxyglutarate through a one-pot bienzymatic cascade of halohydrin dehalogenase and nitrilase, *ChemCatChem*, 2015, **7**(9), 1438–1444 DOI: 10.1002/cctc.201500061

[12] Findrik Blažević, Z.; Milčić, N.; Sudar, M.; Majerić Elenkov, M.: Halohydrin dehalogenases and their potential in industrial application – A viewpoint of enzyme reaction engineering, *Adv. Synth. Catal.*, 2021, **363**(2), 388–410 DOI: 10.1002/adsc.202000984

[13] Ringborg, R.H.; Woodley, J.M.: The application of reaction engineering to biocatalysis, *React. Chem. Eng.*, 2016, **1**(1), 10–22 DOI: 10.1039/C5RE00045A

[14] Švarc, A.; Fekete, M.; Hernandez, K.; Clapés, P.; Findrik Blažević, Z.; Szekrenyi, A.; Skendrović, D.; Vasić-Rački, Đ.; Charnock, S.J.; Vrsalović Presečki, A.: An innovative route for the production of atorvastatin side-chain precursor by DERA-catalysed double aldol addition, *Chem. Eng. Sci.*, 2021, **231**, 116312 DOI: 10.1016/j.ces.2020.116312

[15] Mattey, A.P.; Ford, G.J.; Citoler, J.; Baldwin, C.; Marshall, J.R.; Palmer, R.B.; Thompson, M.; Turner, N.J.; Cosgrove, S.; Flitsch, S.L.: Development of continuous flow systems to access secondary amines through previously incompatible biocatalytic cascades, *Angew. Chem. Int. Ed.*, 2021, **60**(34), 18660–18665 DOI: 10.1002/anie.202103805

[16] Britton, J.; Majumdar, S.; Weiss, G.A.: Continuous flow biocatalysis, *Chem. Soc. Rev.*, 2018, **47**(15), 5891–5918 DOI: 10.1039/C7CS00906B

[17] Klermund, L.; Poschenrieder, S.T.; Castiglione, K.: Biocatalysis in Polymersomes: Improving multienzyme cascades with incompatible reaction steps by compartmentalization, *ACS Catal.*, 2017, **7**(6), 3900–3904 DOI: 10.1021/acscatal.7b00776

[18] Schmidt, S.; Castiglione, K.; Kourist, R.: Overcoming the incompatibility challenge in chemoenzymatic and multi-catalytic cascade reactions, *Chem. Eur. J.*, 2018, **24**(8), 1755–1768 DOI: 10.1002/chem.201703353

[19] Engel, J.; Bornscheuer, U.T.; Kara, S.: Kinetics modeling of a convergent cascade catalyzed by monooxygenase–alcohol dehydrogenase coupled enzymes, *Org. Process Res. Dev.*, 2021, **25**(3), 411–420 DOI: 10.1021/acs.oprd.0c00372

[20] Vasić-Rački, Đ.; Kragl, U.; Liese, A.: Benefits of enzyme kinetics modelling, *Chem. Biochem. Eng. Q.*, 2003, **17**(1), 7–18 http://silverstripe.fkit.hr

[21] Česnik, M.; Sudar, M.; Hernández, K.; Charnock, S.; Vasić-Rački, Đ.; Clapés, P.; Findrik Blažević, Z.: Cascade enzymatic synthesis of L-homoserine – mathematical modelling as a tool for process optimisation and design, *React. Chem. Eng.*, 2020, **5**(4), 747–759 DOI: 10.1039/C9RE00453J

[22] Hernández, K.; Gómez, A.; Joglar, J.; Bujons, J.; Parella, T.; Clapés, P.: 2-Keto-3-Deoxy-l-Rhamnonate Aldolase (YfaU) as catalyst in aldol additions of pyruvate to amino aldehyde derivatives, *Adv. Synth. Catal.*, 2017, **359**(12), 2090–2100 DOI: 10.1002/adsc.201700360

[23] Dong, J.; Fernández-Fueyo, E.; Hollmann, F.; Paul, C.E.; Pesic, M.; Schmidt, S.; Wang, Y.; Younes, S.; Zhang, W.: Biocatalytic oxidation reactions: A chemist's perspective, *Angew. Chem. Int. Ed.*, 2018, **57**(30), 9238–9261 DOI: 10.1002/anie.201800343

[24] Toney, M.D.: Reaction specificity in pyridoxal phosphate enzymes, *Arch. Biochem. Biophys.*, 2005, **433**(1), 279–287 DOI: 10.1016/j.abb.2004.09.037

[25] Sudar, M.; Findrik, Z.; Vasić-Rački, Đ.; Soler, A.; Clapés, P.: A new concept for production of (3*S*,4*R*)-6-[(benzyloxycarbonyl)amino]-5,6-dideoxyhex-2-ulose, a precursor of D-fagomine, *RSC Adv.*, 2015, **5**(85), 69819–69828 DOI: 10.1039/C5RA14414K

[26] Sudar, M.; Česnik, M.; Clapés, P.; Pohl, M.; Vasić-Rački, Đ.; Findrik Blažević, Z.: A cascade reaction for the synthesis of D-fagomine precursor revisited: Kinetic insight and understanding of the system, *N. Biotechnol.*, 2021, **63**, 19–28 DOI: 10.1016/j.nbt.2021.02.004

[27] Sudar, M.; Vasić-Rački, Đ.; Müller, M.; Walter, A.; Findrik Blažević, Z.: Mathematical model of the MenD-catalyzed 1,4-addition (Stetter reaction) of α-ketoglutaric acid to acrylonitrile, *J. Biotechnol.*, 2018, **268**, 71–80 DOI: 10.1016/j.jbiotec.2018.01.013

[28] Börner, T.; Rämisch, S.; Reddem, E.R.; Bartsch, S.; Vogel, A.; Thunnissen, A.M.W.H.; Adlercreutz, P.; Grey, C.: Explaining operational instability

of amine transaminases: Substrate-induced inactivation mechanism and influence of quaternary structure on enzyme–cofactor intermediate stability, *ACS Catal.*, 2017, **7**(2), 1259–1269 DOI: 10.1021/acscatal.6b02100

[29] Dias Gomes, M.; Woodley, J.M.: Considerations when measuring biocatalyst performance, *Molecules*, 2019, **24**(19), 3573 DOI: 10.3390/molecules24193573

[30] Česnik, M.; Sudar, M.; Roldan, R.; Hernandez, K.; Parella, T.; Clapés, P.; Charnock, S.; Vasić-Rački, Đ.; Findrik Blažević, Z.: Model-based optimization of the enzymatic aldol addition of propanal to formaldehyde: A first step towards enzymatic synthesis of 3-hydroxybutyric acid, *Chem. Eng. Res. Des.*, 2019, **150**, 140–152 DOI: 10.1016/j.cherd.2019.06.025

[31] Scherkus, C.; Schmidt, S.; Bornscheuer, U.T.; Gröger, H.; Kara, S.; Liese, A.: A fed-batch synthetic strategy for a three-step enzymatic synthesis of poly-ϵ-caprolactone, *ChemCatChem*, 2016, **8**(22), 3446–3452 DOI: 10.1002/cctc.201600806

[32] Andrić, P.; Meyer, A.S.; Jensen, P.A.; Dam-Johansen, K.: Reactor design for minimizing product inhibition during enzymatic lignocellulose hydrolysis: II. Quantification of inhibition and suitability of membrane reactors, *Biotechnol. Adv.*, 2010, **28**(3), 407–425 DOI: 10.1016/j.biotechadv.2010.02.005

[33] Lindeque, R.M.; Woodley, J.M.: Reactor selection for effective continuous biocatalytic production of pharmaceuticals, *Catalysts*, 2019, **9**(3), 262 DOI: 10.3390/catal9030262

[34] Cho, Y.S.; Lim, H.S.: Comparison of various estimation methods for the parameters of Michaelis-Menten equation based on in vitro elimination kinetic simulation data, *Transl. Clin. Pharmacol.*, 2018, **26**(1), 39–47 DOI: 10.12793/tcp.2018.26.1.39

[35] Srinivasan, B.: A guide to the Michaelis–Menten equation: steady state and beyond, *FEBS J.*, 2021 DOI: 10.1111/febs.16124

[36] Bommarius, A.S.; Riebel, B.R.: Biocatalysis: Fundamentals and applications (Wiley, New York, USA), 1st edition, 2004 ISBN: 978-3-527-30344-1

[37] Lejeune, A.; Vanhove, M.; Lamotte-Brasseur, J.; Pain, R.H.; Frčre, J.M.; Matagne, A.: Quantitative analysis of the stabilization by substrate of Staphylococcus aureus PC1 β-lactamase, *Chem. Biol.*, 2001, **8**(8), 831–842 DOI: 10.1016/S1074-5521(01)00053-9

[38] Vasič-Rački, Đ.; Bongs, J.; Schörken, U.; Sprenger, G.; Liese, A.: Modeling of reaction kinetics for reactor selection in the case of L-erythrulose synthesis, *Bioprocess Biosyst. Eng.*, 2003, **25**, 285–290 DOI: 10.1007/s00449-002-0312-y

[39] Findrik, Z.; Valentović, I.; Vasić-Rački, Đ.: A mathematical model of oxidative deamination of amino acid catalyzed by two D-amino acid oxidases and influence of aeration on enzyme stability, *Appl. Biochem. Biotechnol.*, 2014, **172**(6), 3092–3105 DOI: 10.1007/s12010-014-0735-3

[40] Lindeque, R.M.; Woodley, J.M.: The effect of dissolved oxygen on kinetics during continuous biocatalytic oxidations, *Org. Process Res. Dev.*, 2020, **24**(10), 2055–2063 DOI: 10.1021/acs.oprd.0c00140

[41] McDonald, A.G.; Tipton, K.F.: Parameter reliability and understanding enzyme function, *Molecules*, 2022, **27**(1), 263 DOI: 10.3390/molecules27010263

Appendix II

Z. Findrik Blažević, N. Milčić, M. Sudar, M. Majerić Elenkov, Halohydrin Dehalogenases and Their Potential in Industrial Application – A Viewpoint of Enzyme Reaction Engineering, Adv. Synth. Catal. 363 (2021), 388-410.

Zvjezdana Findrik Blažević: conceptualization, investigation, formal analysis, funding acquisition, writing – original draft, writing – review & editing

Nevena Milčić: investigation, formal analysis, writing – review & editing

Martina Sudar: investigation, formal analysis, writing – review & editing

Maja Majerić Elenkov: funding acquisition, writing – review & editing

JOHN WILEY AND SONS LICENSE TERMS AND CONDITIONS

Nov 16, 2022

This Agreement between Faculty of Chemical Engineering and Technology, University of Zagreb -- Nevena Milčić ("You") and John Wiley and Sons ("John Wiley and Sons") consists of your license details and the terms and conditions provided by John Wiley and Sons and Copyright Clearance Center.

License Number	5421860462821
License date	Nov 04, 2022
Licensed Content Publisher	John Wiley and Sons
Licensed Content Publication	Advanced Synthesis & Catalysis
Licensed Content Title	Halohydrin Dehalogenases and Their Potential in Industrial Application – A Viewpoint of Enzyme Reaction Engineering
Licensed Content Author	Zvjezdana Findrik Blažević, Nevena Milčić, Martina Sudar, et al
Licensed Content Date	Nov 26, 2020
Licensed Content Volume	363
Licensed Content Issue	2
Licensed Content Pages	23
Type of Use	Dissertation/Thesis
Requestor type	Author of this Wiley article
Format	Print and electronic
Portion	Full article
Will you be translating?	No
Title	Mathematical modelling and optimization of biocatalytic synthesis of fluorinated chiral building blocks
Institution name	Faculty of Chemical Engineering and Technology, University of Zagreb
Expected presentation date	Mar 2023
Order reference number	2022-11-04-NM-RightsLink
Requestor Location	Faculty of Chemical Engineering and Technology, University of Zagreb Marulićev trg 19 Zagreb, 10 000 Croatia Attn: Faculty of Chemical Engineering and Technology, University of Zagreb
Publisher Tax ID	EU826007151
Billing Type	Invoice
Billing Address	Faculty of Chemical Engineering and Technology, University of Zagreb Marulićev trg 19 Zagreb, Croatia 10 000 Attn: Faculty of Chemical Engineering and Technology, University of Zagreb
Total	**0.00 EUR**
Terms and Conditions	

TERMS AND CONDITIONS

This copyrighted material is owned by or exclusively licensed to John Wiley & Sons, Inc. or one of its group companies (each a"Wiley Company") or handled on behalf of a society with which a Wiley Company has exclusive publishing rights in relation

to a particular work (collectively "WILEY"). By clicking "accept" in connection with completing this licensing transaction, you agree that the following terms and conditions apply to this transaction (along with the billing and payment terms and conditions established by the Copyright Clearance Center Inc., ("CCC's Billing and Payment terms and conditions"), at the time that you opened your RightsLink account (these are available at any time at http://myaccount.copyright.com).

Terms and Conditions

- The materials you have requested permission to reproduce or reuse (the "Wiley Materials") are protected by copyright.

- You are hereby granted a personal, non-exclusive, non-sub licensable (on a stand-alone basis), non-transferable, worldwide, limited license to reproduce the Wiley Materials for the purpose specified in the licensing process. This license, **and any CONTENT (PDF or image file) purchased as part of your order,** is for a one-time use only and limited to any maximum distribution number specified in the license. The first instance of republication or reuse granted by this license must be completed within two years of the date of the grant of this license (although copies prepared before the end date may be distributed thereafter). The Wiley Materials shall not be used in any other manner or for any other purpose, beyond what is granted in the license. Permission is granted subject to an appropriate acknowledgement given to the author, title of the material/book/journal and the publisher. You shall also duplicate the copyright notice that appears in the Wiley publication in your use of the Wiley Material. Permission is also granted on the understanding that nowhere in the text is a previously published source acknowledged for all or part of this Wiley Material. Any third party content is expressly excluded from this permission.

- With respect to the Wiley Materials, all rights are reserved. Except as expressly granted by the terms of the license, no part of the Wiley Materials may be copied, modified, adapted (except for minor reformatting required by the new Publication), translated, reproduced, transferred or distributed, in any form or by any means, and no derivative works may be made based on the Wiley Materials without the prior permission of the respective copyright owner.**For STM Signatory Publishers clearing permission under the terms of the STM Permissions Guidelines only, the terms of the license are extended to include subsequent editions and for editions in other languages, provided such editions are for the work as a whole in situ and does not involve the separate exploitation of the permitted figures or extracts,** You may not alter, remove or suppress in any manner any copyright, trademark or other notices displayed by the Wiley Materials. You may not license, rent, sell, loan, lease, pledge, offer as security, transfer or assign the Wiley Materials on a stand-alone basis, or any of the rights granted to you hereunder to any other person.

- The Wiley Materials and all of the intellectual property rights therein shall at all times remain the exclusive property of John Wiley & Sons Inc, the Wiley Companies, or their respective licensors, and your interest therein is only that of having possession of and the right to reproduce the Wiley Materials pursuant to Section 2 herein during the continuance of this Agreement. You agree that you own no right, title or interest in or to the Wiley Materials or any of the intellectual property rights therein. You shall have no rights hereunder other than the license as provided for above in Section 2. No right, license or interest to any trademark, trade name, service mark or other branding ("Marks") of WILEY or its licensors is granted hereunder, and you agree that you shall not assert any such right, license or interest with respect thereto

- NEITHER WILEY NOR ITS LICENSORS MAKES ANY WARRANTY OR REPRESENTATION OF ANY KIND TO YOU OR ANY THIRD PARTY, EXPRESS, IMPLIED OR STATUTORY, WITH RESPECT TO THE MATERIALS OR THE ACCURACY OF ANY INFORMATION CONTAINED IN THE MATERIALS, INCLUDING, WITHOUT LIMITATION, ANY IMPLIED WARRANTY OF MERCHANTABILITY, ACCURACY, SATISFACTORY QUALITY, FITNESS FOR A PARTICULAR PURPOSE, USABILITY, INTEGRATION OR NON-INFRINGEMENT AND ALL SUCH WARRANTIES ARE HEREBY EXCLUDED BY WILEY AND ITS LICENSORS AND WAIVED BY YOU.

- WILEY shall have the right to terminate this Agreement immediately upon breach of this Agreement by you.

- You shall indemnify, defend and hold harmless WILEY, its Licensors and their respective directors, officers, agents and employees, from and against any actual or threatened claims, demands, causes of action or proceedings arising from any breach of this Agreement by you.

- IN NO EVENT SHALL WILEY OR ITS LICENSORS BE LIABLE TO YOU OR ANY OTHER PARTY OR ANY OTHER PERSON OR ENTITY FOR ANY SPECIAL, CONSEQUENTIAL, INCIDENTAL, INDIRECT, EXEMPLARY OR PUNITIVE DAMAGES, HOWEVER CAUSED, ARISING OUT OF OR IN CONNECTION WITH THE DOWNLOADING, PROVISIONING, VIEWING OR USE OF THE MATERIALS REGARDLESS OF THE FORM OF ACTION, WHETHER FOR BREACH OF CONTRACT, BREACH OF WARRANTY, TORT, NEGLIGENCE, INFRINGEMENT OR OTHERWISE (INCLUDING, WITHOUT LIMITATION, DAMAGES BASED ON LOSS OF PROFITS, DATA, FILES, USE, BUSINESS OPPORTUNITY OR CLAIMS OF THIRD PARTIES), AND WHETHER OR NOT THE PARTY HAS BEEN ADVISED OF THE POSSIBILITY OF SUCH DAMAGES. THIS LIMITATION SHALL

APPLY NOTWITHSTANDING ANY FAILURE OF ESSENTIAL PURPOSE OF ANY LIMITED REMEDY PROVIDED HEREIN.

- Should any provision of this Agreement be held by a court of competent jurisdiction to be illegal, invalid, or unenforceable, that provision shall be deemed amended to achieve as nearly as possible the same economic effect as the original provision, and the legality, validity and enforceability of the remaining provisions of this Agreement shall not be affected or impaired thereby.

- The failure of either party to enforce any term or condition of this Agreement shall not constitute a waiver of either party's right to enforce each and every term and condition of this Agreement. No breach under this agreement shall be deemed waived or excused by either party unless such waiver or consent is in writing signed by the party granting such waiver or consent. The waiver by or consent of a party to a breach of any provision of this Agreement shall not operate or be construed as a waiver of or consent to any other or subsequent breach by such other party.

- This Agreement may not be assigned (including by operation of law or otherwise) by you without WILEY's prior written consent.

- Any fee required for this permission shall be non-refundable after thirty (30) days from receipt by the CCC.

- These terms and conditions together with CCC's Billing and Payment terms and conditions (which are incorporated herein) form the entire agreement between you and WILEY concerning this licensing transaction and (in the absence of fraud) supersedes all prior agreements and representations of the parties, oral or written. This Agreement may not be amended except in writing signed by both parties. This Agreement shall be binding upon and inure to the benefit of the parties' successors, legal representatives, and authorized assigns.

- In the event of any conflict between your obligations established by these terms and conditions and those established by CCC's Billing and Payment terms and conditions, these terms and conditions shall prevail.

- WILEY expressly reserves all rights not specifically granted in the combination of (i) the license details provided by you and accepted in the course of this licensing transaction, (ii) these terms and conditions and (iii) CCC's Billing and Payment terms and conditions.

- This Agreement will be void if the Type of Use, Format, Circulation, or Requestor Type was misrepresented during the licensing process.

- This Agreement shall be governed by and construed in accordance with the laws of the State of New York, USA, without regards to such state's conflict of law rules. Any legal action, suit or proceeding arising out of or relating to these Terms and Conditions or the breach thereof shall be instituted in a court of competent jurisdiction in New York County in the State of New York in the United States of America and each party hereby consents and submits to the personal jurisdiction of such court, waives any objection to venue in such court and consents to service of process by registered or certified mail, return receipt requested, at the last known address of such party.

WILEY OPEN ACCESS TERMS AND CONDITIONS

Wiley Publishes Open Access Articles in fully Open Access Journals and in Subscription journals offering Online Open. Although most of the fully Open Access journals publish open access articles under the terms of the Creative Commons Attribution (CC BY) License only, the subscription journals and a few of the Open Access Journals offer a choice of Creative Commons Licenses. The license type is clearly identified on the article.

The Creative Commons Attribution License

The Creative Commons Attribution License (CC-BY) allows users to copy, distribute and transmit an article, adapt the article and make commercial use of the article. The CC-BY license permits commercial and non-

Creative Commons Attribution Non-Commercial License

The Creative Commons Attribution Non-Commercial (CC-BY-NC)License permits use, distribution and reproduction in any medium, provided the original work is properly cited and is not used for commercial purposes.(see below)

Creative Commons Attribution-Non-Commercial-NoDerivs License

The Creative Commons Attribution Non-Commercial-NoDerivs License (CC-BY-NC-ND) permits use, distribution and reproduction in any medium, provided the original work is properly cited, is not used for commercial purposes and no modifications or adaptations are made. (see below)

Use by commercial "for-profit" organizations

Use of Wiley Open Access articles for commercial, promotional, or marketing purposes requires further explicit permission from Wiley and will be subject to a fee.

Further details can be found on Wiley Online Library http://olabout.wiley.com/WileyCDA/Section/id-410895.html

Other Terms and Conditions:

v1.10 Last updated September 2015

Questions? customercare@copyright.com or +1-855-239-3415 (toll free in the US) or +1-978-646-2777.

REVIEWS DOI: 10.1002/adsc.202000984

Halohydrin Dehalogenases and Their Potential in Industrial Application – A Viewpoint of Enzyme Reaction Engineering

Zvjezdana Findrik Blažević,[a,*] Nevena Milčić,[a] Martina Sudar,[a] and Maja Majerić Elenkov[b]

[a] University of Zagreb, Faculty of Chemical Engineering and Technology, Savska c. 16, HR-10000 Zagreb, Croatia
tel: +385 1 4597 157
fax: +385 1 4597 133
E-mail: zfindrik@fkit.hr
[b] Ruđer Bošković Institute, Bijenička c. 54, HR-10000 Zagreb, Croatia

Manuscript received: August 18, 2020; Revised manuscript received: November 12, 2020;
Version of record online: November 26, 2020

Supporting information for this article is available on the WWW under https://doi.org/10.1002/adsc.202000984

Abstract: At the moment, there are approx. 100 published papers investigating halohydrin dehalogenases from different aspects; enzymology, molecular biology and reactions they can catalyse. Unquestionably, these enzymes are of great importance and hold an immense potential due to the wide spectrum of different compounds that can be synthesized by their action. These compounds, such as chiral epoxides, β-substituted alcohols, oxazolidinones etc., significantly enrich the chemist's toolbox and, moreover, open the possibility for the synthesis of even more complex compounds. Still, there are many unknowns, and it is the purpose of this work to demonstrate the possibilities and bottlenecks, in scientific sense, that could further help in broadening the applicative potential of these fascinating enzymes.

Keywords: halohydrin dehalogenases; process metrics; epoxides; enzyme kinetics; chiral molecules

1. Introduction

Homochiral molecules are important industrial precursors and intermediates in the production of pharmaceuticals.[1] Of the novel drugs approved by the FDA, majority of chemical drugs in 2019 were single enantiomers of chiral compounds,[2] as well as 45% of those approved in the current year so far (status in August 2020).[3] New methodologies for the synthesis of chiral molecules are reported all the time with the emphasis on green chemistry methodology. Biocatalysis is positioned to be a transformational technology for chemical production since it offers improved synthetic efficiency[4] in a sustainable and environmentally friendly processes.[5] The significance of biocatalysis is progressively increasing because enzymes are a powerful tool for introducing the specificity into molecules produced by organic synthesis. The key for further advancement of biocatalysis is the integration of chemistry, molecular biology, and process development under the umbrella of green chemistry principles.[4] There are currently many industrial biotransformations for the production of pharmaceuticals, fine and bulk chemicals[6] and their number is

Zvjezdana Findrik Blažević (born 1979 in Zagreb, Croatia) studied Chemical Engineering at the University of Zagreb, Faculty of Chemical Engineering and Technology, where she completed her Ph. D. in Chemical Engineering in 2006. She is full professor at the Faculty of Chemical Engineering and Technology, University of Zagreb. Her research is focused on the application of chemical engineering methodology in biocatalysis, especially in the application of enzyme reaction engineering on single- and multi-enzyme reactions and their optimization by the mathematical modelling approach.

Nevena Milčić (born in 1992 in Zagreb, Croatia) graduated environmental engineering (2018) from Faculty of Chemical Engineering and Technology, University of Zagreb, Croatia. Shortly after graduation she joined CarbaZymes project team (Horizon 2020). Since April 2019 she has been employed on the project Enzymatic synthesis of Fluorinated Chiral Building Blocks funded by Croatian Science Foundation. Within project, she is enrolled in Ph.D study (Chemical Engineering and Applied Chemistry) with dual mentorship under Prof. Dr. Zvjezdana Findrik Blažević and Dr. Maja Majerić Elenkov, Senior Research Associate.

Martina Sudar (born in 1987 in Našice, Croatia) studied Process Engineering at the J. J. Strossmayer University of Osijek. She completed her Ph. D. in Chemical Engineering at the University of Zagreb in 2015 at the Faculty of Chemical Engineering and Technology where she works since 2011, currently as assistant professor. Her research is focused on biocatalysis, especially enzyme kinetic characterization for mathematical model development and reaction optimization.

Maja Majerić Elenkov (born in 1970 in Zagreb, Croatia), studied chemistry at the University of Zagreb, where she completed her Ph. D. in organic chemistry in 2003. From 2003 to 2005 she was a postdoctoral fellow in the group of Professor Dick B. Janssen at the University of Groningen (The Netherlands), working on stereoselective transformations catalysed by halohydrin dehalogenases. She is currently appointed as a Senior Research Associate at Ruđer Bošković Institute. Her research focuses on the use of biocatalysts, especially halohydrin dehalogenases for the synthetic transformation of non-natural compounds.

constantly increasing. It is, therefore, expected that their development will continue even stronger as environmental concerns become bigger issues. More than 250 billion US$ worth of various products are generated annually through biotechnological methods.[7] According to Grand View Research Inc. global biotechnology market is expected to reach 727.1 billion US$ by 2025.[8] The pharmaceutical market is still the most important driver for innovation in small and large molecule production technology.[9] Also, pharma industry is the largest market for fine chemicals and consumes 50% of its production.[9]

2. Halohydrin Dehalogenases

Halohydrin dehalogenases (HHDH, E.C. 4.5.1.-), also known as haloalcohol dehalogenases, halohydrin epoxidases or halogen-halide lyases, are versatile biocatalysts. These enzymes can be used for the synthesis of important building blocks and precursors in the pharmaceutical, agrochemical and chemical industries. They are seldom found in nature and living cells but, when present, they have an important role in detoxification of halo-organic compounds.[10] Nowadays, due to the advancement of molecular biology, these enzymes are more accessible; they can easily be expressed in recombinant *E. coli* cells and obtained in larger quantities. Furthermore, they are quite stable when isolated[10d] which presents an important property of an industrial biocatalyst. According to our experience with HHDHs, they show good stability in some cases, while in other they show sensitivity to different organic solvents, or nucleophiles (data not yet published). Still, most of these issues can be solved today by protein engineering, or by a careful choice of reaction conditions. Several HHDHs are also commercially available. Nine HHDHs can be purchased from Enzymicals AG (Greifswald, Germany), HheC can be

purchased from Angel yeast (Yichang, China), whereas Codexis (Redwood City, California, USA) produces HHDH kits.

HHDHs show unprecedented ability to catalyse wide range of bond-formations like carbon-carbon, carbon-chlorine, carbon-nitrogen, carbon-oxygen and carbon-bromine bond.[11] They can be applied for the synthesis of optically active epoxides, β-substituted alcohols, including chiral tertiary alcohols.[10d,e,12] These enzymes were discovered in 1968,[13] but their ability to catalyse epoxide ring-opening with different nucleophiles was demonstrated much later, in 1990s.[14] It was found that they accept azide, nitrite, cyanide, cyanate, thiocyanate, formate etc. as nucleophiles in the epoxide ring-opening reactions which gives access to the corresponding unnatural alcohols like β-nitro and β-azido, as well as β-hydroxynitriles and generally 1,2-difunctionalized organic compounds.[11] All mentioned compounds enrich the synthetic chemist's toolbox and provide powerful possibilities for asymmetric synthesis. Cyanide is an interesting nucleophile as it offers further transformation of compounds into amino, amide or carboxy group-containing molecules by the action of nitrile-amide converting enzymes.[15] Azides also present interesting unnatural nucleophiles since they provide optically pure azidoalcohols in HHDH-catalysed reactions. These azidoalcohols can later be used as precursors for important molecules in organic synthesis and medicinal chemistry, such as amino alcohols, aziridines and triazoles.[16] Some of the mentioned nucleophiles, like halides, nitrite, thiocyanate and formate, are not explored enough for practical application,[10d] and some are even problematic due to the unresolved side reactions that occur.[11] HHDH-catalysed reactions have long been considered as limited to terminal epoxides. Recently, several papers have been published suggesting that HHDHs can open even sterically more demanding and 2,3-disubstituted epoxides.[17] Representative set of substrates converted with various HHDHs are presented in Table 1.

From their discovery up until today, approximately 100 papers on HHDHs were published. The number of publications on a yearly basis (Figure 1) shows that the interest for the application of these enzymes is increasing, especially in the last two decades with the peak of interest in 2015.

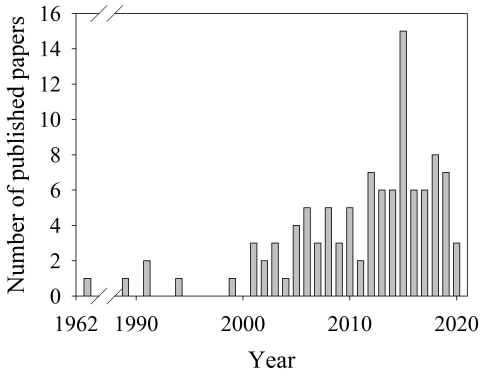

Figure 1. Publications related to the application of HHDHs throughout the years.

2.1. Types of Halohydrin Dehalogenases

Until the early 2010s, all known representatives of HHDHs were classified into three different but related phylogenetic subtypes assigned with letters A (HheA), B (HheB) and C (HheC).[10d,18c] All subtypes share similar homotetrameric structure with catalytic triad made of Ser-Tyr-Arg and extensive binding pocket for nucleophiles.[12b] HheA and HheB enzymes share similar substrate range while HheC clearly differs, showing higher enantioselectivity towards aromatic substrates[25] than A and B-type. The most explored HHDH is HheC, which is the topic of more than 30 publications, and its variants the topic of about 25 more, together covering over half of the papers on this enzyme family. The importance of these enzymes is in its high β-regioselectivity and (*R*)-enantioselectivity in the nucleophilic ring-opening reactions.[22d,26] According to the existing literature, HheC seems to be the only wild-type enzyme exhibiting high enantioselectivity, while others are unselective or moderately enantioselective.[12b] The availability of (*S*)-selective enzymes is poor,[10d] but it is expected that this shortcoming will soon be overcome by the protein engineering techniques.[12b] Wild-type HheA from *Arthrobacter* sp. AD2 is poorly (*S*)-enantioselective towards most aromatic substrates[20b] as a result of relatively spacious active site.[27] With the aim of improving selectivity, (*S*)-enantioselective HheA was evolved by semi-rational design approach with a single mutation of N178 active-site residue.[20b] Possibility of enantioselective biocatalyst with the ability to catalyse wide range of bond forming reactions prompted interest for exploring new biocatalytic pathways and expanding the HHDH enzyme family.[12b] As a result of database mining, based on their phylogenetic relationship, previous classification of HHDHs has been expanded by four new subtypes (D–G) in accordance with similarities in genetic sequences and bioactivity.[12b,18d] The most attractive among those is showing to be HheG from *Ilumatobacter coccineus*. This enzyme shows, opposite to all other HHDHs, high α-position regioselectivity in epoxide ring-opening reactions[28] and can be employed in the ring-opening reactions of sterically demanding cyclic epoxides.[17a] Within these, limonene oxide and cyclo-

Table 1. Substrates converted with various HHDHs.

Halohydrins:

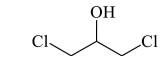 1,3-dichloro-2-propanol[18]	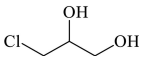 3-chloro-1,2-propanediol[18a–c]	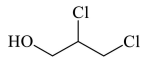 2,3-dichloro-1-propanol[18c,d]
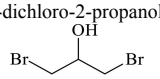 1,3-dibromo-2-propanol[18a–c]	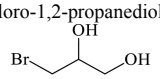 1-bromo-2,3-propanediol[18a]	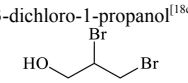 1,3-dibromopropanol[18d]
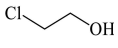 2-chloroethanol[18c,d]	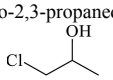 1-chloro-2-propanol[18a–c]	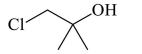 1-chloro-2-methyl-2-propanol[18a]
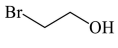 2-bromoethanol[18a–c]	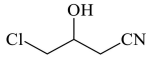 4-chloro-3-hydroxybutyronitrile[18b]	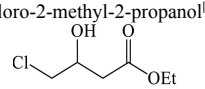 ethyl 4-chloro-3-hydroxybutyrate[18b,d]
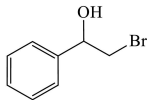 2-bromo-1-phenylethanol[19]	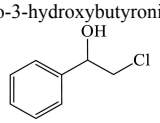 2-chloro-1-phenylethanol[18a–d,20]	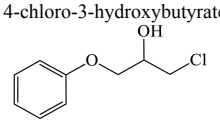 1-chloro-3-phenoxy-2-propanol[19,21]

Epoxides:

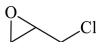 epichlorohydrin[18d]	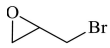 epibromohydrin[18d]	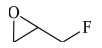 epifluorohydrin[18d]
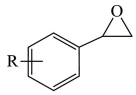 styrene oxides[18d,19,20b,21–22]	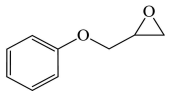 phenyl glycidyl ether[18d,19,21]	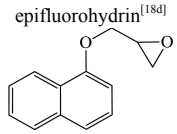 naphthyl glycidyl ether[19,21]
 1,2-epoxybutane[18a]	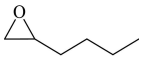 1,2-epoxyhexane[18a]	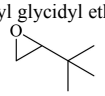 3,3-dimethyl-1,2-epoxybutane[18a]
 2-methyl-1,2-epoxybutane[18a,b,23]	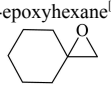 1-oxaspiro[2.5]octane[17a]	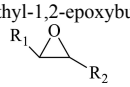 di-substituted *trans*-epoxides[17b]
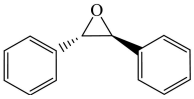 *trans*-stilbene oxide[18d]	 cyclohexene oxide[17a,24]	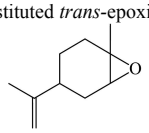 limonene oxide[17a]

Other substrates:

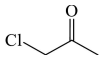 chloroacetone[18c,d]

hexene oxide are exceptions in comparison to other substrates, while they form the products with more than one chiral centre, unlike all the other substrates reported in HHDH studies. Recently, HHDHs from alphaproteobacterium isolate 46_93_T64 and *Pseudomonas pohangensis* were subjected to protein engineering to improve their naturally low enantioselectivity.[21a,b] Among many obtained variants,

the best one showed a 48-fold increase in e.e. in the kinetic resolution of *rac*-PGE in the presence of azide.[21b]

2.2. Industrial Application of Halohydrin Dehalogenases

Industrially, HHDHs are applied for the synthesis of chiral epichlorohydrin.[10a] Epichlorohydrin is used as an intermediate in preparation of synthetic rubbers, epoxy resins, paper chemicals, as a starting material in the production of surfactants, adhesives, insecticides, agricultural chemicals, coatings, ion-exchange resins, solvent, plasticizers and pharmaceuticals.[29] It is also a building block for biologically active compounds such as beta-adrenergic blocking agent (*S*)-atenolol and amino acid derivative (*R*)-carnitine.[29] The most significant industrial application of HHDH is the synthesis of ethyl (*R*)-4-cyano-3-hydroxybutanoate.[30] This is an important precursor in the production of a cholesterol lowering drug atorvastatin,[12b,30b] an ingredient of Lipitor®, the first drug with an annual sale exceeding 10 billion US$.[4] Ma and co-authors[30c] developed this biocatalytic process for the synthesis of ethyl (*R*)-4-cyano-3-hydroxybutanoate (Scheme 1). The starting substrate is prochiral ethyl-4-chloroacetoacetate which is reduced by an (*S*)-selective ketoreductase. In the subsequent reaction, catalysed by HHDH, the product is further transformed, via the corresponding (*S*)-epoxide as an intermediate, to the final product. The use of HHDH for the synthesis of ethyl (*R*)-4-cyano-3-hydroxybutanoate enabled working at the reaction conditions of neutral pH and ambient temperature. The application of biocatalysis in this process significantly reduced the number of formed by-products, waste, organic solvent usage, as well as energy consumption and gas emission thus enabling a green synthesis.[4] The mentioned environmental issues are especially pronounced in the large-scale industrial production of fine chemicals, and the reaction catalysed by HHDH in this process is a nice example of a perfect atom economy.[12c]

3. Case Studies

This review paper is envisioned as an evaluation of the current status of HHDH application with a focus on their potential targeting industrial level. Properties of the selected investigated biocatalytic systems, where syntheses were carried out on preparative scale, are presented in Table 2, including substrate/products, biocatalyst, e.e., reactor volume, product concentrations etc. This section is divided into several subsections depending on the products that can be synthesized by the action of HHDHs.

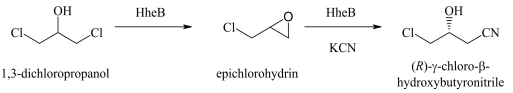

Scheme 2. Conversion of 1,3-dichloropropanol to (*R*)-γ-chloro-β-hydroxybutyronitrile.[31]

3.1. Synthesis of Epihalohydrins or Related Compounds

As HHDHs were first discovered in the context of enzymes related to the degradation of epihalohydrins, these are the compounds occurring in many studies.[14,18e,19,31–32] Thus, synthesis or degradation of epihalohydrins is by far the most studied system catalysed by HHDH starting from the first papers published by Castro and Bartnicki[13] and Nakamura et al.[14,31] who discovered that this enzyme was able to transform halohydrins into epoxides and also that it can accept cyanide as nucleophile (Scheme 2).

Epihalohydrins are compounds important for industrial application as already mentioned. The first kinetic resolution for the synthesis of enantiopure halohydrins and epoxides catalysed by HheC (Scheme 3) was reported by Lutje Spelberg et al.[32c] The enzyme was highly enantioselective towards 2,3-dichloro- and 2,3-dibromo-1-propanol. Enantioselectivity is usually defined by the enantiomeric ratio or *E*-value which represents the ability of enzyme to distinguish between enantiomers in kinetic resolution. It can be calculated by using equation 1 and is independent of the substrate conversion.[33] As a rule of thumb, *E*-values lower than 15 are usually considered unsuitable for analytical purposes. Values between 15–30 can be considered moderate to good, whereas exceeding these values is considered as excellent.[34]

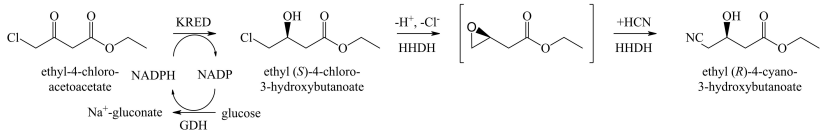

Scheme 1. Industrial application of HHDH in the cascade synthesis of statin side chain precursor ethyl (*R*)-4-cyano-3-hydroxybutanoate.[30c]

Table 2. Process characteristics of some evaluated systems.

$c_{substrate}$ [mM]	$c_{product}$ [mM]	Enzyme	Biocatalyst form	$Y_{isolated\ product}$ [%], $m_{isolated\ product}$ [mg]	X [%]	Reactor	V [mL]	e.e. [%]	$t_{reaction}$ [h]	Ref
200	≈ 75	HHDH from *Corynebacterium* sp. N–I074 produced in *E. coli* JM109/pST001	purified enzyme	n.a.	n.a.	batch	50	n.a.	2	[14]
50	≈ 38	HheB from *Corynebacterium* sp. N–I074 produced in *E. coli* JM109/pST001	purified enzyme	390 mg	n.a.	batch	100	95.2	2	[31]
54-65	n.a.	HheC from *A. radiobacter* AD1 produced in *E. coli*	cell-free extract	37–41%	45	batch	40	> 99	1.5-3	[44]
100-250 mM	n.a.	HheC from *A. radiobacter* AD1 produced in *E. coli*	purified enzyme	44-54%	< 50	batch	13-33	69-98	1-5	[49]
100 mM	n.a.	HheC from *A. radiobacter* AD1 produced in *E. coli*	cell-free extract	87%	100	batch	33.1	99	5	[51]
100 mM	31–92%	HheB2 from *Mycobacterium sp.* GP1 produced in *E. coli* MC1061 cells	cell-free extract	31–92%	100	batch	12.2	racemic	1-3	[32m]
50 mg	40–47%	HheC from *A. radiobacter* AD1	n.a. (preparation provided by Julich Chiral Solutions, Codexis)	40–47%	83-89	batch (cascade-2 enzymes, two steps)	~5.4	> 99	24	[54]
49.5-64.2 mM	n.a.	HheB2 from *Mycobacterium sp.* GP1 and HheC from *A. radiobacter* AD1	n.a. (preparation provided by Julich Chiral Solutions, Codexis)	38-61%	> 99	batch (cascade-2 enzymes, 3 steps)	~5.4	> 99	6-24	[55]
1200 mM	n.a.	variant HHDH (type n.a.)	whole-cells *E. coli* BL21(DE3) co-expressing HHDH and nitrilase	82.7%	100	rep. batch two-step cascade	50	100	6	[48]
200 g/L	n.a.	HHDH-PL from *Parvibaculum lavamentivorans* DS-1	whole-cells *E. coli* BL21 (DE3) expressing HHDH-PL	85%	95	batch	400	99	14	[71c]
10 g/L	n.a.	HheC W249F variant	whole-cells *E. coli* BL21 (DE3) expressing HheC W249F	86%	99	batch	200	97.5	1	[47b]
100 mM		HheC variant	whole-cells *E. coli* coexpressing AdhR, GdhBS, and HheC	n.a.	> 99	batch, two step cascade	20	> 99	2 and 4	[59]

Table 2. continued

$c_{substrate}$ [mM]	$c_{product}$ [mM]	Enzyme	Biocatalyst form	$Y_{isolated\ product}$ [%], $m_{isolated\ product}$ [mg]	X [%]	Reactor	V [mL]	e.e. [%]	$t_{reaction}$ [h]	Ref
100 mM										
50 mM (0.5 g)		HheC W249F variant	purified enzyme	40% 41%	n.a.	batch	65	96.8 95.2	5	[46]
973 mM	232.61 g	HHDH variant produced in *E. coli*	semi-purified lyophilizates	96%	n.a.	two-step batch	~670	> 99.5	8	[30c]
				92%	n.a.		~500	> 99.5	18	
840 mM	61.6 g									
50 mM	n.a.	HheE from marine metagenome HheE5 from *Gamma proteobacterium* IMCC3088	whole cells	50% 48%	100	batch	40	n.a.	24	[17b]
50 mM	n.a.	HheA from *Arthrobacter* sp. AD2	purified enzyme	75-96%	> 99	batch	20	> 99	1.5–3	[45]
168 mM		HheC from *A. radiobacter* AD1 and epoxide hydrolase from *R. ruber*	n.a.	40% 31%	n.a.	batch	24	> 99	24	[64]
20.9 g	9.8 g	HheC from *A. radiobacter* AD1	purified enzyme	29-47%	n.a.	batch	1 L	98.5–99	4 d	[69]

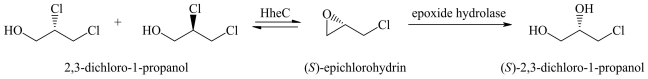

Scheme 3. Conversion of 1,2-dichloropropanol by HheC and epoxide hydrolase.[32c]

$$E = \frac{k_{cat}{}^{R} / K_{m}{}^{R}}{k_{cat}{}^{S} / K_{m}{}^{S}} \quad (1)$$

Lutje Spelberg et al.[32c] were able to synthesize (*S*)-2,3-dichloro-1-propanol ($E > 100$) and (*S*)-2-chloro-1-phenylethanol ($E = 73$) with > 99% e.e.

In another paper, Lutje Spelberg et al.[32b] reported the dynamic kinetic resolution of epihalohydrins in the presence of azide (Scheme 4) catalysed by HheC. The process was very efficient in the case of epibromohydrin as a substrate. On the other hand, with epichlorohydrin the rate of ring-opening by azide was higher than the rate of racemisation, resulting in mixed kinetic and dynamic kinetic resolution. Thus, a requirement for a dynamic kinetic resolution is rapid in situ racemisation of the substrate. The authors show that it is very important to choose the right pH value as all reaction steps are pH dependent. The reaction scheme (Scheme 4) shows high complexity of this reaction system.

Jin and co-authors[32d] investigated a similar system catalysed by the same enzyme; i.e. the first kinetic resolution of *rac*-epichlorohydrin in the presence of nitrite. They evaluated azide, cyanide, chloride, and nitrite as nucleophiles, under the same conditions, and found nitrite to be superior to other nucleophiles. Authors obtained 41% yield on (*R*)-epichlorohydrin with 99% e.e. In a subsequent study, Jin and co-authors[32e] investigated the preparation of (*R*)-epichlorohydrin from 1,3-dichloro-2-propanol in a two-step reaction which combines HheC and epoxide hydrolase in separate reactors. Since this process is comprised of two reactions, it is discussed in detail in the chapter with cascade reactions, along with other similar systems.

The next two studies are focused on process development rather than chirality like most of the other publications. Zou and co-authors[32f] investigated a ring-closure of 1,3-dichloro-2-propanol to epichlorohydrin catalysed by *E. coli* cells expressing HheC from *A. radiobacter*. V_m and K_m for 1,3-dichloro-2-propanol were estimated to be 3 mM min^{-1} and 33 mM, respectively. Furthermore, the product epichlorohydrin was shown to inhibit the reaction and K_i was estimated at 9 mM. To avoid product inhibition and increase productivity, a fed-batch reactor with in situ product removal (ISPR) using different adsorbing resins was tested. 87 mM of product was obtained after 130 min compared to 31 mM without ISPR. This work presents an excellent illustration how kinetic investigation can be applied in process development. The same group of authors[32g] continued to work on a similar system that included the immobilization of HHDH from *A. tumefaciens* CCTCC M 8707 on epoxy support. The immobilized enzyme was reused for 50 batches without significant activity loss and with the obtained volume productivity of 4.2 $g L^{-1} h^{-1}$, which is also an excellent result. Integrating the ISPR resulted in productivity increase up to 8.46 $g L^{-1} h^{-1}$, since macroporous resin used for that purpose was able to selectively adsorb epichlorohydrin and minimize product inhibition. Another advancement in the process development was done by Zou et al.[32h] in the investigation of kinetic resolution of 2,3-dichloro-1-propanol to (*S*)-2,3-dichloro-1-propanol by whole cells of *E. coli* expressing HheC. As this system is limited by the product inhibition,[32f] authors used *n*-heptane-aqueous biphasic medium. This change enabled a

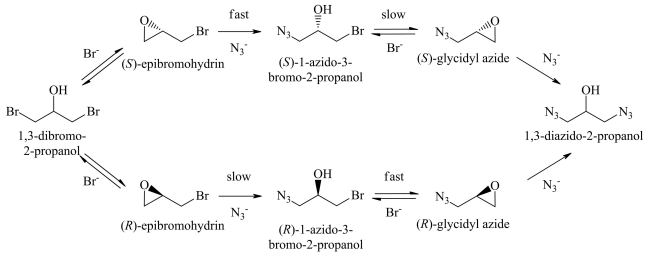

Scheme 4. Overall reaction scheme of the combined dynamic kinetic resolution process of epibromohydrin and subsequent kinetic resolution of the formed product 1-azido-3-bromo-2-propanol catalysed by HheC.[32b]

significant improvement in the tolerated substrate concentration and biocatalyst productivity in comparison to the aqueous system; i.e. 375 mM and 7.64 mmol g_{cell}^{-1} of (*S*)-2,3-dichloro-1-propanol were obtained in two-phase system, in comparison to 150 mM and 2.97 mmol g_{cell}^{-1} in the aqueous system. The process was scaled-up to 2 L and 128.8 mM of (*S*)-2,3-dichloropropanol with 99.1% e.e. and volume productivity of 2.07 g L^{-1} h^{-1} were obtained. Even though these numbers should be increased further for industrial application,[35] they still present a valuable improvement of process metrics and a step closer to applicative system. In a subsequent research,[32k] the same HheC variant was immobilized on A502Ps resin and used for the synthesis of (*S*)-dichloropropanol in an aqueous system and water-saturated ethyl acetate. Better results were obtained in water-saturated ethyl acetate (98% e.e. and 52.34% yield) than in aqueous system and the enzyme was quite stabile (45 batches). However, only low substrate concentrations of 20 mM were applied. In their following work, authors[18e] modified key amino acid residues of the previously used enzyme variant to improve its kinetic parameters. By doing so, they were able to produce enantiopure (*S*)-epichlorohydrin (e.e. > 99%) at substrate concentration of 20 mM. This work is the first report on protein modification by site-directed mutagenesis to regulate the kinetic parameters of HHDH for the forward and the reverse reaction.

Majerić Elenkov and co-authors[32m] studied the transformation of epifluorohydrin catalysed by HheB2 from *Mycobacterium* sp. GP1. Fluorine is an interesting addition for molecules further used as building blocks since it can increase the pharmaceutical effectiveness, biological half-life and the bioabsorption of the potential drug molecule.[36] In this work, the ring-opening reaction was performed in the presence of azide (Scheme 5). Other halogen substituents were tested, but it was found that only with fluorine the reaction stops after the first reaction step, yielding racemic 1-azido-3-fluoro-2-propanol. With other nucleophiles, the reaction proceeded to the unwanted diazido products. This implies that vicinal fluoroalcohols are not substrates for HheB2 and this enzyme is unable to cleave the strong C–F bond.

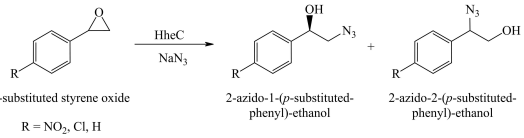

Scheme 6. Kinetic resolution of epoxides by HheC.[37]

3.2. Kinetic Resolution of Aromatic Compounds

1,2-Azidoalcohols are precursors for 1,2-amino alcohols and useful intermediates in carbohydrate chemistry. Lutje Spelberg et al.[37] studied the transformation of *p*-substituted styrene oxides in the reaction catalysed by HheC from *A. radiobacter* AD1 with azide as nucleophile (Scheme 6). The enzyme was found to be highly (*R*)-enantioselective and β-regioselective. The kinetic resolution resulted in high e.e. of the products: (*R*)-azidoalcohol and remaining (*S*)-epoxide. Total enzymatic conversion is achieved with a small excess of sodium azide. The occurrence of chemical azidolysis lowers the selectivity. The Michaelis constant for azide was determined to be 0.2 mM, which implies that 0.5 mM is enough for the reaction rate to be independent of its concentration. By increasing its concentration further, the rate of chemical azidolysis becomes more significant and a decrease in yield and selectivity occurs. This can be overcome by a gradual addition of azide which was nicely discussed in the paper. Of the three tested substrates (Scheme 6), the best one was found to be *p*-nitrostyrene oxide. The enantiomeric purity of the remaining (*S*)-enantiomer was 98% e.e. with 46% yield. At the same time, the enzyme was regioselective and generated the product in 97% e.e. with 47% yield. Non-enzymatic reaction by-product was found in 4% yield, and the product of chemical hydrolysis of the epoxide, *p*-nitrophenylethanediol in 3% yield. This was the first reported highly enantioselective (E > 200) and β-regioselective azidolysis of styrene oxides by HHDH which gave access to optically active 2-amino-1-arylethanols. In 2003 kinetic mechanism on HheC was reported.[38] The reaction was studied on the model substrate, *p*-nitro-2-bromo-1-phenylethanol, and authors performed a detailed kinetic analysis to understand the kinetic mechanism and enantioselectivity of the enzyme. It was revealed that the enzyme is active on both enantiomers; however, the activity and affinity

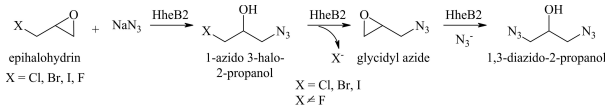

Scheme 5. Reactions catalysed by HheB2 starting from epihalohydrins and sodium azide.[32m]

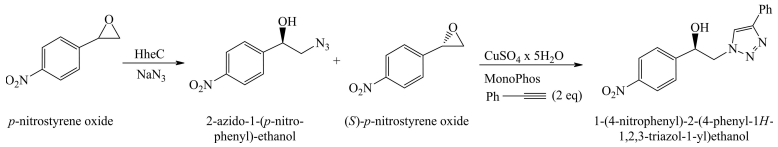

Scheme 7. One pot enzymatic and click reaction.[16a]

towards (*R*)-enantiomer was much higher than towards (*S*)-enantiomer. Finally, it was reported that HheC follows Uni Bi reaction mechanism for both enantiomers, and this information is essential for modifying the selectivity of the enzyme for new applications.[39]

Another work[40] reports a new HHDH, i. e. Syhhdh, applied for the ring-closure via dehalogenation and asymmetric ring-opening reactions. (*S*)-*p*-nitrostyrene oxide with a 99% e.e. and 23.8% yield was obtained from *p*-nitrophenacyl bromide by chemoenzymatic route via one-step chemical synthesis and two-step biocatalysis. In another work[21c] a new HHDH from *P. umsongensis* YCIT1612, able to transform racemic phenyl glycidyl ether to (*S*)-enantiomer with 99% e.e. and 23.5% yield, was reported. HHDH from alphaproteobacterium was reported[19] to catalyse the stereoselective dehalogenation with the best results for racemic 2-bromo-1-phenylethanol. (*S*)-2-bromo-1-phenylethanol was produced with 99% e.e. and 34.5% yield. Campbell-Verduyn et al.[16a] reported the enantioselective azidolysis of aromatic epoxides to 1,2-azidoalcohols that were further ligated to alkynes producing chiral hydroxytriazoles (Scheme 7) in one-pot with excellent e.e. This system is discussed in the section with cascade reactions in more detail.

Mikleušević et al.[26] also investigated the azidolysis of aromatic epoxides (Scheme 8) catalysed by the first highly (*S*)-enantioselective HheA–N178A, a variant form of HheA. They were able to obtain enantiopure (*S*)-β-azidoalcohols and (*R*)-α-azidoalcohols with reduced regioselectivity. The used enzyme variant showed superior enantioselectivity in comparison to the wild-type enzyme. Still, only 2 mM concentrations of substrates were used, and it can be expected that the enantioselectivity would be reduced with the increase of substrate concentration.

Chiral 2-chloro-1-phenylethanol is a precursor for the synthesis of antidepressants fluoxetine, tomoxetine and nisoxetine,[41] while indene bromohydrin is a precursor for the anti-HIV protease inhibitor Indinavir.[42] In a work reported by Wan and co-authors,[43] a new A-type HHDH (HheA10) with high enantioselectivity towards 2-chloro-1-phenylethanol derivatives was found. Chiral resolutions catalysed by the new enzyme enabled enantioenriched aromatic halohydrins and epoxides to be obtained. This research was done solely at 5 mM concentrations of substrate and therefore, more work is required to reveal the true potential of this enzyme. HheG from *I. coccineus* has excellent regioselectivity towards α-position in the azide-mediated ring-opening of styrene oxide derivatives producing the corresponding 2-azido-2-aryil-1-ols with yields up to 96%.[28] The best results were obtained with styrene oxide and 2-(4-methylphenyl) oxirane. This is the first report of the enzymatic synthesis of 2-azido-1-phenylethan-1-ols, and the first enzyme with the selectivity towards the α-position; the position also chemically favoured without the enzyme. Still, the results of non-enzymatic reaction were not reported in this work. Similar group of authors investigated the synthesis of 5-aryl-2-oxazolidinones in a one-step ring-opening of aryl epoxides catalysed by HheC which additionally broadens the application of these enzymes in organic synthesis.[22b]

3.3. Reactions with 2,2-Disubstituted Epoxides and Spiroepoxides

Majerić Elenkov et al.[15b] discovered very high enantioselectivites of HheC in the resolution of 2,2-disubstituted epoxides ($E = 141–200$) and the synthesis of the corresponding β-hydroxynitriles (Scheme 9). These reactions enable the production of enantiopure tertiary alcohols by C–C bond formation. The same group[44] reported another work on the similar topic (Scheme 10). Different substrates were tested with azide and cyanide as nucleophiles. Products obtained

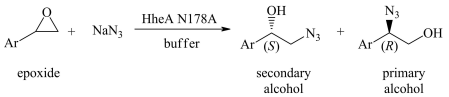

Scheme 8. Conversion of aromatic epoxides catalysed by HheA N187A.[26]

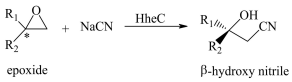

Scheme 9. Kinetic resolution of racemic epoxides by the action of HheC.[15b]

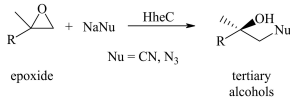

Scheme 10. Kinetic resolution of 2,2-disubstituted epoxides catalysed by HheC.[44]

in these reactions are enantiopure epoxides, β-hydroxynitriles and β-azidoalcohols which are difficult to prepare by other methods. Replacing hydrogen with methyl substituent on the chiral centre increased the *E*-value significantly ($E > 200$) with cyanide as nucleophile. The insignificance of chemical conversion of 2,2-disubstituted epoxides to β-hydroxynitriles was reflected in very high e.e., over 99%. Similar observations were made for azide as nucleophile with most tested substrates. After substrate screening, the best ones were selected for further preparative scale experiments. In the selected three cases e.e. on tertiary alcohols was > 99%, with yields 35–41%, conversions between 42 and 45% and somewhat lower, 71–81%, e. e. of the epoxides.

In the context of reactions with disubstituted epoxides, Molinaro et al.[16b] reported the screening of 96 HHDHs out of which 4 showed complete regioselectivity in the conversion of 2-alkyl-2-aryl-disubstituted epoxides to the corresponding alcohols (Scheme 11). The products are synthetically valuable chiral building blocks that can further be converted to the corresponding amino alcohols and aziridines.

HHDH-catalysed azidolysis of racemic disubstituted *trans*-epoxides to produce two possible regioisomeric azidoalcohols (Scheme 12) was studied by Calderini et al.[17b] They evaluated 19 new and 3 already known HHDHs and found that most of the enzymes were able to convert aliphatic methyl-substituted epoxide substrates to the corresponding azidoalcohols, sometimes with absolute regioselectivity. HheG exhibited high activity towards sterically more demanding disubstituted epoxides and was able to convert cyclic epoxides. This is the first report that HHDH can transform substrates other than terminal epoxides.

Majerić Elenkov et al.[45] found a novel activity of HheA in the first reported azidolysis of spiroepoxides catalysed by HHDH (Scheme 13). Highly regioselective azidolysis of spiroepoxides containing 5–7 membered cyclohexane rings was investigated. Nearly 100% conversion was obtained in enzyme reactions with high yields (above 75%). 5-numbered ring was found to be unstable, undergoing chemical hydrolysis. Comparing chemical azidolysis to HheA-catalysed, the authors showed that biotransformation proceeds with much higher rate and almost complete regioselectivity. HheC was also evaluated and it displayed, besides high regioselectivity, moderate to high enantioselectivity. HheC was even better in some cases, in terms of higher rate than HheA and $E > 200$. By testing several substrates, authors concluded that small variations in substrate configuration have a great influence on activity and enantioselectivity.

3.4. Synthesis of Statin Side Chain Precursors

HHDHs are versatile biocatalysts that can be applied for the synthesis of optically pure intermediates in the statin side chain precursors synthesis. The synthesis of such molecule, methyl 4-cyano-3-hydroxybutanoate (Scheme 14), was studied in the work reported by Majerić Elenkov et al.[46] They used variant HheC–W249P with improved enantioselectivity and activity to obtain the products methyl (*S*)-4-cyano-3-hydroxybutanoate (96.8% e.e. and 40% yield) and

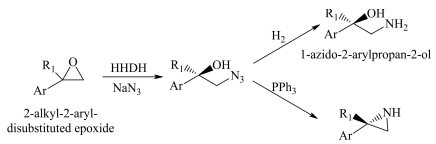

Scheme 11. Azidolysis of aromatic epoxides.[16b]

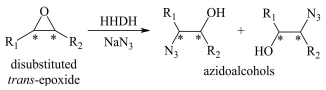

Scheme 12. HHDH-catalysed azidolysis of racemic di-substituted *trans*-epoxides resulting in the formation of two possible regioisomeric azidoalcohols.[17b]

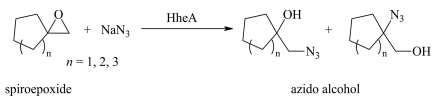

Scheme 13. HheA-catalysed ring-opening of spiroepoxides.[45]

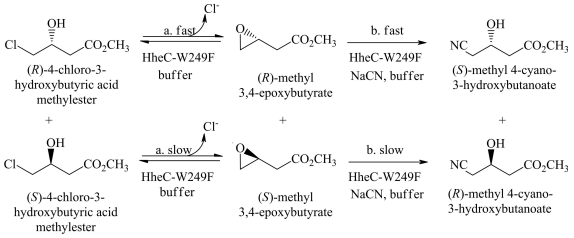

Scheme 14. Sequential kinetic resolution of methyl 4-chloro-3-hydroxybutanoate.[46]

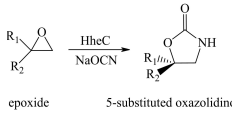

Scheme 15. Synthesis of oxazolidinones with cyanate as nucleophile catalysed by HheC.[49]

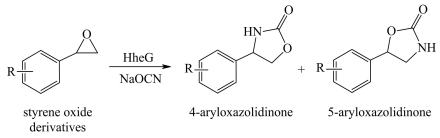

Scheme 17. HheG-catalysed ring-opening of styrene oxide derivatives.[52]

methyl (*S*)-4-chloro-3-hydroxybutanoate (95.2% e.e. and 41% yield) in a kinetic resolution. Substrate concentrations of up to 50 mM were used. A major breakthrough in the synthesis of the statin side chains was reported by Ma and co-authors[30c] who employed in vitro enzyme evolution using gene shuffling technologies to optimise the HHDH performance according to predefined criteria and process parameters. This afforded a 2500-fold improvement in the volumetric productivity per HHDH biocatalyst loading to produce ethyl (*R*)-4-cyano-3-hydroxybutyrate. Considering that this system was conducted as a two-step cascade reaction it is discussed in detail in chapter related to these systems.

Wan et al.[47] used variant HheC–W249F[39] which showed high activity in the synthesis of ethyl (*S*)-4-chloro-3-hydroxybutanoate from cheap substrates such as epichlorohydrin and 1,3-dichloro-2-propanol. Starting from 1,3-dichloro-2-propanol, 86% yield of ethyl (*S*)-4-chloro-3-hydroxybutanoate with 97.5% e.e. was achieved after only 1 hour. This is the first time that ethyl (*S*)-4-chloro-3-hydroxybutanoate was synthesised in this manner. An engineered HHDH-PL F176 M/A187R, within whole cells, was also applied[47b] to synthesize ethyl (*R*)-4-cyano-3-hydroxybutyrate. This engineered enzyme was found to have an increased efficiency for ring-opening and closure. In another work the synthesis of ethyl (*R*)-hydroxyglutarate, a key intermediate in the synthesis of rosuvastatin, was studied in a two-step system.[48] This system will be discussed in more detail in the chapter discussing cascade reactions involving HHDHs.

3.5. Synthesis of Oxazolidinones

Several papers were published on the topic of oxazolidinone synthesis by the action of HHDH. The first one was published by Majerić Elenkov et al.[49]

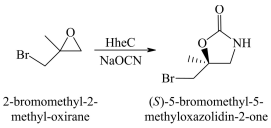

Scheme 16. Synthesis of (*S*)-5-bromomethyl-5-methyloxazolidin-2-one catalysed by HheC.[51]

where a series of 12 epoxides was tested with cyanate as nucleophile. The formed products rapidly underwent cyclization to 2-oxazolidinones, which are interesting building blocks for the preparation of pharmaceutical intermediates since oxazolidinones belong to class of protein synthesis inhibitors with wide antimicrobial activity.[50] The reactions (Scheme 15) yielded 5-substituted oxazolidinones in 69–98% e.e. on a preparative scale with HheC as biocatalyst.

Among the tested substrates, 2-bromomethyl-2-methyloxirane was further investigated together with epibromohydrin in the work by Mikleušević et al.[51] (Scheme 16). Dynamic kinetic resolution of these compounds catalysed by HheC and with OCN^- as a nucleophile was studied. The reaction was performed with the addition of catalytic amounts of bromide ions, necessary for the racemization of the less favoured substrate. Both products, (*S*)-5-bromomethyloxazolidin-2-one and (*S*)-5-bromomethyl-5-methyloxazolidin-2-one, were obtained in high yields (87 and 97%) and optical purities (>99 and 90% e.e.) on 0.5 g scale. The presence of small amounts of bromide in the case of 2-bromomethyl-2-methyloxirane increased the rate of racemization compared to the rate of ring-opening which enabled the efficient dynamic kinetic resolution.

Wan et al.[52] gave the first report on the synthesis of 4-aryloxazolidinones by HheG from *I. coccineus* (Scheme 17). Styrene oxide derivatives were used as substrates and cyanate as nucleophile. Moderate to good yields were obtained with 5–52% e.e. Both products (Scheme 17) were present but mostly 4-aryloxazolidinones (29–77% yield). Authors presented the results of the substrate concentrations influence on the product yields and assumed that the styrene oxide could inhibit the enzyme as a substrate.

3.6. Synthesis of Substituted Epoxides and Related Compounds from Prochiral Ketones in Multi-Step Reactions

Several groups investigated the possibilities to produce chiral epoxide or related chiral substituted alcohol from the corresponding ketone, as opposed to kinetic resolution in which half of the starting material is transformed into the unwanted product. Seisser et al.[53] explored a cascade reaction for converting α-chloroke-

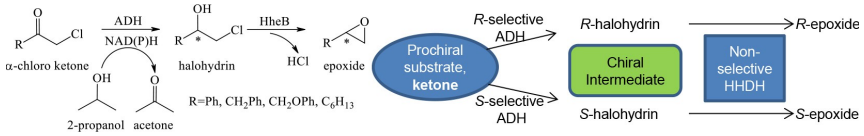

Scheme 18. Cascade reaction to synthesize enantiopure epoxides.[53]

tones into enantiopure epoxides (Scheme 18). Enantioselective alcohol dehydrogenases, i.e. *Rhodococcus ruber* ADH-'A' and *Lactobacillus brevis* ADH, were used as catalysts for the ketone reduction. HheB2 known for its high regioselectivity and low enantioselectivity was used for the second step, i.e., formation of both enantiomers of the corresponding epoxide. As dehydrogenases require coenzyme regeneration, isopropanol was used as a co-substrate, additionally facilitating substrate solubility. Whole *E. coli* cells expressing the enzymes were used. The cascade reaction (Scheme 18) results show that there is some room for improvement considering the product yield, especially in the case of ketone reduction which was poor with *Lb*ADH. Similar authors[54] evaluated this cascade system (Scheme 18) and applied hydroxy-loaded anion exchanger to shift the equilibrium of epoxide formation. 93% yield and >99% e.e. were obtained. The reaction was carried out on a preparative scale (50 mg) for different substrates. Both enantiomers were obtained by using ADHs of opposite enantioselectivities. A continuation of these studies was reported in another paper,[55] for the synthesis of enantiopure β-azidoalcohols and β-hydroxynitriles (Scheme 19). These compounds are building blocks in the synthesis of β-blockers,[56] cholesterol-lowering drugs[46,57] and antidepressants.[58] Schrittwieser and co-authors[55] included another reaction step to the cascade reaction presented in Scheme 18 from their previous work.[53] By adding azide or cyanide nucleophile to the epoxide (Scheme 19), which reacts irreversibly, they were able to obtain enantiopure β-azidoalcohols and β-hydroxynitriles. Enzymes and lyophilized cells containing the enzymes were used in this research. The reactions with cyanide were carried out stepwise, adding HHDH and CN^- after ketone reduction was finished since cyanide inhibits ADH. Cascades involving azide were carried out simultaneously in one-pot. The optical purity of the obtained epoxides was above 99% in all cases. Increase of nucleophile concentration enhances the conversion after 24 hours.

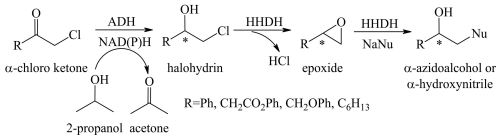

Scheme 19. Biocatalytic cascade sequence for the synthesis of enantiopure β-azidoalcohols and β-hydroxynitriles.[55]

Jin et al.[32e] investigated the preparation of (*R*)-epichlorohydrin from 1,3-dichloro-2-propanol. They set up a two-step reaction with HheC and epoxide hydrolase immobilized on perlite in separate reactors (Scheme 20). Cyclohexane was used as co-solvent to prevent the reverse reaction of the formed epichlorohydrin and to reduce spontaneous hydrolysis. By introducing cyclohexane in the system, yield was increased from the initial 19.2% to 25.1%, which is a significant result. After the completion of the first, unselective reaction step, the reaction mixture was transferred to the second reactor. In the second reactor an enantioselective step, catalysed by epoxide hydrolase, resulted in 99% e.e. of (*R*)-epichlorohydrin at 2.51 mM and 34.3% yield. The same reaction but with the opposite enantiomer production, i.e. (*S*)-epichlorohydrin, was investigated in other papers.[32i,j] Authors[32j] carried out the biotransformation by employing HheC–P175S/W249P and epoxide hydrolase within whole cells with expressed separate enzymes, as well as co-expressed. The latter approach gave better results and (*S*)-epichlorohydrin was obtained in a two-step cascade with 99% e.e. and 54.2–91.2% yield, depending on 1,3-dichloropropanol initial concentration.

Chen et al.[59] studied chiral synthesis of β-hydroxynitriles from prochiral α-haloketones with cyanide as nucleophile (Scheme 21). Low-cost system with co-expressed enzymes (ADH and HHDH) in *E. coli* was used and conversions above 99% were obtained. ADHs of opposite selectivities were chosen to show

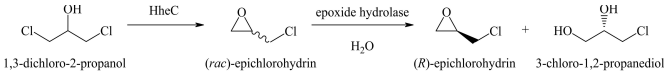

Scheme 20. The synthetic route of (*R*)-epichlorohydrin from 1,3-dichloro-2-propanol by HheC and epoxide hydrolase.[32e]

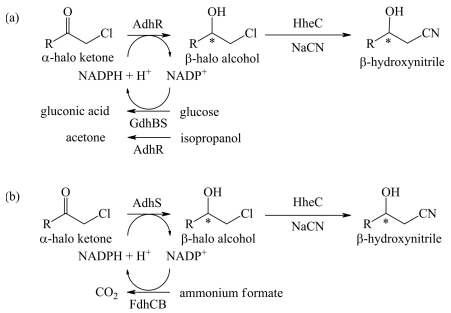

Scheme 21. Multicatalytic cascade leading to chiral β-hydroxynitriles[59] (GdhBS – glucose 1-dehydrogenase from *Bacillus subtilis*, FdhCB – formate dehydrogenase from *Candida boidinii*).

the possibility of obtaining enantiopure form of both products. To achieve efficient coenzyme regeneration, the third, regenerating, enzyme was co-expressed within the cells (Scheme 21). In that manner authors obtained higher efficiency than the one obtained by Schrittwieser et al.[55] which shows the importance of an effective coenzyme regeneration. Authors used substrates at 100 mM and, starting with methyl 4-chloro-3-hydroxybutanoate, enantiopure (*R*)-product and (*S*)-product were obtained in >99% e.e. after 2 and 4 hours, respectively. Besides aforementioned ester, 2-chloroacetophenone showed excellent results with product over 99% e.e. In comparison to the single-enzyme systems, multi-enzyme catalysis allows the realization of very complex schemes and eliminates the need for separation and purification of intermediate products.

Campbell-Verduyn et al.[16a] combined the enantioselective azidolysis of aromatic epoxides with chemical ligation of the product to alkynes producing chiral hydroxytriazoles with excellent e.e. (Scheme 7). That was the first research of the one-pot tandem biocatalytic enantioselective epoxide ring-opening and click reaction to produce optically pure hydroxytriazoles. It is a highly interesting system; however, the concentrations that were used are below industrial application level. The research was continued in another paper in a manner like Chen et al.[59] and was reported by Szymanski et al.[60] (Scheme 22). One-pot four-step synthesis of enantiopure β-hydroxytriazoles combining designer cells and click chemistry was studied. These compounds are β-adrenergic receptor blockers[61] and triazole group in general is a bioisostere of the peptide bond and an important pharmacophore.[62] The reaction was carried out using freshly prepared designer cells and cells in lyophilized form. Four reactions in a sequence enabled the synthesis of β-hydroxytriazoles enantiomers with high e.e. from simple α-haloketones. As in the previously two described cases, authors used the combination of ADH and HHDH of different enantioselectivities within *E. coli* cells to form enantiopure epoxides from the corresponding ketones with azide as nucleophile, which resulted in epoxide ring-opening and the formation of chiral azidoalcohol. The latter was converted to β-hydroxytriazole in a Cu (I)-catalysed [2+3]-dipolar cycloaddition reaction. Two-phase system consisting of buffer and octane as co-solvent, with addition of isopropanol as co-substrate for coenzyme regeneration, was applied. Cells were re-added after 6 hours of experiment after azide addition was started, as it was noticed that the conversion of the starting substrate was not complete, and that the reduction was the slower step of the reaction. After 30 minutes, a model [2+3] cycloaddition partner was added (phenylacetylene), a copper(I) source and a ligand MonoPhos to enhance the rate of the click reaction. It was found that the use of octane as co-solvent resulted in reduction of reactivity due to the extraction of phenylacetylene into the organic phase. It was also shown that lyophilized cells are as efficient as freshly prepared cells and can be stored for a longer period.

Cui et al.[63] studied a cascade composed of stereoselective hydroxylation and enantioselective dehalogenation for the synthesis of optically active β-haloalcohols from halohydrocarbons by the action of P450 and HheA10. Generally, e.e. values improved in one-pot cascades in comparison to sequential reactions. Values above 98% were obtained. In this case only 2 mM substrate concentrations were used.

Ma and co-authors reported an excellent example of a cascade system.[30c] Cascade included HHDH, a green by design two-step, three-enzyme process (Scheme 1) for the synthesis of a key intermediate in the manufacture of atorvastatin (ethyl (*R*)-4-cyano-3-hy-

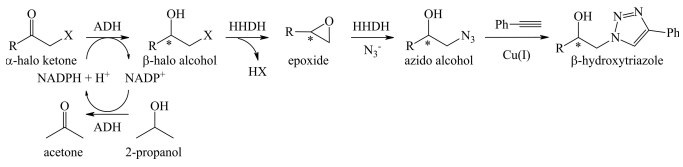

Scheme 22. Multicatalytic cascade leading to enantiopure β-hydroxytriazoles.[60]

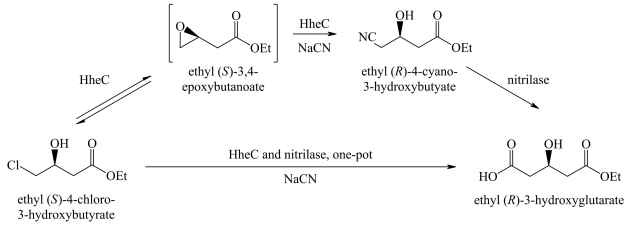

Scheme 23. Synthesis of ethyl (*R*)-3-hydroxyglutarate from ethyl (*S*)-4-chloro-3-hydroxybutyrate catalysed by HheC and nitrilase.[48]

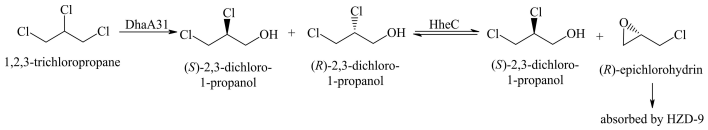

Scheme 24. Synthesis of (*S*)-2,3-dichloro-1-propanol in a cascade reaction catalysed by haloalkane dehalogenase and HHDH.[32l]

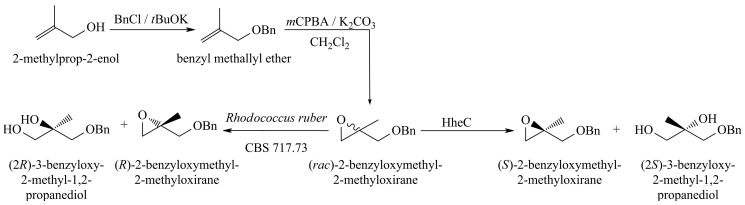

Scheme 25. Enantiocomplementary biocatalytic kinetic resolution of racemic oxirane using epoxide hydrolase and halohydrin dehalogenase.[64]

droxybutyrate). A sequential cascade has shown excellent environmental properties, E-factor 5.8 without water and 18 with water included in the calculation. Volume productivities for the first and second step were 480 and 672 $g\,L^{-1}\,d^{-1}$, respectively. Biocatalyst yields of 178 and 117 $g_{product}\,g_{biocatalyst}^{-1}$, respectively, were obtained.

Another work on a cascade reaction towards the statin side chain precursor (Scheme 23) was reported by Yao et al.[48] Authors used cells with co-expressed and separately expressed enzymes; HheC and nitrilase from *Arabidopsis thaliana*. This paper demonstrates the applicative value of this system. The reaction was carried out in a repetitive batch mode with significant amount of the obtained product. 600 mM were obtained by using co-expressed enzymes, and 900 mM with separately expressed enzymes in one-pot one-step process. The authors also tested a one-pot two-step process which resulted with 1.2 M of product (*R*)-3-hydroxyglutarate.

Bogale et al.[32l] combined haloalkane dehalogenase and HheC in a cascade reaction to transform 1,2,3-trichloropropane to (*S*)-2,3-dichloro-1-propanol with >99% e.e. and 40% yield (out of 44% of theoretical maximum) (Scheme 24). The reaction was carried out in 0.5 L reactor and the enzyme was reused 6-fold. The system was designed as a method to treat large volume liquid waste removal and the production of enantiopure (*S*)-2,3-dichloro-1-propanol.

3.7. Other Related Systems

Fuchs et al.[64] used epoxide hydrolase from *R. ruber* and HheC in a enantiocomplementary chemoenzymatic synthesis of (*R*)- and (*S*)-chromanementhol (Scheme 25). The system works as a kinetic resolution and enantiocomplementary enzymes were used to obtain both enantiomers. This approach can be used for the synthesis of similar structurally related compounds; i.e. bioactive 2-methylchromane derivatives such as clusifoliol (antitumor),[65] rhodadaurichrimaneic acid A (anti-HIV), [66] siccanin (anti-fungal)[67] and troglitazone (diabetes).[68]

Haak et al.[69] reported kinetic resolution catalysed by HheC and established protocols on multigram scale for the synthesis of 3-alkenyl and heteroaryl chloroalcohols (vicinal chloroalcohols) in enantiomerically pure form. Authors discuss rapid in situ hydrolysis of epoxides to the corresponding diols in the context of shifting the reaction equilibrium towards the products and ensuring excellent e.e. of the remaining chloroalcohol. Preparative scale reactions (10 mM) proved the ability to isolate enantiomerically pure chloroalcohols (e.e. >99%) in fair to high yields. Highly efficient kinetic resolution protocol was developed for functionalized vicinal chloroalcohols. Various unsaturated and heteroaromatic chlorohydrins were resolved in high yields (29–47%) and with excellent enantioselectivities (98.5–>99%) (Scheme 26). Starting from 20.9 g of racemic 2-chloro-1-thiophen-2-yl-ethanol, 9.8 g (94% of the theoretical yield) of (*S*)-2-chloro-1-thiophen-2-yl-ethanol was obtained with an excellent e.e. of >99%.[69]

4. Challenges in HHDH-Catalysed Reactions and Possible Solutions from the Viewpoint of Enzyme Reaction Engineering

In the revised literature, i.e. case studies, we observed that reactions are often carried out at low substrate concentration[16a,21c,32c,j,46] or it was noticed that e.e. decreases as the concentration of substrate increases, like in the case of kinetic resolution of phenyl glycidyl ether by HHDH from *P. umsongensis* YCIT1612,[21c] ring opening of aryl epoxides by HheC,[32j] and resolution of methyl 4-chloro-3-hydroxybutanoate by HheC.[46] At low concentration of substrates it is expected that side-reactions would be minimized. Furthermore, it is expected that the enzyme would have some activity towards the opposite enantiomer, which can only be detected if a wide range of concentrations of both enantiomers is evaluated. The available kinetic data showing this for enantiomers of some compounds and certain enzymes (e.g. epichlorohydrin,[18e,32d] 1-nitrophenyl-2-bromoethanol,[38] 2-chloro-1-phenylethanol,[18c,20a,b,38] *p*-nitro-2-bromo-1-phenylethanol,[18c,38–39,70] ethyl 4-chloro-3-hydroxybutyrate,[32i,71] 1,2-epoxybutane[71a,b] and phenyl glycidyl ether[21a,b]) can be found in Table S1.

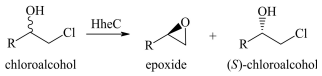

Scheme 26. Enzymatic kinetic resolution of unsaturated and heteroaromatic vicinal chloroalcohols on preparative scale.[69]

Chemical transformations such as hydrolysis intensify with the increase of epoxide concentration as already discussed elsewhere[37] and this could present a problem for the enzymatic transformation. Even if epoxide hydrolase is sometimes applied to avoid the formation of by-products,[32c] the unknown and undetermined side reactions can have a detrimental effect on the process outcome. Therefore, to minimize the effect of chemical transformation and increase the rate of enzymatic transformation, the appropriate reaction conditions must be established. Specifically, higher concentrations of enzyme and/or lower concentrations of substrates may be required to minimize the rate of chemical transformations. A solution to maximize the concentration of the product in cases like this is to select a suitable reactor setup (e.g. fed-batch), as well as process conditions, to maintain the substrate concentration low. The same approach can be used in cases of inhibition by substrate/nucleophile. In these cases, the inhibiting compound can be gradually delivered to the reactor to ensure minimal concentration of inhibitor and maximum possible reaction rate. The results presented in several papers[16a,22b,28,32d,53] lead us to conclusion that HHDHs could be inhibited or deactivated by substrate or nucleophile. It is important to evaluate and distinguish these two effects. Apart from the influences of the substrate on the enzyme, with prolonged reaction time, it is also possible that enzyme operational stability decay occurs, which is very usual for enzymes. To reach a definite conclusion, more information about the reaction kinetics and enzyme operational stability is necessary. A systematic study of the influences of substrate concentration on the initial reaction rate would give conclusive results about the enzyme kinetics and inhibitions present in these reaction systems. The aforementioned general conclusions were drawn from the literature presented in this review.

As industrial biotransformations need to be set up in a way to produce significant amount of product,[35] with high product yield and excellent enantioselectivity, a careful choice of reactor set-up, facilitated by detailed kinetic analysis, is essential. Some of the conclusions from the viewpoint of enzyme reaction engineering which refer to specific papers are given below.

In the azide-mediated ring-opening of styrene oxide derivatives HheG[28] authors evaluated the influence of substrate concentration from 5–60 mM while keeping azide concentration at 1.5 eq. Since they used different concentrations of azide for this investigation, they should not have drawn the conclusions they did. Namely, they state that product inhibition is present in their system, when in fact their results indicate substrate inhibition by azide, at least. By increasing the concentration of azide at constant concentration of epoxide, they found that the best concentration ratio is

1.5:1, because after increasing the ratio further, the yield dropped. The data were extracted from the paper and are presented in Figure 2 indicating that the enzyme might be inhibited at higher concentration of azide. This is further translated to the part of the research where they test the influence of the epoxide on reaction yield all the while keeping the concentration ratio of azide and epoxide at 1.5:1. Thus, higher concentration of epoxide means also higher concentration of azide, so it makes sense that their results obtained at 60 mM of substrate are not satisfactory, when in fact they used 90 mM of azide. Considering that the kinetic parameters were never estimated for this reaction, or any similar one, we could not test the hypotheses further by simulations.

Jin and co-authors[32d] discussed some of the mentioned issues while investigating the first kinetic resolution of *rac*-epichlorohydrin in the presence of nitrite catalysed by HheC. The basic kinetic parameters presented in this work for (*R*)- and (*S*)-epichlorohydrin enantiomers show that both can be accepted as substrates. However, the activity and affinity are higher for (*S*)- than for (*R*)-enantiomer, as expected. Michaelis constant for (*S*)-epichlorohydrin ($K_m = 17.2$ mM) is almost 2-fold lower than for (*R*)-epichlorohydrin ($K_m = 29.0$ mM). In contrast to the Michaelis constant, the calculated k_{cat}/K_m value is higher for (*S*)-epichlorohydrin, (19.4 $mM^{-1} s^{-1}$) than for (*R*)-enantiomer (2.7 $mM^{-1} s^{-1}$). The authors also tested the influence of nitrite concentration on enzyme activity, but unfortunately did not estimate the kinetic constants for this compound. Still, according to the presented data, the Michaelis constant for nitrite can be approximated at ca 22 mM. The authors state that nitrite concentration affects the enantiomeric ratio, obtaining maximum 100% at 60 mM. However, the reactions were performed at 12.8 mM of epichlorohydrin, which is below its Michaelis constant value, and considering the concentration of nitrite used in the reaction, we can assume with certainty that epichlorohydrin concentration will control the rate of enzymatic reaction. Reaction time was not discussed in these experiments, which is also important, while slower reaction needs to run longer. At low concentrations of nitrite, enzymatic reaction will be slower, and maybe not fast enough to overcome chemical reactions in the background, i.e., chemical hydrolysis of epoxide and chemical reaction between nitrite and epoxide. The results presented here could also mean that nitrite inhibits the enzymatic reaction, and that is why at nitrite concentrations above 60 mM, the e.e. once again drops, as the enzymatic reaction becomes slower again. Since concentration vs time curves were not presented in this case, further discussion is not possible. However, by using the data presented in their paper,[32d] as well as their reaction conditions, we tried to evaluate the influence of nitrite concentration on e.e. of the remaining substrate for the two case scenarios: two-substrate Michaelis-Menten kinetics and two-substrate Michaelis-Menten kinetics with included substrate inhibition by nitrite. For the latter case we needed to assume the value of K_i for nitrite which was set at 10 mM. This number is not based on any experimental data, as there are none available, but is solely taken to test our hypothesis. The results presented in Figure 3 prove our hypothesis that nitrite is an inhibitor in this reaction, while the increase of its concentration lowers the e.e. of the obtained remaining substrate.

Lutje Spelberg et al.[32b] presented the data on the effect of bromide and azide on the reaction outcome of dynamic kinetic resolution of epihalohydrins (Scheme 4) but did not analyse nor discuss them in the paper. To us, these data present valuable information showing that by increasing the concentration of azide, the yield of (*S*)-1-azido-3-bromo-2-propanol will in-

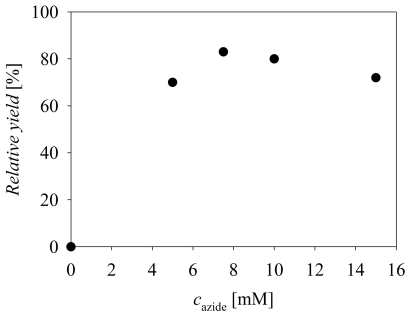

Figure 2. The influence of azide concentration on the relative product yield. The data were extracted from the work of An and co-authors.[28]

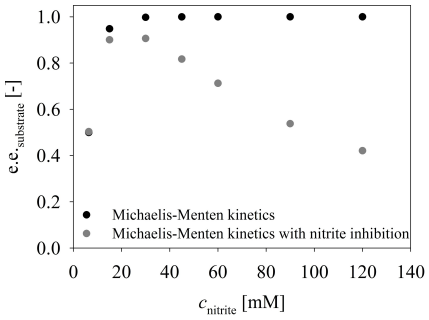

Figure 3. The influence of nitrite concentration on the e.e. of the remaining substrate for double-substrate Michaelis-Menten kinetics (black circles), and double-substrate Michaelis-Menten kinetics with included substrate (nitrite) inhibition (grey circles). Simulations are based on the data reported by Jin and co-authors.[32d]

crease, according to the Michaelis-Menten kinetics. Using the same data, it can also be concluded that azide concentration, while promoting the formation of the desired product, also inhibits the formation of the unwanted (*S*)-glycidyl azide. The same can be concluded for the influence of bromide concentration, which inhibits the formation of (*S*)-glycidyl azide, as suspected in the paper, while promoting the formation of the wanted product. This clearly shows that the interdependencies of all reactions simultaneously occurring in this system are very complex. Further investigation of the kinetics would give a valuable insight on the dependence of the process variables, as well as provide answers to reasons why something occurs. Also, it would probably show that, even though the system is highly effective with epibromohydrin as a substrate, the choice of reaction conditions is of extreme importance for a successful outcome.

From the presented results of one-pot four-step synthesis of enantiopure β-hydroxytriazoles[60] (Scheme 22) we can suggest the possibility that the rate of ketone reduction is negatively affected by the presence of organic solvents. That could be the reason why full ketone conversion was not obtained after 6 hours, as designated in the paper. The results may also indicate that coenzyme regeneration is not efficient enough. The amount of added isopropanol was 1.5 eq, which may be inadequate and possibly explain the slow transformation of haloketone to haloalcohol. Namely, the kinetic model of this coenzyme regeneration system[72] shows that the rate of acetone reduction is faster than the rate of isopropanol oxidation, even at pH 7.0 used in this work. Increasing pH favours the oxidation, even though the reduction rates are usually much higher. Findrik et al.[72] used high concentration of isopropanol; i.e. 1.5 M in comparison to 10 mM substrate in the main reaction. This high concentration ensured high pool of regenerating substrate and, what is even more important, inhibition of the acetone reduction catalysed by the same enzyme. Basically, it ensured that oxidation of isopropanol is the favoured reaction and coenzyme regeneration is more efficient. Modelling approach in general enables finding the optimal reaction conditions and, in turn, shortening of the reaction time. Furthermore, it facilitates the evaluation of increasing the scale by selecting the reactor set-up and proper reaction conditions.

To further demonstrate the potential of the enzyme kinetics research we present a simple example of simulations based on the reported azidolysis of *p*-substituted styrene oxide to form azido alcohols.[37] In this paper Lutje Spelberg et al. report that they detected chemical azidolysis, and chemical hydrolysis of epoxide as background reaction. They also consider gradual addition of azide as a solution to minimize the effect of chemical azidolysis. For this system there is only one kinetic constant reported, i.e. Michaelis constant for azide ($K_m^{azide} = 0.2$ mM, Table S1). To carry out the following simulation we assumed the value of Michaelis constant for the epoxide at 1 mM. We also assumed that the reaction rate constant of chemical azidolysis is 0.001 min mM^{-1}, which is not based on any real data. The reaction rate constant of chemical hydrolysis of epoxide was set to 0.002 min^{-1} according to our findings for similar substrates (data not yet published). We also assumed a value of maximum reaction rate to be 2.2 U mg^{-1}. The enzymatic reaction between epoxide and nucleophile was described by the double-substrate Michaelis-Menten kinetics. Chemical hydrolysis of epoxide was described by the kinetics of the first order, and the rate of chemical azidolysis by the rate of second order. Figure 4 presents the simulations for several reaction conditions in the batch reactor at different initial concentration of substrate/nucleophile,

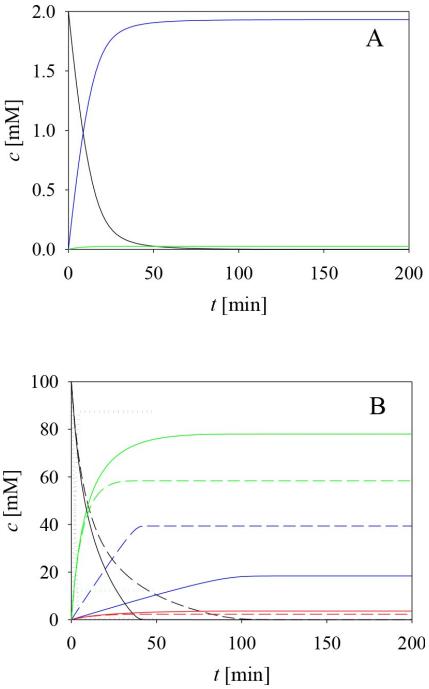

Figure 4. Simulation of azidolysis of *p*-substituted styrene oxide to form azido alcohols[37] and the reported background reactions; i.e. chemical hydrolysis of epoxide, and chemical azidolysis in the batch reactor. **A**. 2 mM substrate concentrations ($\gamma_{HHDH} = 0.1$ mg mL^{-1}). **B**. 100 mM substrate concentrations; solid line: $\gamma_{HHDH} = 0.1$ mg mL^{-1}, long dash line: $\gamma_{HHDH} = 0.5$ mg mL^{-1}, dotted line: $\gamma_{HHDH} = 10$ mg mL^{-1}. Legend: black line – epoxide, blue line – the product of enzymatic reaction, green line – the product of chemical azidolysis, red line – the product of epoxide hydrolysis.

i.e., 2 and 100 mM. From Figure 4A it can be observed that at low substrate concentrations the amount of the by-products is quite low, as reported by Lutje Spelberg et al.[37] 4% of chemical azidolysis product, and 3% of epoxide hydrolysis product. This is very similar to our simulation outcome. The situation drastically changes when 100 mM concentration of substrate is used, which is presented in Figure 4B. This reaction was simulated at three enzyme concentrations demonstrating its influence on the reaction outcome. In the first case where the lowest enzyme concentration was used, only ca 18.5% of enzymatic reaction product was obtained, whereas up to nearly 78% of chemical reaction product. The influence of epoxide hydrolysis was not that pronounced, and only ca 3.5% of this product was obtained. By increasing the concentration of enzyme in the reactor, this ratio can be changed, and up to nearly 90% of enzymatic product can be obtained. Still, these results are not satisfactory, as the used concentrations are too low for industrial application. That is why the reaction was simulated in the fed-batch reactor at the reaction conditions as designated in Figure 5 caption, and the results of the unoptimized simulation show that the concentration of the obtained product is about 392 mM. At the same time the concentration of by-products of chemical azidolysis and epoxide hydrolysis are below 0.01 and 0.1 mM, respectively. As the initial concentration of substrates in the reactor is 2 mM, side reactions have been almost completely resolved by keeping the concentration of epoxide and nucleophile very low throughout the entire reaction duration.

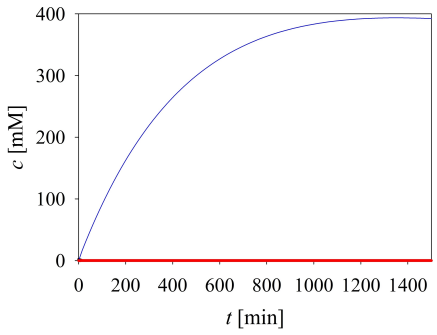

Figure 5. Simulation of azidolysis of *p*-substituted styrene oxide to form azido alcohols[37] and the reported background reactions; i.e. chemical hydrolysis of epoxide, and chemical azidolysis in the fed-batch reactor. ($V_{reactor,0}$ = 10 L, $c_{epoxide}$ = 2 mM, c_{azide} = 2 mM, q = 1 mL min^{-1}, $c_{epoxide,\ feed}$ = $c_{azide,\ feed}$ = 10 M, γ_{HHDH} = 10 mg mL^{-1}). Legend: black line – epoxide, blue line – the product of enzymatic reaction, green line – the product of chemical azidolysis, red line – the product of epoxide hydrolysis.

With this discussion and the presented simulations, hopefully, we have demonstrated the importance of kinetic models and the potential of its applications on HHDH-catalysed reactions.

5. Final Remarks and Process Consideration in Halohydrin Dehalogenase-Catalysed Reactions

Enzymatic epoxide ring-opening reactions are an excellent alternative to the chemical metal-catalysed reactions considering that they take place at room temperature and pressure, neutral pH, and in aqueous media.[10d] At the same time, they can be highly enantioselective. These reactions can be combined with other enzymatic or chemical steps forming products such as chiral 1-(2-aryl-2-hydroxyethyl) triazoles.[16a] The drawback when performing ring-closure reactions is in their reversibility, which can be overcome by several approaches; combining with a second enzyme, i.e., epoxide conversion to diol by epoxide hydrolase, HHDH-catalysed ring-opening reactions employing another nucleophile, or ion exchanger utilization for removal of HX evolved in the reaction for shifting the equilibrium.[10d] Chemical reactions that occur as a result of instability of epoxides or the uncatalyzed chemical reaction between epoxide and nucleophile can have a great influence on the biocatalytic process by negatively affecting the enantioselectivity of the reaction and the purity of the final product. This was shown in the example of the concurrent chemical transformation of epoxide with azide[37] and can be circumvented by slow addition of azide during the process, which is also much safer, considering that azide is explosive under certain circumstances. In general, even though epoxides are considered to be chemically unstable compounds, processes including epoxides can be improved by adjusting the reaction conditions and finding the right reactor set-up. Considering the low solubility of many substrates used with HHDHs, organic solvents should be employed to enable higher productivities[10d] which can negatively affect enzyme activity and stability.[73] Many reports show the application of genetically modified whole cells as biocatalysts that can improve HHDH stability.[59–60] Single enzyme systems or engineered microbial hosts have been used for decades, but the notion of assembling multiple enzymes into synthetic pathways within whole cells is a relatively new development.[74] Extensive possibilities that are coming out of this concept make it a fast growing and potentially high impact field for biomanufacturing fine and platform chemicals, pharmaceuticals and biofuels.[74] By adjusting the expression levels of specific enzymes within the cells, reaction times could be significantly reduced, and conversion

maximized.[12b] Also, higher substrate loadings could be tolerated, which is an important prerequisite for an industrial process. Another important issue is the fact that the application of designer whole cells lowers the cost of the biocatalyst,[60] and resolves the issue of cofactor regeneration where needed.[10d] It is our opinion that the systems involving HHDHs as biocatalysts hold great potential for industrial application. However, we also believe that the key to further exploitation lies in exploring the kinetic properties of these enzymes and understanding the way they behave in the presence of different substrates/products/organic solvents. All this will surely pave the way to higher substrate loadings, higher product concentrations, higher productivities, and eventually broaden their application. From the reviewed papers and presented data it was evident that there are many reported kinetic constants in the literature, which are detailed in Table S1. Those are mainly Michaelis constants, catalytic constants, and in many cases maximum reaction rates. On several occasions, inhibition constants for products or substrates and nucleophiles are also provided. Still, to obtain a full picture of the reaction system, it is crucial to evaluate all aspects of the reaction and determine the influence of all reaction compounds on the reaction rate. It can be seen in Table S1, that 1,3-dichloro-2-propanol is by far the most investigated substrate from this point of view; however, even for this system the data remain scarce in the view of enzyme reaction engineering. For example, if we look at the available data for HheC, it is not clear whether chloride ions remaining as a product after ring closure inhibit the enzyme. Also, it is not clear if the reverse reaction is significant or not, and that would be in fact the start of the kinetic investigation. Of course, one has to bear in mind that the reported kinetic constants mostly serve as a way to show the properties of new enzyme variants created by the site-directed mutagenesis.

In the last part of this review paper we summarized some of the properties of the investigated reaction systems, mostly systems investigated on preparative scale at substrate concentrations of 50 mM and higher (Table 2). We included substrates/products, biocatalysts and their origin, isolated yields, product concentrations, substrate conversions where available, type of reactor and its volume, enantiomeric excess of the product, and reaction time in the table. From these data it is evident that the research on the topic of HHDH-catalysed reaction is mostly done at low concentration scale, in batch systems, and that a lot can be done at lab-scale process development to evaluate further the possibilities of these systems. The presented table thus implies the direction of the needed new research including these enzymes for which we are sure will take place shortly in the future.

Acknowledgements

This work was partially supported by the Croatian Science Foundation (HrZZ, IP-2018-01-4493) and by CAT PHARMA (KK.01.1.1.04.0013), a project co-financed by the Croatian Government and the European Union through the European Regional Development Fund – the Competitiveness and Cohesion Operational Programme.

References

[1] a) R. N. Patel, *Food Technol. Biotechnol.* **2004**, *42*, 305–325; b) W. H. Brooks, W. C. Guida, K. G. Daniel, *Curr. Top. Med. Chem.* **2011**, *11*, 760–770; c) A. Calcaterra, I. D′Acquarica, *J. Pharm. Biomed. Anal.* **2018**, *147*, 323–340.

[2] FDA, *Novel Drug Approvals for 2019*, FDA, **2019**, https://www.fda.gov/drugs/new-drugs-fda-cders-new-molecular-entities-and-new-therapeutic-biological-products/novel-drug-approvals-2019.

[3] FDA, *Novel Drug Approvals for 2020*, FDA, **2020**, https://www.fda.gov/drugs/new-drugs-fda-cders-new-molecular-entities-and-new-therapeutic-biological-products/novel-drug-approvals-2020.

[4] N. Ran, L. Zhao, Z. Chen, J. Tao, *Green Chem.* **2008**, *10*, 361–372.

[5] U. T. Bornscheuer, G. W. Huisman, R. J. Kazlauskas, S. Lutz, J. C. Moore, K. Robins, *Nature* **2012**, *485*, 185–194.

[6] a) A. Liese, K. Seelbach, C. Wandrey, *Industrial Biotransformations*, 2nd ed., Wiley-VCH Verlag GmbH & Co. KGaA, Weinheim, **2006**; b) P. Bajpai, in *Biotechnology in the Chemical Industry: Towards a Green and Sustainable Future*, Elsevier, Amsterdam, Netherlands, **2020**.

[7] J. M. Blamey, F. Fischer, H.-P. Meyer, F. Sarmiento, M. Zinn, in *Biotechnology of Microbial Enzymes: Production, Biocatalysis and Industrial Applications* (Ed.: G. Brahmachari), Academic Press, London, United Kingdom, **2017**, pp. 347–403.

[8] Biotechnology Market Size, Share & Trends Analysis Report by Application (Health, Food & Agriculture, Natural Resources & Environment, Industrial Processing Bioinformatics), by Technology, and Segment Forecasts, 2018–2025, Grand View Research Inc., 2017.

[9] H.-P. Meyer, N. Turner, *Mini-Rev. Org. Chem.* **2009**, *6*, 300–306.

[10] a) K. Faber, W. Kroutil, *Curr. Opin. Chem. Biol.* **2005**, *9*, 181–187; b) P. Dvorak, S. Bidmanova, J. Damborsky, Z. Prokop, *Environ. Sci. Technol.* **2014**, *48*, 6859–6866; c) U. T. Bornscheuer, M. Hesseler, *Eur. J. Lipid Sci. Technol.* **2010**, 552–556; d) M. Majerić Elenkov, L. Tang, A. Meetsma, B. Hauer, D. B. Janssen, *Org. Lett.* **2008**, *10*, 2417–2420; Elenkov, H. W. Hoeffken, L. Tang, B. Hauer, D. B. Janssen, *Adv. Synth. Catal.* **2007**, *349*, 2279–2285; Elenkov, B. Hauer, D. B. Janssen, *Adv. Synth. Catal.* **2006**, *348*, 579–585; Elenkov, W. Szymanski, D. B. Janssen, in *Science of Synthesis: Biocatalysis*

in Organic Synthesis 2 (Eds.: K. Faber, W.-D. Fessner, N. Turner), Georg Thieme Verlag KG, Stuttgart, **2014**, pp. 507–527; e) Z. Y. You, Z. Q. Liu, Y. G. Zheng, *Appl. Microbiol. Biotechnol.* **2013**, *97*, 9–21; f) M. Schallmey, R. J. Floor, W. Szymanski, D. B. Janssen, in *Comprehensive Chirality, Vol. 7* (Eds.: E. M. Carreira, H. Yamamoto), **2012**, pp. 143–155.

[11] G. Hasnaoui-Dijoux, M. Majerić Elenkov, J. H. Lutje Spelberg, B. Hauer, D. B. Janssen, *ChemBioChem* **2008**, *9*, 1048–1051.

[12] a) D. B. Janssen, M. Majerić-Elenkov, G. Hasnaoui, B. Hauer, J. H. Lutje Spelberg, *Biochem. Soc. Trans.* **2006**, *34*, 291–295; b) A. Schallmey, M. Schallmey, *Appl. Microbiol. Biotechnol.* **2016**, *100*, 7827–7839; c) B.-S. Chen, F. Z. R. de Souza, *RSC Adv.* **2019**, *9*, 2102–2115.

[13] C. E. Castro, E. W. Bartnicki, *Biochemistry* **1968**, *7*, 3213–3218.

[14] T. Nakamura, T. Nagasawa, Y. Fujio, I. Watanabe, H. Yamada, *Biochem. Biophys. Res. Commun.* **1991**, *180*, 124–130.

[15] a) J. Chen, R. C. Zheng, Y. G. Zheng, Y. C. Shen, *Adv. Biochem. Eng./Biotechnol.* **2009**, *113*, 33–77; b) M. Majerić Elenkov, B. Hauer, D. B. Janssen, *Adv. Synth. Catal.* **2006**, *348*, 579–585.

[16] a) L. S. Campbell-Verduyn, W. Szymanski, C. P. Postema, R. A. Dierckx, P. H. Elsinga, D. B. Janssen, B. L. Feringa, *Chem. Commun.* **2010**, *46*, 898–900; b) C. Molinaro, A. A. Guilbault, B. Kosjek, *Org. Lett.* **2010**, *12*, 3772–3775.

[17] a) J. Koopmeiners, C. Diederich, J. Solarczek, H. Voß, J. Mayer, W. Blankenfeldt, A. Schallmey, *ACS Catal.* **2017**, *7*, 6877–6886; b) E. Calderini, J. Wessel, P. Süss, P. Schrepfer, R. Wardenga, A. Schallmey, *ChemCatChem* **2019**, *11*, 2099–2106.

[18] a) M. Schallmey, P. Jekel, L. Tang, M. Majerić Elenkov, H. W. Hoffken, B. Hauer, D. B. Janssen, *Enzyme Microb. Technol.* **2015**, *70*, 50–57; Elenkov, H. W. Hoffken, B. Hauer, D. B. Janssen, *Enzyme Microb. Technol.* **2015**, *70*, 50–57; b) F. Xue, Z. Q. Liu, N. W. Wan, Y. G. Zheng, *Appl. Biochem. Biotechnol.* **2014**, *174*, 352–364; c) J. E. van Hylckama Vlieg, L. Tang, J. H. Lutje Spelberg, T. Smilda, G. J. Poelarends, T. Bosma, A. E. van Merode, M. W. Fraaije, D. B. Janssen, *J. Bacteriol.* **2001**, *183*, 5058–5066; d) J. Koopmeiners, B. Halmschlag, M. Schallmey, A. Schallmey, *Appl. Microbiol. Biotechnol.* **2016**, *100*, 7517–7527; e) X. J. Zhang, H. Z. Deng, N. Liu, Y. C. Gong, Z. Q. Liu, Y. G. Zheng, *Bioresour. Technol.* **2019**, *276*, 154–160; f) F. Watanabe, F. Yu, A. Ohtaki, Y. Yamanaka, K. Noguchi, M. Odaka, M. Yohda, *J. Biosci. Bioeng.* **2016**, *122*, 270–275.

[19] F. Xue, X. Ya, Y. Xiu, Q. Tong, Y. Wang, X. Zhu, H. Huang, *Catal. Lett.* **2019**, *149*, 629–637.

[20] a) C. Guo, Y. Chen, Y. Zheng, W. Zhang, Y. Tao, J. Feng, L. Tang, *Appl. Environ. Microbiol.* **2015**, *81*, 2919–2926; b) L. Tang, X. Zhu, H. Zheng, R. Jiang, M. Majerić Elenkov, *Appl. Environ. Microbiol.* **2012**, *78*, 2631–2637; Elenkov, *Appl. Environ. Microbiol.* **2012**, *78*, 2631–2637; c) L. Tang, J. E. T. van Hylckama Vlieg, J. H. Lutje Spelberg, M. W. Fraaije, D. B. Janssen, *Enzyme Microb. Technol.* **2002**, *30*, 251–258; d) K. H. Hopmann, F. Himo, *J. Chem. Theory Comput.* **2008**, *4*, 1129–1137.

[21] a) F. Xue, X. Yu, Y. Shang, C. Peng, L. Zhang, Q. Xu, A. Li, *Int. J. Biol. Macromol.* **2020**, *146*, 80–88; b) F. Xue, L. H. Zhang, Q. Xu, *Appl. Microbiol. Biotechnol.* **2020**, *104*, 2067–2077; c) F. Xue, X. Ya, Q. Tong, Y. Xiu, H. Huang, *Process Biochem.* **2018**, *75*, 139–145.

[22] a) G. Hasnaoui, J. H. Lutje Spelberg, E. de Vries, L. Tang, B. Hauer, D. B. Janssen, *Tetrahedron: Asymmetry* **2005**, *16*, 1685–1692; b) N. Wan, X. Zhou, R. Ma, J. Tian, H. Wang, B. Cui, W. Han, Y. Chen, *Adv. Synth. Catal.* **2020**, *362*, 1201–1207; c) D. Senthilnathan, V. Tamilmani, P. Venuvanalingam, *J. Chem. Sci.* **2011**, *123*, 279–290; d) R. M. de Jong, J. J. Tiesinga, A. Villa, L. Tang, D. B. Janssen, B. W. Dijkstra, *J. Am. Chem. Soc.* **2005**, *127*, 13338–13343; e) K. H. Hopmann, F. Himo, *Biochemistry* **2008**, *47*, 4973–4982.

[23] Q. Liao, X. Du, W. Jiang, Y. Tong, Z. Zhao, R. Fang, J. Feng, L. Tang, *J. Biotechnol.* **2018**, *272–273*, 48–55.

[24] J. Solarczek, T. Klunemann, F. Brandt, P. Schrepfer, M. Wolter, C. R. Jacob, W. Blankenfeldt, A. Schallmey, *Sci. Rep.* **2019**, *9*, 5106.

[25] J. H. Lutje Spelberg, H. E. J. de Vries, in *Enzyme Catalysis in Organic Synthesis*, 3rd ed. (Eds.: K. Drauz, H. Gröger, O. May), Wiley-VCH Verlag GmbH & Co. KGaA, Weinheim, Germany, **2012**, pp. 363–416.

[26] A. Mikleušević, I. Primožič, T. Hrenar, B. Salopek-Sondi, L. Tang, M. Majerić Elenkov, *Tetrahedron: Asymmetry* **2016**, *27*, 930–935.

[27] R. M. de Jong, K. H. Kalk, L. Tang, D. B. Janssen, B. W. Dijkstra, *J. Bacteriol.* **2006**, *188*, 4051–4056.

[28] M. An, W. Liu, X. Zhou, R. Ma, H. Wang, B. Cui, W. Han, N. Wan, Y. Chen, *RSC Adv.* **2019**, *9*, 16418–16422.

[29] N. Kasai, T. Suzuki, Y. Furukawa, *J. Mol. Catal. B* **1998**, *4*, 237–252.

[30] a) S. C. Davis, R. J. Fox, G. W. Huisman, V. Gavrilovic, L. M. Newman (Codexis Inc.), *U. S. Patent 8101395B2*, **2005**; b) Z. Y. You, Z. Q. Liu, Y. G. Zheng, *Appl. Microbiol. Biotechnol.* **2014**, *98*, 11–21; c) S. K. Ma, J. Gruber, C. Davis, L. Newman, D. Gray, A. Wang, J. Grate, G. W. Huisman, R. A. Sheldon, *Green Chem.* **2010**, *12*, 81–86.

[31] T. Nakamura, T. Nagasawa, F. Yu, I. Watanabe, H. Yamada, *Tetrahedron* **1994**, *50*, 11821–11826.

[32] a) A. J. van den Wijngaard, P. T. Reuvekamp, D. B. Janssen, *J. Bacteriol.* **1991**, *173*, 124–129; b) J. H. Lutje Spelberg, L. Tang, R. M. Kellogg, D. B. Janssen, *Tetrahedron: Asymmetry* **2004**, *15*, 1095–1102; c) J. H. Lutje Spelberg, J. E. T. van Hylckama Vlieg, T. Bosma, R. M. Kellogg, D. B. Janssen, *Tetrahedron: Asymmetry* **1999**, *10*, 2863–2870; d) H.-X. Jin, Z. C. Hu, Z. Q. Liu, Y. G. Zheng, *Biotechnol. Appl. Biochem.* **2012**, *59*, 170–177; e) H.-X. Jin, Z.-Q. Liu, Z.-C. Hu, Y.-G. Zheng, *Biochem. Eng. J.* **2013**, *74*, 1–7; f) S. P. Zou, E. H. Du, Z. C. Hu, Y. G. Zheng, *Biotechnol. Lett.* **2013**, *35*, 937–942; g) S. P. Zou, K. Gu, Y. G. Zheng, *Biotechnol. Prog.*

2018, *34*, 784–792; h) S. P. Zou, Y. G. Zheng, E. H. Du, Z. C. Hu, *J. Biotechnol.* **2014**, *188*, 42–47; i) F. Xue, Z.-Q. Liu, Y.-J. Wang, N.-W. Wan, Y.-G. Zheng, *J. Mol. Catal. B* **2015**, *115*, 105–112; j) F. Xue, Z.-Q. Liu, Y.-J. Wang, H.-Q. Zhu, N.-W. Wan, Y.-G. Zheng, *Catal. Commun.* **2015**, *72*, 147–149; k) X. J. Zhang, P. X. Shi, H. Z. Deng, X. X. Wang, Z. Q. Liu, Y. G. Zheng, *Bioresour. Technol.* **2018**, *263*, 483–490; l) T. F. Bogale, I. Gul, L. Wang, J. Deng, Y. Chen, M. Majerić Elenkov, L. Tang, *Catalysts* **2019**, *10*, 3; Elenkov, L. Tang, *Catalysts* **2019**, *10*, 3; m) M. Majerić Elenkov, M. Čičak, A. Smolko, A. Knežević, *Tetrahedron Lett.* **2018**, *59*, 406–408; n) A. J. van den Wijngaard, D. B. Janssen, B. Witholt, *Microbiology* **1989**, *135*, 2199–2208.

[33] A. J. J. Straathof, J. A. Jongejan, *Enzyme Microb. Technol.* **1997**, *21*, 559–571.

[34] K. Faber, *Biotransformations in Organic Chemistry*, 7th ed., Springer International Publishing AG, Cham, **2018**.

[35] P. Tufvesson, J. Lima-Ramos, M. Nordblad, J. M. Woodley, *Org. Process Res. Dev.* **2011**, *15*, 266–274.

[36] a) E. P. Gillis, K. J. Eastman, M. D. Hill, D. J. Donnelly, N. A. Meanwell, *J. Med. Chem.* **2015**, *58*, 8315–8359; b) Y. Zhou, J. Wang, Z. Gu, S. Wang, W. Zhu, J. L. Acena, V. A. Soloshonok, K. Izawa, H. Liu, *Chem. Rev.* **2016**, *116*, 422–518; c) W. K. Hagmann, *J. Med. Chem.* **2008**, *51*, 4359–4369.

[37] J. H. Lutje Spelberg, J. E. van Hylckama Vlieg, L. Tang, D. B. Janssen, R. M. Kellogg, *Org. Lett.* **2001**, *3*, 41–43.

[38] L. Tang, J. H. Lutje Spelberg, M. W. Fraaije, D. B. Janssen, *Biochemistry* **2003**, *42*, 5378–5386.

[39] L. Tang, A. E. van Merode, J. H. Lutje Spelberg, M. W. Fraaije, D. B. Janssen, *Biochemistry* **2003**, *42*, 14057–14065.

[40] D. Hu, H.-H. Ye, M.-C. Wu, F. Feng, L.-J. Zhu, X. Yin, J.-F. Li, *Catal. Commun.* **2015**, *69*, 72–75.

[41] a) A. Kamal, G. B. R. Khanna, R. Ramu, *Tetrahedron: Asymmetry* **2002**, *13*, 2039–2051; b) Y. Nakajima, H. Hamashima, K. Washizuka, Y. Tomishima, H. Ohtake, E. Imamura, T. Miura, H. Kayakiri, M. Kato, *Bioorg. Med. Chem. Lett.* **2005**, *15*, 251–254.

[42] Y. Igarashi, S. Otsutomo, M. Harada, S. Nakano, *Tetrahedron: Asymmetry* **1997**, *8*, 2833–2837.

[43] N. W. Wan, J. Tian, H. Wang, M. Tian, Q. He, R. Ma, B. Cui, W. Han, Y. Chen, *Bioorg. Chem.* **2018**, *81*, 529–535.

[44] M. Majerić Elenkov, H. W. Hoeffken, L. Tang, B. Hauer, D. B. Janssen, *Adv. Synth. Catal.* **2007**, *349*, 2279–2285.

[45] M. Majerić Elenkov, I. Primožič, T. Hrenar, A. Smolko, I. Dokli, B. Salopek-Sondi, L. Tang, *Org. Biomol. Chem.* **2012**, *10*, 5063–5072.

[46] M. Majerić Elenkov, L. Tang, B. Hauer, D. B. Janssen, *Org. Lett.* **2006**, *8*, 4227–4229.

[47] a) N. W. Wan, Z. Q. Liu, F. Xue, Y. G. Zheng, *J. Biotechnol.* **2015**, *214*, 27–32; b) N. W. Wan, Z.-Q. Liu, F. Xue, Z.-Y. Shen, Y.-G. Zheng, *ChemCatChem* **2015**, *7*, 2446–2450.

[48] P. Yao, L. Wang, J. Yuan, L. Cheng, R. Jia, M. Xie, J. Feng, M. Wang, Q. Wu, D. Zhu, *ChemCatChem* **2015**, *7*, 1389–1389.

[49] M. Majerić Elenkov, L. Tang, A. Meetsma, B. Hauer, D. B. Janssen, *Org. Lett.* **2008**, *10*, 2417–2420.

[50] a) F. D. Lowy, in *Infectious Diseases, Vol. 2*, 4th ed. (Eds.: J. Cohen, W. G. Powderly, S. M. Opal), Elsevier, China, **2017**, pp. 1230–1232.e1231; b) D. I. Diekema, R. N. Jones, *Drugs* **2000**, *59*, 7–16.

[51] A. Mikleušević, Z. Hameršak, B. Salopek-Sondi, L. Tang, D. B. Janssen, M. Majerić Elenkov, *Adv. Synth. Catal.* **2015**, *357*, 1709–1714.

[52] N. Wan, J. Tian, X. Zhou, H. Wang, B. Cui, W. Han, Y. Chen, *Adv. Synth. Catal.* **2019**, *361*, 4651–4655.

[53] B. Seisser, I. Lavandera, K. Faber, J. H. Lutje Spelberg, W. Kroutil, *Adv. Synth. Catal.* **2007**, *349*, 1399–1404.

[54] J. H. Schrittwieser, I. Lavandera, B. Seisser, B. Mautner, J. H. Lutje Spelberg, W. Kroutil, *Tetrahedron: Asymmetry* **2009**, *20*, 483–488.

[55] J. H. Schrittwieser, I. Lavandera, B. Seisser, B. Mautner, W. Kroutil, *Eur. J. Org. Chem.* **2009**, *2009*, 2293–2298.

[56] J. S. Yadav, P. T. Reddy, S. Nanda, A. B. Rao, *Tetrahedron: Asymmetry* **2002**, *12*, 3381–3385.

[57] M. Müller, *Angew. Chem. Int. Ed.* **2005**, *44*, 362–365; *Angew. Chem.* **2005**, *117*, 366–369.

[58] R. J. Hammond, B. W. Poston, I. Ghiviriga, B. D. Feske, *Tetrahedron Lett.* **2007**, *48*, 1217–1219.

[59] S.-Y. Chen, C.-X. Yang, J.-P. Wu, G. Xu, L.-R. Yang, *Adv. Synth. Catal.* **2013**, *355*, 3179–3190.

[60] W. Szymanski, C. P. Postema, C. Tarabiono, F. Berthiol, L. Campbell-Verduyn, S. de Wildeman, J. G. de Vries, B. L. Feringa, D. B. Janssen, *Adv. Synth. Catal.* **2010**, *352*, 2111–2115.

[61] S. Su, J. R. Giguere, S. E. Schaus, J. A. Porco, *Tetrahedron* **2004**, *60*, 8645–8657.

[62] Y. Zhou, Y. Zhao, K. M. O'Boyle, P. V. Murphy, *Bioorg. Med. Chem. Lett.* **2008**, *18*, 954–958.

[63] H.-B. Cui, L.-Z. Xie, N.-W. Wan, Q. He, Z. Li, Y.-Z. Chen, *Green Chem.* **2019**, *21*, 4324–4328.

[64] M. Fuchs, Y. Simeo, B. T. Ueberbacher, B. Mautner, T. Netscher, K. Faber, *Eur. J. Org. Chem.* **2009**, *2009*, 833–840.

[65] a) N. P. Seeram, H. Jacobs, S. McLean, W. F. Reynolds, *Phytochemistry* **1998**, *49*, 1389–1391; b) T. Tanaka, F. Asai, M. Iinuma, *Phytochemistry* **1998**, *49*, 229–232.

[66] Y. Kashiwada, K. Yamazaki, Y. Ikeshiro, T. Yamagishi, T. Fujioka, K. Mihashi, K. Mizuki, L. M. Cosentino, K. Fowke, S. L. Morris-Natschke, K.-H. Lee, *Tetrahedron* **2001**, *57*, 1559–1563.

[67] K. J. Asabashi, *J. Antibiot.* **1962**, *15*, 161–168.

[68] K. Matsumoto, S. Miyake, M. Yano, Y. Ueki, Y. Tominaga, *The Lancet* **1997**, *350*, 1748–1749.

[69] R. M. Haak, C. Tarabiono, D. B. Janssen, A. J. Minnaard, J. G. de Vries, B. L. Feringa, *Org. Biomol. Chem.* **2007**, *5*, 318–323.

[70] a) L. Tang, D. E. Torres Pazmino, M. W. Fraaije, R. M. de Jong, B. W. Dijkstra, D. B. Janssen, *Biochemistry* **2005**, *44*, 6609–6618; b) J. H. Lutje Spelberg, L. Tang, M. van Gelder, R. M. Kellogg, D. B. Janssen, *Tetrahedron: Asymmetry* **2002**, *13*, 1083–1089.

[71] a) H. Arabnejad, M. Dal Lago, P. A. Jekel, R. J. Floor, A. W. H. Thunnissen, A. C. Terwisscha van Scheltinga, H. J. Wijma, D. B. Janssen, *Protein Eng. Des. Sel.* **2017**, *30*, 173–187; b) M. Schallmey, R. J. Floor, B. Hauer, M. Breuer, P. A. Jekel, H. J. Wijma, B. W. Dijkstra, D. B. Janssen, *ChemBioChem* **2013**, *14*, 870–881; c) N.-W. Wan, Z.-Q. Liu, K. Huang, Z.-Y. Shen, F. Xue, Y.-G. Zheng, Y.-C. Shen, *RSC Adv.* **2014**, *4*, 64027–64031; d) N. W. Wan, Z. Q. Liu, F. Xue, K. Huang, L. J. Tang, Y. G. Zheng, *Appl. Microbiol. Biotechnol.* **2015**, *99*, 4019–4029.
[72] Z. Findrik, Đ. Vasić-Rački, S. Lutz, T. Daussmann, C. Wandrey, *Biotechnol. Lett.* **2005**, *27*, 1087–1095.
[73] M. N. Gupta, *Eur. J. Biochem.* **1992**, *203*, 25–32.
[74] B. Lin, Y. Tao, *Microb. Cell Fact.* **2017**, *16*, 106.

Advanced Synthesis & Catalysis

Supporting Information

Halohydrin Dehalogenases and Their Potential in Industrial Application – A Viewpoint of Enzyme Reaction Engineering

Zvjezdana Findrik Blažević,* Nevena Milčić, Martina Sudar, and Maja Majerić Elenkov

Supplement

Halohydrin dehalogenases and their potential in industrial application – a viewpoint of enzyme reaction engineering

Zvjezdana Findrik Blažević[a]*, Nevena Milčić[a], Martina Sudar[a], Maja Majerić Elenkov[b]

[a] University of Zagreb, Faculty of Chemical Engineering and Technology, Savska c. 16, HR-10000 Zagreb, Croatia
[*corresponding author, e-mail: zfindrik@fkit.hr, tel: +385 1 4597 157, fax: +385 1 4597 133]
[b] Ruđer Bošković Institute, Bijenička c. 54, Zagreb 10000, Croatia

Table S1 Kinetic parameters of different halohydrin dehalogenases collected from the current literature.

Substrate	Nu^-	Enzyme	K_m [mM]	V_m [U mg^{-1}]	k_{cat} [s^{-1}]	K_i [mM]	Reference
1,3-Dichloro-2-propanol	-	HheC	0.010	-	37	-	[1]
		HheC	0.010 ± 0.002	-	9.3 ± 0.9		[2]
		HheC	8.5	9.0	-	Chloroacetic acid / 0.5	[3]
		HheC	10^{-2}	-	9.7	-	[4]
		HheC	0.019 ± 0.005	-	12.87 ± 0.61		[5]
		E. coli BL21 (DE3) cells expressing HheC	33	3 U mL^{-1}	-	Epichlorohydrin / 9	[6]
		$HheC_{PS}$	20.8	42.7	17.3	-	[7]
		$HheC_{PS}$ I81W	19.3	34.1	14.2		
		$HheC_{PS}$ F86N	16.8	25.9	10.8		
		$HheC_{PS}$ V94R	15.8	12	5.0		
		HheC N176A	> 3.2	-	> 3.3		[2]
		HheC N176D	> 4.4	-	> 0.97		
		HheC Y187F	0.012 ± 0.005	-	18.7 ± 1.1		
		HheC W249F	0.024 ± 0.007i	-	16.0 ± 0.9		
		HheC W139C	0.12	-	30.4		[8]
		HheC C153S	< 0.05	-	0.8 ± 0.07		[9]
		HheC H12	< 0.05	-	0.9 ± 0.1		
		HHDH from *A. tumefaciens* CCTCC M 87071	39.3	3.1 mM min^{-1}	54.9		[10]

		HHDH from *A. tumefaciens* CCTCC M 87071 with mutated 14 residues	18.4	9.1 mM min^{-1}	1011.1		
		HheC-C153S	< 0.05	-	6.0 ± 0.3		[11]
		HheC2360	10.4 ± 1.9	-	4.8 ± 0.4		[11]
		HheC C153S	< 0.1	-	6.6 ± 0.2		[12]
		HheC2656	2.8 ± 0.2	-	13.5 ± 0.3		[11]
		HHDH from *A. tumefaciens*	24.66	6.99 mmol min^{-1}	-		[13]
		HHDH from *A. tumefaciens* immobilized on ES-103B	34.04	5.35 mmol min^{-1}	-		[13]
		HHDH from *Bradyrhizobium erythrophlei* (HheB8)	13.2	21.5	-		[14]
		HHDH from *Tistrella mobilis* ZJB1405	26.8 ± 1.9	170.1 ± 2.5	74.2 ± 0.9		[15]
		HheA from *Agromyces mediolanus* ZJB120203	2.44	3.13	-		[16]
		HheA from *Arthrobacter* sp. AD2	8.5	9.0	-		[16]
		HheA from *Agromyces mediolanus* ZJB120203	4.58	3.84	-		[16]
		HheC CT1	0.029 ± 0.001	-	11.15 ± 0.08		[5]
		HheC CT2	0.014 ± 0.002		13.34 ± 0.27		[5]
		HheC CT3	0.021 ± 0.002		9.25 ± 0.13		[5]
		HheC CT4	0.155 ± 0.011		4.77 ± 0.07		[5]
		HheC CT5	0.476 ± 0.044		1.86 ± 0.04		[5]
		HheC CT6	3.456 ± 0.281		0.14 ± 0.01		[5]
		HheC CSL1	0.009 ± 0.001		21.14 ± 0.31		[5]
		HheC CSL2	0.014 ± 0.002		12.44 ± 0.27		[5]
		HheC CSL3	0.018 ± 0.004		22.56 ± 0.62		[5]
		HheC BB9	0.054 ± 0.006		45.01 ± 0.90		[17]
		HheC DG9	0.059 ± 0.013		76.27 ± 3.77		[17]
		HheC FE5	0.077 ± 0.005		53.56 ± 0.75		[17]
		HheC ZB1	0.057 ± 0.006		70.32 ± 1.51		[17]
		HheC ZB8	0.056 ± 0.005		70.32 ± 1.21		[17]
		HHDH-PL from *Parvibaculum lavamentivorans* DS-1	30.5 ± 1.12		4651 ± 8.2		[18]
		HheA	16.0 ± 2.2		2.7 ± 0.9		[19]

		HheA-D1	16.8 ± 3.0		2.5 ± 0.1		[19]
		HheC T134A + C153S	< 0.1		18.0 ± 0.3	1,3-Dichloro-2-propanol / 8.9 ± 0.5	[12]
1,3-Dibromo-2-propanol	-	HheC	-	-	> 20		[4]
		HheC T134A + C153S	< 0.1		34.9 ± 3.5	1,3-Dibromo-2-propanol / 1.7 ± 0.4	[12]
		HheC2656	1.5 ± 0.2	-	22.9 ± 1.5		[11]
		HheC2360	0.59 ± 0.05		7.8 ± 0.2		[11]
		HheC-C153S	< 0.05		6.6 ± 0.3		[11]
		HheC C153S	< 0.1		10.1 ± 0.1		[12]
		HHDH from *Tistrella mobilis* ZJB1405	20.5 ± 1.4		340.8 ± 2.9		[15]
		HHDH-PL from *Parvibaculum lavamentivorans* DS-1	43.9 ± 1.5		8015 ± 13.5		[18]
(*S*)-Epichlorohydrin	Cl^-	$HheC_{PS}$	1.38	0.42	0.18	-	[7]
		$HheC_{PS}$ I81W	4.01	0.49	0.20		
		$HheC_{PS}$ F86N	7.31	0.51	0.21		
		$HheC_{PS}$ V94R	6.75	0.57	0.24		
	NO_2^-	HheC	17.2	714.3	333.3		[20]
(*R*)-Epichlorohydrin	NO_2^-	HheC	29.0	166.8	77.8	-	[20]
rac-Epichlorohydrin	NO_2^-	HheC	19.3	384.5	179.4	-	[20]
	CN^-	*Corynebacterium* sp. strain N-1074	$K_m^{1,3\text{-DCP}}$ = 15.0 mM K_m^{cyanide}= 8.06 mM	27.8			[21]
2,3-Dichloro-1-propanol	-	HheC	0.82	-	6.5	-	[1]
		HHDH from *A. tumefaciens* CCTCC M 87071	K_m = 47.1 mM	2.0 mM min^{-1}	24.8		[10]
		HHDH from *A. tumefaciens* CCTCC M 87071 with mutated14 residues	28.6	6.7 mM min^{-1}	522.2		[10]
2,3-Dibromo-1-propanol	-	HheC	< 0.2	-	15.5	-	[4]
		HHDH-PL from *Parvibaculum lavamentivorans* DS-1	36.3 ± 0.6		4255 ± 21.5		[18]
		HHDH from *Tistrella mobilis* ZJB1405	8.9 ± 0.8	3.2 ± 1.3	1.4 ± 0.6		[15]
1-Chloro-2-propanol	-	HheC T134A + C153S	0.4 ± 0.1	-	1.0 ± 0.1	1-Chloro-2-propanol /32.8 ± 6.8	[12]
		HheC C153S	0.8 ± 0.1		1.5 ± 0.1	1-Chloro-2-propanol /108 ± 34	
		HheC2656	39.8 ± 3.4		1.23 ± 0.05	-	[11]
		HheC2360	19.6 ± 1.3		0.3 ± 0.01		

		HheC-C153S	0.7 ± 0.1		18.2 ± 0.6		
1-Bromo-2-propanol	-	HHDH-PL from *Parvibaculum lavamentivorans* DS-1	31.2 ± 2.2	-	5243 ± 9.9	-	[18]
1-Chloro-2-methyl-2-propanol	-	HheC	0.26 ± 0.06	-	68 ± 5	-	[22]
		HheC W139F	6.7 ± 0.76		44 ± 3		
		HheC W238F	0.11 ± 0.02		74 ± 2		
		HheC W249F	2.5 ± 0.59		80 ± 7		
		HheC C153S	0.53 ± 0.02		35.1 ± 0.5		[11]
		HheC2360	16.5 ± 0.8		6.5 ± 0.1		
		HheC2656	8.0 ± 0.6		10.5 ± 0.3		
		HheC C153S	0.31 ± 0.02		37.2 ± 0.4		[12]
		HheC T134A + C153S	1.2 ± 0.3		170 ± 22	1-Chloro-2-methyl-2-propanol / 4.9 ± 1.1	[12]
1-Chloro-3-cyano-2-propanol	-	HHDH-PL from *Parvibaculum lavamentivorans* DS-1	4.1 ± 0.3	-	519 ± 11.2	-	[18]
2-Chloroethanol	-	HheC	0.84	-	3.9	-	[1]
		HheC	0.84		0.5		[4]
Chloroacetone	-	HheC	2.4	-	235	-	[1]
2-Bromoethanol	-	HheC	< 0.2	-	26.5	-	[1]
		HheC	< 0.2		12.4		[4]
		HHDH-PL from *Parvibaculum lavamentivorans* DS-1	14.5 ± 0.4		4070 ± 32.2		[18]
(*R*)-1-Nitrophenyl-2-bromoethanol	-	HheC	0.009	-	22	-	[4]
(*S*)-1-Nitrophenyl-2-bromoethanol	-	HheC	0.43		7		
(*R*)-2-Chloro-1-phenylethanol	-	HheC	0.37	-	48.5	-	[1]
		HheC	0.37		12.1		[4]
		HheC	0.45 ± 0.04		14.83 ± 1.4		[23]
		P84V/F86P mutant	0.72 ± 0.13		25.1 ± 1.89		
		P84V/F86P/N176A mutant	2.54 ± 0.43		6.57 ± 0.85		
		P84V/F86P/T134C/N176A mutant	6.73 ± 0.58		3.54 ± 0.32		
		P84V/F86P/T134A/N176A mutant	8.02 ± 1.03		2.77 ± 0.2		
		T134V/L142M mutant	0.23 ± 0.07		5.61 ± 0.63		
		L142F/N176H mutant	0.19 ± 0.05		4.45 ± 0.37		
		HheA	22.6 ± 3.0		0.72 ± 0.04		[24]
		HheA V136Y/L141G	7.9 ± 0.4		0.70 ± 0.01		
		HheA V136Y/L141G/N178A	> 50		> 2.1		
		HheA N178A	> 50		> 1.0		
(*S*)-2-Chloro-1-phenylethanol	-	HheC	4.2		8.9	-	[1]

		HheC	4.2		2.2		[4]
		HheC	4.53 ± 0.46		2.37 ± 0.23		[23]
		P84V/F86P/T134C/N176A mutant	0.52 ± 0.11		13.56 ± 1.21		
		P84V/F86P/T134A/N176A mutant	0.42 ± 0.06		15.06 ± 1.03		
		T134V/L142M mutant	9.70 ± 1.18		2.19 ± 0.17		
		L142F/N176H mutant	10.31 ± 1.01		1.57 ± 0.09		
		HheA	21.2 ± 1.5		0.94 ± 0.03		[24]
		HheA V136Y/L141G	37.9 ± 6.0		0.67 ± 0.05		
		HheA V136Y/L141G/N178A	10.7 ± 0.5		2.87 ± 0.22		
		HheA N178A	4.8 ± 0.5		5.3 ± 0.14		
		P84V/F86P mutant	2.19 ± 0.61		4.24 ± 1.11		[23]
		P84V/F86P/N176A mutant	0.60 ± 0.09		29.98 ± 2.10		
rac-2-Chloro-1-phenylethanol	-	HheC-C153S	1.3 ± 0.1	-	12.6 ± 0.3	-	[11]
		HheC2360	5.3 ± 1.4		3.8 ± 0.4		
		HheC2656	3.6 ± 0.1		6.39 ± 0.08		
		HheC C153S	0.7 ± 0.1		11.7 ± 0.3	2-Chloro-1-phenylethanol / 56.6 ± 7.1	[12]
		HheC T134A + C153S	23.1 ± 5.5		100 ± 19	2-Chloro-1-phenylethanol / 8.5 ± 2.2	
		HHDH from *Tistrella mobilis* ZJB1405	28.2 ± 2.1	17.3 ± 1.5	7.5 ± 0.7	-	[15]
		HHDH-PL from *Parvibaculum lavamentivorans* DS-1	32.0 ± 1.9	-	1534 ± 21.3		[18]
rac-*p*-Nitro-2-bromo-1-phenylethanol	-	HheC	6.2	-	20	-	[4]
		HheC Asp80Asn	0.02 ± 0.002		0.1 ± 0.002		[25]
		HheC W139C	0.15		110		[8]
		HheC C153S	0.06 ± 0.01		2.5 ± 0.1		[9]
		HheC H12	0.05 ± 0.01		2.4 ± 0.2		
(*S*)-*p*-Nitro-2-bromo-1-phenylethanol	-	HheC	0.43 ± 0.05		7 ± 1	PNSHH/ 1; PNSO/ 0.01; HBr/1.2	[4, 22]
		HheC	0.250	r_0 = 2.6	-	-	[26]
		HheC N176A	> 0.89	-	> 7.2 x 10^{-3}		[2]
		HheC N176D	> 1.26	-	> 0.2		
		HheC Y187F	0.65 ± 0.01		9.1 ± 0.5		
		HheC W139F	0.06 ± 0.01		13 ± 1		[22]
		HheC W238F	0.23 ± 0.03		4 ± 0.2		
		HheC W249F	0.61 ± 0.08		2.3 ± 0.3		
(*R*)-*p*-Nitro-2-bromo-1-phenylethanol	-	HheC	0.028	r_0 = 35	16.3	-	[26]
		HheC	0.009 ± 0.003	-	22 ± 1		[4, 22]

		HheC	< 0.01		75		[1]
	I^-	HheC	-		-	I^- / 2.3	[26]
	Br^-					Br^- / 4.3	
	Cl^-					Cl^- / 13	
	F^-					F^-/ 29	
	N_3^-					N_3^-/ 2.7	
	NO_2^-					NO_2^-/ 20	
	CN^-					CN^-/ > 50	
	OCN^-					OCN^-/ 4.5	
	SCN^-					SCN^-/ 30	
	NO_3^-					NO_3^-/ 44	
	CH_3COO^-					CH_3COO^-/ 33	
	CH_3CH_2OH					CH_3CH_2OH / > 50	
	$(CH_3)_2CHNH_2$					$(CH_3)_2CHNH_2$/ > 50	
	-	HheC Tyr145Phe	0.13		0.072	-	[1]
		HheC Arg149Lys	0.056		0.33		
		HheC Arg149Gln	> 0.40		> 0.15		
		HheC N176A	> 1.4		> 0.76		[2]
		HheC N176D	> 1.5		6.3		
		HheC Y187F	0.17 ± 0.02		89 ± 3		
		HheC W139F	0.15 ± 0.04		38 ± 5		[22]
		HheC W238F	0.007 ± 0.003		21 ± 1		
		HheC W249F	0.050 ± 0.01		170 ± 13		
p-Nitrostyrene oxide	N_3^-	HheC	azide / 0.2	-			[27]
Ethyl (*S*)-4-chloro-3-hydroxybutyrate	-	HheC C153S	0.16 ± 0.01	-	2.68 ± 0.06	-	[11]
		HheC C153S	0.08 ± 0.01		2.9 ± 0.2		[9]
		HheC H12	0.06 ± 0.02		1.8 ± 0.2		
		HheC C153S W249F	0.23 ± 0.03		0.6 ± 0.1		
		H12 W249F	0.07 ± 0.02		4.1 ± 0.2		
		HheC2360	1.9 ± 0.2		8.3 ± 0.3		[11]
		HheC2656	3.5 ± 0.3		16.2 ± 0.5		
		HHDH from *Tistrella mobilis* ZJB1405	29.3 ± 1.5	62.5 ± 2.1	28.1 ± 0.9		[15]
Ethyl (*R*)-4-chloro-3-hydroxybutyrate	-	HheC C153S	< 0.05	-	4.0 ± 0.3	-	[11]
		HheC2360	2.8 ± 0.2		6.3 ± 0.2		
		HheC2656	2.5 ± 0.1		14.5 ± 0.3		
		HHDH-PL WT	7.3 ± 0.3		2222 ± 34		[28]
		HHDH-PL F176M/A187R	5.9 ± 0.2		3132 ± 35		
	CN^-	HHDH-PL WT	10.1 ± 0.1		752 ± 18		
	CN^-	HHDH-PL F176M/A187R	5.4 ± 0.2		1112 ± 27		

	-	HHDH-PL from *Parvibaculum lavamentivorans* DS-1	9.9 ± 1.4		2935 ± 9.6		[18]
		HheC2656	3.5 ± 0.3		16.2 ± 0.5		[11]
		HheC C153S	0.06 ± 0.01		5.6 ± 0.5		[9]
		HheC H12	0.07 ± 0.01		2.3 ± 0.2		
		HheC C153S W249F	0.07 ± 0.01		2.6 ± 0.3		
		H12 W249F	0.07 ± 0.02		20.5 ± 0.3		
Ethyl 4-chloroacetoacetate	-	HheC	3.5451	909 U L^{-1}	-	COBE / 0.000239	[29]
		HheC F136V/W249F	7.23	266 U L^{-1}		-	
tert-Butyl (*3 R,5 S*)-6-chloro-3,5-dihydroxyhexanoate	-	HheC2360	8.5 ± 0.2	-	204 ± 9	-	[30]
		HheC2360 W86V	4.3 ± 0.1		517 ± 13		
		HheC2360 V84G/W86V	3.1 ± 0.3		653 ± 17		
		HheC2360 V84G/W86F	1.7 ± 0.2		671 ± 14		
rac-1,2-Epoxybutane	CN^-	HheC C153S	0.5 ± 0.1	-	1.9 ± 0.5	-	[9]
	HCN	HheC-C153S	HCN / 0.6 ± 0.1		1.1 ± 0.1		[11]
	CN^-	HheC H12	2.0 ± 0.1		3.7 ± 0.1		[9]
	HCN	HheC2656	HCN / 3.1 ± 0.9		63.9 ± 8.5		[11]
	HCN	HheC2360	HCN / 4.1 ± 0.7		91.7 ± 6.6		[11]
	CN^-	HHDH from *Corynebacterium* sp. N-I074	1,2-epoxybutane/330 CN^-/ 135	90.9	-		[31]
	HCN	HheC C153S	HCN / 0.6 ± 0.1		1.7 ± 0.2		[12]
	HCN	HheC T134A + C153S	HCN / 0.8 ± 0.1		18.0 ± 0.7		[12]
(*R*)-1,2-Epoxybutane	CN^-	HheC C153S	1.0 ± 0.1	-	2.7 ± 0.1	-	[9]
	CN^-	HheC H12	2.5 ± 0.1		2.5 ± 0.1		
	CN^-	HheC C153S W249F	0.49 ± 0.08		5.9 ± 0.2		
	CN^-	H12 W249F	0.7 ± 0.1		7.4 ± 0.4		
	HCN	HheC-C153S	HCN / 0.3 ± 0.1		1.1 ± 0.1		[11]
	HCN	HheC2360	HCN / 5.2 ± 1.1		88.6 ± 9.1		
	HCN	HheC2656	HCN / 2.1 ± 0.2		52.6 ± 2.1		
(*S*)-1,2-Epoxybutane	CN^-	HheC C153S	0.7 ± 0.3	-	3.1 ± 0.5	-	[9]
	CN^-	HheC H12	1.1 ± 0.2		1.7 ± 0.2		
	CN^-	HheC C153S W249F	1.10 ± 0.06		6.2 ± 1.4		
	CN^-	H12 W249F	1.6 ± 0.2		7.7 ± 0.3		
	HCN	HheC-C153S	HCN / 0.5 ± 0.1		1.3 ± 0.1		[11]
	HCN	HheC2360	HCN / 5.4 ± 0.6		110.3 ± 5.4		
	HCN	HheC2656	HCN / 2.4 ± 0.4		33.4 ± 2.6		
rac-1,2-Epoxy-2-methylbutane	HCN	HheC-C153S	HCN / 0.9 ± 0.2	-	2.5 ± 0.2	-	[11]
		HheC2360	HCN / 11.0 ± 1.8		57.5 ± 5.8		
		HheC2656	HCN / 1.7 ± 0.4		31.3 ± 2.5		

		HheC C153S	HCN / 0.3 ± 0.05		1.5 ± 0.1		[12]
		HheC T134A + C153S	HCN / 1.6 ± 0.5		16.7 ± 1.9		
Ethyl (*S*)-3,4-epoxybutyrate	HCN	HheC2360	HCN / 4.1 ± 1.1	-	46.6 ± 6.0	-	[11]
		HheC2656	HCN / 1.4 ± 0.1		17.5 ± 0.5		
		HheC-C153S	HCN / 1.8 ± 0.4		4.8 ± 0.4		
3,3-Dimethylepoxybutane	HCN	HheC T134A + C153S	HCN / 0.9 ± 0.1	-	4.9 ± 0.3	-	[12]
		HheC C153S	HCN / 4.7 ± 1.0		1.4 ± 0.1		
rac-1,2-Epoxyhexane	HCN	HheC-C153S	HCN / 1.4 ± 0.2	-	0.51 ± 0.03	-	[11]
		HheC2360	HCN / 3.1 ± 0.8		62.0 ± 7.1		
		HheC2656	HCN / 1.7 ± 0.4		19.0 ± 0.8		
		HheC C153S	HCN / 4.1 ± 0.8		2.2 ± 0.2		[12]
		HheC T134A + C153S	HCN / 6.3 ± 0.9		18.9 ± 1.5		
Chlorocyclohexanol	-	HheG	30.0 ± 3.0; n = 2.9 ± 0.6		0.3 ± 0.03		[32]
Cyclohexene oxide	NaCN	HheG	cyclohexene oxide / 22.2 ± 2.0 NaCN / 19.8 ± 0.5 $n^{\text{cyclohexene oxide}}$ = 2.6 ± 0.5 n^{NaCN} = 3.3 ± 0.3		(2 ± 0.00) 10^{-4}		
Cyclohexene oxide	NaN_3	HheG	cyclohexene oxide / 23.7 ± 2.6 NaN_3 / 8.6 ± 0.5 $n^{\text{cyclohexene oxide}}$ = 3.0 ± 0.9 n^{NaN3} = 1.7 ± 0.2		7.8 ± 0.35		
(+)-*cis*-/(+)-*trans*-limonene oxide	NaN_3	HheG	19.4 ± 2.4, n = 1.7 ± 0.3		44 ± 0.01		
3-Chloro-1,2-propanediol	-	HheC	48	3.1	-	-	[1]
		HheC	2.20	-	3.7		[4]
		HheC C153S	4.0 ± 0.2		3.17 ± 0.05		[11]
		HheC2360	> 85		0.2		
		HheC2656	58.0 ± 21.7		0.4 ± 0.1		
		HheC T134A + C153S	5.5 ± 0.5		1.6 ± 0.1		[12]
		HheC C153S	2.8 ± 0.2		2.8 ± 0.1		
3-Bromopropane-1,2-diol	-	HheC	0.43	-	20.1	-	[4]
		HheC-C153S	0.16 ± 0.02		6.1 ± 0.1		[11]
		HheC2360	22.6 ± 1.8		5.7 ± 0.2		
		HheC2656	57.4 ± 2.8		10.8 ± 0.3		
		HheC C153S	0.7 ± 0.1		10.9 ± 0.5	3-Bromopropane-1,2-diol /77 ± 19	[12]

		HheC T134A + C153S	0.7 ± 0.1		37.0 ± 2.8	3-Bromopropane-1,2-diol / 33.3 ± 9.1	
(*R*)-Phenyl glycidyl ether	NaN_3	HHDH from *Pseudomonas pohangensis*	29.4	36.6	14.7	-	[33]
		HHDH N160L	51.0	2.4	0.96		
		HHDH Q159L	20.5	23.2	9.3		
		HHDH alphaproteobacteria isolate 46_93_T64	37.6 ± 1.2	-	6.4 ± 0.8		[34]
		HHDH N179L	64 ± 2.4		0.3 ± 0.01		
		HHDH R89Y/N179L	44.6 ± 1.8		0.26 ± 0.01		
(*S*)-Phenyl glycidyl ether	NaN_3	HHDH from *Pseudomonas pohangensis*	49.1	6.2	2.49	-	[33]
		HHDH N160L	26.7	27.42	11.0		
		HHDH Q159L	40.8	2.15	0.86		
		HHDH alphaproteobacteria isolate 46_93_T64	10.0 ± 0.6	-	16.7 ± 0.9		[34]
		HHDH N179L	13.5 ± 0.5		5.9 ± 0.2		
		HHDH R89Y/N179L	17.2 ± 0.6		4.8 ± 0.4		

HheC - from *A. radiobacter* AD1

References:

[1] J. E. van Hylckama Vlieg, L. Tang, J. H. Lutje Spelberg, T. Smilda, G. J. Poelarends, T. Bosma, A. E. van Merode, M. W. Fraaije, D. B. Janssen, *J. Bacteriol.* **2001**, *183*, 5058-5066.
[2] L. Tang, D. E. Torres Pazmino, M. W. Fraaije, R. M. de Jong, B. W. Dijkstra, D. B. Janssen, *Biochemistry* **2005**, *44*, 6609-6618.
[3] A. J. van den Wijngaard, P. T. Reuvekamp, D. B. Janssen, *J. Bacteriol.* **1991**, *173*, 124-129.
[4] L. Tang, J. H. Lutje Spelberg, M. W. Fraaije, D. B. Janssen, *Biochemistry* **2003**, *42*, 5378-5386.
[5] X. Wang, S. Han, Z. Yang, L. Tang, *J. Biotechnol.* **2015**, *212*, 92-98.
[6] S. P. Zou, E. H. Du, Z. C. Hu, Y. G. Zheng, *Biotechnol. Lett.* **2013**, *35*, 937-942.
[7] X. J. Zhang, H. Z. Deng, N. Liu, Y. C. Gong, Z. Q. Liu, Y. G. Zheng, *Bioresour. Technol.* **2019**, *276*, 154-160.
[8] L. Tang, Y. Li, X. Wang, *J. Biotechnol.* **2010**, *147*, 164-168.
[9] H. Arabnejad, M. Dal Lago, P. A. Jekel, R. J. Floor, A. W. H. Thunnissen, A. C. Terwisscha van Scheltinga, H. J. Wijma, D. B. Janssen, *Protein Eng. Des. Sel.* **2017**, *30*, 173-187.
[10] Z. Q. Liu, A. C. Gao, Y. J. Wang, Y. G. Zheng, Y. C. Shen, *J. Ind. Microbiol. Biotechnol.* **2014**, *41*, 1145-1158.
[11] M. Schallmey, R. J. Floor, B. Hauer, M. Breuer, P. A. Jekel, H. J. Wijma, B. W. Dijkstra, D. B. Janssen, *ChemBioChem* **2013**, *14*, 870-881.
[12] M. Schallmey, P. Jekel, L. Tang, M. Majerić Elenkov, H. W. Hoffken, B. Hauer, D. B. Janssen, *Enzyme Microb. Technol.* **2015**, *70*, 50-57.
[13] S. P. Zou, K. Gu, Y. G. Zheng, *Biotechnol. Prog.* **2018**, *34*, 784-792.
[14] F. Xue, J. Gao, L. Zhang, H. Li, H. Huang, *Catal. Lett.* **2018**, *148*, 1181-1189.
[15] F. Xue, Z.-Q. Liu, Y.-J. Wang, N.-W. Wan, Y.-G. Zheng, *J. Mol. Catal. B: Enzym.* **2015**, *115*, 105-112.
[16] F. Xue, Z. Q. Liu, N. W. Wan, Y. G. Zheng, *Appl. Biochem. Biotechnol.* **2014**, *174*, 352-364.
[17] X. Wang, H. Lin, Y. Zheng, J. Feng, Z. Yang, L. Tang, *J. Biotechnol.* **2015**, *206*, 1-7.
[18] N.-W. Wan, Z.-Q. Liu, K. Huang, Z.-Y. Shen, F. Xue, Y.-G. Zheng, Y.-C. Shen, *RSC Adv.* **2014**, *4*, 64027-64031.
[19] L. Tang, R. Jiang, K. Zheng, X. Zhu, *Enzyme Microb. Technol.* **2011**, *49*, 395-401.

[20] H.-X. Jin, Z. C. Hu, Z. Q. Liu, Y. G. Zheng, *Biotechnol. Appl. Biochem.* **2012**, *59*, 170-177.
[21] T. Nakamura, T. Nagasawa, F. Yu, I. Watanabe, H. Yamada, *Tetrahedron* **1994**, *50*, 11821-11826.
[22] L. Tang, A. E. van Merode, J. H. Lutje Spelberg, M. W. Fraaije, D. B. Janssen, *Biochemistry* **2003**, *42*, 14057-14065.
[23] C. Guo, Y. Chen, Y. Zheng, W. Zhang, Y. Tao, J. Feng, L. Tang, *Appl. Environ. Microbiol.* **2015**, *81*, 2919-2926.
[24] L. Tang, X. Zhu, H. Zheng, R. Jiang, M. Majerić Elenkov, *Appl. Environ. Microbiol.* **2012**, *78*, 2631-2637.
[25] R. M. de Jong, J. J. Tiesinga, H. J. Rozeboom, K. H. Kalk, L. Tang, D. B. Janssen, B. W. Dijkstra, *EMBO J.* **2003**, *22*, 4933-4944.
[26] J. H. Lutje Spelberg, L. Tang, M. van Gelder, R. M. Kellogg, D. B. Janssen, *Tetrahedron: Asymmetry* **2002**, *13*, 1083-1089.
[27] J. H. Lutje Spelberg, J. E. van Hylckama Vlieg, L. Tang, D. B. Janssen, R. M. Kellogg, *Org. Lett.* **2001**, *3*, 41-43.
[28] N. W. Wan, Z. Q. Liu, F. Xue, K. Huang, L. J. Tang, Y. G. Zheng, *Appl. Microbiol. Biotechnol.* **2015**, *99*, 4019-4029.
[29] S.-Y. Chen, X.-J. He, J.-P. Wu, G. Xu, L.-R. Yang, *Biotechnol. Bioprocess Eng.* **2014**, *19*, 26-32.
[30] Y. Luo, Y. Chen, H. Ma, Z. Tian, Y. Zhang, J. Zhang, *Scientific Reports* **2017**, *7*, 42064.
[31] T. Nakamura, T. Nagasawa, Y. Fujio, I. Watanabe, H. Yamada, *Biochem. Biophys. Res. Commun.* **1991**, *180*, 124-130.
[32] J. Koopmeiners, C. Diederich, J. Solarczek, H. Voß, J. Mayer, W. Blankenfeldt, A. Schallmey, *ACS Catal.* **2017**, *7*, 6877-6886.
[33] F. Xue, X. Yu, Y. Shang, C. Peng, L. Zhang, Q. Xu, A. Li, *Int. J. Biol. Macromol.* **2020**, *146*, 80-88.
[34] F. Xue, L. H. Zhang, Q. Xu, *Appl. Microbiol. Biotechnol.* **2020**, *104*, 2067-2077.

Appendix III

N. Milčić, M. Sudar, I. Dokli, M. Majerić Elenkov, Z. Findrik Blažević, Halohydrin dehalogenase-catalysed synthesis of enantiopure fluorinated building blocks: bottlenecks found and explained by applying a reaction engineering approach, React. Chem. Eng. 8, 673 (2023) 673-686.

Nevena Milčić: conceptualization, methodology, investigation, formal analysis, validation, writing – original draft, writing – review & editing

Martina Sudar: methodology, investigation, formal analysis, writing – review & editing

Irena Dokli: methodology, investigation, formal analysis, writing – review & editing

Maja Majerić Elenkov: funding acquisition, methodology, writing – review & editing

Zvjezdana Findrik Blažević: conceptualization, methodology, formal analysis, funding acquisition, writing – original draft, writing – review & editing

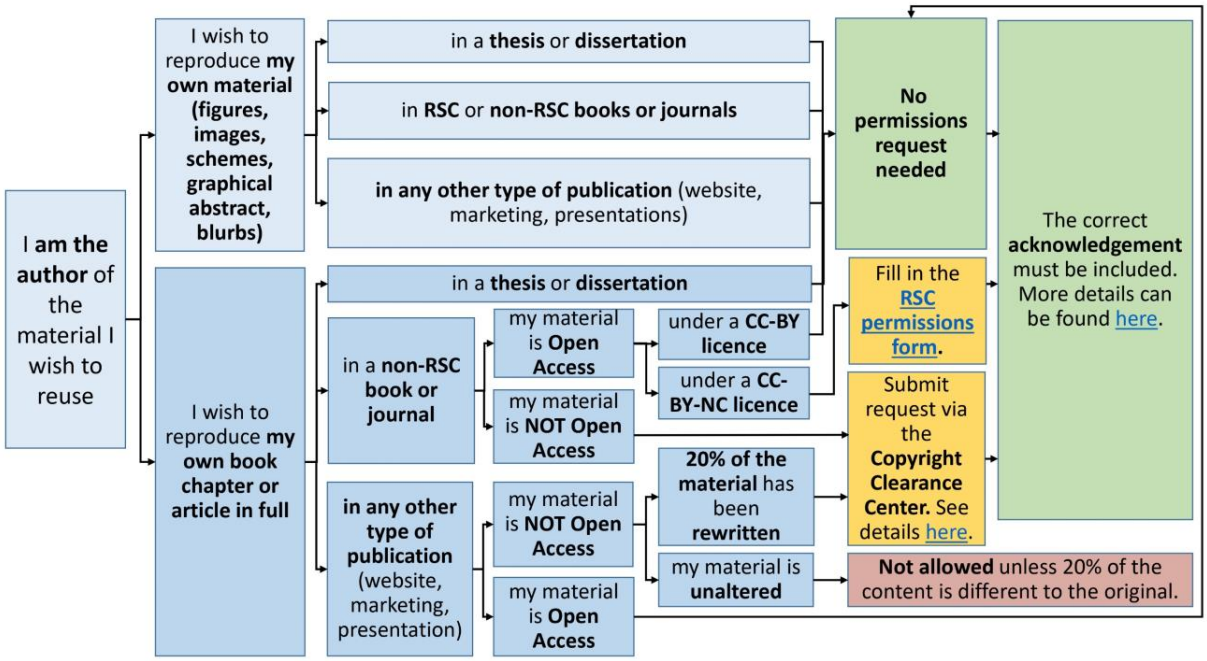

Reproduced from Milčić et. al 2023, with permission from the Royal Society of Chemistry.

Reaction Chemistry & Engineering

ROYAL SOCIETY OF CHEMISTRY

PAPER

Cite this: *React. Chem. Eng.*, 2023, **8**, 673

Halohydrin dehalogenase-catalysed synthesis of enantiopure fluorinated building blocks: bottlenecks found and explained by applying a reaction engineering approach†

Nevena Milčić, [a] Martina Sudar, [a] Irena Dokli, [b] Maja Majerić Elenkov [b] and Zvjezdana Findrik Blažević *[a]

Received 29th October 2022,
Accepted 6th December 2022

DOI: 10.1039/d2re00461e

rsc.li/reaction-engineering

Optically pure fluorinated organic azides represent synthetically valuable building blocks in a range of industrial applications. Since direct fluorination of molecules is challenging from both economic and environmental perspectives, the development of novel methods for modifying existing fluorinated synthons is highly desirable. In this work, enantioselective azidolysis of fluorinated aromatic epoxides catalysed by halohydrin dehalogenases (HHDHs) was explored. A series of 11 fluorinated epoxides were evaluated as substrates from the viewpoint of hydrolytic stability and enzyme kinetics. The synthesis of enantiopure (*R*)-2-azido-1-[4-(trifluoromethyl)phenyl]ethanol with the HheC-W249P variant was selected for detailed kinetic investigation. Reaction bottlenecks were identified and discussed from the reaction engineering perspective. Epoxide hydrolysis, enzyme inhibition and operational stability decay were found to undesirably affect the reaction outcome. Understanding the kinetic limitations and applying model-based process simulations enabled the selection of the reactor type and initial conditions favouring biotransformation. High substrate loadings are not suitable since they support hydrolysis, enzyme deactivation, and substrate inhibition. By selecting a repetitive batch reactor set-up, a reaction yield of 95% could be obtained, together with the increase in the reaction selectivity of 100% compared to the batch reactor. To the best of our knowledge, the developed mathematical model represents so far the first of its kind with HHDH enzymes, thus bringing valuable insights into the kinetic and catalytic performance of this enzyme group, as well as the reaction type. It is expected that, with minor adaptations, it could be generalized and applied to give qualitative insight into the behaviour of similar systems.

1. Introduction

Fluorine-containing building blocks (BBs) are of great importance in the agrochemical and pharmaceutical industries because the introduction of the F-atom into a molecule alters the biochemical reactivity and can induce, or enhance, a wide range of fundamental properties, *e.g.*, target efficacy, intrinsic activity, lipophilicity, biological half-life, *etc.*[1–6] However, direct fluorination, *i.e.*, the subsequent incorporation of a fluorine moiety into target molecules, is often a costly process performed under harsh conditions and with toxic reagents. Hence, methods of modifying existing fluorinated synthons are preferred.[7,8] If the BB not only contains a valuable fluorinated functional group but is also enantiomerically pure, its importance and applicability increase. Although long perceived as a green promising tool, biocatalysis is nowadays acknowledged as a mature technology for asymmetric biotransformations. Biocatalysis offers not only the possibility of obtaining optically pure compounds, but also numerous advantages over chemical synthesis in terms of cost-effectiveness and environmental impact.[9,10] Halohydrin dehalogenases (HHDHs) belong to the class of lyases (E.C. 4.5.1.-) and catalyse the reversible conversion of vicinal halohydrins and their corresponding epoxides.[11–13] The synthetic value of the HHDH enzyme group lies in their ability to employ a broad range of unnatural nucleophiles in an epoxide ring-opening reaction (azide, cyanide, cyanate, thiocyanate, nitrite, and formate), thus enabling access to novel C–C, C–S, C–N, and C–O bonds. In addition, HHDH-catalysis is often highly regioselective and enantioselective. Therefore, products of high optical purity

[a] *University of Zagreb, Faculty of Chemical Engineering and Technology, Savska c. 16, HR-10000 Zagreb, Croatia. E-mail: zfindrik@fkit.hr*
[b] *Ruđer Bošković Institute, Bijenička c. 54, HR10000 Zagreb, Croatia*
† Electronic supplementary information (ESI) available. See DOI: **https://doi.org/10.1039/d2re00461e**

can be obtained. Optical purity represents an important requirement in the pharmaceutical and fine chemical industries. HHDH-catalysis offers access to various 1,2-difunctionalized organic compounds such as β-nitro alcohols, β-azido alcohols and β-hydroxynitriles.[14–24] The importance of HHDH enzymes is best illustrated by industrial application of a C-type variant in the industrial production of the key intermediate of atorvastatin, an active ingredient of a cholesterol-lowering drug sold under the brand name Lipitor.[25] In this research, the azidolysis of fluorinated styrene oxide derivatives is in the focus. The resulting organic azides are versatile compounds that provide an excellent starting point for the synthetic preparation of amines and the corresponding derivatives, nitrogen heterocycles, such as the extensively studied 1,2,3-triazoles, *etc.*[26,27] In our previous research,[28] we showed that HHDHs can be employed in the kinetic resolution of fluorinated aromatic epoxides, giving access to the corresponding enantioenriched or enantiopure fluorinated β-azido alcohols of synthetic relevance. Although HHDHs are potent biocatalysts, lower productivity on the preparative scale occurs as a result of chemical side reactions in the system. This was also considered in our previous work where the issues in the published research with HHDH-catalysed reactions were discussed and explained from the reaction engineering point of view.[13] Reaction engineering methods offer numerous advantages for a deeper understanding and improvement of biocatalytic processes. Kinetic characterization of the biocatalytic system can reveal and address various challenges, such as the existence and extent of side reactions, deactivation and inhibition of enzymes.[29,30] Furthermore, by applying a mathematical model, different reaction conditions and scenarios can be simulated without the need for extensive experimentation.[31] Since mathematical modelling methodology has never been experimentally applied to HHDH-catalysed systems yet, kinetic data could not only provide valuable insight into enzyme characteristics and process bottlenecks, but could also be utilised in finding potential solutions.[13] In this study, we conducted kinetic characterization on the substrate scope of diverse fluorinated aromatic epoxides, gaining insight into challenges regarding their use. (*R*)-2-Azido-1-[4-(trifluoromethyl)phenyl]ethanol synthesis was chosen for the development of a comprehensive mathematical model and the evaluation of different reaction outcomes through process simulations.

2. Experimental

2.1 Materials

Tris(hydroxymethyl)aminomethane (Tris) was obtained from Acros Organics (Belgium); β-mercaptoethanol from Honeywell Fluka (USA); glycerol and dimethyl sulfoxide (DMSO) from Gram-mol d.o.o. (Croatia); ethylenediaminetetraacetic acid (EDTA), Luria-Bertani broth, agar, ampicillin and arabinose from Carl Roth (Germany); protease inhibitor cOmplete™ tablets from Roche (Switzerland); methanol (MeOH), acetonitrile (MeCN) and ethyl acetate (EtOAc) from Fisher Scientific (USA). Commercially unavailable *para*-nitro-2-bromo-1-phenylethanol (PNSHH) and *para*-nitro styrene oxide (PNSO) were synthesised as reported elsewhere,[32] while 2-(2-fluorophenyl)oxirane (**1a**), 2-(3-fluorophenyl)oxirane (**1b**), 2-(4-fluorophenyl)oxirane (**1c**), 2-(2-fluorophenyl)-2-methyloxirane (**1d**), 2-(3-fluorophenyl)-2-methyloxirane (**1e**), 2-(4-fluorophenyl)-2-methyloxirane (**1f**), 2-(2,6-difluorophenyl) oxirane (**1g**), 2-(3,4-difluorophenyl)oxirane (**1h**), 2-(2,4-difluorophenyl)oxirane (**1i**), 2-(2,4,5-trifluorophenyl)oxirane (**1j**), 2-[4-(trifluoromethyl)phenyl]oxirane (**1k**) and 2-azido-1-[4-(trifluoromethyl)phenyl]ethanol (**2k**) were synthesized as part of a separate study.[33]

2.2 Enzyme production

HheC from *Agrobacterium radiobacter* and its variants, W249P and ISM-4, were prepared as described previously.[34] In short, overexpression of HHDHs was performed within *E. coli* MC1061 cells cultivated in Luria-Bertani medium augmented with arabinose and ampicillin. Cell pellets were collected *via* centrifugation (5000 rpm, 15 min, 4 °C) and sonicated in TEMG buffer (10 mM Tris-SO_4 pH 7.5, 1 mM EDTA, 1 mM β-mercaptoethanol, 10% glycerol) with addition of a protease inhibitor. The cell-free extract (CFE) was separated from the cell debris *via* centrifugation (11 000 rpm, 40 min, 4 °C) and used without further purification in biocatalytic reactions. The protein content in the CFE was determined by the Bradford method,[35] while the HHDH activity was assessed with the activity assay described below.

2.3 Enzyme activity assay

The HHDH activity was determined *via* an assay described elsewhere.[32,36] Briefly, the initial reaction rates were determined in the ring-closure reaction of *para*-nitro-2-bromo-1-phenylethanol (PNSHH) to *para*-nitro styrene oxide (PNSO) (Scheme 1). Assays were performed in Eppendorf tubes (V_r = 500 μL) in a ThermoMixer C (Eppendorf, Germany) at 1000 rpm and 25 °C in a buffer solution (100 mM Tris-SO_4 with 5% DMSO v/v, pH 7.5 at 25 °C). The reaction mixture contained 5 mM PNSHH and the reaction was initiated by addition of the CFE to its final concentration of 0.1 mg mL^{-1}. The reaction mixture was sampled 5 times within 10% conversion and 10 μL aliquots were diluted in 390 μL of MeCN prior to filtration through 0.22 μm Chromafil Xtra H-PTFE (Macherey-Nagel, Germany). Concentrations of the substrate (PNSHH) and product (PNSO)

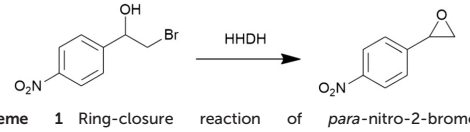

Scheme 1 Ring-closure reaction of *para*-nitro-2-bromo-1-phenylethanol (PNSHH) to *para*-nitro styrene oxide (PNSO) catalysed by HHDH enzymes.

were monitored by HPLC (see 2.9). Specific enzyme activities were calculated based on product formation employing eqn (1), where dc/dt is a change in product concentration over time and γ_E is the enzyme concentration in the reactor.

$$\text{S.A.} = \frac{dc_{\text{product}}}{dt} \cdot \frac{1}{\gamma_E} \quad (1)$$

2.4 Kinetics of hydrolytic decomposition

The first step in the kinetic characterization of epoxides was to determine their hydrolytic stability under conditions relevant for conducting biotransformation (500 mM Tris-SO_4 buffer, pH 7.5 at 25 °C, 1000 rpm). Experimental data were collected by applying the initial reaction rate method. This means that a series of experiments were conducted at different concentrations of epoxides (0–20 mM), and the initial reaction rates were estimated within substrate conversion of 10%. Graphs presenting the dependence of the initial reaction rate on the epoxide concentration were constructed. Based on the linear dependencies and molecularity of the reaction, it was assumed that the reactions follow pseudo-first-order kinetics. Kinetic parameters, that is hydrolysis constants (k_h), were estimated using SCIENTIST software (see 2.10).[37]

2.5 Preliminary kinetic measurements for the selection of the biocatalytic system

Preliminary kinetic measurements were performed on a set of 11 substrates by varying the epoxide concentration while keeping all the other conditions (V_r = 500 μL, 500 mM Tris-SO_4 buffer, pH 7.5 at 25 °C, 5% v/v DMSO, 1000 rpm) and sodium azide concentration (10 mM) constant (Scheme 2). Sampling was performed 5 times within 10% substrate conversion with respect to the conditions of the initial reaction rate method. Aliquots (10 μL) were extracted in EtOAc (500 μL) for 20 s on a Vortex V-1 Plus (Biosan, Latvia) and dried on a Na_2SO_4 layer. The samples were analysed as described in section 2.9 and a decrease in substrate concentration was monitored. The initial reaction rate of the enzymatic reaction (r_0) was calculated by subtracting the rate of hydrolytic decomposition (r_h in eqn (2), Table 1) from the total epoxide consumption according to eqn (3) (Table 1), and the data were used to estimate the values of kinetic parameters of Michaelis–Menten kinetics (K_m, V_m, K_i) applying non-linear regression methods (see 2.10).

2.6 Kinetic measurements on the selected biocatalytic system

Biocatalytic synthesis of (*R*)-2-azido-1-[4-(trifluoromethyl) phenyl]ethanol ((*R*)-**2k**) was selected for detailed kinetic characterization and model development (Scheme 3). The selected system can in fact be divided into three individual reactions as shown in the ESI† (S-1). The first is a biocatalytic reaction between (*R*)-**1k** and sodium azide for (*R*)-**2k** synthesis (S-1-A). The second reaction is an undesirable chemical reaction in which *rac*-**1k** and sodium azide participate in the formation of the α-regioisomer of the product, *rac*-2-azido-2-[4-(trifluoromethyl)phenyl]ethanol (*rac*-**3k**) (S-1-B). The third reaction is the hydrolytic decomposition of *rac*-**1k**, resulting in *rac*-2-[4-(trifluoromethyl)phenyl]-1,2-ethanediol (*rac*-**4k**) (S-1-C).

Detailed kinetic measurements were performed starting from individual substrates in each reaction. The effect of the concentration of one compound on the specific enzyme activity, *i.e.*, the reaction rate, was monitored, while the effects of all the other concentrations and conditions were excluded by being kept constant. In this way, the influences of all reaction components on the biocatalytic reaction were examined. For example, (*S*)-**1k** does not participate in the biocatalytic reaction, and *rac*-**4k** is formed as a by-product *via* chemical hydrolysis, but the influence of these compounds on the biocatalytic reaction was evaluated, since they are inevitably present in the system and can interfere with the reaction in focus.

Experiments were performed in a ThermoMixer C (Eppendorf, Germany). In the initial reaction rate experiments common conditions were V_r = 500 μL, 500 mM Tris-SO_4 buffer, pH 7.5 at 25 °C, 5% v/v DMSO, 1000 rpm, while individual concentrations for each measurement are given in the description of Fig. 1. Sampling was performed 5 times within 10% substrate conversion and product formation was monitored. The samples were processed and analysed as described in sections 2.5 and 2.9, respectively. Specific enzyme activities were calculated employing eqn (1) and the kinetic parameters of Michaelis–Menten kinetics (K_m, V_m, K_i) were estimated based on experimental data and equations of presumed kinetic models applying non-linear regression methods (see 2.10).

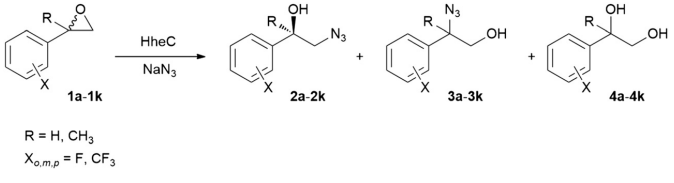

Scheme 2 Azide-mediated kinetic resolution of fluorinated aromatic epoxides (**1a**–**1k**) catalysed by HheC. The biocatalytic products are β-azido alcohols (**2a**–**2k**), α-azido alcohols (**3a**–**3k**) are produced by chemical azidolysis, while diols (**4a**–**4k**) are produced by spontaneous chemical hydrolysis. Investigated molecules are listed in Table 2.

Table 1 Kinetic equations for azidolysis of epoxides **1a**–**1k** and the developed mathematical model for **2k** synthesis

Kinetic equations		Mass-balance equations		Operational stability	
$r_h = k_h \cdot c_{rac\text{-epoxide}}$	(2)	$\frac{dc_{(R)\text{-}\mathbf{1k}}}{dt} = -0.5 \cdot r_h - r_1$	(7)	$\frac{d\gamma_{W249P}}{dt} = -k_d \cdot \gamma_{W249P}$	(12)
$\frac{dc_{epoxide}}{dt} = -r_0 - r_h$	(3)	$\frac{dc_{(S)\text{-}\mathbf{1k}}}{dt} = -0.5 \cdot r_h$	(8)	$k_d = \frac{c_{0,\mathbf{1k}} \cdot a}{c_{0,\mathbf{1k}} + b}$	(13)
$r_0 = \frac{V_m \cdot c_{epoxide}}{K_m^{epoxide} + c_{epoxide}}$	(4)	$\frac{dc_{NaN_3}}{dt} = -r_1$	(9)		
$r_0 = \frac{V_m \cdot c_{epoxide}}{K_m^{epoxide} + c_{epoxide} + \frac{c_{epoxide}^2}{K_i^{epoxide}}}$	(5)	$\frac{dc_{\mathbf{2k}}}{dt} = r_1$	(10)		
$r_1 = \frac{V_{m0} \cdot e^{-k_d \cdot t} \cdot c_{(R)\text{-}\mathbf{1k}} \cdot c_{NaN_3} \cdot \gamma_{W249P}}{\left(K_m^{NaN_3} + c_{NaN_3}\right) \cdot \left(K_m^{(R)\text{-}\mathbf{1k}} \cdot \left(1 + \frac{c_{\mathbf{2k}}}{K_i^{\mathbf{2k}}} + \frac{c_{(S)\text{-}\mathbf{1k}}}{K_i^{(S)\text{-}\mathbf{1k}}} + \frac{c_{\mathbf{4k}}}{K_i^{\mathbf{4k}}} + \frac{c_{DMSO}}{K_i^{DMSO}}\right) + c_{(R)\text{-}\mathbf{1k}} + \frac{c_{(R)\text{-}\mathbf{1k}}^2}{K_i^{(R)\text{-}\mathbf{1k}}}\right)}$	(6)	$\frac{dc_{\mathbf{4k}}}{dt} = r_h$	(11)		

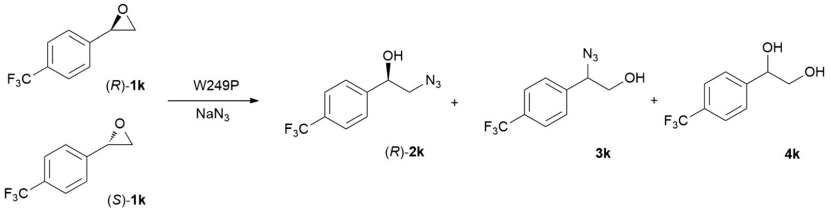

Scheme 3 (*R*)-**2k** synthesis through W249P-catalysed and azide-mediated kinetic resolution of *rac*-**1k**.

2.7 Batch and repetitive batch experiments

In order to confirm the accuracy and applicability of the developed mathematical model, model validation was performed by conducting experiments in a batch reactor and repetitive batch reactor. Experiments were conducted at different concentrations of the substrate (**1k**, sodium azide) and enzyme, whereas experimental details for individual reactors are given in the description of Fig. 3. Conducting the reaction in the repetitive batch mode in fact means that the concentrations of the substrate and product in the reactor were monitored over time and, according to the consumption of the substrate, a new amount was added in portions when it was depleted. Experimental details of the repetitive experiment are given in the description of Fig. 4. Data sampling and processing were conducted in the same manner as in the kinetic measurements. It is important to emphasize that the total volume of the taken samples was always below 10% of the working volume.

2.8 Enzyme stability

The enzyme kinetic stability during incubation with substrates and the enzyme operational stability in the batch reactor were assessed. To test the kinetic stability the enzyme was incubated in buffer (Tris-SO_4, pH 7.5 at 25 °C) and in the presence of different concentrations of the substrate and nucleophile. The influences of both epoxide and sodium azide concentrations were evaluated, but the experiments were carried out in the presence of only one substrate at a time, so that the biocatalytic reaction between them would not occur. The effects of different epoxide (5, 20, 50 mM) and sodium azide (20, 50, 100 mM) concentrations on the enzyme stability (0.40 mg mL^{-1}) during incubation were investigated. First, the incubation/reaction was started by adding a certain amount of enzyme to the reactor. At regular intervals, sampling was performed and the enzyme in the aliquot was separated from the rest of the reaction mixture (*i.e.* substrates, products, solvent) on an Amicon™ Ultra-0.5 centrifugal unit (Merck, USA; 4 °C, 14 000 rpm, 5 min). The enzyme was fully recovered from the filter, washed three times with buffer, and used for the initiation of the activity assay (see 2.3). Prior to measurements, the enzyme was resuspended in buffer to the same final volume, adjusted to match the final protein concentration of 0.40 mg mL^{-1} at the beginning of the stability monitoring. Based on the rate of product formation, specific enzyme activities were calculated according to eqn (1), and from the decline of specific activities over time, data on enzyme stability were obtained and numerically expressed as estimated operational stability decay constants (k_d) (see 2.10).

2.9 Chromatographic analyses

Instruments. Liquid chromatography analyses were performed on an LC-40 Nexera Lite from Shimadzu (Japan) with a PDA detector. Gas chromatography analyses were performed on a GC-2014 from Shimadzu (Japan) with an FID.

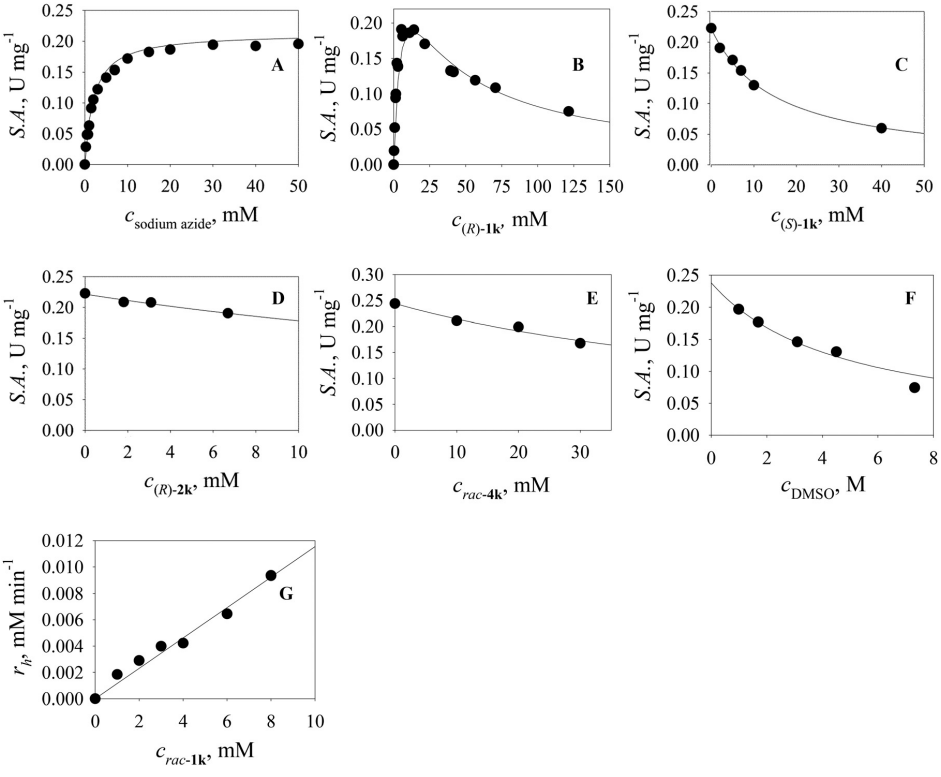

Fig. 1 Kinetics of azidolysis of *rac*-**1k** (V_r = 500 μL; 500 mM Tris-SO_4; pH 7.5; 25 °C; DMSO 10% v/v; 1000 rpm; γ_{W249P} = 0.652 mg mL^{-1}). Dependence of the enzyme specific activity on the concentration of: A. sodium azide 0–50 mM ($c_{(R)\text{-}1k}$ = 10 mM); B. (*R*)-**1k** 0–120 mM ($c_{sodium\ azide}$ = 10 mM); C. (*S*)-**1k** 0–40 mM ($c_{(R)\text{-}1k}$ = 10 mM, $c_{sodium\ azide}$ = 10 mM); D. (*R*)-**2k** 0–6.5 mM ($c_{(R)\text{-}1k}$ = 10 mM, $c_{sodium\ azide}$ = 10 mM). E. *rac*-**4k** 0–30 mM ($c_{(R)\text{-}1k}$ = 20 mM, $c_{sodium\ azide}$ = 10 mM); F. DMSO 0–7 M ($c_{(R)\text{-}1k}$ = 20 mM, $c_{sodium\ azide}$ = 10 mM). G. Influence of *rac*-**1k** concentration on its hydrolytic degradation 0–8 mM. Black dots – experimental data, line – mathematical model.

Activity assay (HPLC). The PNSHH and PNSO concentrations in the enzyme activity assay were determined on a Kinetex core–shell C18 column (2.6 μm, 100 × 4.6 mm; Phenomenex, USA) with gradient analysis, using previously prepared calibration curves (ESI† S-2). Mobile phases: mobile phase A was 80% v/v MeCN in ultrapure water with 0.1% v/v TFA, while mobile phase B was ultrapure water with 0.1% v/v TFA. Analysis: 40–30% phase B from 0 to 5 min, 30–40% phase B from 5 to 5.5 min, 40% phase B to 7 min. Conditions: flow rate 1.5 mL min^{-1}, wavelength 310 nm, oven temperature 30 °C, duration 7 min. Retention times: PNSHH 3.6 min; PNSO 3.9 min.

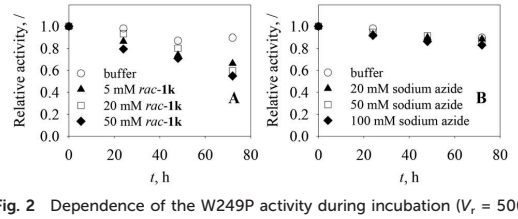

Fig. 2 Dependence of the W249P activity during incubation (V_r = 500 μL; 500 mM Tris-SO_4; pH 7.5; 25 °C; DMSO 10% v/v; 1000 rpm; γ_{W249P} = 0.40 mg mL^{-1}) with different concentrations of: A. *rac*-**1k** (0, 5, 20, 50 mM); B. sodium azide (0, 20, 50, 100 mM).

Substrate screening (HPLC). The concentrations of epoxides **1a–1k** for hydrolysis assessment and preliminary kinetics measurements were determined on a Kinetex core–shell C18 column (2.6 μm, 100 × 4.6 mm; Phenomenex, USA) with an isocratic method using previously prepared calibration curves (ESI† S-3). Mobile phase: 50% v/v MeOH in ultrapure water. Analysis: 5 to 15 min, depending on the epoxide analysed. Conditions: flow rate 1 mL min^{-1}, wavelength 254 nm, oven temperature 30 °C. Retention times: **1a** 11.4 min; **1b** 10.4 min; **1c** 7.7 min; **1d** 12.6 min; **1e** 11.9 min; **1f** 11.0 min; **1g** 7.4 min; **1h** 9.7 min; **1i** 10.3 min; **1j** 12.6 min; **1k** 10.1 min.

Selected system – achiral analysis (HPLC). **1k** and **2k** were analyzed on a Kinetex core–shell C18 column (2.6 μm, 100 × 4.6 mm; Phenomenex, USA) with gradient analysis, using

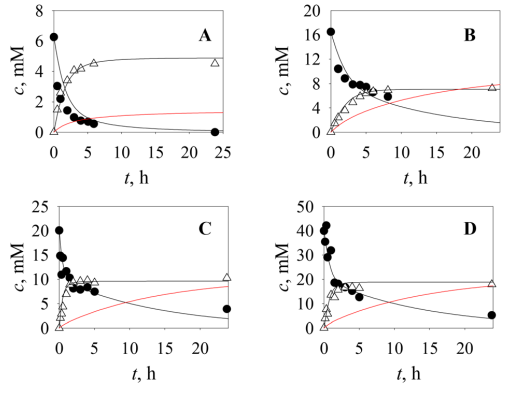

Fig. 3 Validation of the mathematical model in batch reactor experiments (V_r = 2 mL; 500 mM Tris-SO_4; pH 7.5; 25 °C; DMSO 10% v/v; 1000 rpm) conducted with different initial conditions: A. $c_{\text{sodium azide}}$ = 5 mM, $c_{(R)\text{-}\mathbf{1k}}$ = 6.26 mM, γ_{W249P} = 0.30 mg mL^{-1}; B. $c_{\text{sodium azide}}$ = 25 mM, $c_{rac\text{-}\mathbf{1k}}$ = 16.5 mM, γ_{W249P} = 0.33 mg mL^{-1}; C. $c_{\text{sodium azide}}$ = 10 mM, $c_{rac\text{-}\mathbf{1k}}$ = 20.1 mM, γ_{W249P} = 2.0 mg mL^{-1}; D. $c_{\text{sodium azide}}$ = 20 mM, $c_{rac\text{-}\mathbf{1k}}$ = 40.3 mM, γ_{W249P} = 2.0 mg mL^{-1}. Legend: experimental data represented as symbols (black dots – (*R*)-**1k**; white triangles – (*R*)-**2k**), mathematical model as lines (black lines – **1k** and **2k**, red line – **4k**). Due to the weak response, **4k** was not monitored experimentally but was simulated by the model.

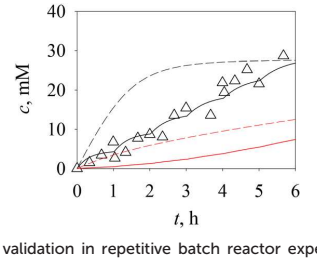

Fig. 4 Model validation in repetitive batch reactor experiments (V_r = 500 μL; 500 mM Tris-SO_4; pH 7.5; 25 °C; DMSO 10% v/v; 1000 rpm) with initial conditions $c_{\text{sodium azide}}$ = 5 mM, $c_{rac\text{-}\mathbf{1k}}$ = 10 mM, γ_{W249P} = 2 mg mL^{-1}, with addition of 5 mM NaN_3 and 10 mM *rac*-**1k** every one hour until 5th hour. Legend: experimental data represented as symbols (white triangles – (*R*)-**2k**), mathematical model as lines (black lines – **2k**, red line – **4k**). Dashed lines represent concentrations of (*R*)-**2k** and **4k** that would be obtained in a batch reactor when the same amount of substrates would be used all at once ($c_{\text{sodium azide}}$ = 30 mM, $c_{rac\text{-}\mathbf{1k}}$ = 60 mM, γ_{W249P} = 2 mg mL^{-1}), instead of in a repetitive manner. Due to the weak response, **4k** was not monitored experimentally but was simulated by the model.

previously prepared calibration curves (ESI† S-4). Mobile phases: mobile phase A was 90% v/v MeCN in ultrapure water, while mobile phase B was ultrapure water. Analysis: 60–40% phase B from 0 to 15 min, 40–60% phase B from 15 to 20 min, 60% phase B to 22 min. Conditions: flow rate 1 mL min^{-1}, wavelength 190 nm, oven temperature 30 °C, duration 22 min. Retention times: **1k** 14.8 min; **2k** 12.3 min.

Selected system – chiral analysis of the substrate (GC). (*R*)-**1k** and (*S*)-**1k** were analyzed on a capillary column Chirasil-DEX CB (25 m × 0.25 mm; Agilent Technologies, USA) with an isothermal method using previously prepared calibration curves (ESI† S-5). Analysis: 120 °C during 10 min. Conditions: split injector at 250 °C, FID at 300 °C. Retention times: (*R*)-**1k** 6.2 min; (*S*)-**1k** 6.6 min.

Selected system – chiral analysis of the product (HPLC). (*R*)-**2k** and (*S*)-**2k** were monitored on a Chiralcel OJ-3 column (3 μm, 100 × 4.6 mm; Daicel, Japan) with isocratic analysis, while the (*R*)-**2k** concentration was determined by using previously prepared calibration curves (ESI† S-6). Mobile phase: 2.5% v/v isopropanol in *n*-hexane. Analysis: 32 min. Conditions: flow rate 1 mL min^{-1}, wavelength 220 nm, oven temperature 30 °C. Retention times: (*R*)-**2k** 26.7 min; (*S*)-**2k** 29.0 min.

2.10 Data processing and mathematical modelling

All data were processed by using the software package SCIENTIST.[37] The values of kinetic parameters were estimated from experimentally obtained data and kinetic model equations (Table 1) by employing non-linear regression methods (*i.e.*, simplex and least squares fit) implemented in the SCIENTIST software.[37] The simplex method was used for more complex models where the initial values of parameters were not known, *e.g.* substrate inhibition kinetics. By applying this approach we obtained the values of kinetic parameters closer to the optimal ones. Subsequently, the least squares fit method was used to obtain the optimal values of kinetic parameters. First, the hydrolytic stability of the 11 epoxides was assessed. Based on the linear dependence and the reaction molecularity, it was assumed that the reaction rate is a pseudo-first order (eqn (2), Table 1). This means that in the hydrolysis reaction, one molecule of epoxide and one molecule of water participate, but the latter is in such an excess that the concentration can be considered unchanged throughout the experimental period and mathematically included as a part of the hydrolysis constant (k_h). Hydrolytic constants were estimated in each case based on experimental data (ESI† S-7) and eqn (2) (Table 1) by employing linear regression analysis.

In the second step, the kinetic resolution of epoxides with sodium azide catalysed by HheC was examined. In cases where a biocatalytic reaction occurred, the basic reaction kinetics was investigated. The substrate concentration decline in the biocatalytic reaction was monitored and the rate of the enzymatic reaction was calculated by subtracting the rate of hydrolytic decomposition from the total epoxide consumption (eqn (3), Table 1). Specific enzyme activities were calculated (eqn (1)) and the kinetic parameters were estimated by employing the standard Michaelis–Menten kinetic model (eqn (4), Table 1) or the Michaelis–Menten model with included substrate inhibition (eqn (5), Table 1), depending on the trend of the obtained experimental data.

In the selected biocatalytic system, *i.e.* kinetic resolution of *rac*-**1k**, detailed kinetic measurements were performed and the kinetic model was developed. The reaction rate of

azidolysis is represented by r_1 (eqn (6), Table 1) and defined by a double substrate Michaelis–Menten kinetics with included substrate inhibition by (*R*)-**1k** and competitive inhibitions by **2k**, (*S*)-**1k**, **4k** and DMSO which were experimentally verified. The equation also includes the operational stability decay of the enzyme, which was described by the 1st order kinetics. By coupling kinetic models (eqn (2) and (6), Table 1) with mass balance equations for the batch reactor (eqn (7)–(11), Table 1), the mathematical model was developed. A coefficient of 0.5 in eqn (7) and (8) defines that the racemic mixture is composed of 50% of each enantiomer, and the amount of **1k** that enters the reactor is divided between the mass balances for both enantiomers.

In order to complete the mathematical model, it was necessary to estimate the operational stability decay rate constants (k_d). The constants were estimated from individual activity measurements performed with the enzyme separated

Table 2 The hydrolytic reaction rate constants (k_h) for selected epoxides (**1a**–**1k**) and estimated kinetic parameters (V_m, K_m, K_i, k) in *rac*-epoxide azidolysis catalysed by HheC from *Agrobacterium radiobacter*

Compound	Epoxide	Structure	k_h [min^{-1}]	V_m [U mg^{-1}]	K_m [mM]	K_i [mM]
2-(2-Fluorophenyl)oxirane	**1a**		0.0042 (R^2 = 0.9996)	0.47	12.24	—
2-(3-Fluorophenyl)oxirane	**1b**	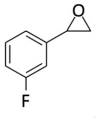	0.0063 (R^2 = 0.9935)	0.14	2.35	—
2-(4-Fluorophenyl)oxirane	**1c**	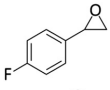	0.0025 (R^2 = 0.9449)	37.78	304.33	0.08
2-(2-Fluorophenyl)-2-methyloxirane	**1d**	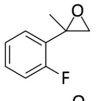	0.0059 (R^2 = 0.9899)	First order kinetics, k = 0.0098 min^{-1}		
2-(3-Fluorophenyl)-2-methyloxirane	**1e**	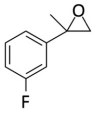	0.0057 (R^2 = 0.9984)	4.77	405.39	0.15
2-(4-Fluorophenyl)-2-methyloxirane	**1f**	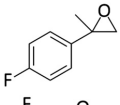	0.0078 (R^2 = 0.9963)		n.a.	
2-(2,6-Difluorophenyl)oxirane	**1g**	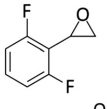	0.0028 (R^2 = 0.9984)	First order kinetics, k = 0.0079 min^{-1}		
2-(3,4-Difluorophenyl)oxirane	**1h**	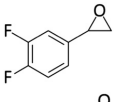	0.0048 (R^2 = 0.9835)		n.a.	
2-(2,4-Difluorophenyl)oxirane	**1i**	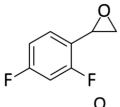	0.0052 (R^2 = 0.9977)		n.a.	
2-(2,4,5-Trifluorophenyl)oxirane	**1j**	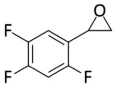	0.0039 (R^2 = 0.9976)		n.a.	
2-(4-(Trifluoromethyl)phenyl)oxirane	**1k**	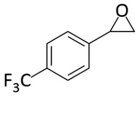	0.0012 (R^2 = 0.9921)	0.52	14.32	—

during the reaction, whereby it was assumed that the operational stability decay rate of the enzyme could be described by 1st order kinetics (eqn (12), Table 1). The estimated constants were incorporated into the main mathematical model (eqn (6), Table 1). The dependence of the decay rate constants on the initial concentration of epoxide in the reactor was described with eqn (13) (Table 1) which was based on experimental findings.

3. Results and discussion

3.1 Substrate selection based on hydrolytic stability and preliminary kinetic characterization

In theory, HHDH-catalysed azidolysis of racemic aromatic epoxides results in optically pure or enriched 1,2-azidoalcohols and unreacted enantiomers of epoxides, both valuable fluorinated building blocks. However, there are several challenges regarding the utilization of styrene oxide derivatives as substrates that should be addressed. Fluorinated aromatic epoxides are only sparingly soluble in water (*e.g. para*-fluorostyrene oxide solubility at 25 °C is 0.26 g L^{-1}),[38] as well as susceptible to spontaneous hydrolysis,[39] which reduces the product yield. There are numerous scientific papers reporting about novel and attractive HHDH activities in a highly enantioselective fashion;[20,21,23,24,40] however, the aforementioned challenges are more pronounced when conducting reactions on a higher scale than the millimolar one, which is usually utilised for screening.[13] In this study, we originally selected 11 fluorinated aromatic epoxides as potential substrates (**1a–1k**, Table 2). The set of epoxides was selected based on the importance of their kinetic resolution products. Small, optically pure, aromatic molecules with a fluorine substituent represent highly valuable building blocks in the pharmaceutical, agrochemical and fine chemical industries.[1,4] Although the selected epoxides differ only in the number and position of fluorine atoms, final properties, such as hydrolytic stability and the enzyme affinity towards them, can vary widely. This is why all of the substrates were initially screened in an aqueous medium for hydrolytic decomposition, and those distinguished as more stable were kinetically characterized in HheC-catalysed azidolysis. The estimated hydrolytic constants for the pseudo-first order kinetics are presented in Table 2. Depending on the structure, different stabilities were obtained. Epoxide **1k**, with k_h of 0.0012 min^{-1}, is hydrolytically the most stable, followed by **1c** with a reaction rate constant of 0.0025 min^{-1}. With epoxide **1f**, a rather high hydrolytic constant was obtained (k_h = 0.0078 min^{-1}), which in practice means that the half-life time, calculated as $\ln 2/k_h$, is inconveniently low ($t_{1/2}$ = 1.5 h). Due to the considerable instability, **1f** was excluded from further studies, while the remaining 10 epoxides were evaluated in the azidolysis reaction (Table 2). Preliminary screening showed that HheC displays a somewhat lower activity towards the epoxide bearing three F-substituents at different positions (**1j**), hence it was omitted as well. From the epoxides with two F-substituents (**1g**, **1h**, **1i**), **1g** was selected as the representative on account of having the highest stability among the group. Therefore, in the second phase of research, epoxides **1a–1e**, **1g** and **1k** were kinetically characterized in HheC-catalysed azidolysis. From the estimated values of the kinetic parameters (Table 2), several conclusions can be drawn. In the evaluated concentration range, azidolysis of epoxides **1d** and **1g** follows the first order kinetics with reaction rate constants of the same order of magnitude as the hydrolysis rate constant. This means that increasing the concentration of the substrate is prerequisite for acceleration of the azidolysis reaction; however, at the same time, the rate of chemical hydrolysis significantly increases. Due to the linear response, to which chemical azidolysis may also contribute, **1d** and **1g** were excluded from further research. Although azidolysis of **1a** can be described with the Michaelis–Menten equation, in separate studies, *ortho*-substituted epoxides proved to be poorer substrates for HheC in terms of lower reaction enantioselectivity.[33] While the enzyme obviously accepts substrates with substituents in the *meta*-position (**1b** and **1e**), the maximum reaction rates are somewhat lower compared to those in the *para*-position (**1c** and **1k**). In this work, *para*-substituted fluorinated epoxides proved to be the best candidates for HheC-catalysed reactions. Based on the elimination, when the enzyme activity, affinity and hydrolytic stability were assessed, **1c** and **1k** were considered for further evaluation.

3.2 Enzyme selection based on batch experiments

After narrowing the substrate selection to **1c** and **1k**, two HheC enzyme variants were introduced to the research, W249P and ISM-4. In our previous study,[28] we showed that W249P exhibits significantly higher activity compared to the wild-type enzyme towards fluorinated styrene oxide derivatives. In this work, the estimated kinetic parameters show that their maximum reaction rates are comparable, but the W249P variant shows better affinity towards **1k** (Tables 2 and 4, K_m values). ISM-4, obtained by Wu *et al.*[41] through iterative saturation mutagenesis, proved to have improved thermostability but similar activity towards substrate 1,3-dichloro-2-propanol as the wild-type. We conducted batch experiments with both substrates and variants under the

Table 3 Azidolysis of **1k** with W249P and ISM-4 variants. Reaction conditions: 20 mM *rac*-epoxide, 20 mM sodium azide, 10% v/v DMSO, V_r = 3 mL, 1000 rpm, 25 °C, γ_{W249P} = 1 mg mL^{-1} or γ_{ISM-4} = 2 mg mL^{-1} (the enzyme concentration was selected to achieve the same activity towards model substrate PNSHH)

Enzyme variant	Conversion[a,b]	ee_S	ee_P	*E*-Value
W249P	52 (49)	94	>99	>200
ISM-4	51 (50)	98	>99	>200

[a] Conversion determined after 2 h of reaction. [b] Intrinsic value in parentheses is the conversion catalysed by the enzyme.

Table 4 Estimated kinetic parameters for the kinetic resolution of **1k** with the W249P variant

Parameter	Unit	Value
V_m	U mg^{-1}	0.404 ± 0.019
$K_m^{NaN_3}$	mM	2.014 ± 0.198
$K_m^{(R)\text{-}\mathbf{1k}}$	mM	1.095 ± 0.171
$K_i^{(R)\text{-}\mathbf{1k}}$	mM	32.861 ± 2.962
$K_i^{(S)\text{-}\mathbf{1k}}$	mM	2.256 ± 0.140
$K_i^{\mathbf{2k}}$	mM	6.136 ± 0.895
$K_i^{\mathbf{4k}}$	mM	6.532 ± 0.501
K_i^{DMSO}	mM	373.011 ± 29.862
k_h	min^{-1}	$1.154 \cdot 10^{-3} \pm 1.211 \cdot 10^{-4}$
a	min^{-1}	$0.00218 \pm 3.141 \cdot 10^{-5}$
b	mM	7.168 ± 0.332

same conditions, whereas the enzyme concentration was adjusted according to the same activity towards the PNSHH substrate. Azidolysis of **1k** proceeded with complete regioselectivity and $E > 200$ in the case of both variants (ESI† S-8, Table 3). Although both enzymes displayed activity towards **1c**, azidolysis was not completely enantioselective. Thus, **1k** was imposed as a more interesting substrate and as such was chosen for further research. In comparison of ISM-4 and W249P, the latter was chosen for further research due to its higher enzyme activity. The selected biocatalytic system is kinetic resolution of *rac*-**1k** with the W249P enzyme, *i.e.*, synthesis of (*R*)-**2k** with the remaining unreacted (*S*)-**1k**. These compounds represent valuable and diverse building blocks in medicinal chemistry, primarily on account of chirality and possession of the CF_3 moiety, which has electron-withdrawing properties important for defense against oxidative metabolism of small molecules.[42] Structural analogues of (*R*)-**2k** have a broad spectrum of applications in scientific research, *i.e.*, research focused on the synthesis of molecules displaying antiplasmodial, antibacterial, antitubercular and beta-blocker activities.[43,44]

3.3 Solvent ratio

As an aromatic epoxide, **1k** is only sparingly soluble in aqueous medium. Low solubility limits the substrate availability to the enzyme, thus kinetic measurements above *ca.* 10 mM are impossible without introduction of a solvent into the reaction mixture. DMSO is the most commonly used solvent for HHDH-catalysed reactions based on its low toxicity and amphipathic properties. By utilizing 10% DMSO, good substrate solubility is achieved up to 150 mM or more (maximum experimentally tested value), thus enabling kinetic measurements in this concentration range. The utilized DMSO volume ratio does not induce protein structure degradation as a side effect, which was discussed in our previous research.[36] However, due to possible competitive inhibition by DMSO,[36] the solvent concentration effect on the enzyme activity also needs to be tested and included in the kinetic model.

3.4 Enzyme kinetics

The kinetics of (*R*)-**2k** synthesis was determined from the independent experimental measurements obtained by the initial reaction rate methods and the dependencies of enzyme specific activities on concentrations were plotted (Fig. 1). Based on the experimental data obtained by employing the initial reaction rate method, the kinetic equations were written for two reactions taking place simultaneously (eqn (2) and (6), Table 1). Based on the equations and experimental data, the apparent kinetic parameters were estimated (Table 4). When compared to the kinetic parameters of HheC (Table 2), it can be observed that a very similar maximum activity was obtained, but the affinity of W249P towards **1k** was significantly better by an order of magnitude. The reaction rate for (*R*)-**2k** synthesis was described by double-substrate Michaelis–Menten kinetics with substrate (*R*)-**1k** inhibition, competitive inhibition by (*S*)-**1k**, **4k** and DMSO, and product inhibition by (*R*)-**2k**. Although the V_m value is rather low (0.4 U mg^{-1}), low K_m values point out to a high affinity for substrates. The K_m value for sodium azide is twice as high as that for the epoxide, which indicates a stronger binding affinity for the epoxide. While sodium azide displays the usual Michaelis–Menten behaviour (Fig. 1-A), (*R*)-**1k** exhibits substrate inhibition (Fig. 1-B), which is manifested in a decrease in specific activity at concentrations higher than 10 mM. Although the reaction is completely enantioselective, as shown and described in the ESI† (S-9), the influence of the (*S*)-**1k** enantiomer was investigated since the kinetic resolution is always initiated from a racemic mixture. It was shown that the opposite enantiomer of **1k** has a rather strong inhibitory effect (Fig. 1-C). The resulting biocatalytic product (*R*)-**2k** also proved to display inhibitory properties (Fig. 1-D), although to a lesser extent, which is manifested in a three-fold higher inhibition constant (Table 4). In addition to the main biocatalytic reaction, other two reactions occur: hydrolytic decomposition of *rac*-**1k**, whereby *rac*-**4k** is produced, and chemical reaction between *rac*-**1k** and sodium azide, whereby *rac*-**3k** is formed (ESI† S-1-B). The spontaneous formation of α-azido alcohols and its effect on the specific activity of the enzyme have not been investigated, since it was found in batch experiments that the **3k** percentage in the final product is negligibly low (about 1% of the product is formed after 6 h). On the other hand, the influence of hydrolysis was thoroughly examined. In addition to the evaluation of the hydrolytic decomposition rate (Fig. 1-G), the influence of the concentration of the formed **4k** on the specific activity was evaluated (Fig. 1-E). The diol (**4k**) has an effect on the enzyme activity similar to (*R*)-**2k**. Finally, the effect of the DMSO concentration on the enzyme activity was assessed and described as competitive inhibition (Fig. 1-F).[36]

3.5 Enzyme stability during incubation with substrates

Enzyme stability during incubation at different concentrations of the epoxide and nucleophile was

investigated. W249P proved to be very stable in reaction buffer medium during the investigated time (Fig. 2, empty circles). To evaluate if different reaction compounds affect the enzyme activity over time, W249P was also incubated at different concentrations of the epoxide (Fig. 2-A) and nucleophile (Fig. 2-B). It was found that azide ions do not affect the stability of the enzyme, since the retained activity within the observed time in the buffer medium was the same as that in the presence of the highest concentration of the nucleophile used. However, in the presence of **1k**, faster W249P deactivation occurred. It was therefore expected that the substrate will have a negative effect on the enzyme operational stability as well, based on our previous experience.[31,45] This is valuable information indicating a possibility that the enzyme operational stability will follow a similar trend in the reactor.

3.6 Model validation

The mathematical model of the reaction in the batch reactor is represented by the kinetic (eqn (2) and (6), Table 1) and the reactor model (eqn (7)–(11), Table 1). Its validation was done by conducting experiments in the batch reactor at different initial concentrations of the substrate, nucleophile and enzyme. The enzyme operational stability was monitored in a repeated set of experiments and decay rates were estimated from the enzyme activity in time. The estimated k_d values were included in the model. The mathematical model described the data well (Fig. 3), which can be substantiated by the statistical data provided in the ESI† (S-10). By using lower concentrations of **1k** (Fig. 3-A and B), it is possible to circumvent the region where substrate inhibition is severe, thus achieving a satisfactory concentration of (*R*)-**2k**. At higher concentrations of **1k** (Fig. 3-C and D), it is necessary to considerably increase the amount of enzyme since the enzymatic reaction rate is reduced by inhibition with (*R*)- and (*S*)-**1k**, while, at the same time, the hydrolysis rate is faster. Fig. 4 presents a comparison between batch and repetitive batch reactors, where the total substrate concentration used is the same in both cases, but in the latter, it is distributed in several portions, each time after substrate consumption. By feeding the substrate into the reactor, the same amount of (*R*)-**2k** can be produced while less **4k** is formed, on account of a more favourable distribution of epoxide concentrations over time, which will be discussed in more detail later (see 3.7).

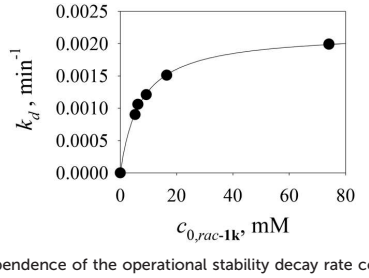

Fig. 5 Dependence of the operational stability decay rate constant on the **1k** initial concentration. The deactivation constants were estimated from enzyme stability monitoring during batch experiments.

Batch experiments were performed in duplicate. Besides monitoring the concentrations of the substrate and products by chromatographic analyses, samples were taken to monitor the enzyme activity in the reactor (ESI,† S-11).

From the obtained activity profiles in time, the operational stability decay rate constants were estimated (ESI† S-12) using eqn (12) (Table 1). As initially anticipated, it was found that the operational stability decay rate is dependent on the initial epoxide concentration in the batch reactor (Fig. 5). The mathematical expression describing hyperbolic dependence of the deactivation constant on the initial concentrations of epoxide is given by eqn (13) (Table 1), and the parameters for k_d estimation are presented in Table 4. Knowing the dependence of the operational stability decay rate constant on the initial concentration of the epoxide is very valuable information allowing the selection of conditions in different reactors where enzyme deactivation, although inevitable, will be minimized.

3.7 Model based remarks

Although at first sight this system may seem like a simple reaction, (*R*)-**2k** synthesis is not a trivial task due to the presence of hydrolytic decomposition of the substrate, inhibition by almost all reaction compounds (except the nucleophile) and the concentration dependent operational stability decay rate of the enzyme. The reaction was first simulated in the batch reactor due to the simplicity of its set-up. As substrate inhibition becomes more prominent at concentrations above 10 mM (*R*)-**1k**, its concentration should be kept around this value to ensure the maximum reaction rate. A lower substrate concentration is also beneficial for reduction of the hydrolysis effect and enzyme operational stability decay, as they are more pronounced at higher epoxide concentrations. Hydrolysis leads not only to the accumulation of diol in the reactor, which slows down the reaction, but also to the decrease in the final yield of (*S*)-**1k**. The beneficial influence of lower epoxide concentrations on the resolution outcome is already shown by Fig. 3-B, where 16 mM *rac*-**1k** was employed with 0.33 mg mL^{-1} enzyme. Here, the reaction yield was 88% after 5 h, where the yield (*Y*, %) is defined as the ratio of the quantity of the obtained product to the theoretically possible maximum product quantity. At higher epoxide concentrations, the reaction yield drastically drops, as demonstrated *via* process simulations (Fig. 6-A). If higher substrate concentrations are used, the concentration of the enzyme in the reactor must be sufficiently high to convert (*R*)-**1k** to (*R*)-**2k** fast enough to minimize substrate conversion to the unwanted diol. In Fig. 3-D, 2 mg mL^{-1} enzyme was employed to resolve 40 mM *rac*-**1k** with a yield of 90% after 2 h. With process simulations it is also demonstrated how the change in enzyme concentration affects the process outcome. As shown in

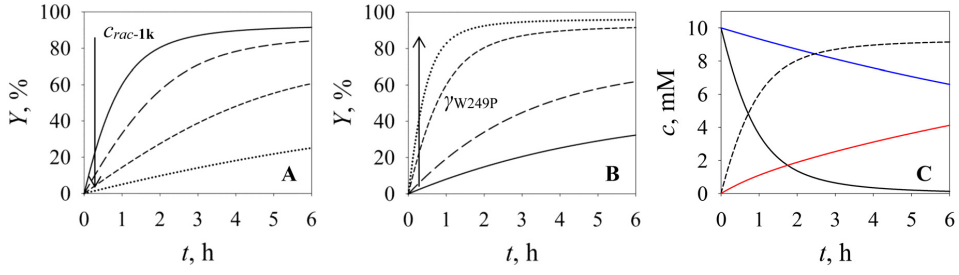

Fig. 6 Batch reactor set-up: simulation of A. influence of epoxide concentration on the reaction outcome (γ_{W249P} = 1 mg mL^{-1}, concentration of azide is equimolar to concentration of *rac*-**1k**), legend: full line – 20 mM, long dashed line – 50 mM, short dashed line – 100 mM, dotted line – 200 mM. B. Influence of enzyme concentration on the reaction outcome ($c_{rac\text{-}1k}$ = 20 mM, $c_{sodium\ azide}$ = 20 mM), legend: full line – 0.1 mg mL^{-1}, long dashed line – 0.25 mg mL^{-1}, short dashed line – 1 mg mL^{-1}, dotted line – 2 mg mL^{-1}. C. Reaction progress of the biocatalytic reaction (conditions: $c_{rac\text{-}1k}$ = 20 mM, $c_{sodium\ azide}$ = 20 mM, γ_{W249P} = 1 mg mL^{-1}), legend: full black line – (*R*)-**1k**, full blue line – (*S*)-**1k**, short dashed line – (*R*)-**2k**, red line – **4k**.

Fig. 6-B, lower enzyme concentrations (full line for 0.1 mg mL^{-1} and long-dashed line for 0.25 mg mL^{-1}) result in a dramatic yield drop, because hydrolysis becomes the predominant process. However, very good outcome is achieved in the case when 1 mg mL^{-1} (short-dashed line) and 2 mg mL^{-1} (dotted line) enzyme concentrations are utilized. In the case when 1 mg mL^{-1} enzyme catalyzes 20 mM *rac*-**1k** resolution with an equimolar concentration of sodium azide, a reaction yield of 90% is obtained after 3 h (Fig. 6-B, short-dashed line). The outcome should also be revised in terms of reaction time, since a longer contact of unreacted (*S*)-**1k** with the aqueous medium favours the hydrolysis reaction. The progress of the biocatalytic reaction under given conditions (equimolar *rac*-**1k** and sodium azide at 20 mM, 1 mg mL^{-1} enzyme) is shown in Fig. 6-C. After 3 h, the reaction selectivity (*i.e.* the ratio of the formed desired alcohol to the total amount of undesired diol) is 3.5, while only an hour later it drops to 2, as (*S*)-**1k** is consumed in the hydrolytic reaction. It is apparent that the reaction, when conducted in the batch reactor, should be precisely monitored and terminated as soon as the desired yield is achieved. This is a demonstration of utility of model-based simulations, especially in shortage of equipment for inline concentration monitoring.

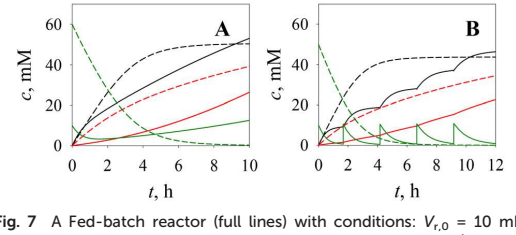

Fig. 7 A Fed-batch reactor (full lines) with conditions: $V_{r,0}$ = 10 mL, $c_{0,rac\text{-}1k}$ = 20 mM, $c_{0,sodium\ azide}$ = 20 mM, γ_{W249P} = 2 mg mL^{-1}, $q_{sodium\ azide}$ = 0.25 μL min^{-1} ($c_{sodium\ azide,\ piston}$ = 6.9 M), $q_{rac\text{-}1k}$ = 0.4 μL min^{-1} ($c_{rac\text{-}1k,\ piston}$ = 5.2 M); batch reactor (dashed lines) with conditions: $c_{rac\text{-}1k}$ = 120 mM, $c_{0,azide}$ = 100 mM, γ_{W249P} = 2 mg mL^{-1}. B Repetitive batch reactor (full lines) with initial conditions $c_{sodium\ azide}$ = 10 mM, $c_{rac\text{-}1k}$ = 20 mM, γ_{W249P} = 2 mg mL^{-1} and addition of 10 mM sodium azide and 20 mM *rac*-**1k** according to (*R*)-enantiomer consumption; batch reactor (dashed lines) with conditions: c_{azide} = 80 mM, $c_{rac\text{-}1k}$ = 100 mM, γ_{W249P} = 2 mg mL^{-1}. Green line – (*R*)-**1k**, black line – **2k**, red line – **4k**.

If the reaction is performed in the fed-batch reactor with substrate feed or in the repetitive batch reactor with sequential addition of substrate(s), the (*R*)-**1k** concentration can be kept at the optimum concentration range for a certain time. However, feed/addition of the racemic mixture also causes (*S*)-**1k** accumulation in the reactor, which represents a problem with prolonged reaction times. The reason for the reaction rate decrease is that (*S*)-**1k**, although not reacting, acts as a potent inhibitor, decreasing the rate of the main reaction and consequently leading to accumulation of inhibiting substrate (*R*)-**1k** as well (Fig. 7-A). Moreover, higher **1k** concentrations favour diol formation, whereby not only inhibition by **4k** becomes a problem, but also optically pure and valuable (*S*)-**1k** is consumed. In Fig. 7, **2k** and **4k** concentrations obtained in the fed-batch (Fig. 7-A) and repetitive batch reactor (Fig. 7-B) were compared with those obtained in the batch reactor. The initial concentrations in the simulations were adjusted so that the total amount of substrates consumed for reactors with substrate feeding is the same as that for the batch reactor, except that in the latter case the entire amount is added at once. This means that in the batch reactor 120 mM *rac*-**1k** is added at the beginning of the experiment (Fig. 7-A, green dashed line), while in the fed-batch reactor the same total amount of *rac*-**1k** is distributed over 10 hours of inflow, keeping the concentration in the reactor most of the time at or below 10 mM (Fig. 7-A, green full line). Similarly, in the repetitive batch reactor portions of 20 mM *rac*-**1k** are added five times, every time after its consumption (Fig. 7-B, green full line), while in the batch reactor the process starts with 100 mM *rac*-**1k** (Fig. 7-B, green dashed line). Despite the previously mentioned challenges, with reaction engineering, *i.e.*, simulating reactions with gradual/continuous addition of

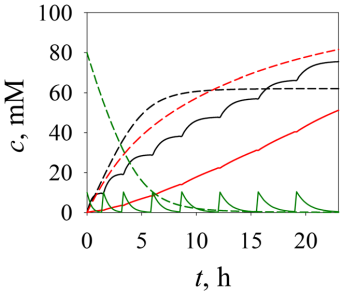

Fig. 8 Repetitive batch reactor (full lines) with initial conditions $c_{\text{sodium azide}}$ = 200 mM, $c_{rac\text{-}\mathbf{1k}}$ = 20 mM, γ_{W249P} = 2 mg mL^{-1} and addition of 20 mM *rac*-**1k** according to (*R*)-enantiomer consumption; batch reactor (dashed lines) with conditions: $c_{\text{sodium azide}}$ = 200 mM, $c_{rac\text{-}\mathbf{1k}}$ = 160 mM, γ_{W249P} = 2 mg mL^{-1}. Green line – (*R*)-**1k**, black line – **2k**, red line – **4k**.

substrates, it is possible to achieve an improved outcome. In Fig. 7-A it is evident that after 9 h the same amount of (*R*)-**2k** is formed in both batch and fed-batch reactors, while the reaction selectivity is improved from 1.3 to 2.2 in the fed-batch. Similarly, in the repetitive batch reactor (Fig. 7-B) after the same time (here, 12 h is taken as an example), (*R*)-**2k** formation is slightly enhanced, while the selectivity increases from 1.3 to 2.0 in the repetitive batch. Keeping the concentration of *rac*-**1k** at the optimal level is highly important for the reaction outcome due to the concentration-dependent enzyme inhibition and deactivation. At higher epoxide concentrations, the importance of gradual addition of the substrate to the reactor is even greater. Insufficient knowledge of the system could lead to the choice of initial conditions in the batch reactor where the final concentration of **4k** is higher than the one of (*R*)-**2k** (Fig. 8, dashed lines). On the other hand, by distributing 160 mM *rac*-**1k** in 8 portions (Fig. 8, full lines), a reaction yield of 95% could be obtained, together with the increase in reaction selectivity from 0.7 to 1.4.

3.8 Challenges regarding industrial implementation of the halohydrin dehalogenase catalysed synthesis of fluorinated building blocks

The previous sections of the paper identified the kinetic limitations of the investigated enzyme and the possibilities brought by mathematical models and process simulations for evading or minimizing unwanted outcomes. In this section, the suitability of the investigated system for the scale-up is discussed, along with the topics to be addressed in the future. At the current stage, the optimized system offered a high reaction yield of 95%, which is in agreement with the requirements for scale-up in the industrial sector of pharmaceutical and fine chemical production. However, the obtained product concentration of roughly 20 g L^{-1} is still beneath the required threshold of 50 g L^{-1}, which should be fulfilled to design the economically profitable scale-up process.[46] Although the fed-batch and repetitive batch reactors present progress in comparison with the batch reactor, prolonging the reaction further is not a valid option since accumulation of inhibiting products, *i.e.*, (*R*)-**2k** and *rac*-**4k**, leads to a decrease in the rate of the biocatalytic reaction. Increasing the enzyme concentration can accelerate the reaction and intensify the volume productivity, but meeting the process targets in terms of enzyme consumption should also be taken into account. The biocatalyst yield, expressed as kilograms of the formed product *via* kilograms of the employed enzyme, should not be below 10.[46,47] Although in this study enzyme consumption is not within the threshold, it is worth noting that the required biocatalyst yield for whole-cell catalysis is fairly lower, on account of 3–5 times lower cost of biocatalyst preparation.[48] The current study was performed with a crude enzyme extract, but according to our experience, *E. coli* cells harbouring wild type HheC offer high stability. Moreover, whole-cell biotransformations with HHDHs are often encountered in the literature.[49–53] In order to increase the reaction productivity, non-conventional media should be considered. Future research should focus on HHDH compatibility with alternative media in order to reduce the hydrolysis impact and to minimize the inhibition by distribution of enzymes and inhibitors in different phases. In a biphasic system, the organic phase could increase the substrate solubility, thus enhancing bioavailability, and serve as protection for the substrate from the water involved in the hydrolytic reaction, while the aqueous phase could protect the enzyme from too high concentrations of inhibitors, *i.e.* substrates and products. Biphasic systems could, at the same time, facilitate downstream processing.[54,55] Furthermore, due to addressed enzyme deactivation, immobilization methods should be investigated. This could hypothetically enable the biocatalytic reaction in continuous processes in biphasic systems. We are currently focused on these topics with the aim of improving the industrial applicability of HHDH enzymes.

4. Conclusion

In this work, reaction engineering methodology was utilised for the exploration of HHDH-catalysed transformation of fluorinated compounds. The reactions in focus were kinetic resolutions of fluorinated styrene oxide derivatives with incorporation of the synthetically valuable azido group. Kinetic studies on HHDH substrates revealed that the examined fluorinated derivatives of styrene oxide are hydrolytically unstable, which is not always evident when screening HHDH activities towards substrates at low concentrations. Hydrolysis reactions are described with pseudo-first order kinetics, which in practice implies a faster undesired reaction at concentrations higher than a millimolar scale. In addition, preliminary screening showed that *para*-substituted derivatives are the best choice for this biotransformation type. The azidolysis of *rac*-2-[4-

(trifluoromethyl)phenyl]oxirane was selected for kinetic characterization based on moderate hydrolytic stability, high enzyme affinity and complete reaction enantioselectivity. However, its synthesis on a larger scale is not a simple assignment due to the presence of numerous inhibitions and concentration-dependent enzyme deactivation, all of which favour hydrolysis on a synthetically relevant concentration scale. Although inevitable, the hydrolysis effect can be reduced by carrying out the reaction in an appropriate reactor under carefully chosen conditions, which can be found by employing process simulations. A substantial improvement in the reaction outcome can be achieved by gradually feeding/repetitively adding *rac*-epoxide in portions into the reactor, which keeps the reacting enantiomer concentration in the area of maximum enzyme activity. In this way, the reaction yield could reach 95% with improvement in the selectivity of 100%. The developed mathematical kinetic model, the first of its kind for any of the HHDH enzymes, provides valuable insight into the kinetic characteristics of the enzyme pointing out to its limitations, and as such provides guidance for further process improvements. This model, with minor adaptations, could serve as a step towards wider applicative value of HHDHs.

Author contributions

Nevena Milčić: conceptualization, investigation, methodology, validation, visualization, writing – original draft. Martina Sudar: investigation, methodology, writing – review & editing. Irena Dokli: investigation, methodology, writing – review & editing. Maja Majerić Elenkov: conceptualization, methodology, supervision, funding acquisition, project administration, resources, writing – review & editing. Zvjezdana Findrik Blažević: conceptualization, methodology, validation, visualization, supervision, funding acquisition, project administration, resources, writing – original draft.

Conflicts of interest

There are no conflicts to declare.

Acknowledgements

This work was financially supported by the Croatian Science Foundation (HrZZ, IP-2018-01-4493). N. M. is supported by a PhD scholarship from the Croatian Science Foundation through the Career Development Project for Young Researchers. We would like to thank Prof. Lixia Tang for providing us plasmids.

Notes and references

1 E. P. Gillis, K. J. Eastman, M. D. Hill, D. J. Donnelly and N. A. Meanwell, *J. Med. Chem.*, 2015, **58**, 8315–8359.
2 M. G. Perrone, P. Vitale, A. Panella, A. Tolomeo and A. Scilimati, in *Fluorinated Pharmaceuticals: Advances in Medicinal Chemistry*, ed. A. D. Westwell, Future Medicine, London, United Kingdom, 2015, ch. 9, pp. 126–139.
3 J. Wang, M. Sánchez-Roselló, J. L. Aceña, C. del Pozo, A. E. Sorochinsky, S. Fustero, V. A. Soloshonok and H. Liu, *Chem. Rev.*, 2014, **114**, 2432–2506.
4 P. Jeschke, *Eur. J. Org. Chem.*, 2022, **2022**, e202101513.
5 Y. Ogawa, E. Tokunaga, O. Kobayashi, K. Hirai and N. Shibata, *iScience*, 2020, **23**, 101467.
6 M. Inoue, Y. Sumii and N. Shibata, *ACS Omega*, 2020, **5**, 10633–10640.
7 A. Palumbo Piccionello, I. Pibiri, S. Buscemi and A. Pace, in *Fluorine in Life Sciences: Pharmaceuticals, Medicinal Diagnostics, and Agrochemicals*, ed. G. Haufe and F. R. Leroux, Elsevier, Amsterdam, Netherlands, 2019, ch. 5, pp. 213–239.
8 T. Liang, C. N. Neumann and T. Ritter, *Angew. Chem., Int. Ed.*, 2013, **52**, 8214–8264.
9 E. L. Bell, W. Finnigan, S. P. France, A. P. Green, M. A. Hayes, L. J. Hepworth, S. L. Lovelock, H. Niikura, S. Osuna, E. Romero, K. S. Ryan, N. J. Turner and S. L. Flitsch, *Nat. Rev. Methods Primers*, 2021, **1**, 46.
10 R. A. Sheldon and J. M. Woodley, *Chem. Rev.*, 2018, **118**, 801–838.
11 A. Schallmey and M. Schallmey, *Appl. Microbiol. Biotechnol.*, 2016, **100**, 7827–7839.
12 G. Hasnaoui-Dijoux, M. Majerić Elenkov, J. H. Lutje Spelberg, B. Hauer and D. B. Janssen, *ChemBioChem*, 2008, **9**, 1048–1051.
13 Z. Findrik Blažević, N. Milčić, M. Sudar and M. Majerić Elenkov, *Adv. Synth. Catal.*, 2021, **363**, 388–410.
14 M. M. Elenkov, L. Tang, A. Meetsma, B. Hauer and D. B. Janssen, *Org. Lett.*, 2008, **10**, 2417–2420.
15 M. Majerić Elenkov, I. Primožič, T. Hrenar, A. Smolko, I. Dokli, B. Salopek-Sondi and L. Tang, *Org. Biomol. Chem.*, 2012, **10**, 5063–5072.
16 N.-W. Wan, Z.-Q. Liu, F. Xue, Z.-Y. Shen and Y.-G. Zheng, *ChemCatChem*, 2015, **7**, 2446–2450.
17 M. Majerić Elenkov, M. Čičak, A. Smolko and A. Knežević, *Tetrahedron Lett.*, 2018, **59**, 406–408.
18 E. Calderini, J. Wessel, P. Süss, P. Schrepfer, R. Wardenga and A. Schallmey, *ChemCatChem*, 2019, **11**, 2099–2106.
19 J. H. Schrittwieser, I. Lavandera, B. Seisser, B. Mautner and W. Kroutil, *Eur. J. Org. Chem.*, 2009, **2009**, 2293–2298.
20 R. M. Haak, C. Tarabiono, D. B. Janssen, A. J. Minnaard, J. G. de Vries and B. L. Feringa, *Org. Biomol. Chem.*, 2007, **5**, 318–323.
21 R. M. Haak, F. Berthiol, T. Jerphagnon, A. J. A. Gayet, C. Tarabiono, C. P. Postema, V. Ritleng, M. Pfeffer, D. B. Janssen, A. J. Minnaard, B. L. Feringa and J. G. de Vries, *J. Am. Chem. Soc.*, 2008, **130**, 13508–13509.
22 G. Hasnaoui, J. H. Lutje Spelberg, E. de Vries, L. Tang, B. Hauer and D. B. Janssen, *Tetrahedron: Asymmetry*, 2005, **16**, 1685–1692.
23 F.-R. Zhang, N.-W. Wan, J.-M. Ma, B.-D. Cui, W.-Y. Han and Y.-Z. Chen, *ACS Catal.*, 2021, **11**, 9066–9072.

24 Q. Xu, K.-S. Huang, Y.-F. Wang, H.-H. Wang, B.-D. Cui, W.-Y. Han, Y.-Z. Chen and N.-W. Wan, *ACS Catal.*, 2022, **12**, 6285–6293.

25 S. K. Ma, J. Gruber, C. Davis, L. Newman, D. Gray, A. Wang, J. Grate, G. W. Huisman and R. A. Sheldon, *Green Chem.*, 2010, **12**, 81–86.

26 H. Tanimoto and K. Kakiuchi, *Nat. Prod. Commun.*, 2013, **8**, 1021–1034.

27 J. Tomaszewska, K. Koroniak and H. Koroniak, *ARKIVOC*, 2017, **2017**, 421–432.

28 I. Dokli, N. Milčić, P. Marin, M. S. Miklenić, M. Sudar, L. Tang, Z. F. Blažević and M. M. Elenkov, *Catal. Commun.*, 2021, **152**, 106285.

29 M. Sudar and Z. Findrik Blažević, in *Enzyme Cascade Design and Modelling*, ed. S. Kara and F. Rudroff, Springer International Publishing, Cham, Switzerland, 2021, ch. 5, pp. 91–108.

30 N. Milčić, I. Ćevid, M. M. Çakar, M. Sudar and Z. Findrik Blažević, *Hung. J. Ind. Chem.*, 2022, **50**, 45–55.

31 M. Česnik, M. Sudar, R. Roldan, K. Hernandez, T. Parella, P. Clapés, S. Charnock, Đ. Vasić-Rački and Z. Findrik Blažević, *Chem. Eng. Res. Des.*, 2019, **150**, 140–152.

32 J. H. Lutje Spelberg, L. Tang, M. van Gelder, R. M. Kellogg and D. B. Janssen, *Tetrahedron: Asymmetry*, 2002, **13**, 1083–1089.

33 I. Dokli, Z. Brkljača, P. Švaco, L. Tang, V. Stepanić and M. Majerić Elenkov, *Org. Biomol. Chem.*, 2022, DOI: **10.1039/D2OB01955H**.

34 A. Mikleušević, Z. Hameršak, B. Salopek-Sondi, L. Tang, D. B. Janssen and M. Majerić Elenkov, *Adv. Synth. Catal.*, 2015, **357**, 1709–1714.

35 M. M. Bradford, *Anal. Biochem.*, 1976, **72**, 248–254.

36 N. Milčić, V. Stepanić, I. Crnolatac, Z. Findrik Blažević, Z. Brkljača and M. Majerić Elenkov, *Chem. – Eur. J.*, 2022, **28**, e202201923.

37 *SCIENTIST Handbook*, Micromath®, Salt Lake City, 1986–1995.

38 Fischer Scientific, **www.fishersci.at**.

39 E. Y. Lee and M. L. Shuler, *Biotechnol. Bioeng.*, 2007, **98**, 318–327.

40 E. Mehić, L. Hok, Q. Wang, I. Dokli, M. S. Miklenić, Z. Findrik Blažević, L. Tang, R. Vianello and M. Majerić Elenkov, *Adv. Synth. Catal.*, 2022, **364**, 2461.

41 Z. Wu, W. Deng, Y. Tong, Q. Liao, D. Xin, H. Yu, J. Feng and L. Tang, *Appl. Microbiol. Biotechnol.*, 2017, **101**, 3201–3211.

42 D. A. Nagib and D. W. C. MacMillan, *Nature*, 2011, **480**, 224–228.

43 P. K. Bangalore, S. K. Vagolu, R. K. Bollikanda, D. K. Veeragoni, P. C. Choudante, S. Misra, D. Sriram, B. Sridhar and S. Kantevari, *J. Nat. Prod.*, 2020, **83**, 26–35.

44 H. Ankati, Y. Yang, D. Zhu, E. R. Biehl and L. Hua, *J. Org. Chem.*, 2008, **73**, 6433–6436.

45 Đ. Vasić-Rački, J. Bongs, U. Schörken, G. Sprenger and A. Liese, *Bioprocess Biosyst. Eng.*, 2003, **25**, 285–290.

46 P. Tufvesson, J. Lima-Ramos, N. Al Haque, K. V. Gernaey and J. M. Woodley, *Org. Process Res. Dev.*, 2013, **17**, 1233–1238.

47 P. Tufvesson, M. Nordblad, U. Krühne, M. Schürmann, A. Vogel, R. Wohlgemuth and J. M. Woodley, *Org. Process Res. Dev.*, 2015, **19**, 652–660.

48 P. Tufvesson, J. Lima-Ramos, M. Nordblad and J. M. Woodley, *Org. Process Res. Dev.*, 2011, **15**, 266–274.

49 N.-W. Wan, Z.-Q. Liu, K. Huang, Z.-Y. Shen, F. Xue, Y.-G. Zheng and Y.-C. Shen, *RSC Adv.*, 2014, **4**, 64027–64031.

50 S.-P. Zou, Y.-G. Zheng, E.-H. Du and Z.-C. Hu, *J. Biotechnol.*, 2014, **188**, 42–47.

51 H.-X. Jin, Z.-Q. Liu, Z.-C. Hu and Y.-G. Zheng, *Biochem. Eng. J.*, 2013, **74**, 1–7.

52 P. Yao, L. Wang, J. Yuan, L. Cheng, R. Jia, M. Xie, J. Feng, M. Wang, Q. Wu and D. Zhu, *ChemCatChem*, 2015, **7**, 1438–1444.

53 D. Hu, H.-H. Ye, M.-C. Wu, F. Feng, L.-J. Zhu, X. Yin and J.-F. Li, *Catal. Commun.*, 2015, **69**, 72–75.

54 M. M. C. H. van Schie, J.-D. Spöring, M. Bocola, P. Domínguez de María and D. Rother, *Green Chem.*, 2021, **23**, 3191–3206.

55 C. Cao and T. Matsuda, *Org. Synth. Using Biocatal.*, 2016, pp. 67–97.

Electronic Supplementary Material (ESI) for Reaction Chemistry & Engineering.

Supplementary material

Reaction system

S-1. Reactions in the selected system for kinetic characterization and model development:

A. main reaction: biocatalytic synthesis of (*R*)-2-azido-1-[4-(trifluoromethyl)phenyl]ethanol (**2k**);

B. side reaction: spontaneous chemical synthesis of *rac*-2-azido-2-[4-(trifluoromethyl)phenyl]ethanol (**3k**);

C. side reaction: spontaneous hydrolysis of *rac*-**1k** to *rac*-2-[4-(trifluoromethyl)phenyl]-1,2-ethanediol (**4k**).

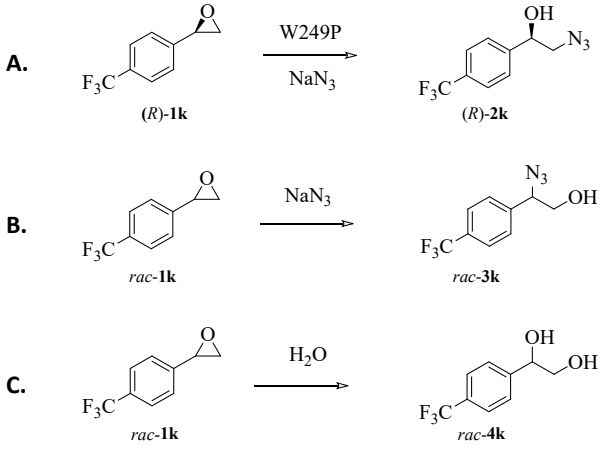

Calibration curves

S-2. Calibration curves for **A.** *para*-nitro-2-bromo-1-phenylethanol (PNSHH) and **B.** *para*-nitro styrene oxide (PNSO).

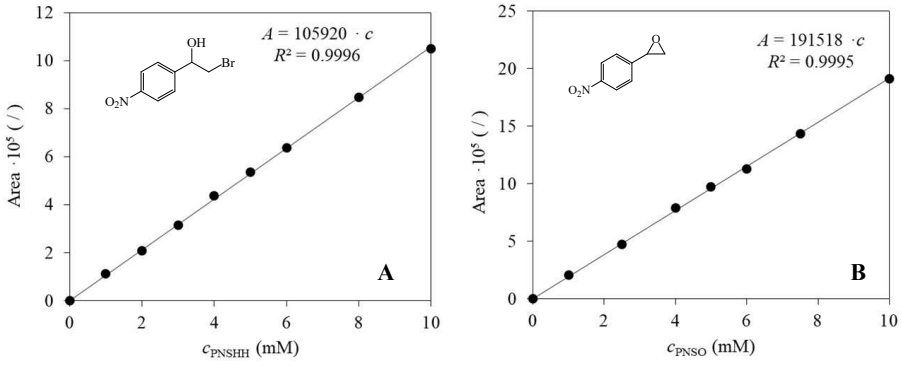

S-3. Calibration curves for the substrates (**1a**-**1k**): **A.** 2-(2-fluorophenyl)oxirane (**1a**); **B.** 2-(3-fluorophenyl)oxirane (**1b**); **C.** 2-(4-fluorophenyl)oxirane (**1c**); **D.** 2-(2-fluorophenyl)-2-methyloxirane (**1d**); **E.** 2-(3-fluorophenyl)-2-methyloxirane (**1e**); **F.** 2-(4-fluorophenyl)-2-methyloxirane (**1f**); **G.**– 2-(2,6-difluorophenyl)oxirane (**1g**); **H.** 2-(3,4-difluorophenyl)oxirane (**1h**); **I.** 2-(2,4-difluorophenyl)oxirane (**1i)**; **J.** 2-(2,4,5-trifluorophenyl)oxirane (**1j**); **K.** 2-[4-(trifluoromethyl)phenyl]oxirane (**1k**).

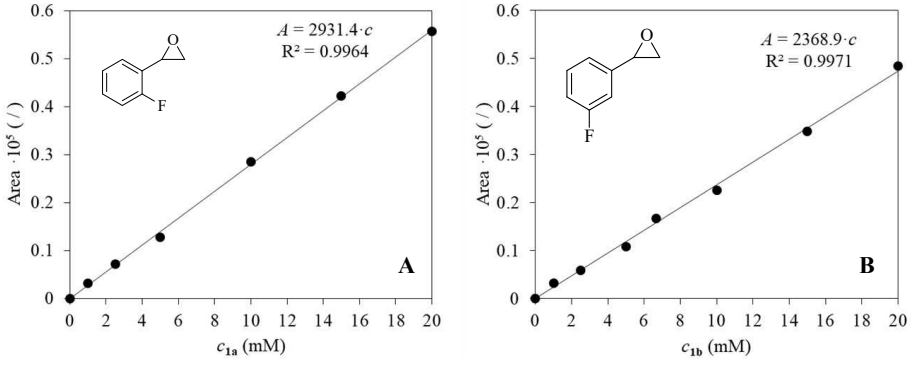

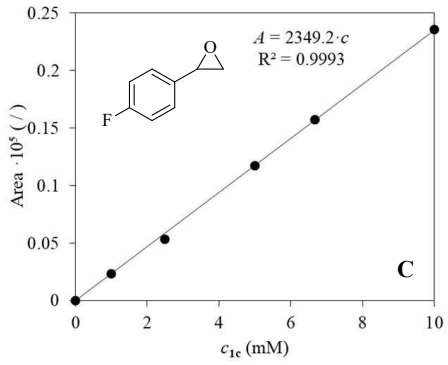
A = 2349.2·c
R² = 0.9993
Area ·10⁵ (/)
c1c (mM)
C

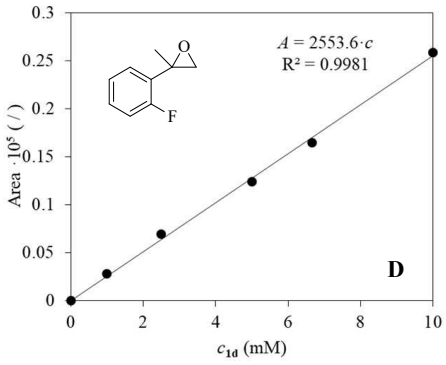
A = 2553.6·c
R² = 0.9981
Area ·10⁵ (/)
c1d (mM)
D

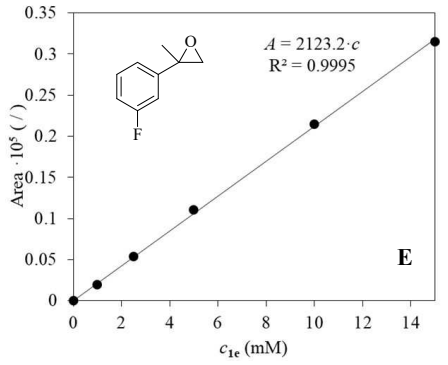
A = 2123.2·c
R² = 0.9995
Area ·10⁵ (/)
c1e (mM)
E

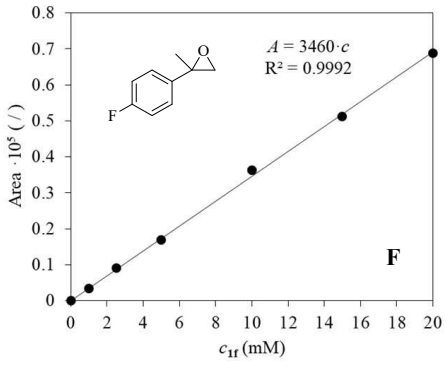
A = 3460·c
R² = 0.9992
Area ·10⁵ (/)
c1f (mM)
F

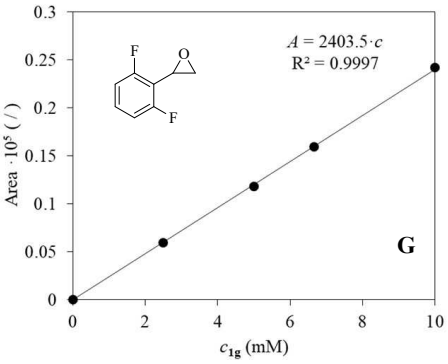
A = 2403.5·c
R² = 0.9997
Area ·10⁵ (/)
c1g (mM)
G

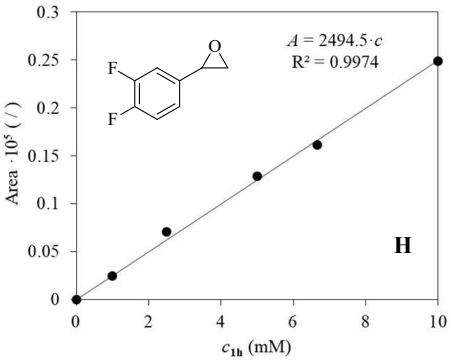
A = 2494.5·c
R² = 0.9974
Area ·10⁵ (/)
c1h (mM)
H

3

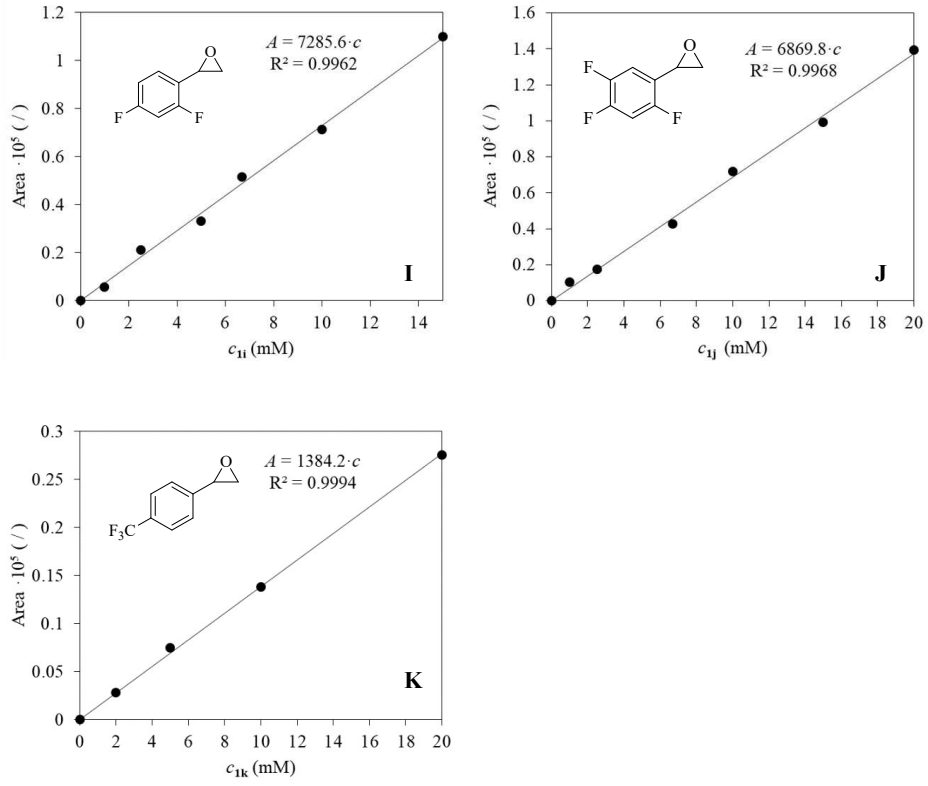

S-4. Calibration curves for the selected system: **A.** substrate (**1k**) and **B.** product (**2k**).

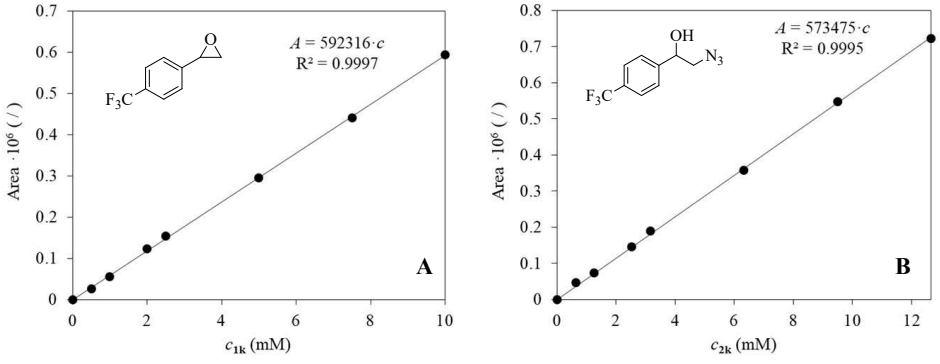

S-5. Calibration curves for individual enantiomers of the substrate: **A.** (*R*)-**1k** and **B.** (*S*)-**1k**

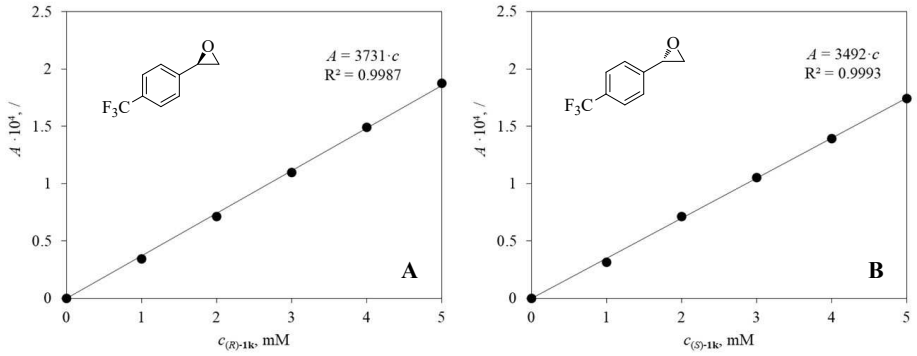

S-6. Product (*R*)-**2k** calibration curve on chiral column

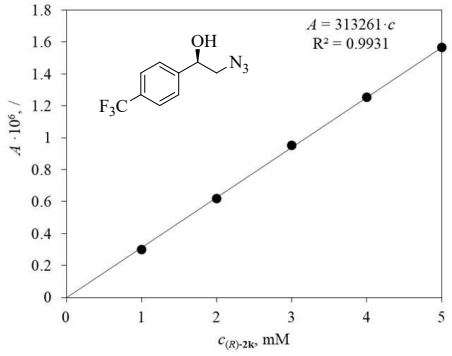

Hydrolysis kinetics

S-7. Determination of hydrolytic constants for substrates **1a**-**1k**. **A. 1a**; **B. 1b**; **C. 1c**; **D. 1d**; **E. 1e**; **F. 1f**; **G. 1g**; **H. 1h**; **I. 1i**; **J. 1j**; **K. 1k**. The graph for **1k** is given in the main paper (*See* 3.5)

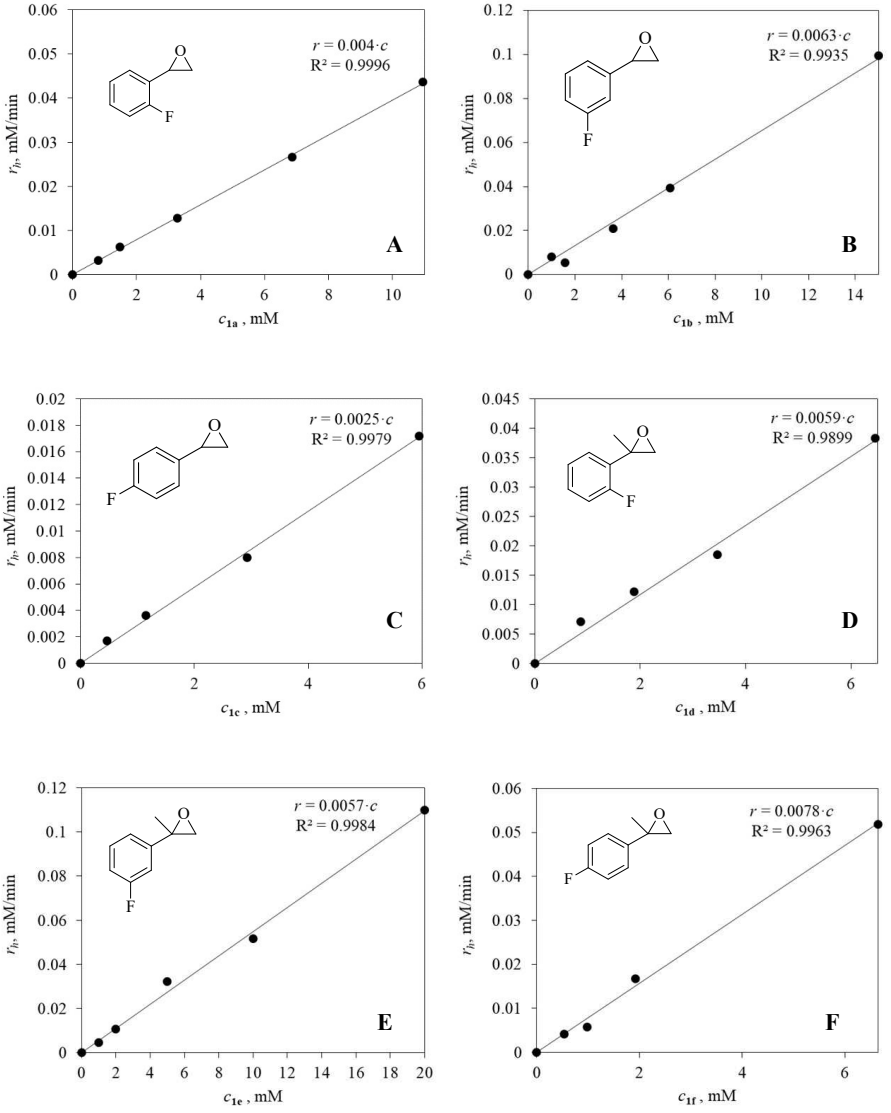

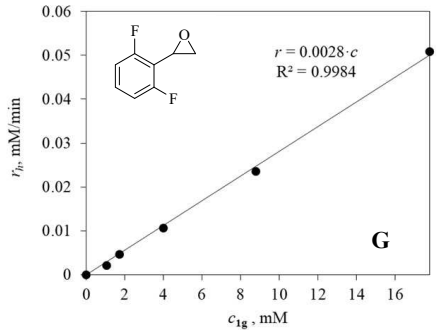
r = 0.0028·c
R² = 0.9984
G
r_h, mM/min
c_{1g}, mM

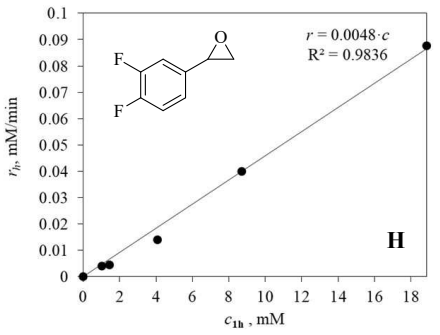
r = 0.0048·c
R² = 0.9836
H
r_h, mM/min
c_{1h}, mM

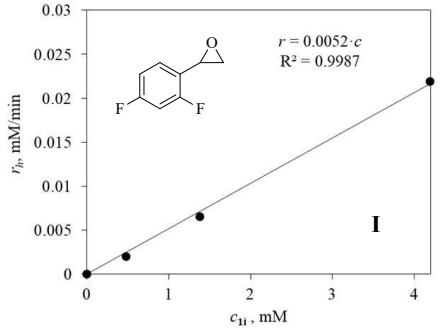
r = 0.0052·c
R² = 0.9987
I
r_h, mM/min
c_{1i}, mM

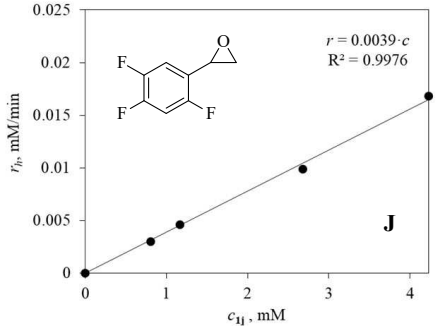
r = 0.0039·c
R² = 0.9976
J
r_h, mM/min
c_{1j}, mM

Reaction enantioselectivity

S-8. Azidolysis curves of **A. 1c** with W249P, **B. 1c** with ISM-4, **C. 1k** with W249P, **D. 1k** with ISM-4. Legend: black squares (*R*)-**1c**; white squares (*S*)-**1c**; black triangles (*R*)-**1k**; white triangles (*S*)-**1k**. Reaction conditions: 20 mM *rac*-epoxide, 20 mM NaN_3, 10% *v/v* DMSO, V_r = 3 mL, 1000 rpm, 25 °C, γ_{W249P} =1 mg/mL (left panel), γ_{ISM-4} = 2 mg/mL (right panel).

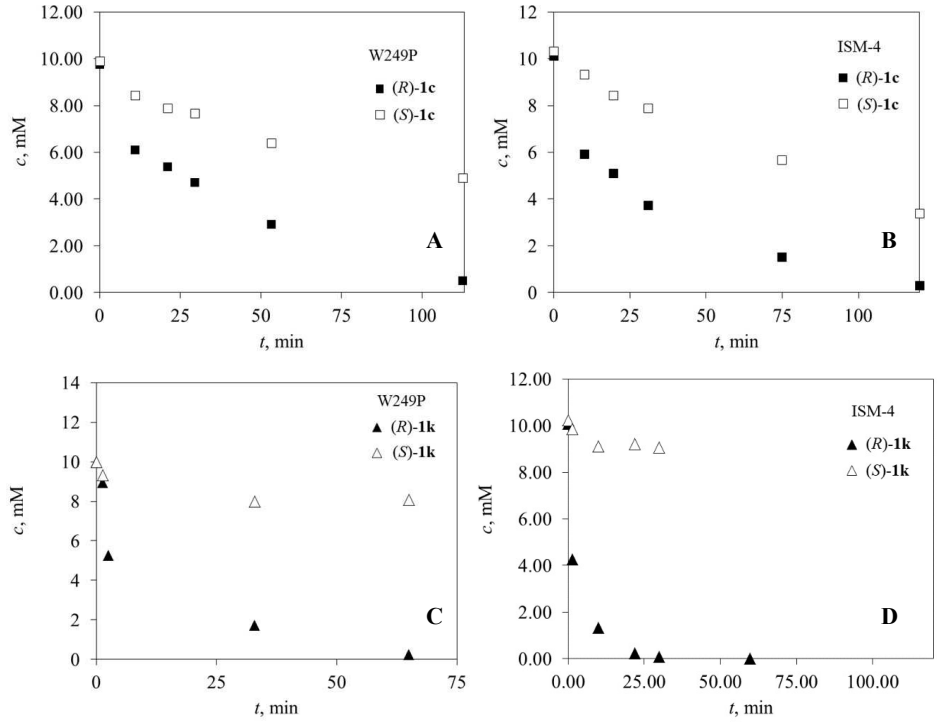

S-9. Proof of complete reaction enantioselectivity, i.e. absence of (*S*)-**1k** azidolysis with W249P enzyme. In order to check whether the enzymatic reaction is completely enantioselective towards (*R*)-**1k**, a reaction in the batch reactor was performed starting with (*S*)-**1k** and high enzyme concentration (3 mg/mL). Even after 24 h, the formation of the biocatalytic product (*S*)-**2k** was not recorded at all. Also, the consumption of the (*S*)-enantiomer over time follows the model-predicted consumption in the hydrolytic reaction, which is another proof that (*S*)-**1k** is not consumed, except in hydrolysis, in any other reaction (including the biocatalytic reaction). Conditions: $c_{(S)\text{-}\mathbf{1k}}$ = 20 mM, $c_{\text{sodium azide}}$ = 20 mM, γ_{W249P} =3 mg/mL. Due to the weak response, **4k** was not monitored experimentally but was confirmed by the model.

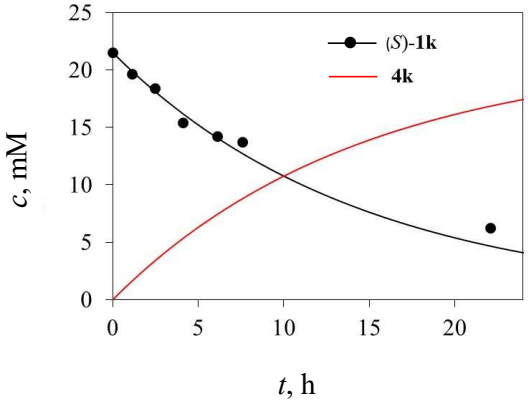

Model validation

S-10. Model validation statistics for experiments conducted in batch reactor (**Fig 3.** in main text) that provides information about fitting of experimental data and models. Validation of mathematical model in batch reactor experiments (V_r = 500 µL; 500 mM Tris-SO_4; pH 7.5; 25 °C; DMSO 10% *v/v*; 1000 rpm) conducted with different initial conditions: **A.** $c_{\text{sodium sodium azide}}$ = 5 mM, $c_{(R)\text{-}\mathbf{1k}}$ = 6.26 mM, γ_{W249P} = 0.30 mg mL^{-1}; **B.** $c_{\text{sodium sodium azide}}$ = 25 mM, $c_{rac\text{-}\mathbf{1k}}$ = 16.5 mM, γ_{W249P} = 0.33 mg mL^{-1}; **C.** $c_{\text{sodium sodium azide}}$ = 10 mM, $c_{rac\text{-}\mathbf{1k}}$ = 20.1 mM, γ_{W249P} = 2.0 mg mL^{-1}; **D.** $c_{\text{sodium azide}}$ = 20 mM, $c_{rac\text{-}\mathbf{1k}}$ = 40.3 mM, γ_{W249P} = 2.0 mg mL^{-1}.

Batch experiment	Standard deviation (σ)	Coefficient of determination (R^2)	Correlation coefficient (ρ)	Model selection criterion (MSC)
Fig 3-A	0.802	0.924	0.953	1.490
Fig 3-B	1.148	0.987	0.977	1.929
Fig 3-C	1.737	0.981	0.907	1.560
Fig 3-D	1.043	0.913	0.955	1.494

S-11. Experimentally determined and model-confirmed enzyme operational stability decay during batch experiments (V_r = 500 µL; 500 mM Tris-SO_4; pH 7.5; 25 °C; DMSO 10% *v/v*; 1000

rpm). Initial conditions: **A.** $c_{\text{sodium sodium azide}}$ = 5 mM, $c_{(R)\text{-}\mathbf{1k}}$ = 6.26 mM, γ_{W249P} = 0.3 mg mL^{-1}; **B.** $c_{\text{sodium azide}}$ = 5 mM, $c_{rac\text{-}\mathbf{1k}}$ = 5.3 mM, γ_{W249P} = 0.2 mg mL^{-1}; **C.** $c_{\text{sodium sodium azide}}$ = 10 mM, $c_{rac\text{-}\mathbf{1k}}$ = 9.2 mM, γ_{W249P} = 0.2 mg mL^{-1}; **D.** $c_{\text{sodium sodium azide}}$ = 25 mM, $c_{rac\text{-}\mathbf{1k}}$ = 16.5 mM, γ_{W249P} = 0.33 mg mL^{-1}; **E.** $c_{\text{sodium sodium azide}}$ = 50 mM, $c_{rac\text{-}\mathbf{1k}}$ = 74.1 mM, γ_{W249P} = 0.4 mg mL^{-1}.

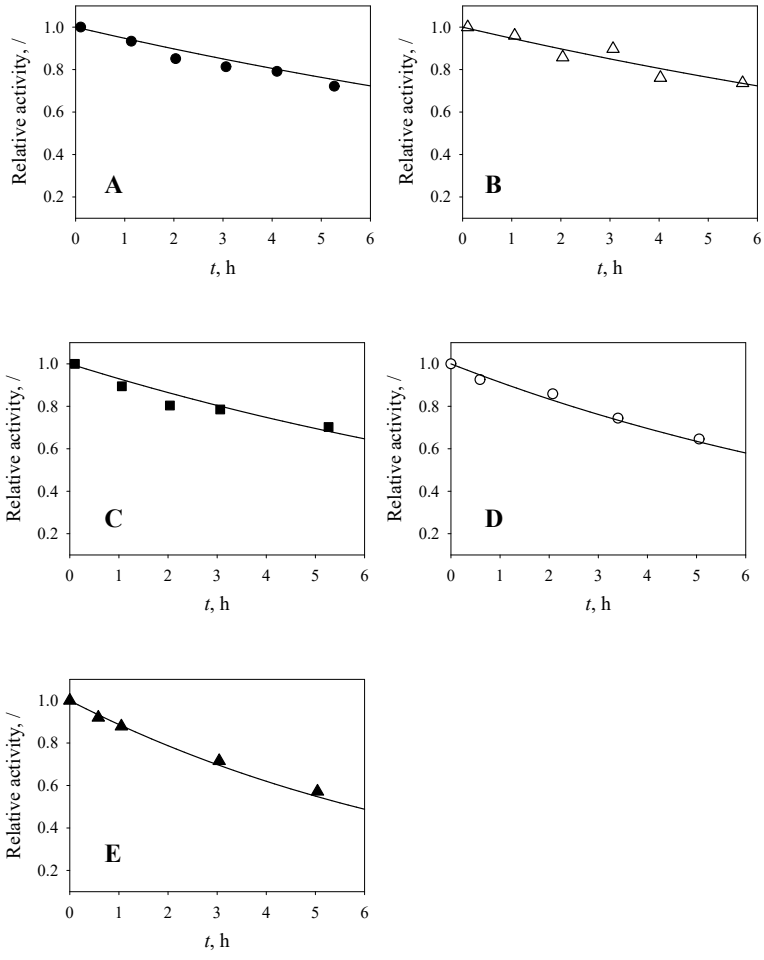

S-12. Table of enzyme operational stability decay rate constants of the first order. Initial conditions: **A.** $c_{\text{sodium azide}}$ = 5 mM, $c_{(R)\text{-}\mathbf{1k}}$ = 6.26 mM, γ_{W249P} = 0.3 mg mL^{-1}; **B.** $c_{\text{sodium azide}}$ = 5 mM, $c_{rac\text{-}\mathbf{1k}}$ = 5.3 mM, γ_{W249P} = 0.2 mg mL^{-1}; **C.** $c_{\text{sodium azide}}$ = 10 mM, $c_{rac\text{-}\mathbf{1k}}$ = 9.2 mM, γ_{W249P} = 0.2 mg mL^{-1}; **D.** $c_{\text{sodium azide}}$ = 25 mM, $c_{rac\text{-}\mathbf{1k}}$ = 16.5 mM, γ_{W249P} = 0.33 mg mL^{-1}; **E.** $c_{\text{sodium azide}}$ = 50 mM, $c_{rac\text{-}\mathbf{1k}}$ = 74.1 mM, γ_{W249P} = 0.4 mg mL^{-1}.

Experiment	$c_{0,\mathbf{1k}}$, mM	k_d, min^{-1}
A	6.26	$0.00106 \pm 5.7 \cdot 10^{-5}$
B	5.26	$0.00095 \pm 1.4 \cdot 10^{-4}$
C	9.22	$0.00121 \pm 1.5 \cdot 10^{-4}$
D	16.5	$0.001512 \pm 7.7 \cdot 10^{-5}$
E	74.1	$0.001992 \pm 6.8 \cdot 10^{-5}$

Appendix IV

N. Milčić, V. Stepanić, I. Crnolatac, Z. Findrik Blažević, Z. Brkljača, M. Majerić Elenkov, Inhibitory Effect of DMSO on Halohydrin Dehalogenase: Experimental and Computational Insights into the Influence of an Organic Co-solvent on the Structural and Catalytic Properties of a Biocatalyst, Chem. Eur. J. 28 (2022)

Nevena Milčić: investigation, methodology, formal analysis, validation, writing – original draft, writing – review & editing

Višnja Stepanić: investigation, formal analysis, writing – review & editing

Ivo Crnolatac: investigation, formal analysis, writing – review & editing

Zvjezdana Findrik Blažević: conceptualization, methodology, funding acquisition writing – review & editing

Zlatko Brkljača: investigation, methodology, formal analysis, validation, writing – original draft, writing – review & editing

Maja Majerić Elenkov: conceptualization, methodology, funding acquisition, formal analysis, validation, writing – original draft, writing – review & editing

JOHN WILEY AND SONS LICENSE TERMS AND CONDITIONS

Nov 16, 2022

This Agreement between Faculty of Chemical Engineering and Technology, University of Zagreb -- Nevena Milčić ("You") and John Wiley and Sons ("John Wiley and Sons") consists of your license details and the terms and conditions provided by John Wiley and Sons and Copyright Clearance Center.

License Number	5421860798674
License date	Nov 04, 2022
Licensed Content Publisher	John Wiley and Sons
Licensed Content Publication	Chemistry - A European Journal
Licensed Content Title	Inhibitory Effect of DMSO on Halohydrin Dehalogenase: Experimental and Computational Insights into the Influence of an Organic Co-solvent on the Structural and Catalytic Properties of a Biocatalyst
Licensed Content Author	Nevena Milčić, Višnja Stepanić, Ivo Crnolatac, et al
Licensed Content Date	Sep 13, 2022
Licensed Content Volume	28
Licensed Content Issue	56
Licensed Content Pages	11
Type of Use	Dissertation/Thesis
Requestor type	Author of this Wiley article
Format	Print and electronic
Portion	Full article
Will you be translating?	No
Title	Mathematical modelling and optimization of biocatalytic synthesis of fluorinated chiral building blocks
Institution name	Faculty of Chemical Engineering and Technology, University of Zagreb
Expected presentation date	Mar 2023
Order reference number	2022-11-04-NM-RightsLinkDMSO
Requestor Location	Faculty of Chemical Engineering and Technology, University of Zagreb Marulićev trg 19 Zagreb, 10 000 Croatia Attn: Faculty of Chemical Engineering and Technology, University of Zagreb
Publisher Tax ID	EU826007151
Billing Type	Invoice
Billing Address	Faculty of Chemical Engineering and Technology, University of Zagreb Marulićev trg 19 Zagreb, Croatia 10 000 Attn: Faculty of Chemical Engineering and Technology, University of Zagreb
Total	**0.00 EUR**
Terms and Conditions	

INFRINGEMENT OR OTHERWISE (INCLUDING, WITHOUT LIMITATION, DAMAGES BASED ON LOSS OF PROFITS, DATA, FILES, USE, BUSINESS OPPORTUNITY OR CLAIMS OF THIRD PARTIES), AND WHETHER OR NOT THE PARTY HAS BEEN ADVISED OF THE POSSIBILITY OF SUCH DAMAGES. THIS LIMITATION SHALL APPLY NOTWITHSTANDING ANY FAILURE OF ESSENTIAL PURPOSE OF ANY LIMITED REMEDY PROVIDED HEREIN.

- Should any provision of this Agreement be held by a court of competent jurisdiction to be illegal, invalid, or unenforceable, that provision shall be deemed amended to achieve as nearly as possible the same economic effect as the original provision, and the legality, validity and enforceability of the remaining provisions of this Agreement shall not be affected or impaired thereby.

- The failure of either party to enforce any term or condition of this Agreement shall not constitute a waiver of either party's right to enforce each and every term and condition of this Agreement. No breach under this agreement shall be deemed waived or excused by either party unless such waiver or consent is in writing signed by the party granting such waiver or consent. The waiver by or consent of a party to a breach of any provision of this Agreement shall not operate or be construed as a waiver of or consent to any other or subsequent breach by such other party.

- This Agreement may not be assigned (including by operation of law or otherwise) by you without WILEY's prior written consent.

- Any fee required for this permission shall be non-refundable after thirty (30) days from receipt by the CCC.

- These terms and conditions together with CCC's Billing and Payment terms and conditions (which are incorporated herein) form the entire agreement between you and WILEY concerning this licensing transaction and (in the absence of fraud) supersedes all prior agreements and representations of the parties, oral or written. This Agreement may not be amended except in writing signed by both parties. This Agreement shall be binding upon and inure to the benefit of the parties' successors, legal representatives, and authorized assigns.

- In the event of any conflict between your obligations established by these terms and conditions and those established by CCC's Billing and Payment terms and conditions, these terms and conditions shall prevail.

- WILEY expressly reserves all rights not specifically granted in the combination of (i) the license details provided by you and accepted in the course of this licensing transaction, (ii) these terms and conditions and (iii) CCC's Billing and Payment terms and conditions.

- This Agreement will be void if the Type of Use, Format, Circulation, or Requestor Type was misrepresented during the licensing process.

- This Agreement shall be governed by and construed in accordance with the laws of the State of New York, USA, without regards to such state's conflict of law rules. Any legal action, suit or proceeding arising out of or relating to these Terms and Conditions or the breach thereof shall be instituted in a court of competent jurisdiction in New York County in the State of New York in the United States of America and each party hereby consents and submits to the personal jurisdiction of such court, waives any objection to venue in such court and consents to service of process by registered or certified mail, return receipt requested, at the last known address of such party.

WILEY OPEN ACCESS TERMS AND CONDITIONS

Wiley Publishes Open Access Articles in fully Open Access Journals and in Subscription journals offering Online Open. Although most of the fully Open Access journals publish open access articles under the terms of the Creative Commons Attribution (CC BY) License only, the subscription journals and a few of the Open Access Journals offer a choice of Creative Commons Licenses. The license type is clearly identified on the article.

The Creative Commons Attribution License

The Creative Commons Attribution License (CC-BY) allows users to copy, distribute and transmit an article, adapt the article and make commercial use of the article. The CC-BY license permits commercial and non-

Creative Commons Attribution Non-Commercial License

The Creative Commons Attribution Non-Commercial (CC-BY-NC)License permits use, distribution and reproduction in any medium, provided the original work is properly cited and is not used for commercial purposes.(see below)

Creative Commons Attribution-Non-Commercial-NoDerivs License

The Creative Commons Attribution Non-Commercial-NoDerivs License (CC-BY-NC-ND) permits use, distribution and reproduction in any medium, provided the original work is properly cited, is not used for commercial purposes and no modifications or adaptations are made. (see below)

Use by commercial "for-profit" organizations

Use of Wiley Open Access articles for commercial, promotional, or marketing purposes requires further explicit permission

Cover Profile
doi.org/10.1002/chem.202202870

Chemistry Europe
European Chemical Societies Publishing

www.chemeurj.org

Inhibitory Effect of DMSO on Halohydrin Dehalogenase: Experimental and Computational Insights into the Influence of an Organic Co-solvent on the Structural and Catalytic Properties of a Biocatalyst


Nevena Milčić


Višnja Stepanić


Ivo Crnolatac


Zvjezdana Findrik Blažević


Zlatko Brkljača


Maja Majerić Elenkov

Invited for the cover of this issue are Zlatko Brkljača, Maja Majerić Elenkov and co-workers at the Ruđer Bošković Institute and University of Zagreb. The image depicts the enzyme halohydrin dehalogenase HheC, which is made up of four identical subunits, with marked catalytic residues and volumetric maps of water and DMSO in the active site. Read the full text of the article at 10.1002/chem.202201923.

What is the most significant result of this study?

Our research addresses a fast-developing area of biocatalysis, focusing on the interactions between the enzyme halohydrin dehalogenase and solvent molecules. The ability of enzymes to operate in organic solvents is the basis of extensive research in enzymology. We have performed the first comprehensive study of the mechanisms by which DMSO, the most commonly used co-solvent in the halohydrin dehalogenase-catalyzed reactions, influences the activity and stability of the enzyme HheC. The contribution of this work is manifold. It involved experimental kinetic studies and investigation of the structural changes that occur under operational conditions. MD simulations of this tetrameric enzyme in aqueous-organic media, applied for the first time in the study of halohydrin dehalogenases, in general, provide unique information about interactions at the molecular level.

What was the inspiration for this cover design?

As the most of the team members are experimentalists, we were delighted to see the beauty of the enzyme HheC and its interactions with solvent molecules at the molecular level. The significance and indispensable role of solvent molecules for the catalytic activity of the biocatalyst, as well as the dynamic differences between its subunits, are captured at the molecular-level during the MD simulations.

Who designed the cover?

The cover was designed by Zlatko Brkljača.

What other topics are you working on at the moment?

In addition to DMSO, we are interested in finding organic solvents that are more suitable for performing halohydrin dehalogenase-catalysed synthesis. Evaluation of other solvents and their impacts on the catalytic performance of halohydrin dehalogenase is currently in progress in our laboratories.

Chemistry
A European
Journal

Chemistry Europe
European Chemical Societies Publishing

Front Cover:
Z. Brkljača, M. Majerić Elenkov and co-workers
Inhibitory Effect of DMSO on Halohydrin Dehalogenase: Experimental and Computational Insights into the Influence of an Organic Co-solvent on the Structural and Catalytic Properties of a Biocatalyst

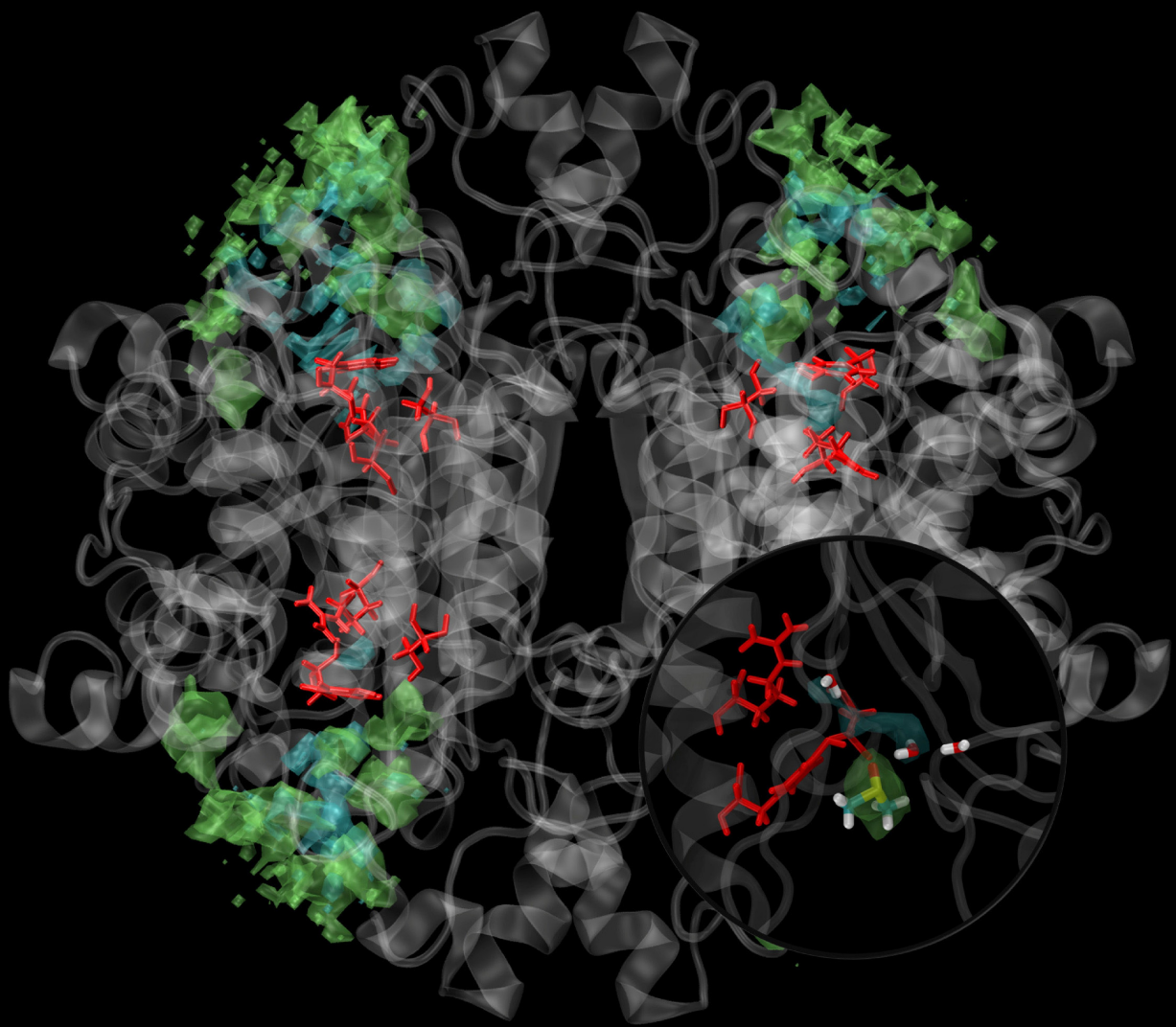

WILEY-VCH

56/2022

Chemistry–A European Journal
Research Article
doi.org/10.1002/chem.202201923
Chemistry Europe
European Chemical Societies Publishing
www.chemeurj.org

Type your text

Inhibitory Effect of DMSO on Halohydrin Dehalogenase: Experimental and Computational Insights into the Influence of an Organic Co-solvent on the Structural and Catalytic Properties of a Biocatalyst

Nevena Milčić,[a] Višnja Stepanić,[b] Ivo Crnolatac,[c] Zvjezdana Findrik Blažević,[a] Zlatko Brkljača[+],*[c] and Maja Majerić Elenkov*[c]

Abstract: Although the application of organic solvents in biocatalysis is well explored, in-depth understanding of the interactions of solvent with proteins, in particular oligomeric ones, is still scant. Understanding these interactions is essential in tailoring enzymes for industrially relevant catalysis in nonaqueous media. In our study, the homotetrameric enzyme halohydrin dehalogenase (HHDH) from *Agrobacterium radiobacter* AD1 (HheC) was investigated, as a model system, in DMSO/water solvent mixtures. DMSO, the most commonly used co-solvent for biocatalytic transformations, was found to act as a mixed-type inhibitor with a prevalent competitive contribution. Even 5% (*v*/*v*) DMSO inhibits the activity of HheC by half. Molecular dynamics (MD) simulations showed that DMSO keeps close to Ser-Tyr catalytic residues forming alternate H-bonds with them. Stability measurements paired with differential scanning calorimetry, dynamic light scattering methods and MD studies revealed that HheC maintains its structural integrity with as much as 30% (*v*/*v*) DMSO.

Introduction

The ability of halohydrin dehalogenases (HHDHs) to catalyse epoxide ring-opening reactions in an enantioselective fashion[1–4] as well as their implementation in enzymatic cascades,[5–14] have been intensively explored over the years primarily due to the synthetic value of the products.[11,15–17] Because of the poor solubility of substrates, biocatalytic reactions are usually performed with the addition of a small amount of organic solvent (OS).[18] Dimethyl sulfoxide (DMSO) is a suitable co-solvent for biocatalysis due to its amphipathic, nontoxic, and recyclable nature.[19] It is a solvent of choice for the majority of performed HHDH-catalysed biotransformations, used in concentrations up to 5% (*v*/*v*).[1,2,4,20–30] Such systems allow substrates to be dissolved in higher concentrations, thus being more available for enzymatic transformation. However, for industrial use the substrate solubility limit is still too low. Larger amounts of DMSO are required to increase industrial space-time-yield, which could unfavourably reflect on the enzyme performance. It has been shown that the effects of organic co-solvents on enzyme activity and stability depend on the chemical and physicochemical properties of OS and the type of enzyme.[31] Interactions between an enzyme and an OS can result in molecular changes in the enzyme structure, such as loss of structural water, changes in its flexibility and conformational alterations.[32–34] OS molecules may also act as enzyme inhibitors.[35] In general, enzymes are more tolerant to hydrophobic OSs than hydrophilic ones as the latter can cause destructive structural changes due to easier penetration into the enzyme and greater capacity to replace structural water within the enzyme hydration shell.[36] Understanding complex enzyme–OS interactions is of primary concern in the rational design of OS resistant enzymes. A combination of experimental and computational methods is a useful and efficient pathway to provide insights into these complex interactions.[37]

For a long time, only a few HHDHs were known and solely one member, HheC from *Agrobacterium radiobacter* AD1, was studied extensively.[15] However, in recent years, several novel genes that encode HHDHs have been discovered,[38–41] extending the potential for the synthetic application of these biocatalysts. Although there are several reports of HHDH-catalysed transformations in aqueous-organic media,[42–46] no mechanistic study on the influence of OSs on the HHDHs properties has been performed to date.

[a] *N. Milčić, Prof. Z. Findrik Blažević*
Faculty of Chemical Engineering and Technology
University of Zagreb
Savska c. 16, 10000 Zagreb (Croatia)

[b] *Dr. V. Stepanić*
Laboratory for Machine Learning and Knowledge Representation
Ruđer Bošković Institute
Bijenička c. 54, 10000 Zagreb (Croatia)

[c] *Dr. I. Crnolatac, Dr. Z. Brkljača,[+] Dr. M. Majerić Elenkov*
Division of Organic Chemistry and Biochemistry
Ruđer Bošković Institute
Bijenička c. 54, 10000 Zagreb (Croatia)
E-mail: Zlatko.Brkljaca@irb.hr
Maja.Majeric.Elenkov@irb.hr

[+] *Present Address: Selvita Ltd., 10000 Zagreb, Croatia, E-mail: zlatko.brkljaca@selvita.com*

Supporting information for this article is available on the WWW under https://doi.org/10.1002/chem.202201923

In the present study, the combination of experimental and computational methods was applied to elucidate the behaviour of homotetrameric enzyme HheC in aqueous-organic media, with the focus on its interactions with OS molecules. DMSO was chosen because it is the most frequently used co-solvent in biocatalysis with HHDHs due to its miscibility with water, while HheC was selected as a representative of the enzyme group.

Results and Discussion

General structural properties of HheC

HheC is a functional homotetramer. It consists of four identical subunits possessing the Rossmann fold.[47] Two subunits are bound in a dimer through their α-helices, α5 and α6, making intermolecular four-helix bundle. Dimers are assembled in tetramer through interactions of helices α8, β-strand β7, and their connecting loops (Figure 1). The C-terminal domain of each subunit interacts with the diagonal subunit of another dimer. Such a C-terminal extension is absent in other HHDHs.[48] Although it is not essential for catalytic activity, it is found to regulate HheC's enantioselectivity.[49] Without monomer association, this enzyme cannot perform catalysis.[50] Upon formation of tetramer, nearly one third of the surface of each HheC subunit becomes buried in the interface (Table S1 in the Supporting Information), which significantly contributes to protein stability, as the reduced surface area offers protection against denaturation. Generally, oligomerization is a common strategy found in nature for enhancing protein stability and regulating its activity.[51] The flexibility of amino acid residues belonging to the C-tail and the loops surrounding the entrance to the catalytic site is significantly reduced in tetramer as compared to monomeric state (Figure S1, right).

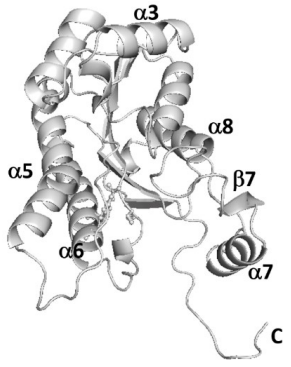

Figure 1. Cartoon view of the HheC monomer.

Structure and stability of HheC in the presence of DMSO

MD simulations on tetramer showed that regardless of solvent environment, it overall exhibits high level of structural stability (Figures 2A and S2 right; results of repeated simulations, that is, replicas, can be found in Figure S3A and B). The subunits in tetramer possess quite uniform behaviour with no significant deviations in the conformational phase space and amino acid residue fluctuations with change of DMSO proportion (Figures S4 and S5). However, their mutual positioning is changed, as observed from principal component analysis (PCA), which is shown in Figures 2B and S3 C. When going from 0 to 50% (*v*/*v*) DMSO system, the distinct sheering of the main structural motifs of subunits occurs. It is found that the most prominent structural changes occur in the most solvent accessible and flexible regions of the protein, which can be clearly observed in the case of helix α3 (Figures 2C, D and S1, left). More precisely, the distance between diagonally opposite helices α3 in 20 and 50% DMSO is approximately 4 Å longer compared to the water case.

The significant structural changes with DMSO addition are reflected in calculated solvent accessible surface area (SASA). The tetramer in 50% DMSO shows reduction in SASA compared to 0 and 20% DMSO system (Tables 1 and S2 in the case of replicas). DMSO addition leads to dehydration of HheC, with a number of water molecules exiting the first solvation shell being greater than the number of DMSO molecules entering into it. Water makes more hydrogen bonds (HBs) with HheC than DMSO and the total number of HBs of HheC (all residues considered) with OS molecules decreases with the addition of DMSO, although not proportionally, most probably due to the fact that water encompasses the protein more closely compared to DMSO (illustrated by volumetric maps in Figure S6).

The SASA reduction could also imply that DMSO establishes a non-negligible number of hydrophobic interactions with HheC at its 50% (*v*/*v*) ratio. This would further imply that hydrophobic regions of the protein, which are usually buried inside, become somewhat more exposed toward the OS.

Table 1. SASA, solvent occupancy (DMSO or water) and hydrogen bonds (HBs) at the tetramer surface.

DMSO *v*/*v* [%]	SASA[a] [Å^2]	Average number of solvent molecules in the first solvent shell[b]		Number of HBs[c]	
		H_2O	DMSO	H_2O	DMSO
0	37157.8 ± 377.5	1846.9 ± 29.5	/	1711.6 ± 26.6	/
20	37639.6 ± 310.4	1584.0 ± 25.3	144.5 ± 9.6	1592.5 ± 21.6	36.8 ± 5.8
50	35977.1 ± 244.9	1243.1 ± 21.3	281.0 ± 11.8	1335.8 ± 21.2	73.0 ± 7.0

[a] Average SASA of HheC. [b] Average number of solvent molecules inside the first solvation shell (all water/DMSO molecules found within 3.5/4.5 Å from the heavy (non-hydrogen) atoms of the protein). [c] Average number of HBs between solvent molecules and the protein. Only HBs satisfying both conditions; distance below 3.5 Å and angle below 30°, are counted.

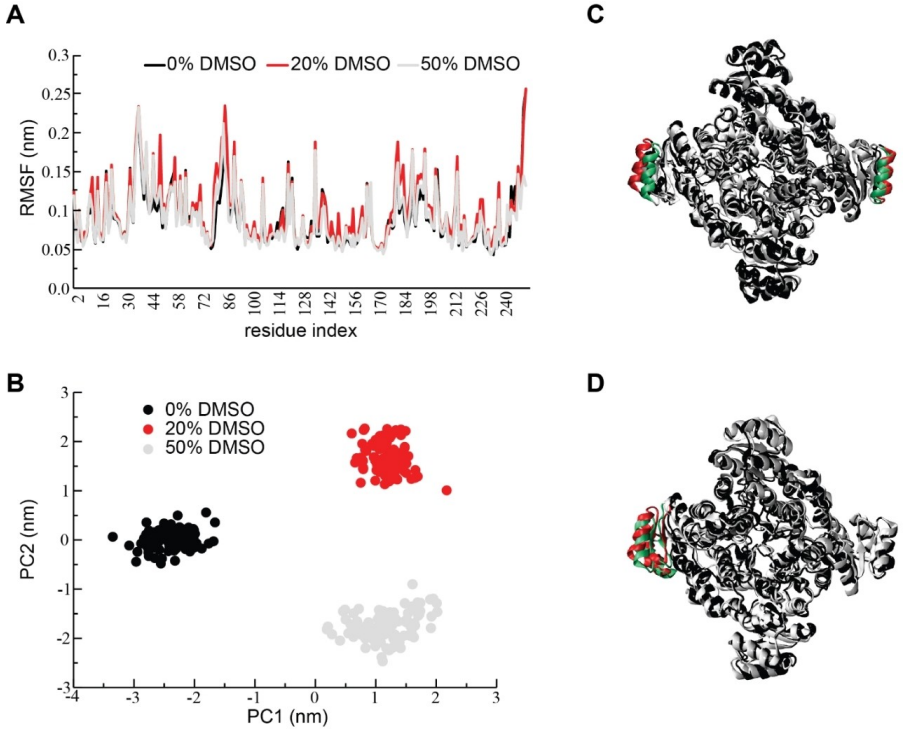

Figure 2. A) Root mean square fluctuation (RMSF) values obtained as the average fluctuation of equivalent residues in the four tetramer subunits, for HheC in three solvent mixtures. B) PCA plot calculated from coordinates of the Cα atoms of the tetramer in the three simulated systems (last 100 ns of each simulation). All structures are projected onto the first two common principal components PC1 and PC2 explaining 30.8 and 21.2% of variance, respectively. Aligned structures corresponding to lowest and highest C) PC1 and D) PC2 values, respectively. Differences along PC1 and PC2 are most easily observed through changes in positioning helix α3 (coloured green and red for lower and upper extreme, respectively), with them moving away one from another in the former, but rotating/skewing in the latter case.

Overall, that might lead to a change in electrostatics of the protein, thus promoting its propensity toward aggregation. DMSO is also found to form small clusters at its hotspots around the protein (Figure S6).

Although the tetramer structure stays conserved and no subunit dissociation or unfolding were recorded during the simulated time, the observed concentration dependent subunit shifting could entail that more drastic changes might occur during the significantly prolonged simulation times.

Experimental stability measurements showed that HheC remains stable for days in media containing up to 30% DMSO. At 40% DMSO enzyme starts losing its activity over the time (with a half-life $t_{1/2}$ of 41 h, compared to 520 h for pure aqueous media), with DMSO being fully detrimental to the enzyme stability at a concentration of 50% ($t_{1/2}$ = 40 min) (Table 2). A steep stability curve indicates that the enzyme abruptly loses catalytic activity when exposed to 50% DMSO (Figure S7).

In parallel, we employed differential scanning calorimetry (DSC) to determine HheC thermally induced denaturation in a buffer medium and in the presence of different DMSO volume ratios; 5, 20, 30, 40 and 50% (*v*/*v*; Figure 3). Thermal unfolding of HheC in buffer aqueous solution occurs at T_m of 60 °C

Table 2. The effect of DMSO concentration on HheC stability during incubation.

DMSO *v*/*v* [%]	k_d [min^{-1}]	$t_{1/2}$ [h]	Residual activity[a] [%]
0	$2.22\times10^{-5}\pm1.44\times10^{-6}$	520	97
30	$2.39\times10^{-5}\pm5.21\times10^{-6}$	484	96.5
40	$2.81\times10^{-4}\pm9.31\times10^{-6}$	41	67
50	$1.67\times10^{-2}\pm2.53\times10^{-3}$	0.7	0

[a] After 24 h.

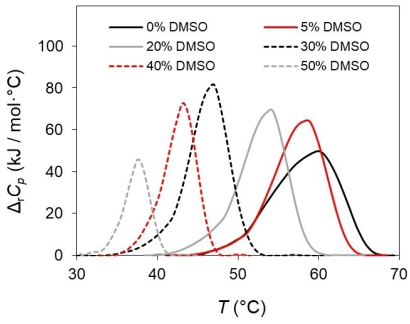

Figure 3. Shift of DSC thermograms, represented as baseline-subtracted molar heat capacity traces of HheC enzyme, with increasing amounts of DMSO in the buffer (100 mM Tris-SO_4, pH 7.5, $\gamma_{HheC} = 0.85$ mg mL^{-1}).

(Table 3), compared to 55 °C obtained by thermofluor-based assay under somewhat different conditions (50 mM Tris-SO_4, pH 8).[52] The unfolding transition peak is quite broad, characterized by $\Delta T_{1/2}$ of 10.1 °C. Furthermore, the geometry of the transition peak, broad with distinctive shoulder towards lower temperatures, indicates a multistate denaturation process. Thermograms obtained under DMSO presence reveal a definite co-solvent contribution to thermal denaturation. An increment in DMSO concentration results in narrowing and shifting of denaturation heat absorption peaks and, consequently, T_m values toward the lower temperature region (Table 3), that is, process cooperativity increases while thermal stability declines.

Progressive thermal destabilization with DMSO concentration increase is also manifested through the linear decrease in $\Delta T_{1/2}$ values (Figure S8). Moreover, the transition peak geometry changes at higher DMSO concentrations (40 and 50%), showing a more symmetrical appearance, thereby suggesting two-state unfolding process. The destabilization of the enzyme tertiary and secondary conformation is further corroborated by the unfolding process enthalpy, which declines abruptly in buffer medium with 40 and 50% DMSO. In buffer medium and with 5, 20, and 30% DMSO, ΔH remains around 500 kJ mol^{-1} K^{-1} (Table 3). It appears that 30% of DMSO is a critical ratio for reduction of kinetic stability as well as thermodynamic in terms of process enthalpy.

Table 3. HheC thermal unfolding characteristics,[a] extracted from the DSC scans.

DMSO *v/v* [%]	T_m [°C]	ΔH [kJ mol^{-1} K^{-1}]	ΔT @ $^1/_2$ *h* [°C]
0	60.0	509	10.1
5	58.6	517	7.5
20	54.1	502	6.5
30	46.9	513	5.7
40	43.2	358	4.4
50	37.7	175	3.4

[a] Melting temperature (T_m), enthalpy (ΔH) and peak width at half height (ΔT @ $^1/_2$ *h*).

It is well established that environmental stress causes protein unfolding and/or aggregation. Protein structural transformations of different extent may lead to changes in its size and shape, which can be identified using the dynamic light scattering (DLS) technique. The increase in size greater than the one found in the crystal structure of an enzyme is usually attributed to protein aggregation.[53] Thus, we chose DLS to evaluate the influence of DMSO concentration on the global structure of HheC. Number size distribution (NSD) and volume size distribution (VSD) were used to characterize the distribution of particles with a different hydrodynamic diameter (D_h). NSD weights particles according to their number and is a measure of relative protein concentration, whereas VSD weights particles according to the volume they occupy and is suitable for early detection of aggregates formation.[54]

In the buffer medium, all the particles were found between 4 and 15 nm in size, with a maximum of distribution around 8.5 nm (85 Å; Figure 4), which corresponds to the size of crystal tetrameric HheC (146.44×72.04×97.42 Å).[47] NSD displays almost no redistribution over 7 days, indicating that the enzyme structure remains very stable during the observed period (Figure 4A). Although their overall portion is rather minute, VSD suggests the existence of aggregates after 24 h onwards, where distribution maxima move toward higher values over time (Figure S9). Resembling the behaviour of HheC in the buffer medium, no change in NSD in 30% (*v/v*) DMSO was observed during the first 2 days (Figure 4B). At 72 h, around 30% of the particles aggregated, while at 96 h, this value increased to 80%. After 120 h, there are no particles smaller than 40 nm left, and their size extends to 6 μm. When protein is exposed to a

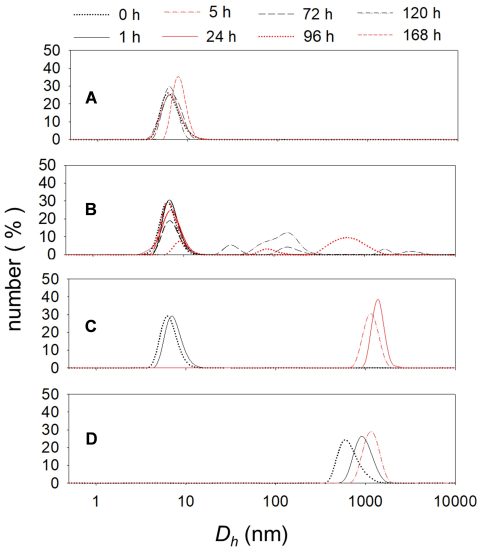

Figure 4. Number size distribution in A) buffer medium or B) 30, C) 40 and D) 50% DMSO ($\gamma_{HheC} = 1.0$ mg mL^{-1}, 100 mM Tris-SO_4, pH 7.5, 25 °C, 1000 rpm).

denaturing agent, the shift in its size to larger particles is commonly ascribed to random protein rearrangement into a looser structure and molecular aggregation.[53] Under harsh conditions, denaturation and protein unfolding may occur, followed by rapid and unspecific aggregation due to hydrophobic interactions among unfolded chains.[55] This effect occurs faster at higher concentrations of OSs, especially hydrophilic ones.[31] In 40% DMSO, after 5 h, the smallest HheC particles were about 700 nm in size (Figure 4C). In 50% DMSO co-solvent, the distribution maximum was determined to be at 600 nm after mixing the protein sample with the co-solvent and equilibration for 60 s, indicating almost instant structural changes (Figure 4D).

The shift in particle size distribution towards greater values was accompanied by an increase in solution turbidity, also indicating rapid aggregation (Figure S10). These results show the clear correlation between the HheC stability at the different DMSO content (Table 2) and the extent of aggregation. However, faster protein aggregation is expected here, as 10 times greater concentration was used for DLS measurements. Protein concentration plays an important role in aggregation phenomenon, as the increase in concentration directly implies a greater possibility for collision and consequent aggregation.[56–58]

Protein aggregation is often related to protein unfolding. As the large and oligomeric proteins tend to unfold stepwise, we would expect that unfolding of tetrameric HheC starts with the subunit dissociation. However, in all DMSO/water mixtures, the formation of monomeric HheC was not detected implying that the rate of aggregation is faster than the rate of subunit dissociation, or that HheC aggregate directly from the tetrameric state. In many cases non-native aggregation is preceded by partial or complete protein unfolding; however, proteins can also directly associate from the near-native structure without going through the intermediate state. Such protein association can be initiated by electrostatic forces, or combination of electrostatic and hydrophobic interactions.[56] Although conformational changes are considered necessary for aggregation occurrence, it is presumed they can be subtle and take place within an oligomeric structure.[57,59] However, these findings do not rule out the possibility that dissociation of tetrameric structure occurs, since the change in size from tetramer to monomer does not meet the recommended minimum difference of a factor of 3 for the resolution of the DLS technique.[60]

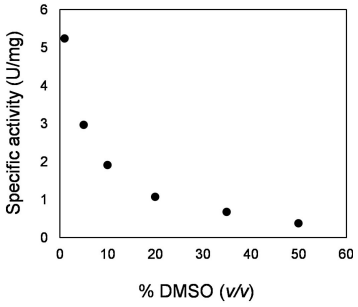

Figure 5. The effect of the DMSO concentration on the dehalogenation activity of HheC (c_{PNSHH} = 5 mM, γ'_{CFE} = 0.1 mg mL^{-1}, 100 mM Tris-SO_4 pH 7.5 with different DMSO ratios, V_R = 500 µL, 25 °C, 1000 rpm).

Enzyme kinetic activity profile

Although HheC remains stable, its catalytic activity, evaluated using *para*-nitro-2-bromo-1-phenylethanol (PNSHH test, Scheme S1) changes rapidly by adding DMSO. Reactions performed over the range of DMSO from 1 to 50% (*v*/*v*) showed a steady decline in the enzyme activity with increasing co-solvent concentration (Figure 5). At 10% DMSO, the specific activity of the enzyme drops below the half of its value, while at 50% co-solvent content, the relative activity is below 10%.

In the active site

MD simulations performed on tetrameric state upon molecular docking indicated possible effective binding of DMSO to catalytic residues (Figure S11), and provide detailed insight in the substrate and halide binding sites with respect to the prevalence of solvent molecules and their dynamic interactions with the amino acid residues forming these sites. In halide/nucleophile binding site, DMSO does not replace the bound water. On average 1.5 water molecules make interactions with the residues constituting this site (Table 4). However, DMSO binds alternately to the catalytic residues Ser132 and Tyr145 through formation of, on average, 0.3 and 0.8 HBs with them, in the case of 20 and 50% DMSO systems, respectively (Table 4,

Table 4. Average numbers of solvent molecules (DMSO or water) and their HBs with the residues Ser132 or Tyr145 in the active site for the HheC tetramer.

DMSO *v*/*v* (%)	Average number of solvent molecules				Number of HBs[c] (Ser132/Tyr145)	
	Substrate binding site[a]		Halide binding site[b]			
	H_2O	DMSO	H_2O	DMSO	H_2O	DMSO
0	19.9 ± 2.0	/	1.7 ± 0.4	/	2.1 ± 0.5	/
20	15.5 ± 1.8	2.6 ± 0.5	1.7 ± 0.3	0.3 ± 0.2	1.5 ± 0.5	0.3 ± 0.3
50	11.1 ± 1.5	2.8 ± 0.5	1.3 ± 0.3	0.2 ± 0.2	2.1 ± 0.5	0.8 ± 0.3

[a] Average number of solvent molecules inside the ligand binding region defined as the region inside a sphere of radius of 8 Å centred around the centre of mass of Tyr187. [b] Defined as the intersection of the two conditions; all water molecules found at or below 5 Å from Cα atom of His179 AND all water molecules found at or below 8 Å from Cα atom of Tyr187. [c] Average number of HBs between solvent molecules and Ser132 OR Tyr145. Only HBs with distance below 3.5 Å and angle below 30°, are counted.

Figure 6). This finding is concurrent with the loss of water molecules surrounding the catalytic site (Figures 7 and S12). Water density decreases, while DMSO density increases inside the substrate binding site with rising DMSO concentration. The water 3D density profiles are significantly more dispersed compared to the more localized density distribution of DMSO, particularly in the vicinity of the residues Ser132 and Tyr145.

This finding, together with the observation that the active site is significantly more constrained in the presence of DMSO (Figure S13, less variance along both components PC1 and PC2 in 20 and 50% DMSO compared to 0% DMSO), suggest that DMSO has significantly stronger propensity and higher specificity toward the catalytic triad than water. To confirm this assumption, we calculated mean residence times of water and DMSO, by using autocorrelation function methodology.[61,62] The mean residence time water spends in the vicinity of OH-group of the catalytic residues (monitored region was 4 Å from OH-group of Ser132) is between 1 and 2.8 ns for the studied systems. The residence time of DMSO is considerably longer, 8.5 and 23 ns for 20 and 50% DMSO, respectively. We found strong evidence from MD simulations that DMSO exerts inhibiting effects on HheC through binding to the catalytic residues.

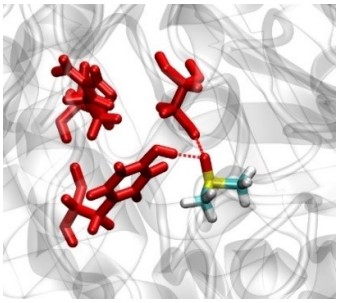

Figure 6. Snapshot of the MD simulation showing the DMSO molecule bound to the catalytic residues and forming HBs with OH groups of Ser132 and/or Tyr145 of HheC subunit. See the Supporting video.

In addition, although DMSO molecules do not enter halide binding site, they accumulate near amino acid residues which form the loop enclosing the halide binding site and participating in formation of the so-called tunnel 2 observed in HheC in extensive MD simulations of HheC carried previously.[48] In addition to helix 3, helix 7 is observed to vary the most by DMSO addition (Figure S4). This is rather interesting because helix 7 has a direct effect on the available tunnels for substrate binding and product release, in particular also affecting tunnel 2.[48] The changes in conformation found herein when increasing DMSO concentration could directly influence the available tunnels, and thus impact the catalytic activity of the enzyme.

Enzyme inhibitory effect

In order to gain experimental insight into the mode of inhibition, a set of initial reaction rates measurements was performed at different PNSHH concentrations (1–5 mM) over a co-solvent range of 1–50% (*v*/*v*) (Figure S14). A double reciprocal Lineweaver-Burk plot was constructed (Figure 8), presenting dependencies of the inverse specific activities (1/

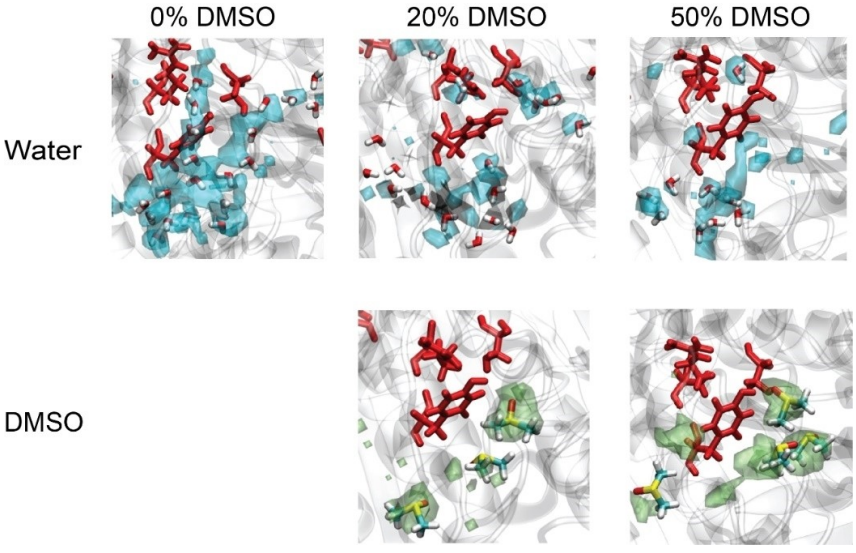

Figure 7. Volumetric maps (isovalue = 0.5) of water (blue) and DMSO (green) inside the substrate binding site of HheC (4 Å from Ser132), obtained from the last 100 ns of the respective tetramer simulations.

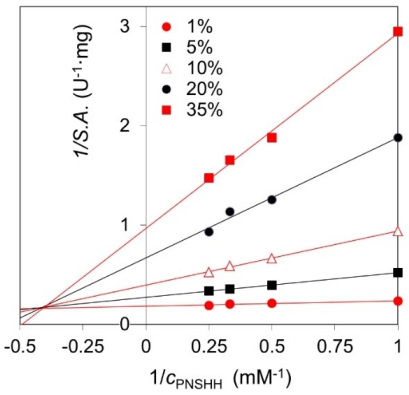

Figure 8. Lineweaver-Burk plot showing the dependence of HheC specific activity reciprocal value on the reciprocal value of PNSHH concentration over a DMSO range of 0–35 % (*v*/*v*).

S.A., mg U^{-1}) over inverse substrate concentrations ($1/c_{PNSHH}$, mM^{-1}). Each individual line unites values for same DMSO ratios, while line slope increases with increase of co-solvent content.

The interdependence of Lineweaver-Burk lines indicates the type of inhibition occurring.[63] The intersection of the lines is not positioned on the *y*- or *x*-axis, which corresponds to mixed inhibition; a form of reversible inhibition that cannot be classified as a single type but contains both elements of competitive and uncompetitive behaviour. Inhibition parameters (Table 5) were estimated by the nonlinear regression methods, as described in Experimental Section.

DMSO can compete with the substrate for binding to the free enzyme, thus reducing enzyme affinity, that is, increasing K_m. Furthermore, co-solvent can bind to the HheC-PNSHH complex, hence lowering V_m.[49] A lower value of the competitive inhibition constant indicates that its share in the activity reduction is predominant. The inhibitory effect of DMSO towards different enzymes has also been observed in other studies.[65–67]

In research applications and industrial synthesis, HHDHs are often used in ring-opening reactions with different nucleophiles for obtaining synthetically valuable β-substituted alcohols and 1,2-difunctionalized organic compounds.[15] Therefore, the reverse reaction between PNSO and bromide ions was characterized. Since Michaelis constant for PNSO is not available from literature, the effect of PNSO concentration on the specific activity of the enzyme was examined prior to co-solvent experiments (Figure S15A). Reactions performed in DMSO presence over the range 1 to 50 % (*v*/*v*; 0.14–7.04 M) demonstrated a strong inhibitory effect (Figure S15B). Under assumption of mixed inhibition, parameters were estimated as described in Experimental Section (Table 5). Values obtained by kinetic measurements of up to 35 % DMSO were included in the parameter estimation, since specific activity at 50 % is obviously a synergistic result of inhibition and protein aggregation. In the ring-opening reaction, competitive inhibition is also found superior ($K_i^c < K_i^u$). Although still considerable, the overall effect of inhibition is slightly lower compared to the ring-closing reaction (Figure S16).

DMSO is often employed as a co-solvent of choice in screening HHDH activities of usually poorly soluble unnatural substrates. However, we show that even at 5 % (*v*/*v*), DMSO can inhibit the activity of HheC by half. Moreover, DMSO does not act as an equally potent inhibitor for all enzyme reactions, which could, in some cases, lead to wrong conclusions of insufficient enzyme affinity. In other words, while performing screening of novel substrates, the lower enzyme activity may not necessarily reflect a weaker affinity for a substrate, but it may result from stronger DMSO inhibition, even though the utilized volume ratio is kept the same (stemming from distinct binding propensities of the different substrates). Suppressed HHDH activity also prolongs the time required for biocatalytic transformations, extending the contact time of substrates/products with water, which further favours unwanted hydrolysis and other chemical side reactions. This should also be considered while screening new activities, as background reactions can reduce product optical purity and yield. We can conclude that inhibitory effect of DMSO cannot be generalized; hence, detailed kinetic studies should be conducted with each enzyme of interest. In addition, inhibition behaviour is related not only to the enzyme but also to the nature of organic solvent, as diverse solvent molecules may have different binding affinities to the active site of the enzyme or even demonstrate other inhibition modes. For example, DMF does not reduce the HheC activity at the same extent as DMSO (Table S4). However, it has a negative effect on the enzyme stability with a half-life of 1 h even at 20 % DMF. Evaluation of other organic solvents and their impact on the catalytic performance of HheC is in progress and will be reported in due course.

Table 5. Kinetic parameters in PNSHH ring-closing and PNSO ring-opening reactions in presence of DMSO.

Ring-closing reaction of PNSHH		Ring-opening reaction of PNSO		
Kinetic parameter	Value	Kinetic parameter	Value	Unit
V_m	26.205 ± 0.090	V_m	1.171 ± 0.246	U mg^{-1}
$K_m^{PNSHH[a]}$	0.009 ± 0.003	K_m^{PNSO}	1.489 ± 0.114	mM
K_{i1}^c	3.922 ± 0.319	K_{i2}^c	10.380 ± 0.585	mM
K_{i1}^u	998.942 ± 85.226	K_{i2}^u	104.529 ± 4.219	mM
		K_i^{PNSO}	0.201 ± 0.015	mM

[a] Determined elsewhere[64]

Conclusion

In this study, the underlying mechanisms for the observed decay in HheC activity in the presence of the water-miscible co-solvent DMSO was elucidated by performing kinetics, DLS and DSC measurements as well as MD simulations. DMSO was found to act as a mixed-type inhibitor with a prevalent competitive contribution in both ring-opening and ring-closing reactions. MD simulations revealed that DMSO molecules replace water molecules both on the surface and in the active site of the enzyme, thereby forming hydrogen bonds and hydrophobic interactions with HheC as well as showing a tendency to form small patches close to the protein surface. On the other hand, we found that the native structure of HheC is retained in the presence of DMSO in concentrations up to 30%. To the best of our knowledge, such high structural tolerance to the action of elevated amounts of DMSO has not been reported for any natural HHDH to date. Last but not least, HheC shows high structural integrity compared to other natural enzymes under given conditions. The stability of HheC, demonstrated both experimentally and in MD simulations of the tetramer, is worth emphasising, as for most studied enzymes in the literature, complete destabilization occurs at significantly lower DMSO concentrations. Above 30% (*v/v*) DMSO, HheC starts losing its active structure, finally attaining a fully aggregated form in the presence of 50% DMSO. These investigations provide an understanding of the co-solvent effect, being a crucial component in tailoring HheC for industrially relevant catalysis in nonaqueous media. For the first time, a comprehensive investigation of the co-solvent effect on HHDH's structural and catalytic properties has been conducted, giving guidelines for appropriate solvent use in future biocatalysis.

Experimental Section

General experimental procedures/data. Chemicals and solvents were purchased as follows: acrylamide and tris(hydroxymethyl)aminomethane from Acros Organics (Geel, Belgium); β-mercaptoethanol and Coomassie Brilliant Blue G-250 from Honeywell Fluka (North Carolina, USA); glycerol, sodium hydroxide, DMSO from Gram-mol d.o.o. (Zagreb, Croatia); EDTA, ammonium sulfate, lysogeny broth, agar, ampicillin, arabinose and sodium dodecyl sulfate from Carl Roth (Karlsruhe, Germany); protease inhibitor cOmplete™ tablets from Roche (Basel, Switzerland); bovine serum albumin and phosphoric acid from Sigma-Aldrich (Missouri, USA); methyl *tert*-butyl ether from VWR International (Pennsylvania, USA); acetonitrile and ammonium persulfate from Fisher Scientific (New Hampshire, USA); tetramethylethylenediamine from TCI Europe N.V. (Zwijndrecht, Belgium); sodium azide from Alfa Aesar (Kandel, Germany); while *para*-nitro-2-bromo-1-phenylethanol (PNSHH) and *para*-nitro styrene oxide (PNSO) where synthesized according to the previously described method.[24]

Protein expression and characterization: Cell-free extract (CFE) of HheC was prepared as reported previously.[27] Single-step purification was carried out by ion-exchange chromatography on HiPrep Q HP 16/10 column with 20 mL bed volume (Cytiva, Marlborough, UK) on an ÄKTA FPLC system (GE Healthcare, Chicago, USA). Column was equilibrated with TEMG buffer (10 mM Tris-SO_4 pH 7.5, 1 mM EDTA, 1 mM β-mercaptoethanol, 10% (*v/v*) glycerol), while TEMG containing 0.45 M $(NH_4)_2SO_4$ was used to elute the proteins according existing method.[68] Fractions containing the target enzyme were inspected for activity by applying the PNSHH assay and their purity was confirmed by SDS-PAGE (Figure S17). The two fractions of the highest purity and protein content were concentrated and desalinated by repeated washing on Amicon Ultra-15 centrifugal filter (Merck Millipore, Darmstadt, Germany). Protein concentration (CFE and purified protein) was determined by the Bradford method.[69]

Activity assay: HHDH activity assay was adapted from literature.[24] The initial reaction rates were determined in ring-closing reaction of PNSHH to PNSO (Scheme S1). Activity was monitored in 500 µL screw capped tubes in ThermoMixer C (Eppendorf, Hamburg, Germany) at 1000 rpm and 25 °C in buffer (100 mM Tris-SO_4, pH 7.5) with selected DMSO volume ratio (1–50% (*v/v*)), containing PNSHH (5 mM) and CFE (0.1 mg mL^{-1}). Sampling was performed 5 times within 10% PNSHH conversion. Aliquots (10 µL) were immediately diluted in 390 µL acetonitrile and filtered through 0.22 µm Chromafil Xtra H-PTFE (Macherey-Nagel, Düren, Germany). PNSHH and PNSO concentrations were determined by HPLC analyses using previously prepared calibration curves (Figure S18). Specific enzyme activity (*S.A.*) was calculated from a linear change in PNSO concentration over time using Equation (1).

$$S.A. = \frac{V_R}{V_E} \cdot \frac{dc}{dt} \cdot \frac{1}{\gamma_E} \quad (1)$$

Stability measurements: Enzyme kinetic stability measurements were performed in screw capped tubes in ThermoMixer C from Eppendorf (Hamburg, Germany) at 1000 rpm and 25 °C throughout 72 h. Incubation media consisted of Tris-SO_4 buffer (100 mM Tris-SO_4, pH 7.5) with DMSO at selected volume ratios (5–50% (*v/v*)). Multiple times during the stability monitoring interval, the enzyme was sampled and used to initiate individual activity assays (ring-closing reactions of PNSHH to PNSO) as described.

DSC measurements: HheC thermal stability measurements were performed in a microcalorimeter Nano-DSC (TA Instruments, New Castle, USA). Samples were prepared by dissolving purified protein to a final concentration of 0.85 mg mL^{-1} in buffer (100 mM in Tris-SO_4, pH 7.5 at 25 °C) and buffer/DMSO mixtures (5, 20, 30, 40, 50%), followed by degassing for 10 min on a degassing station (TA Instruments, New Castle, USA). Analyses were performed in 300 µL cell volume, with 600 s equilibration time, in the temperature range of 20–70 °C at a scan rate of 1 °C min^{-1}. Prior to protein thermal profiling, reference calorimetry was performed with every buffer-DMSO mixture, and the obtained scans were later subtracted from the protein measurements. Results were evaluated with TA Instruments Nano Analyze software package, and thermal unfolding characteristics (T_m: melting temperature, ΔH: enthalpy, $\Delta T @ {}^1/_2\ h$: peak width at half height) were extracted.

Particle size distribution: Measurements of the particle size distributions (PSDs) were performed by DLS on a Zetasizer Ultra (Malvern Panalytical, Malvern, UK). The parameters required for monitoring protein NSDs in 30, 40 and 50% DMSO solutions were determined as follows: kinematic viscosity with manual glass U-tube viscosimeter CFRC-150 (Cannon Instrument Company, State College, USA), density with digital density meter DMA 35 (Anton Paar, Zagreb, Croatia) and refractive index with refractometer (Carl Zeiss Jena GmbH, Jena, Germany; Table S3). Purified enzyme was filtered through a 0.45 µm Chromafil Xtra H-PTFE (Macherey-Nagel, Düren, Germany) to remove larger particles that may interfere with the measurement. The enzyme at a concentration of 1.0 mg mL^{-1} was incubated in cuvettes in Tris-SO_4 (100 mM, pH 7.5) and with 30, 40 and 50% (*v/v*) DMSO. Incubation was performed through one

week at 25 °C and 1000 rpm. Each measurement was performed in triplicate with an equilibration time of 60 s.

Estimation of kinetic parameters: The values of the deactivation constant (k_d, min^{-1}) and half-life ($t_{1/2}$, h) were estimated from experimental results obtained within enzyme stability measurements. Estimations were based on Equations (2) and (3), respectively, assuming that the activity decay can be described by first-order kinetics.

$$\frac{dS.A.}{dt} = -k_d \cdot t \tag{2}$$

$$t_{1/2} = \frac{\ln 2}{k_d} \tag{3}$$

Enzyme kinetics in PNSHH ring-closing (Scheme S1, Equation (4)) and PNSO ring-opening (Scheme S2, Equation (5)) reactions are described with Michaelis-Menten expressions with inhibitions. The parameters of maximum reaction rate (V_m), Michaelis constants (K_m), inhibition constants (K_i^c: competitive, K_i^u: uncompetitive, K_i^{PNSO}: substrate inhibition) were estimated using experimental data, kinetic Equations (4) and (5) and nonlinear regression methods available within the SCIENTIST software package.[63,70]

$$r_1 = \frac{V_{m1} \cdot c_{PNSHH}}{K_m^{PNSHH} \cdot \left(1 + \frac{c_{DMSO}}{K_{i1}^c}\right) + c_{PNSHH} \cdot \left(1 + \frac{c_{DMSO}}{K_{i1}^u}\right)} \tag{4}$$

$$r_2 = \frac{V_{m2} \cdot c_{PNSO}}{K_m^{PNSO} \cdot \left(1 + \frac{c_{DMSO}}{K_{i2}^c}\right) + c_{PNSO} \cdot \left(1 + \frac{c_{DMSO}}{K_{i2}^u}\right) + \frac{c_{PNSO}^2}{K_i^{PNSO}}} \tag{5}$$

Molecular dynamics simulations methodology: We performed all-atom molecular dynamics (MD) simulations of wild type HheC in water and mixed solvent environments (water/DMSO mixtures), in tetramer and hypothetical monomer states. The protein structure (water removed) was obtained from crystal structure with the PDB ID 1ZMT. The protein was parameterized using AMBER ff14SB force field.[71] The monomer was immersed in the rectangular boxes containing 29348 water molecules, 25253 water/1380 DMSO molecules, and 16253 water/3450 DMSO molecules, corresponding to mixtures with 0, 20 and 50% DMSO/H_2O (*v*/*v*), respectively. Similarly, in the case of the HheC tetrameric state, 80000 water molecules, 64000 water/3680 DMSO molecules, and 40000 water/9200 DMSO species were used to solvate the tetramer, corresponding to 0, 20 and 50% DMSO/H_2O (*v*/*v*) mixtures, respectively. To account for ionic strength and to neutralize the net charge of the simulation boxes, sodium cations and chloride anions were added to each simulated system. Water molecules and salt ions were described by the standard TIP3P water model and parameters developed by Cheatham III et al. (ion parameters used in AMBER force fields), respectively.[72] The DMSO parameters were obtained using general AMBER force field.[73] Missing partial charges of DMSO solvent were estimated by a restrained single-conformer fit to the electrostatic potential (RESP).[74] The potential was obtained from the HF/6-31G(d)//B3LYP/6-31G(d) quantum mechanical calculations.

All prepared systems were subjected to the equivalent minimization/equilibration procedure. The simulation boxes were first minimized using steepest descent algorithm (5000 steps), and were subsequently relaxed for the duration of 10 ns at $T = 298$ K (NVT ensemble) with the time step of 2 fs, where we used Berendsen thermostat (time constant for temperature coupling set at 1 ps), and where position restraints on all heavy atoms (all atoms other than hydrogens) of the protein were imposed (500 $kJ\,mol^{-1}\,nm^{-2}$). After the initial relaxation in the canonical ensemble, systems were equilibrated at $T = 298$ K (NPT ensemble), where we again used Berendsen thermostat to maintain temperature (time constant for temperature coupling set at 1 ps) and Berendsen barostat to maintain constant pressure of 1 bar (time constant for pressure coupling set to 5.0 ps) for 10 ns with the time step of 2 fs with weak position restraints again applied on the equivalent set of atoms as aforementioned (100 $kJ\,mol^{-1}\,nm^{-2}$). Finally, we propagated production runs with all systems simulated for at least 200 ns. More precisely, hypothetical monomer simulations were propagated for t(0% DMSO) = 300 ns, t(20%DMSO) = 240 ns and t(50% DMSO) = 400 ns, and tetramer simulations were propagated for t(0% DMSO) = 240 ns, t(20% DMSO) = 300 ns and t(50% DMSO) = 250 ns. Production simulations were propagated in NPT ensemble without any restraints, with Nose-Hoover thermostat incorporated to maintain temperature at $T = 298$ K (time constant for temperature coupling of 1 ps), whereas Parrinello-Rahman barostat was used to maintain constant pressure of 1 bar (time constant for pressure coupling set to 5.0 ps). All simulations were performed with periodic boundary conditions in all three directions, with long-range electrostatic interactions beyond a 1.2 nm cutoff taken into account by using the particle mesh Ewald method.[75] In the subsequent analysis only the last 100 ns of each individual simulation was considered. All MD simulations and analyses (e.g., root mean square deviation (RMSD), root mean square fluctuation (RMSF), principal component analysis (PCA), hydrogen bonds (HBs) analysis) were conducted using GROMACS 2018.[76] The systems are visualized by programs VMD[77] and PyMOL.[78] Additionally, one replica of each simulated system was propagated for 200 ns, using the same conditions as described above. Starting structures for each replica were taken from already simulated systems, corresponding to structures extracted at $t = 50$ ns. The extracted structures were equilibrated using Berendsen barostat in duration of 1 ns, whereby starting velocities of the prepared systems were randomly generated following Boltzmann distribution, constituting different starting points in their respective phase spaces.

Acknowledgements

This work was financially supported by the Croatian Science Foundation (HrZZ, IP-2018-01-4493). Additionally, N.M. is supported by a PhD scholarship from the Croatian Science Foundation through the Career Development Project for Young Researchers. The authors are thankful to Croatian Ministry of Science and Education for supporting the computational cluster Isabella where MD calculations were performed (http://www.srce.unizg.hr/en/usluge/isabella-cluster). We would like to thank to Prof. Lixia Tang for helpful comments on the manuscript and to Drs. Fabio Faraguna and Marko Racar for giving us access to Zetasizer and helping us with measurements.

Conflict of Interest

The authors declare no conflict of interest.

Keywords: activity · biocatalysis · DMSO · halohydrin dehalogenase · molecular dynamics

[1] G. Hasnaoui-Dijoux, M. Majerić Elenkov, J. H. Lutje Spelberg, B. Hauer, D. B. Janssen, *ChemBioChem* **2008**, *9*, 1048–1051.
[2] M. Majerić Elenkov, H. W. Hoeffken, L. Tang, B. Hauer, D. B. Janssen, *Adv. Synth. Catal.* **2007**, *349*, 2279–2285.
[3] M. Majerić Elenkov, B. Hauer, D. B. Janssen, *Adv. Synth. Catal.* **2006**, *348*, 579–585.
[4] A. Mikleušević, I. Primožič, T. Hrenar, B. Salopek-Sondi, L. Tang, M. Majerić Elenkov, *Tetrahedron: Asymmetry* **2016**, *27*, 930–935.
[5] L. Martínez-Montero, D. Tischler, P. Süss, A. Schallmey, M. C. R. Franssen, F. Hollmann, C. E. Paul, *Catal. Sci. Technol.* **2021**, *11*, 5077–5085.
[6] J.-F. Wu, N.-W. Wan, Y.-N. Li, Q.-P. Wang, B.-D. Cui, W.-Y. Han, Y.-Z. Chen, *iScience* **2021**, *24*, 102883.
[7] E. Calderini, P. Süss, F. Hollmann, R. Wardenga, A. Schallmey, *Catalysts* **2021**, *11* (8), 1–18.
[8] X.-Y. Zhou, N.-W. Wan, Y.-N. Li, R. Ma, B.-D. Cui, W.-Y. Han, Y.-Z. Chen, *Adv. Synth. Catal.* **2021**, *363*, 4343–4348.
[9] S.-Y. Chen, C.-X. Yang, J.-P. Wu, G. Xu, L.-R. Yang, *Adv. Synth. Catal.* **2013**, *355*, 3179–3190.
[10] H.-B. Cui, L.-Z. Xie, N.-W. Wan, Q. He, Z. Li, Y.-Z. Chen, *Green Chem.* **2019**, *21*, 4324–4328.
[11] S. K. Ma, J. Gruber, C. Davis, L. Newman, D. Gray, A. Wang, J. Grate, G. W. Huisman, R. A. Sheldon, *Green Chem.* **2010**, *12*, 81–86.
[12] B. Seisser, I. Lavandera, K. Faber, J. H. L. Spelberg, W. Kroutil, *Adv. Synth. Catal.* **2007**, *349*, 1399–1404.
[13] J. H. Schrittwieser, I. Lavandera, B. Seisser, B. Mautner, W. Kroutil, *Eur. J. Org. Chem.* **2009**, *2009*, 2293–2298.
[14] W. Szymanski, C. P. Postema, C. Tarabiono, F. Berthiol, L. Campbell-Verduyn, S. de Wildeman, J. G. de Vries, B. L. Feringa, D. B. Janssen, *Adv. Synth. Catal.* **2010**, *352*, 2111–2115.
[15] Z. Findrik Blažević, N. Milčić, M. Sudar, M. Majerić Elenkov, *Adv. Synth. Catal.* **2021**, *363*, 388–410.
[16] M. Schallmey, P. Jekel, L. Tang, M. Majerić Elenkov, H. W. Höffken, B. Hauer, D. B. Janssen, *Enzyme Microb. Technol.* **2015**, *70*, 50–57.
[17] J. Koopmeiners, C. Diederich, J. Solarczek, H. Voß, J. Mayer, W. Blankenfeldt, A. Schallmey, *ACS Catal.* **2017**, *7*, 6877–6886.
[18] M. M. C. H. van Schie, J.-D. Spöring, M. Bocola, P. Domínguez de María, D. Rother, *Green Chem.* **2021**, *23*, 3191–3206.
[19] L. Ostermeier, R. Oliva, R. Winter, *Phys. Chem. Chem. Phys.* **2020**, *22*, 16325–16333.
[20] H. Arabnejad, M. Dal Lago, P. A. Jekel, R. Floor, A.-M. W. H. Thunnissen, A. C. Terwisscha van Scheltinga, H. Wijma, D. B. Janssen, *Protein Eng. Des. Sel.* **2016**, *30*, 175–189.
[21] M. An, W. Liu, X. Zhou, R. Ma, H. Wang, B. Cui, W. Han, N. Wan, Y. Chen, *RSC Adv.* **2019**, *9*, 16418–16422.
[22] R. M. Haak, F. Berthiol, T. Jerphagnon, A. J. A. Gayet, C. Tarabiono, C. P. Postema, V. Ritleng, M. Pfeffer, D. B. Janssen, A. J. Minnaard, B. L. Feringa, J. G. de Vries, *J. Am. Chem. Soc.* **2008**, *130*, 13508–13509.
[23] G. Hasnaoui, J. H. Lutje Spelberg, E. de Vries, L. Tang, B. Hauer, D. B. Janssen, *Tetrahedron: Asymmetry* **2005**, *16*, 1685–1692.
[24] J. H. Lutje Spelberg, L. Tang, M. van Gelder, R. M. Kellogg, D. B. Janssen, *Tetrahedron: Asymmetry* **2002**, *13*, 1083–1089.
[25] M. Majerić Elenkov, I. Primožič, T. Hrenar, A. Smolko, I. Dokli, B. Salopek-Sondi, L. Tang, *Org. Biomol. Chem.* **2012**, *10*, 5063–5072.
[26] M. Majerić Elenkov, M. Čičak, A. Smolko, A. Knežević, *Tetrahedron Lett.* **2018**, *59*, 406–408.
[27] A. Mikleušević, Z. Hameršak, B. Salopek-Sondi, L. Tang, D. B. Janssen, M. Majerić Elenkov, *Adv. Synth. Catal.* **2015**, *357*, 1709–1714.
[28] C. Molinaro, A.-A. Guilbault, B. Kosjek, *Org. Lett.* **2010**, *12*, 3772–3775.
[29] L. Tang, X. Zhu, H. Zheng, R. Jiang, M. Majerić Elenkov, *Appl. Environ. Microbiol.* **2012**, *78*, 2631–2637.
[30] S.-P. Zou, Z.-C. Wang, C. Qin, Y.-G. Zheng, *Biotechnol. Lett.* **2016**, *38*, 1579–1585.
[31] S. Wang, X. Meng, H. Zhou, Y. Liu, F. Secundo, Y. Liu, *Catalysts* **2016**, *6*, 1–16.
[32] M. Khabiri, B. Minofar, J. Brezovský, J. Damborský, R. Ettrich, *J. Mol. Model.* **2013**, *19*, 4701–4711.
[33] H. Cui, T. H. J. Stadtmüller, Q. Jiang, K.-E. Jaeger, U. Schwaneberg, M. D. Davari, *ChemCatChem* **2020**, *12*, 4073–4083.
[34] M. Dirkmann, J. Iglesias-Fernández, V. Muñoz, P. Sokkar, C. Rumancev, A. von Gundlach, O. Krenczyk, T. Vöpel, J. Nowack, M. A. Schroer, S. Ebbinghaus, C. Herrmann, A. Rosenhahn, E. Sanchez-Garcia, F. Schulz, *ChemBioChem* **2018**, *19*, 153–158.
[35] S. Dutta Banik, M. Nordblad, J. M. Woodley, G. H. Peters, *ACS Catal.* **2016**, *6*, 6350–6361.
[36] V. Stepankova, S. Nevolova, T. Koudelakova, Z. Prokop, R. Chaloupkova, J. Damborský, *ACS Catal.* **2013**, *3*, 2823–2836.
[37] M. Nachiappan, G. R. R. Mariadasse, P. Saritha, M. Amala, D. Prabhu, R. Sundarraj, C. Pandian, J. Jeyaraman in *Frontiers in Protein Structure, Function, and Dynamics* (Eds.: D. B. Singh, T. Tripathi), SpringerLink, New York, **2020**, pp. 23–55.
[38] A. Schallmey, M. Schallmey, *Appl. Microbiol. Biotechnol.* **2016**, *100*, 7827–7839.
[39] M. Schallmey, J. Koopmeiners, E. Wells, R. Wardenga, A. Schallmey, *Appl. Environ. Microbiol.* **2014**, *80*, 7303–7315.
[40] J. Koopmeiners, B. Halmschlag, M. Schallmey, A. Schallmey, *Appl. Microbiol. Biotechnol.* **2016**, *100*, 7517–7527.
[41] J. Wessel, G. Petrillo, M. Estevez-Gay, S. Bosch, M. Seeger, W. P. Dijkman, J. Iglesias-Fernández, A. Hidalgo, I. Uson, S. Osuna, A. Schallmey, *FEBS J.* **2021**, *288*, 4683–4701.
[42] H.-X. Jin, Z.-Q. Liu, Z.-C. Hu, Y.-G. Zheng, *Biochem. Eng. J.* **2013**, *74*, 1–7.
[43] S.-P. Zou, Y.-G. Zheng, E.-H. Du, Z.-C. Hu, *J. Biotechnol.* **2014**, *188*, 42–47.
[44] D. Roiban, P. Sutton, R. Splain, C. Morgan, A. Fosberry, K. Honicker, P. Homes, C. Boudet, A. Dann, J. Guo, K. Brown, L. Ihnken, D. Fuerst, *Org. Process Res. Dev.* **2017**, *21*, 1302–1310.
[45] X.-J. Zhang, P.-X. Shi, H.-Z. Deng, X.-X. Wang, Z.-Q. Liu, Y.-G. Zheng, *Bioresour. Technol.* **2018**, *263*, 483–490.
[46] F. Dong, H. Chen, C. A. Malapit, M. B. Prater, M. Li, M. Yuan, K. Lim, S. D. Minteer, *J. Am. Chem. Soc.* **2020**, *142*, 8374–8382.
[47] R. M. de Jong, J. J. W. Tiesinga, H. J. Rozeboom, K. H. Kalk, L. Tang, D. B. Janssen, B. W. Dijkstra, *EMBO J.* **2003**, *22*, 4933–4944.
[48] M. Estévez-Gay, J. Iglesias-Fernández, S. Osuna, *Catalysts* **2020**, *10*, 1–14.
[49] R. M. de Jong, J. J. W. Tiesinga, A. Villa, L. Tang, D. B. Janssen, B. W. Dijkstra, *J. Am. Chem. Soc.* **2005**, *127*, 13338–13343.
[50] L. Tang, J. E. T. van Hylckama Vlieg, J. H. Lutje Spelberg, M. W. Fraaije, D. B. Janssen, *Enzyme Microb. Technol.* **2002**, *30*, 251–258.
[51] K. Hashimoto, A. R. Panchenko, *Proc. Natl. Acad. Sci. USA* **2010**, *107*, 20352–20357.
[52] Z. Wu, W. Deng, Y. Tong, Q. Liao, D. Xin, H. Yu, J. Feng, L. Tang, *Appl. Microbiol. Biotechnol.* **2017**, *101*, 3201–3211.
[53] J. A. J. Housmans, G. Wu, J. Schymkowitz, F. Rousseau, *FEBS J.* **2021**, 1–30.
[54] J. Stetefeld, S. A. McKenna, T. R. Patel, *Biophys. Rev. Lett.* **2016**, *8*, 409–427.
[55] L. Wen, M. Lyu, H. Xiao, H. Lan, Z. Zuo, Z. Yin, *Mol. Pharm.* **2018**, *15*, 2257–2267.
[56] W. Wang, S. Nema, D. Teagarden, *Int. J. Pharm.* **2010**, *390*, 89–99.
[57] D. March, V. Bianco, G. Franzese, *Polymer* **2021**, *13*, 1–14.
[58] S. Nikfarjam, E. V. Jouravleva, M. A. Anisimov, T. J. Woehl, *Biomol. Eng.* **2020**, *10*, 1–14.
[59] G. Meric, A. S. Robinson, C. J. Roberts, *Annu. Rev. Chem. Biomol. Eng.* **2017**, *8*, 139–159.
[60] Y. Casamayou-Boucau, A. G. Ryder, *Anal. Chim. Acta* **2020**, *1138*, 18–29.
[61] S. Chowdhuri, A. Chandra, *J. Phys. Chem. B.* **2006**, *110*, 9674–9680.
[62] S. Bandyopadhyay, S. Chakraborty, B. Bagchi, *J. Am. Chem. Soc.* **2005**, *127*, 16660–16667.
[63] "Appendix I: Enzyme Kinetics", *Organic Chemistry of Enzyme-Catalyzed Reactions* (Ed: R. B. Silverman), Academic Press, San Diego, **2002**, 563–596.
[64] L. Tang, J. H. Lutje Spelberg, M. W. Fraaije, D. B. Janssen, *Biochemistry* **2003**, *42*, 5378–5386.
[65] A. Kumar, T. Darreh-Shori, *ACS Chem. Neurosci.* **2017**, *8*, 2618–2625.
[66] L. Misuri, M. Cappiello, F. Balestri, R. Moschini, V. Barracco, U. Mura, A. Del-Corso, *J. Enzyme Inhib. Med. Chem.* **2017**, *32*, 1152–1158.
[67] G.-H. Kwak, S. H. Choi, J.-R. Kim, H.-Y. Kim, *BMB Rep.* **2009**, *42*, 580–585.
[68] J. van Hylckama Vlieg, L. Tang, J. H. Lutje Spelberg, T. Smilda, G. J. Poelarends, T. Bosma, A. E. J. van Merode, M. Fraaije, D. B. Janssen, *J. Bacteriol.* **2001**, *183*, 5058–5066.
[69] M. M. Bradford, *Anal. Biochem.* **1976**, *72*, 248–254.
[70] *SCIENTIST Handbook*, Micromath®, Salt Lake City, **1986–1995**.
[71] J. A. Maier, C. Martinez, K. Kasavajhala, L. Wickstrom, K. E. Hauser, C. Simmerling, *J. Chem. Theory Comput.* **2015**, *11*, 3696–3713.

[72] I. S. Joung, T. E. Cheatham, *J. Phys. Chem. B.* **2008**, *112*, 9020–9041.
[73] J. Wang, R. M. Wolf, J. W. Caldwell, P. A. Kollman, D. A. Case, J . *Comput. Chem.* **2004**, *25*, 1157–1174.
[74] P. Cieplak, W. D. Cornell, C. Bayly, P. A. Kollman, *J. Comput. Chem.* **1995**, *16*, 1357–1377.
[75] T. Darden, D. York, L. Pedersen, *J. Chem. Phys.* **1993**, *98*, 10089–10092.
[76] M. J. Abraham, T. Murtola, R. Schulz, S. Páll, J. C. Smith, B. Hess, E. Lindahl, *SoftwareX* **2015**, *1–2*, 19–25.
[77] W. Humphrey, A. Dalke, K. Schulten, *J. Mol. Graphics* **1996**, *14*, 33–38.
[78] L. Schrödinger, *The {PyMOL} Molecular Graphics System*, Version ~ 2.3.2, **2015**.

Manuscript received: June 21, 2022
Accepted manuscript online: August 23, 2022
Version of record online: September 13, 2022

Chemistry–A European Journal

Supporting Information

Inhibitory Effect of DMSO on Halohydrin Dehalogenase: Experimental and Computational Insights into the Influence of an Organic Co-solvent on the Structural and Catalytic Properties of a Biocatalyst

Nevena Milčić, Višnja Stepanić, Ivo Crnolatac, Zvjezdana Findrik Blažević, Zlatko Brkljača,* and Maja Majerić Elenkov*

TABLE OF CONTENTS:

Buried surface area

Table S1. Buried surface area for the tetramers calculated as the difference between four times SASA (solvent accessible surface area) of the hypothetical monomer and SASA of its respective tetramer.

DMSO v/v (%)	SASA / Å^2		Buried surface area / Å^2
	Hypothetical monomer	Tetramer	
0	13113	37158	**15294**
20	13301	37640	**15564**
50	13535	35977	**18163**

RMSF analysis of HheC in water

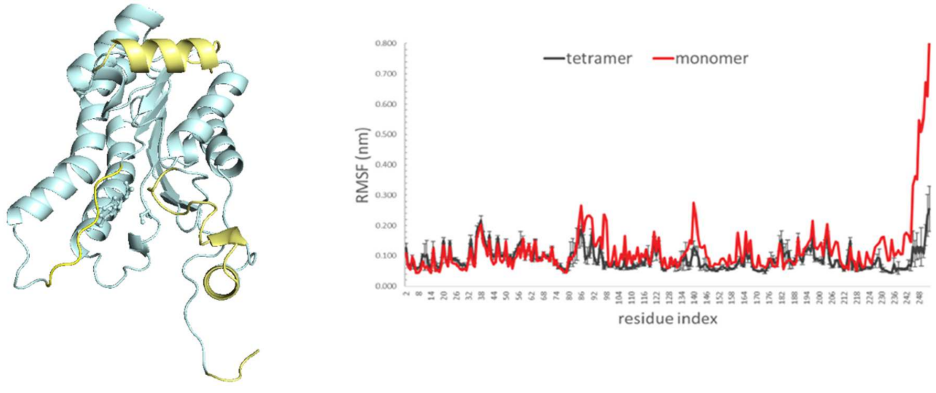

Figure S1. The most flexible parts (yellow coloured, root mean square fluctuation (RMSF) > 0.15 nm) of a HheC tetrameric subunit in water (left). Comparison of RMSF values of Cα atoms of amino acid residues in monomer (red) and average tetramer subunit (black) (right).

RMSD analysis

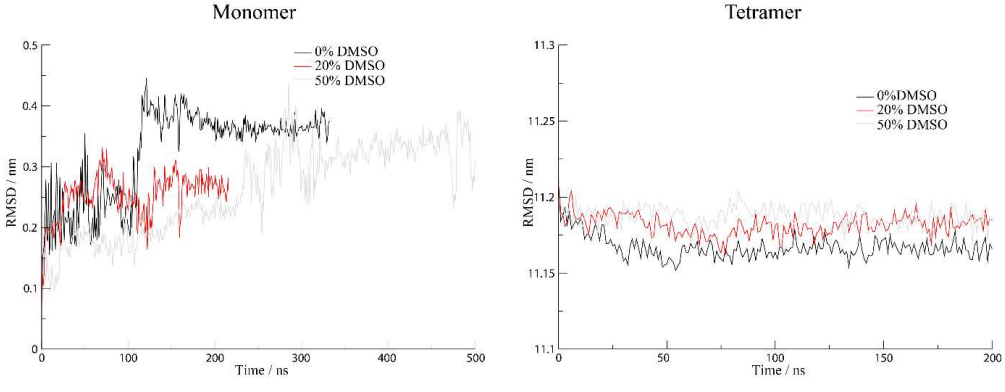

Figure S2. Root mean square deviations (RMSD) of all propagated systems. RMSD values were calculated taking into account atoms constituting the protein backbone.

MD simulations - replicas

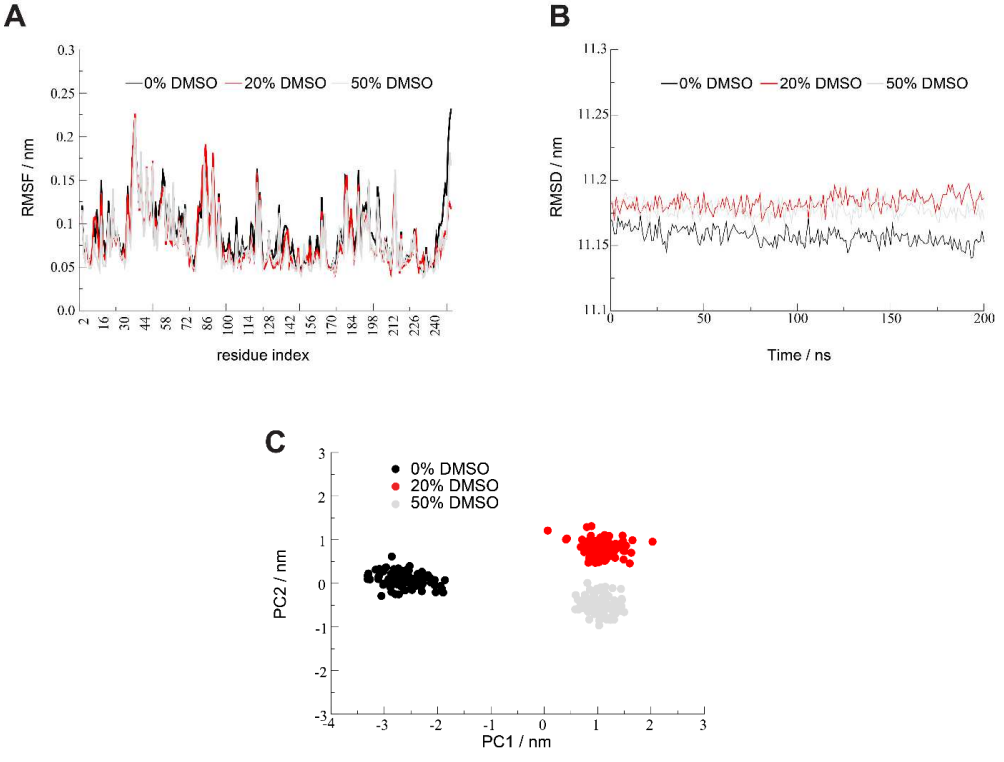

Figure S3. (A) RMSF values obtained as the average fluctuation of equivalent residues in the four tetramer subunits, for HheC in three solvent mixtures. (B) RMSD profiles of all propagated systems. RMSD values were calculated taking into account atoms constituting the protein backbone. (C) PCA plot calculated from coordinates of Cα atoms of tetramer in the three simulated systems (last 100 ns of each original simulation, identical eigenvectors as in Figure 2B).

Overall, extremely similar structural features of the tetramers are observed from the simulations of replicas (comparisons of Figure S3A and Figure 2A, Figure S3B and Figure S2 right panel, and Figure S3C and Figure 2B). Only minor difference between the original simulations and replicas can be observed in the behaviour of 20% DMSO and 50% DMSO systems with regard to their position in PC2, with their corresponding structures now situated somewhat closer compared to the original simulations. However, their PC1 positions are virtually unchanged. Moreover, protein–solvent interactions remain virtually identical between original simulations and replicas (compare Table 2 vs Table S2). Thus, the original simulation results are reproduced with additional simulations.

PCA plots for simulated systems

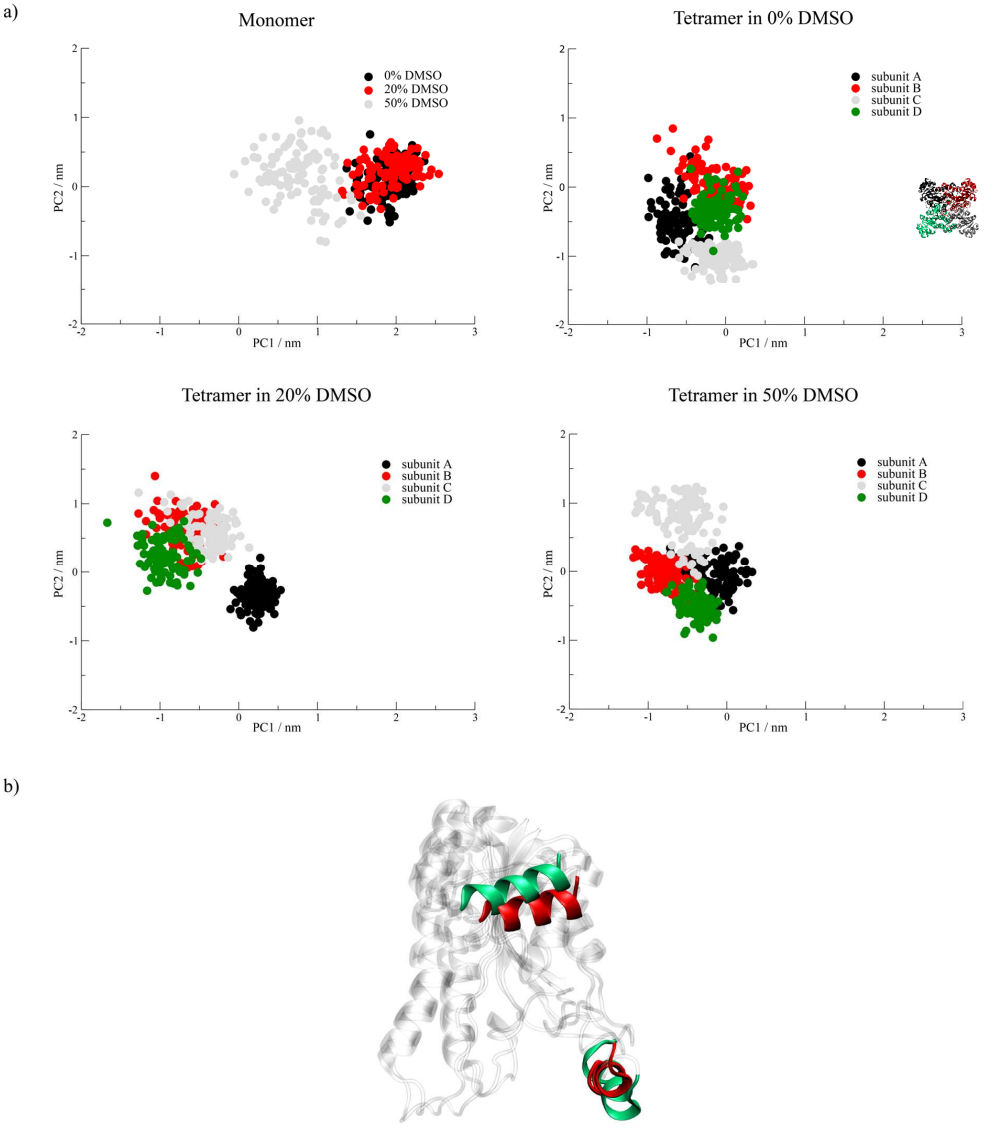

Figure S4. a) Principal component analysis (PCA) of the simulated systems was performed on the basis of first 239 Cα atoms of the protein backbone where all monomer structures, stemming from all performed simulations (hypothetical monomer and tetramer), taken into account. Tail constituting C-terminus of the protein (Cα atoms belonging to residues 240-253) was discarded from the analysis since this region showcases the highest variance between different monomers/subunits, thus blurring the conformational analysis. All structures are projected onto the first two common principal components PC1 and PC2 explaining 33.3% and 11.5% of variance, respectively. b) Aligned structures corresponding to the extreme cases along PC1, with the structures containing green and red helices representing lower and higher extreme, respectively. Lower extreme roughly corresponds to the structure of subunits in tetramers, while upper extreme approximates 20% and 50% DMSO hypothetical monomer systems. Helices α3 and α7 (consult Figure 1) are coloured as they represent the most variable regions of the monomers/monomeric subunits along PC1. Conformational space of hypothetical monomer significantly differs from the conformational space of tetramer subunits, particularly in DMSO/water mixtures.

RMSF analyses of HheC in water/DMSO mixtures

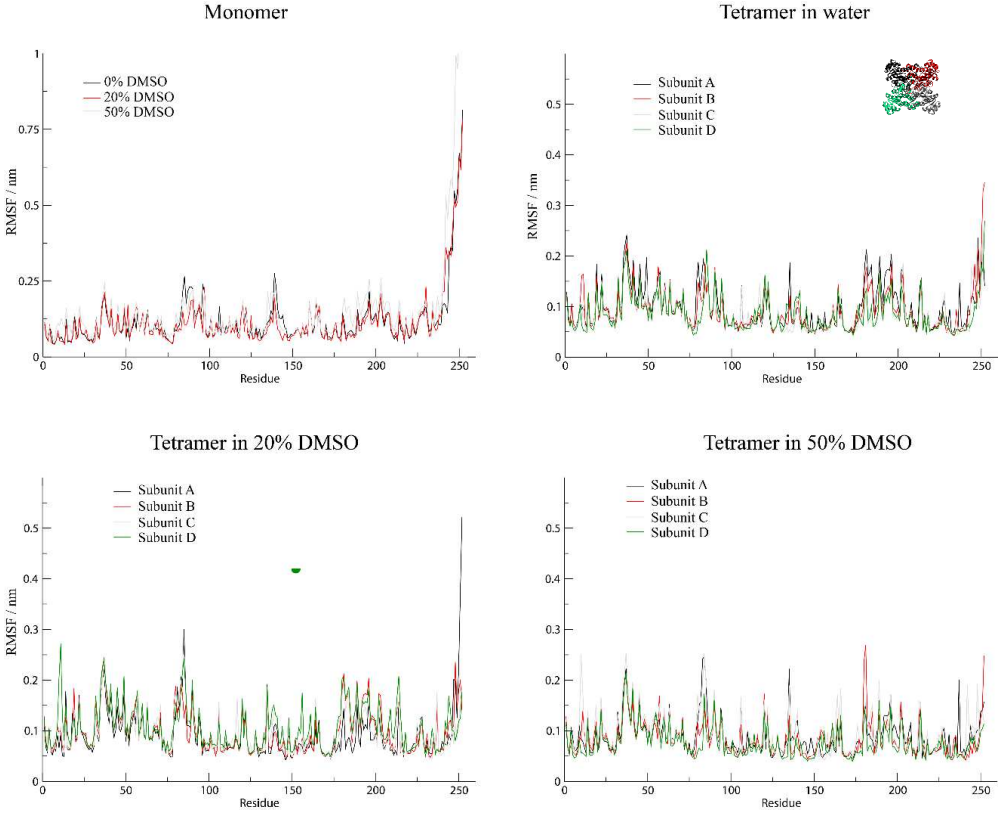

Figure S5. RMSF per amino acid residue, for all propagated systems. For tetrameric form of the protein HheC, RMSF values were calculated for each subunit independently.

SASA, solvent occupancy and HBs at the protein surface - replicas

Table S2. SASA, solvent occupancy (DMSO or water) and HBs at the protein surface.

DMSO v/v (%)	SASA[a] (Å^2)	Average Number of Solvent Molecules in the First Solvent Shell[b]		Number of HBs[c]	
		H_2O	DMSO	H_2O	DMSO
0	37742.1 ± 278.8	1873.8 ± 23.6	/	1720.1 ± 23.8	/
20	37339.4 ± 249.3	1597.6 ± 23.7	143.3 ± 9.0	1596.3 ± 24.7	38.2 ± 5.9
50	36690.8 ± 264.9	1241.5 ± 22.9	289.4 ± 11.3	1334.8 ± 23.2	78.3 ± 6.9

[a] Average SASA of HheC. [b] Average number of solvent molecules inside the first solvation shell (all water/DMSO molecules found within 3.5/4.5 Å from the heavy (non-hydrogen) atoms of the protein). [c] Average number of HBs between solvent molecules and the protein. Only HBs satisfying both conditions; distance below 3.5 Å and angle below 30º, are counted.

Volumetric maps of water and DMSO around the protein

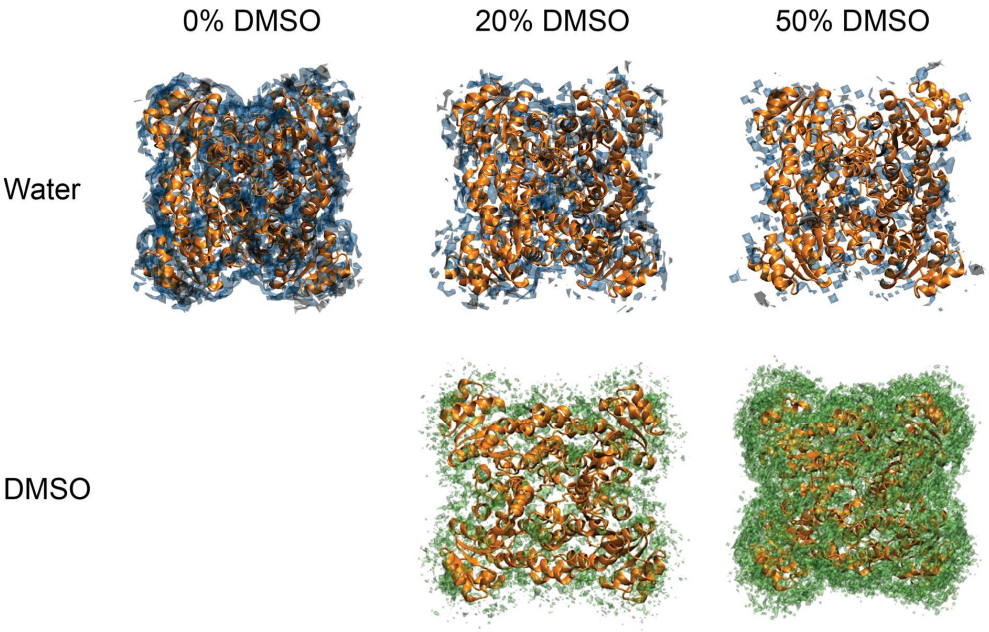

Figure S6. Volumetric maps of water (isovalue = 0.7, atom radius = 0.5, grid resolution = 2 Å) and DMSO (isovalue = 0.5, atom radius = 0.2, grid resolution = 1 Å) around the protein (all solvent molecules within 4 Å from the protein surface are taken into account). Upper panel: Water density around tetramer in pure water simulation, 20% DMSO and 50% DMSO, from left to right respectively. Lower panel: DMSO density in 20% and 50% DMSO, from left to right, respectively.

Stability of HheC in the presence of DMSO

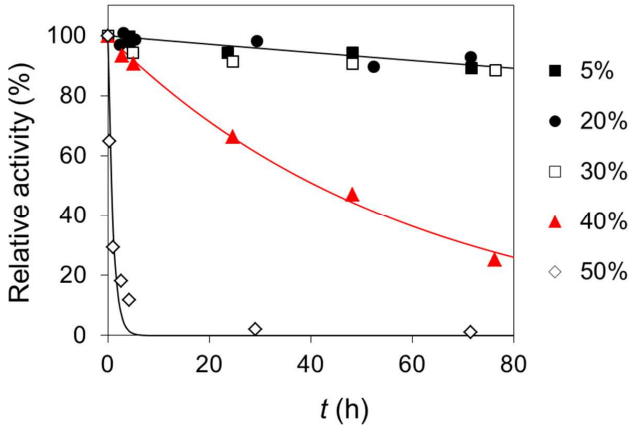

Figure S7. HheC kinetic stability during incubation in aqueous media containing different volume ratios of DMSO (c_{PNSHH} = 5 mM, γ_{CFE} = 0.1 mg/mL, 100 mM Tris-SO_4 pH 7.5, 0 −50% (v/v) DMSO, V_R = 500 µL, 25 °C, 1000 rpm). Legend: symbols – experimental points; line – model.

DSC measurements

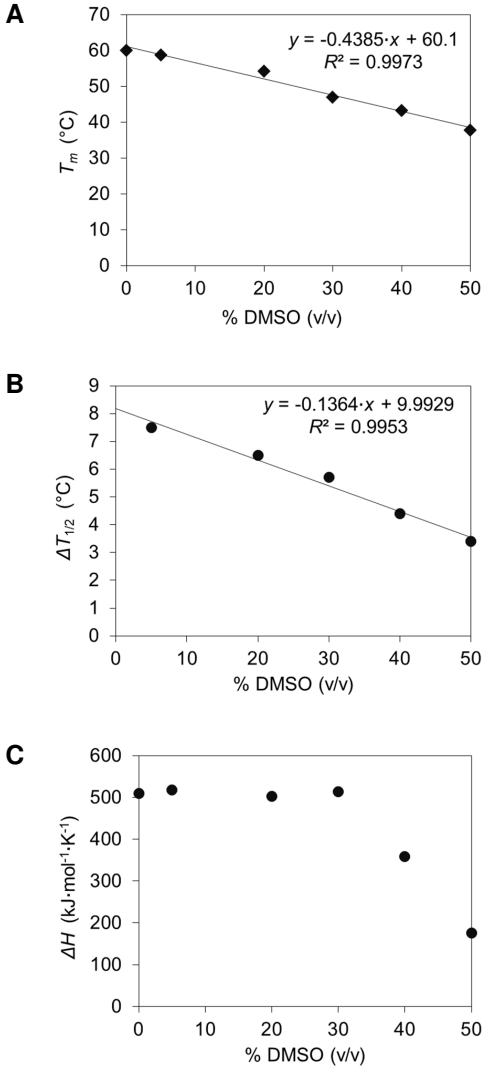

Figure S8. Interdependencies of HheC thermal unfolding parameters. Dependence of DMSO content (% v/v) on: (A) T_m (°C) ; (B) $\Delta T_{1/2}$ (°C) ; (C) ΔH (kJ·mol^{-1}·K^{-1}).

DMSO-water mixture properties

Table S3. Parameters for 30, 40 and 50% DMSO mixtures determined prior to DLS measurements.*

DMSO v/v (%)	n (/)	ρ (g/cm^3)	ν (mm^2/s)	μ (g/cm^3)
30	1.38	1.0397	1.895	1.9705
40	1.40	1.0558	2.355	2.4868
50	1.41	1.0713	2.945	3.1547

* n – refractive index, ν – kinematic viscosity, μ – dynamic viscosity. Dynamic viscosity was calculated from density and kinematic viscosity measurements.

Enzyme aggregation

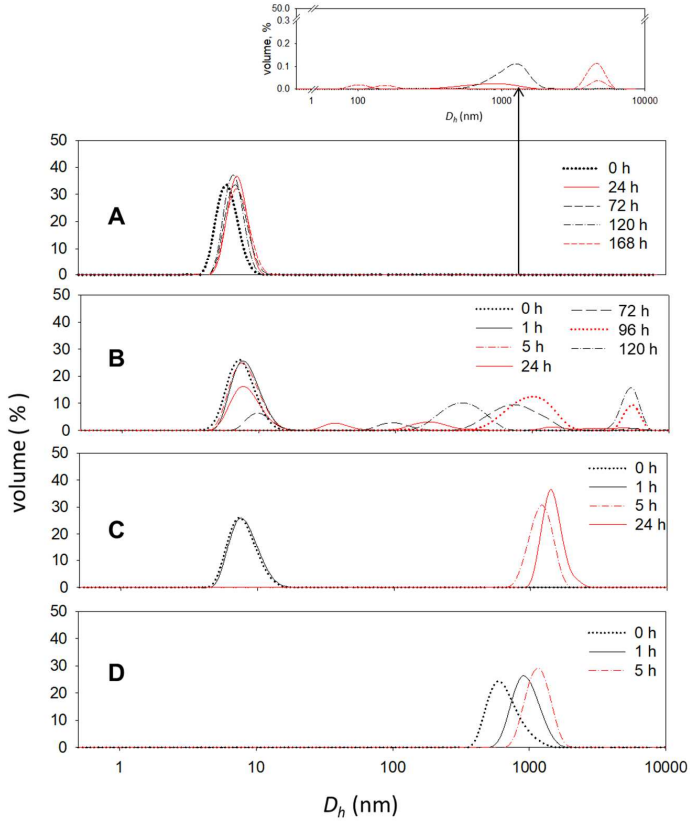

Figure S9. Volume size distribution in (A) buffer medium; (B) 30% DMSO; (C) 40% DMSO; (D) 50% DMSO (γ_{HheC} =1 mg/mL, 100 mM Tris-SO_4 pH 7.5, 25°C, 1000 rpm).

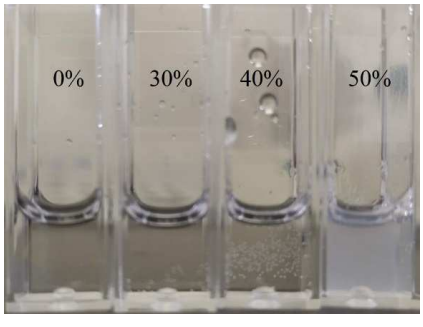

Figure S10. Visual detection of aggregation occurrence by turbidity change in DLS cuvettes upon mixing HheC solution with 50% DMSO.

Molecular docking

To investigate possible inhibitory effect of DMSO, we firstly performed molecular docking. Molecular docking in the substrate binding site of HheC successfully reproduced the experimental binding pose of the substrate PNSO (Figure S11). The best docked pose of DMSO molecule in the substrate binding site was found to be the one close to the halide binding site with the sulfoxide group forming HBs with OH-groups from Tyr145 and Ser132 (Figure S11).

The scores for the substrate PNSO and DMSO, normalized by their heavy atom numbers, were 4.3 and 6.7, respectively. Comparison of the docked binding modes of DMSO and the referent ligand PNSO and the greater ligand efficiency of DMSO, pointed to the competitive inhibiting effect of DMSO on the catalytic activity of HheC. This finding provided a first hint at the possibility of DMSO being an inhibitor of HheC.

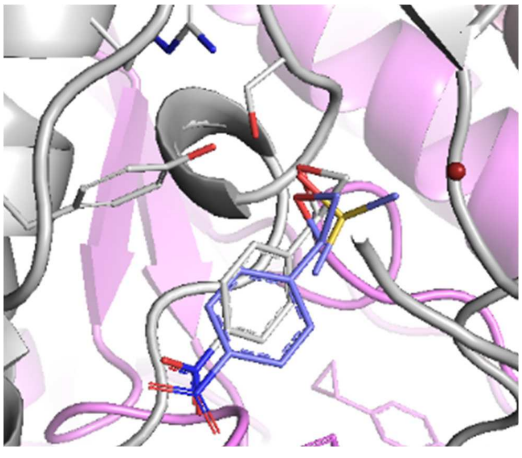

Figure S11. The crystal PNSO ligand (white C atoms) and its and DMSO binding poses predicted by molecular docking (C atoms coloured blue). The catalytic triad constituted by amino acids Ser132, Tyr145 and Arg149 is shown in the stick representation. The red sphere denotes halide binding site. Another subunit belonging to HheC tetramer from the crystal structure 1ZMT is shown in pink.

Molecular docking calculations were carried out using the program GOLD. The calculations were performed considering the binding site conformation of the crystal structure of HheC with the Protein Data Bank (PDB) code 1ZMT, in which HheC is complexed with its substrate (*R*)-PNSO, with water molecule present in the halide binding pocket. Prior to docking all water molecules and the ligand were removed. The binding site was defined as all atoms lying within 15 Å radius of the hydroxyl oxygen of the catalytic residue Tyr145. The PLP fitness function (dimensionless) was used as a scoring function along with default values of all other program parameters.

Volumetric maps of water and DMSO inside the substrate binding sites

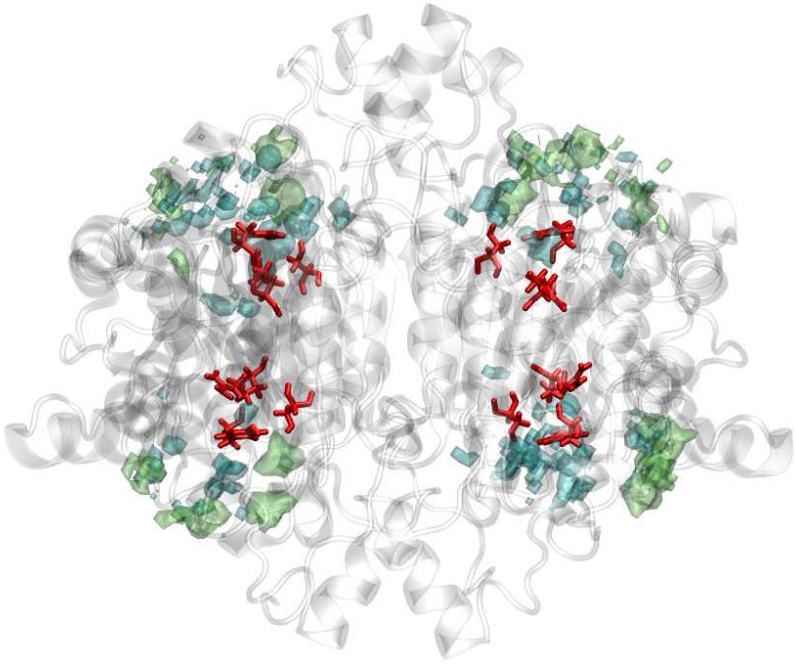

Figure S12. Volumetric maps (isovalue = 0.5) of water (blue) and DMSO (green) inside the substrate binding sites of HheC tetramer (4 Å from Ser132), at 50% DMSO.

PCA plots for the HheC catalytic site

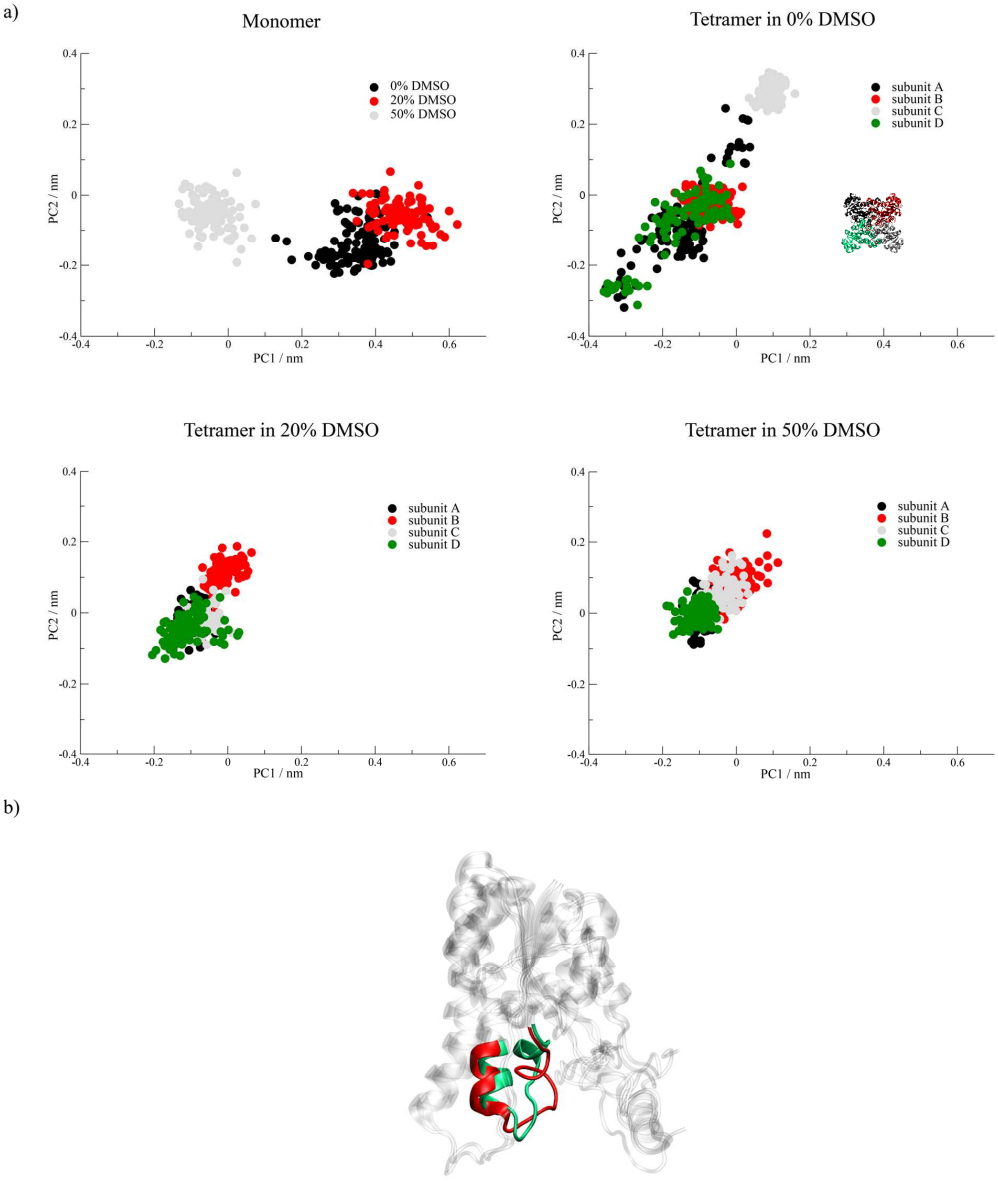

Figure S13. a) PCA for the simulated systems was performed on the basis of Cα atoms belonging to residues 132 to 149, constituting active site and the region surrounding it, with all monomers, stemming from the hypothetical monomer simulations or subunits constituting the tetramer, taken into account. All structures are projected onto the first two common principal components PC1 and PC2 explaining 41.0% and 15.7% of variance, respectively. b) Aligned structures corresponding to the extreme cases (lowest and highest values) along PC1. Structures containing green and red helices correspond to lower and upper extreme values of PC1, respectively. Helices corresponding to residues 132-149 are highlighted.

Kinetic measurements

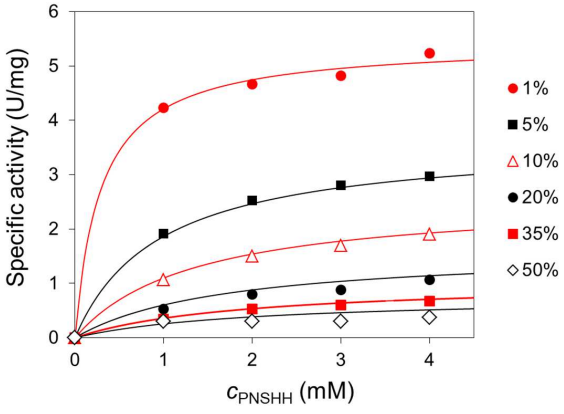

Figure S14. Dependence of the HheC specific activity on the concentration of DMSO (0-50%) and PNSHH (0-4 mM) (25 °C, 1000 rpm, c_{PNSHH} = 5 mM, V_R = 500 µL, 100 mM Tris-SO_4 pH 7.5, γ_{HheC} = 0.01 mg/mL).

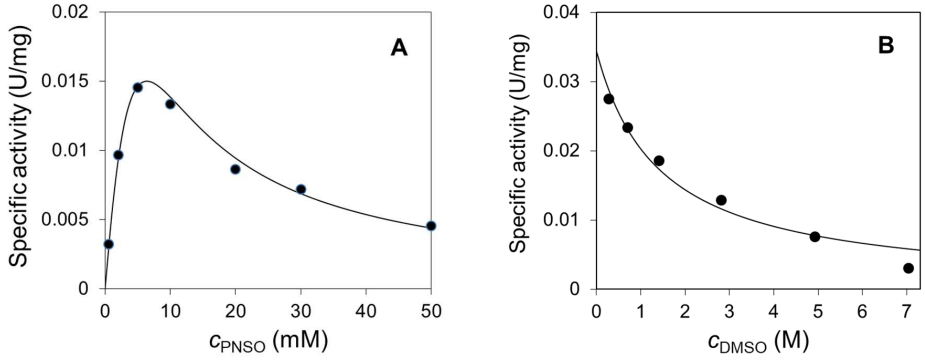

Figure S15. Dependence of the HheC specific activity in PNSO ring-opening reactions with bromide ions on the concentration of (A) PNSO 0-50 mM (c_{NaBr} = 10 mM, γ_{HheC} = 0.4 mg/mL, V_R = 500 µL, 25 °C, 1000 rpm, 100 mM Tris-SO_4 pH 7.5, 10% v/v DMSO); (B) DMSO 0 – 50% v/v (c_{PNSO} = 7.5 mM, c_{NaBr} = 10 mM, γ_{HheC} = 0.4 mg/mL, V_R = 500 µL, 25 °C, 1000 rpm, 100 mM Tris-SO_4 pH 7.5 with different DMSO ratios).

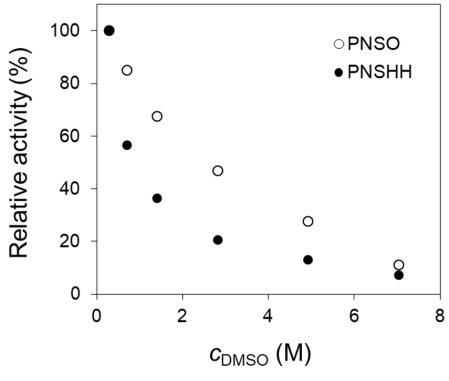

Figure S16. Comparison of the DMSO effect on the relative activity in epoxide ring-opening reaction (c_{PNSO} = 7.5 mM, c_{NaBr} = 10 mM, γ_{CFE} = 0.4 mg/mL) and epoxide ring-closure reaction (c_{PNSHH} = 4 mM, γ_{CFE} = 0.01 mg/mL). DMSO 0 – 50% (v/v) corresponds to 0.14 – 7.04 M (V_r = 500 µL, 25 °C, 1000 rpm, 100 mM Tris-SO_4 pH 7.5 with different DMSO ratios).

Activity and stability of HheC in the presence of DMF

Table S4. DMF effect on the relative activity and stability of DMF evaluated on PNSHH test.*

DMF v/v (%)	Relative activity (%)	$t_{1/2}$ (h)
0	100	520
20	73	1.0
35	22	0.57
50	4	0.51

* Conditions: V_R = 500 µL, 100 mM Tris-SO_4 pH 7.5, c_{PNSHH} = 5 mM, γ_{HheC} = 0.1 mg/mL. Incubation media: 100 mM Tris-SO_4 pH 7.5 with DMF at selected volume ratios (20, 35 and 50%).

SDS-PAGE of purified HheC

Figure S17. SDS-PAGE gel: left – page ruler, right – purified HheC

Reactions catalysed by HheC

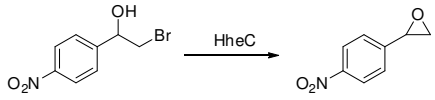

Scheme S1. PNSHH-test: ring-closure reaction of PNSHH to PNSO.

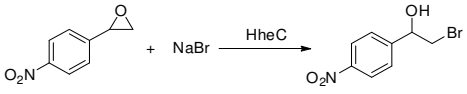

Scheme S2. Ring-opening reaction of PNSO to PNSHH.

HPLC calibration curves

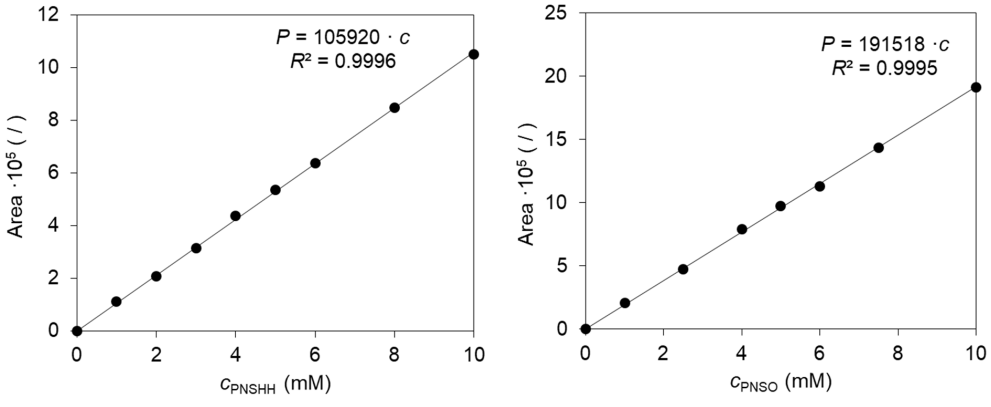

Figure S18. HPLC calibration curves for PNSHH (left) and PNSO (right). Stationary phase: Phenomenex Kinetex® C18 (5 µm, 4.6 × 250 mm). Mobile phase A: 0.1% (v/v) TFA in UPW; mobile phase B: 0.1% (v/v) TFA in ACN:UPW 80:20. Method: decrease in eluent B from 40 to 30% in first 5 minutes, return to 40% B from 5th to 6th minute, stopping the method at 7th minute ; wavelength 275 nm; column oven temperature: 30 °C ; retention times: PNSHH 3.61 min, PNSO 3.97 min

Appendix V

N. Milčić, P. Švaco, M. Sudar, L. Tang, Z. Findrik Blažević, M. Majerić Elenkov, Impact of organic solvents on the catalytic performance of halohydrin dehalogenase, Appl. Microbiol. Biotechnol. (2023)

Nevena Milčić: investigation, methodology, formal analysis, validation, writing – original draft, writing – review & editing

Petra Švaco: investigation, formal analysis, validation, writing – review & editing

Martina Sudar: investigation, formal analysis, validation, writing – review & editing

Lixia Tang: investigation, methodology, formal analysis

Zvjezdana Findrik Blažević: conceptualization, methodology, formal analysis, funding acquisition, writing – original draft, writing – review & editing

Maja Majerić Elenkov: conceptualization, methodology, formal analysis, funding acquisition, writing – original draft, writing – review & editing

This publication was republished as an integral part of PhD thesis with the permission of Applied Microbiology and Biotechnology.

SPRINGER NATURE LICENSE
TERMS AND CONDITIONS

Apr 02, 2023

This Agreement between Faculty of Chemical Engineering and Technology, University of Zagreb -- Nevena Milčić ("You") and Springer Nature ("Springer Nature") consists of your license details and the terms and conditions provided by Springer Nature and Copyright Clearance Center.

License Number	5520801465058
License date	Apr 02, 2023
Licensed Content Publisher	Springer Nature
Licensed Content Publication	Applied Microbiology and Biotechnology
Licensed Content Title	Impact of organic solvents on the catalytic performance of halohydrin dehalogenase
Licensed Content Author	Nevena Milčić et al
Licensed Content Date	Mar 7, 2023
Type of Use	Thesis/Dissertation
Requestor type	academic/university or research institute
Format	print and electronic
Portion	full article/chapter
Will you be translating?	no
Circulation/distribution	1 - 29
Author of this Springer Nature content	yes
Title	Mathematical modelling and optimization of biocatalytic synthesis of fluorinated chiral building blocks
Institution name	Faculty of Chemical Engineering and Technology, University of Zagreb
Expected presentation date	May 2023
Requestor Location	Faculty of Chemical Engineering and Technology, University of Zagreb Marulićev trg 19 Zagreb, 10 000 Croatia Attn: Faculty of Chemical Engineering and Technology, University of Zagreb
Total	**0.00 EUR**

Terms and Conditions

Springer Nature Customer Service Centre GmbH Terms and Conditions

The following terms and conditions ("Terms and Conditions") together with the terms specified in your [RightsLink] constitute the License ("License") between you as Licensee and Springer Nature Customer Service Centre GmbH as Licensor. By clicking 'accept' and completing the transaction for your use of the material ("Licensed Material"), you confirm your acceptance of and obligation to be bound by these Terms and Conditions.

1. Grant and Scope of License

1. 1. The Licensor grants you a personal, non-exclusive, non-transferable, non-sublicensable, revocable, world-wide License to reproduce, distribute, communicate to the public, make available, broadcast, electronically transmit or create derivative works using the Licensed Material for the purpose(s) specified in your RightsLink Licence Details

only. Licenses are granted for the specific use requested in the order and for no other use, subject to these Terms and Conditions. You acknowledge and agree that the rights granted to you under this License do not include the right to modify, edit, translate, include in collective works, or create derivative works of the Licensed Material in whole or in part unless expressly stated in your RightsLink Licence Details. You may use the Licensed Material only as permitted under this Agreement and will not reproduce, distribute, display, perform, or otherwise use or exploit any Licensed Material in any way, in whole or in part, except as expressly permitted by this License.

1. 2. You may only use the Licensed Content in the manner and to the extent permitted by these Terms and Conditions, by your RightsLink Licence Details and by any applicable laws.

1. 3. A separate license may be required for any additional use of the Licensed Material, e.g. where a license has been purchased for print use only, separate permission must be obtained for electronic re-use. Similarly, a License is only valid in the language selected and does not apply for editions in other languages unless additional translation rights have been granted separately in the License.

1. 4. Any content within the Licensed Material that is owned by third parties is expressly excluded from the License.

1. 5. Rights for additional reuses such as custom editions, computer/mobile applications, film or TV reuses and/or any other derivative rights requests require additional permission and may be subject to an additional fee. Please apply to journalpermissions@springernature.com or bookpermissions@springernature.com for these rights.

2. Reservation of Rights

Licensor reserves all rights not expressly granted to you under this License. You acknowledge and agree that nothing in this License limits or restricts Licensor's rights in or use of the Licensed Material in any way. Neither this License, nor any act, omission, or statement by Licensor or you, conveys any ownership right to you in any Licensed Material, or to any element or portion thereof. As between Licensor and you, Licensor owns and retains all right, title, and interest in and to the Licensed Material subject to the license granted in Section 1.1. Your permission to use the Licensed Material is expressly conditioned on you not impairing Licensor's or the applicable copyright owner's rights in the Licensed Material in any way.

3. Restrictions on use

3. 1. Minor editing privileges are allowed for adaptations for stylistic purposes or formatting purposes provided such alterations do not alter the original meaning or intention of the Licensed Material and the new figure(s) are still accurate and representative of the Licensed Material. Any other changes including but not limited to, cropping, adapting, and/or omitting material that affect the meaning, intention or moral rights of the author(s) are strictly prohibited.

3. 2. You must not use any Licensed Material as part of any design or trademark.

3. 3. Licensed Material may be used in Open Access Publications (OAP), but any such reuse must include a clear acknowledgment of this permission visible at the same time as the figures/tables/illustration or abstract and which must indicate that the Licensed Material is not part of the governing OA license but has been reproduced with permission. This may be indicated according to any standard referencing system but must include at a minimum 'Book/Journal title, Author, Journal Name (if applicable), Volume (if applicable), Publisher, Year, reproduced with permission from SNCSC'.

4. STM Permission Guidelines

4. 1. An alternative scope of license may apply to signatories of the STM Permissions Guidelines ("STM PG") as amended from time to time and made available at https://www.stm-assoc.org/intellectual-property/permissions/permissions-guidelines/.

4. 2. For content reuse requests that qualify for permission under the STM PG, and which may be updated from time to time, the STM PG supersede the terms and conditions contained in this License.

4. 3. If a License has been granted under the STM PG, but the STM PG no longer apply at the time of publication, further permission must be sought from the Rightsholder. Contact journalpermissions@springernature.com or bookpermissions@springernature.com for these rights.

5. Duration of License

5. 1. Unless otherwise indicated on your License, a License is valid from the date of purchase ("License Date") until the end of the relevant period in the below table:

Reuse in a medical communications project	Reuse up to distribution or time period indicated in License
Reuse in a dissertation/thesis	Lifetime of thesis
Reuse in a journal/magazine	Lifetime of journal/magazine
Reuse in a book/textbook	Lifetime of edition
Reuse on a website	1 year unless otherwise specified in the License
Reuse in a presentation/slide kit/poster	Lifetime of presentation/slide kit/poster. Note: publication whether electronic or in print of presentation/slide kit/poster may require further permission.
Reuse in conference proceedings	Lifetime of conference proceedings
Reuse in an annual report	Lifetime of annual report
Reuse in training/CME materials	Reuse up to distribution or time period indicated in License
Reuse in newsmedia	Lifetime of newsmedia
Reuse in coursepack/classroom materials	Reuse up to distribution and/or time period indicated in license

6. Acknowledgement

6. 1. The Licensor's permission must be acknowledged next to the Licensed Material in print. In electronic form, this acknowledgement must be visible at the same time as the figures/tables/illustrations or abstract and must be hyperlinked to the journal/book's homepage.

6. 2. Acknowledgement may be provided according to any standard referencing system and at a minimum should include "Author, Article/Book Title, Journal name/Book imprint, volume, page number, year, Springer Nature".

7. Reuse in a dissertation or thesis

7. 1. Where 'reuse in a dissertation/thesis' has been selected, the following terms apply: Print rights of the Version of Record are provided for; electronic rights for use only on institutional repository as defined by the Sherpa guideline (www.sherpa.ac.uk/romeo/) and only up to what is required by the awarding institution.

7. 2. For theses published under an ISBN or ISSN, separate permission is required. Please contact journalpermissions@springernature.com or bookpermissions@springernature.com for these rights.

7. 3. Authors must properly cite the published manuscript in their thesis according to current citation standards and include the following acknowledgement: '*Reproduced with permission from Springer Nature*'.

8. License Fee

You must pay the fee set forth in the License Agreement (the "License Fees"). All amounts payable by you under this License are exclusive of any sales, use, withholding, value added or similar taxes, government fees or levies or other assessments. Collection and/or remittance of such taxes to the relevant tax authority shall be the responsibility of the party who has the legal obligation to do so.

9. Warranty

9. 1. The Licensor warrants that it has, to the best of its knowledge, the rights to license reuse of the Licensed Material. **You are solely responsible for ensuring that the material you wish to license is original to the Licensor and does not carry the copyright of another entity or third party (as credited in the published**

version). If the credit line on any part of the Licensed Material indicates that it was reprinted or adapted with permission from another source, then you should seek additional permission from that source to reuse the material.

9. 2. EXCEPT FOR THE EXPRESS WARRANTY STATED HEREIN AND TO THE EXTENT PERMITTED BY APPLICABLE LAW, LICENSOR PROVIDES THE LICENSED MATERIAL "AS IS" AND MAKES NO OTHER REPRESENTATION OR WARRANTY. LICENSOR EXPRESSLY DISCLAIMS ANY LIABILITY FOR ANY CLAIM ARISING FROM OR OUT OF THE CONTENT, INCLUDING BUT NOT LIMITED TO ANY ERRORS, INACCURACIES, OMISSIONS, OR DEFECTS CONTAINED THEREIN, AND ANY IMPLIED OR EXPRESS WARRANTY AS TO MERCHANTABILITY OR FITNESS FOR A PARTICULAR PURPOSE. IN NO EVENT SHALL LICENSOR BE LIABLE TO YOU OR ANY OTHER PARTY OR ANY OTHER PERSON OR FOR ANY SPECIAL, CONSEQUENTIAL, INCIDENTAL, INDIRECT, PUNITIVE, OR EXEMPLARY DAMAGES, HOWEVER CAUSED, ARISING OUT OF OR IN CONNECTION WITH THE DOWNLOADING, VIEWING OR USE OF THE LICENSED MATERIAL REGARDLESS OF THE FORM OF ACTION, WHETHER FOR BREACH OF CONTRACT, BREACH OF WARRANTY, TORT, NEGLIGENCE, INFRINGEMENT OR OTHERWISE (INCLUDING, WITHOUT LIMITATION, DAMAGES BASED ON LOSS OF PROFITS, DATA, FILES, USE, BUSINESS OPPORTUNITY OR CLAIMS OF THIRD PARTIES), AND WHETHER OR NOT THE PARTY HAS BEEN ADVISED OF THE POSSIBILITY OF SUCH DAMAGES. THIS LIMITATION APPLIES NOTWITHSTANDING ANY FAILURE OF ESSENTIAL PURPOSE OF ANY LIMITED REMEDY PROVIDED HEREIN.

10. Termination and Cancellation

10. 1. The License and all rights granted hereunder will continue until the end of the applicable period shown in Clause 5.1 above. Thereafter, this license will be terminated and all rights granted hereunder will cease.

10. 2. Licensor reserves the right to terminate the License in the event that payment is not received in full or if you breach the terms of this License.

11. General

11. 1. The License and the rights and obligations of the parties hereto shall be construed, interpreted and determined in accordance with the laws of the Federal Republic of Germany without reference to the stipulations of the CISG (United Nations Convention on Contracts for the International Sale of Goods) or to Germany´s choice-of-law principle.

11. 2. The parties acknowledge and agree that any controversies and disputes arising out of this License shall be decided exclusively by the courts of or having jurisdiction for Heidelberg, Germany, as far as legally permissible.

11. 3. This License is solely for Licensor's and Licensee's benefit. It is not for the benefit of any other person or entity.

Questions? For questions on Copyright Clearance Center accounts or website issues please contact springernaturesupport@copyright.com or +1-855-239-3415 (toll free in the US) or +1-978-646-2777. For questions on Springer Nature licensing please visit https://www.springernature.com/gp/partners/rights-permissions-third-party-distribution

Other Conditions:

Version 1.4 - Dec 2022

Questions? E-mail us at customercare@copyright.com.

Applied Microbiology and Biotechnology
https://doi.org/10.1007/s00253-023-12450-2

Impact of organic solvents on the catalytic performance of halohydrin dehalogenase

Nevena Milčić[1] · Petra Švaco[2] · Martina Sudar[1] · Lixia Tang[3] · Zvjezdana Findrik Blažević[1] · Maja Majerić Elenkov[2]

Received: 17 October 2022 / Revised: 15 February 2023 / Accepted: 21 February 2023

Abstract
Biocatalytic transformations in organic synthesis often require the use of organic solvents to improve substrate solubility and promote the product formation. Halohydrin dehalogenases (HHDHs) are enzymes that catalyze the formation and conversion of epoxides, important synthetic class of compounds that are often sparingly soluble in water and prone to hydrolysis. In this study, the activity, stability, and enantioselectivity of HHDH from *Agrobacterium radiobacter* AD1 (HheC) in form of cell-free extract were evaluated in various aqueous-organic media. A correlation was discovered between the enzyme activity in the ring-closure reaction and logP of the solvent. Knowledge of such a relationship makes biocatalysis with organic solvents more predictable, which may reduce the need to experiment with a variety of solvents in the future. The results revealed a high enzyme compatibility with hydrophobic solvents (e.g., *n*-heptane) in terms of activity and stability. Regarding the HHDH applicability in an organic medium, inhibitions by a number of solvents (e.g., THF, toluene, chloroform) proved to be a more challenging problem than the protein stability, especially in the ring-opening reaction, thus suggesting which solvents should be avoided. In addition, solvent tolerance of the thermostable variant ISM-4 was also evaluated, revealing increased stability and to a lesser extent enantioselectivity compared to the wild-type. This is the first time such a systematic analysis has been reported, giving insight into the behavior of HHDHs in nonconventional media and opening new opportunities for the future biocatalytic applications.

Key points
- *HheC performs better in the presence of hydrophobic than hydrophilic solvents.*
- *Enzyme activity in the PNSHH ring-closure reaction is a function of the logP.*
- *Thermostability of ISM-4 variant is accompanied by superior solvent tolerance.*

Keywords Biocatalysis · Halohydrin dehalogenase · Organic solvents · Protein stability

Introduction

Halohydrin dehalogenases (HHDHs; EC 4.5.1.-) are enzymes that catalyze the formation and conversion of epoxides (Scheme S1) (de Jong 2003). They can be applied in the kinetic resolution of racemic epoxides by utilizing a range of anionic nucleophiles such as azide, cyanide, cyanate, and nitrite (Hasnaoui-Dijoux et al. 2008; Findrik Blažević et al. 2021). The ring-opening products and the remaining epoxides are versatile and important synthetic intermediates for fine chemicals and pharmaceuticals (Schneider 2007). The limitation of low yield from the kinetic resolution (50% is the maximum yield) can be overcome by combining HHDHs in a cascade with enzymes such as alcohol dehydrogenases (Seisser et al. 2007; Schrittwieser et al. 2009; Ma et al. 2010; Szymanski et al. 2010; Chen et al. 2013) and monooxygenases (Cui et al. 2019; Calderini et al. 2021). In such a system, chirality is introduced into the molecule in the first step, followed by HHDH-catalyzed non-enantioselective transformation to the final product. Dynamic kinetic resolution is another approach

✉ Maja Majerić Elenkov
majeric@irb.hr

[1] Faculty of Chemical Engineering and Technology, University of Zagreb, Savska c, 16 Zagreb, Croatia

[2] Ruđer Bošković Institute, Bijenička c, 54 Zagreb, Croatia

[3] University of Electronic Science and Technology, No. 4, Section 2, North Jianshe Road, Chengdu, China

Published online: 07 March 2023

in which HHDH can be combined with a transition metal catalyst (Haak et al. 2008) or used solely, however only for a limited number of substrates (Lutje Spelberg et al. 2004; Mikleušević et al. 2015). HHDHs are attractive biocatalysts for synthetic application due to their stereoselectivity, versatile reactivity, and feasible merging with other enzyme(s) in a cascade. In addition, HHDHs can be easily expressed in recombinant form in *E. coli*, do not require cofactors for their activity and are relatively stable (Tang et al. 2002), which presents important properties of an industrial biocatalyst. The low solubility of hydrophobic substrates in aqueous media (e.g., 2 mM for aromatic epoxides) limits the application of HHDHs, since higher substrate loading is an important prerequisite for a biotechnological process. The hydrolytic instability of epoxides is additional limitation for the preparative scale since this side reaction negatively reflects on the product yield. HHDH-catalyzed laboratory-scale transformations are usually performed in aqueous media with the addition of up to 5% (v/v) dimethyl sulfoxide (DMSO). However, recent studies by our group have shown that even small amounts of DMSO can have strong unfavorable effect on reaction rate, mainly due to distinct mixed-type inhibitory properties with predominant competitive contribution (Milčić et al. 2022). At higher DMSO concentration (>30% (v/v)), enzyme conformational changes are induced, and structural integrity is disrupted. Kinetic inhibition studies were confirmed by computational analysis, indicating the need to explore alternative solvents for HHDH-biocatalysis (Milčić et al. 2022).

The use of organic solvents (OSs) as reaction media offers significant advantages and might solve issues regarding solubility and hydrolytic stability (van Schie et al. 2021), at the same time facilitating product extraction and enzyme separation (Cao and Matsuda 2016). Although there are several reports on HHDH-catalyzed transformations in organic-aqueous media (Jin et al. 2013; Zou et al. 2014; Roiban et al. 2017; Zhang et al. 2018; Dong et al. 2020; Staar et al. 2022), no systematic evaluation of the influence of various OSs on the catalytic properties of HHDHs has been performed so far. In general, OSs negatively affect enzyme structure, consequently activity and stability, and may behave as enzyme inhibitors, yet generalization cannot be made, and experimental evaluation is required for each biocatalyst-solvent system. New efforts should be endeavored to find more compatible solvents, as well as novel resistant enzyme variants, with the goal of new industrial implementation of HHDHs. Striving to increase biocatalytic applicability of HHDH, we studied biocatalytic properties of enzyme from *Agrobacterium radiobacter* AD1 (HheC) in the presence of various OSs. Besides wild-type HheC, we examined the thermostable variant ISM-4, obtained previously by some of us employing iterative saturation mutagenesis (Wu et al. 2017), since resistance to high temperatures is often accompanied with enhanced stability and activity in OSs (Arabnejad et al. 2016).

Materials and methods

General

Acrylamide and tris(hydroxymethyl)aminomethane (Tris) were purchased from Acros Organics (Geel, Belgium); β-mercaptoethanol and Coomassie brilliant blue G-250 from Honeywell Fluka (North Carolina, United States); glycerol, sodium hydroxide, dimethyl sulfoxide (DMSO) from Gram-mol d.o.o. (Zagreb, Croatia); EDTA, ammonium sulfate, Lauria-Bretani medium, agar, ampicillin, arabinose, and sodium dodecyl sulfate (SDS) from Carl Roth (Karlsruhe, Germany); protease inhibitor cOmplete™ tablets from Roche (Basel, Switzerland); bovine serum albumin and phosphoric acid from Sigma-Aldrich (Missouri, United States); ethanol, cyclohexane, *n*-hexane, and *n*-heptane from Scharlau (Barcelona, Spain); dimethylformamide (DMF) from Carlo Erba Reagents S.r.l. (Milan, Italy); methanol (MeOH), acetone, tetrahydrofuran (THF), ethyl acetate (EtOAc), methyl *tert*-butyl ether (MTBE), diisopropyl ether (DIPE), chloroform, toluene, and isopropyl alcohol (*i*-PrOH) from VWR International (Pennsylvania, United States); acetonitrile (MeCN) and ammonium persulfate from Fisher Scientific (New Hampshire, United States); and tetramethylethylenediamine from TCI Europe N.V. (Zwijndrecht, Belgium). *para*-Nitro-2-bromo-1-phenylethanol (PNSHH) and *para*-nitro styrene oxide (PNSO) were synthesized as reported elsewhere (Lutje Spelberg et al. 2002).

Enzyme preparation and characterization

Cell-free extracts (CFE) of wild-type HheC and ISM-4 variant were produced as previously described (Mikleušević et al. 2015). Ion-exchange chromatography was performed on HiPrep Q HP 16/10 column (Cytiva, Marlborough, UK) to obtain purified enzyme (Milčić et al. 2022). The produced enzymes were characterized via Bradford method (protein concentration) (Bradford 1976), PNSHH assay (enzyme activity) (Lutje Spelberg et al. 2002), and SDS-PAGE (enzyme overexpression and purity).

Activity assays

Enzyme activity was assessed according to an established protocol described elsewhere (Lutje Spelberg et al. 2002; Milčić et al. 2022). Briefly, ring-closure reaction of PNSHH to PNSO (PNSHH assay) was performed according to the initial reaction rate method, i.e., within 10% conversion of the substrate (Scheme S2). Reaction mixtures were prepared in

screw capped tubes to minimize solvent evaporation and reactions were conducted on ThermoMixer C (Eppendorf, Hamburg, Germany) (V_R = 500 µL, pH 7.5, 100 mM Tris-SO_4 with 5% (v/v) DMSO or specified volume ratio of solvent tested, 1000 rpm, 25 or 50 °C, c_{PNSHH} = 5 mM, γ_{CFE} = 0.1 mg/mL). Samples from the reaction (10 µL) were diluted in MeCN (390 uL) to stop the reaction, and further separated from the enzyme through a filter. Filters used were 0.2 µm Chromafil Xtra H-PTFE or PTFE (Macherey-Nagel, Düren, Germany), depending on reaction medium. Likewise, ring-opening reaction of PNSO to PNSHH (Scheme S3) with bromide ions was performed with hydrophobic OSs (c_{PNSO} = 5 mM, c_{NaBr} = 5 mM, γ_{CFE} = 1 mg/mL, with all the other conditions same as ones in PNSHH assay). Samples were analyzed by HPLC and the concentrations of PNSHH and PNSO were determined using previously prepared calibration curves. Specific enzyme activity was calculated through product formation over time when substrate conversion was less than 10% (Equation 1), whereby V_R stands for reactor volume, V_E for volume of enzyme added, dc/dt for change of product concentration over time, and γ_E for enzyme concentration in stock solution.

$$S.A. = \frac{V_R}{V_E} \cdot \frac{dc}{dt} \cdot \frac{1}{\gamma_E} \quad (1)$$

Stability measurements

Measurements of the kinetic stability of the enzymes during incubation with OSs were performed in screw-top tubes in ThermoMixer C from Eppendorf (Hamburg, Germany) at 1000 rpm and 25 or 50 °C over a prolonged period, i.e., 24 h–4 weeks, depending on activity retained. For water-immiscible OSs, an individual incubation reaction was initiated for each activity measurement. Aqueous-organic media consisted of Tris-SO_4 buffer (500 mM Tris-SO_4, pH 7.5 at 25 °C) and OSs in selected volume ratios with 0.65 mg/mL of CFE. Aliquots of the enzyme from the incubation medium were taken regularly to evaluate activity. Based on the results of linear product formation over time within 10% conversion, the specific enzyme activities were calculated. Under the common assumption that activity decline is described by 1st order kinetics, the deactivation constants (Equation 2) were estimated using nonlinear regression methods within software package SCIENTIST (SCIENTIST handbook), and were used to calculate half-life times (Equation 3).

$$\frac{dS.A.}{dt} = -k_d \cdot t \quad (2)$$

$$t_{1/2} = \frac{1n2}{k_d} \quad (3)$$

Enantioselectivity assays

Kinetic resolution experiments were performed at room temperature as follows. Tris-SO_4 buffer (50 mM, pH 7.5) was added to a round-bottom flask equipped with magnetic stirrer at room temperature (25 °C) followed by a stock solution of sodium azide in water (10 mM final concentration), stock solution of racemic 2-(benzyl)oxirane (BNO) in OS (5 mM final concentration), and 200 µL of cell-free enzyme extract (4 mL total volume of reaction mixture) (Scheme S4). Experiments at elevated temperatures (30, 40, 50, 60, 70, 80, and 90 °C) were performed in screw-top tubes in TS-100C thermoshaker from BioSan (Riga, Latvia) at 1000 rpm. The progress of the reaction was followed by periodically taking samples (0.5 mL) from the reaction mixture. Samples were extracted with MTBE (1 mL), dried over anhydrous Na_2SO_4 and analyzed by GC. Enantioselectivity was determined by measuring the substrate (BNO) and product 2-azido-1-phenylethanol (BNA) enantiomeric access (ee) at different time intervals. E values were calculated from ee_p and ee_s according to Equation 4. Data reported for conversion (c) were calculated according to Equation 5.

$$E = \ln\left[\left(1-ee_s\right)/\left(1+ee_s/ee_p\right)\right]/\ln\left[\left(1+ee_s\right)/\left(1+ee_s/ee_p\right)\right] \quad (4)$$

$$c = ee_s/\left(ee_s+ee_p\right) \quad (5)$$

Analytical methods

HPLC analysis

Concentrations of PNSHH and PNSO were determined on LC-40 Nexera Lite from Shimadzu (Kyoto, Japan) with PDA detector at 275 nm and 30 °C. Kinetex Core-shell C18 column (2.6 µm, 100 × 4.6 mm) from Phenomenex (Torrance, USA) was used with organic phase A (80% MeCN in ultrapure water containing 0.1% TFA) and aqueous phase B (ultrapure water containing 0.1% TFA) at flow rate of 1.5 mL/min. Gradient elution was used from 40 to 30% of phase B over 5 min with a return to initial 30% over the next 2 min. The retention times for PNSHH and PNSO were 3.3 and 3.7 min, respectively.

GC analysis

Chiral GC analyses were performed using an Agilent 8860 instrument (Wilmington, USA) equipped with FID detector (set at 300 °C) and a split injector (set at 250 °C). A Hydrodex g-DiMOM column (25 m×0.25 mm) from Macherey-Nagel (Dueren, Germany) was used with the temperature program: 90 °C, 3 °C/min to 170 °C and N_2 as carrier gas (170 kPa). Retention times were as follows: 7.4 min

(*R*)-BNO, 7.6 min (*S*)-BNO, 23.3 min (*R*)-BNA and 23.6 min (*S*)-BNA.

Results

HheC is by far the best-studied wild-type HHDH enzyme due to its high stereoselectivity and as such was chosen as a group representative for systematic exploration of OSs tolerance in terms of biocatalytic properties (activity, stability, and enantioselectivity).

The impact of the enzyme formulation on HheC stability

The stability of two HheC formulations, cell-free extract (CFE) and purified enzyme, was compared. The stability of wild-type HheC in buffer medium at concentration around 0.1 mg/mL was determined at 25 °C and 1000 rpm, while the concentration in CFE was estimated to be 60% of total proteins (Mikleušević et al. 2015). CFE was found to be very stable, with half-live of 21 days, while the purified enzyme was less stable form ($t_{1/2}$ < 6 days) (Fig. S1), which implies that non-target proteins shelter HheC enzyme from external environment. Further measurements in this work were performed with CFE on account of higher stability along with easier and more cost-effective preparation.

Activity of wild-type HheC in water-organic solvent mixtures

The enzyme activity in the ring-closure reaction (Scheme S2) was examined in the presence of 15 different OSs: dimethyl sulfoxide (DMSO), dimethylformamide (DMF), methanol (MeOH), acetone, acetonitrile (MeCN), isopropyl alcohol (*i*-PrOH), tetrahydrofuran (THF), ethyl acetate (EtOAc), methyl *tert*-butyl ether (MTBE), diisopropyl ether (DIPE), chloroform, toluene, cyclohexane, *n*-hexane, and *n*-heptane. These commonly accessible OSs were selected to cover a broad range of logP values. The effect of each OS was examined in the range of the minimum volume ratio required to dissolve 5 mM PNSHH (2-5% (v/v)) to the maximum ratio at which the enzyme still retained activity in a given assay. Graphs depicting the dependence of specific enzyme activity on the volume ratio of OSs were constructed (Fig. S2). Afterwards, enzyme activity in ring-opening reaction with bromide ions (Scheme S3) was assessed in the same way in presence of set of hydrophobic OSs. Activity profiles for PNSO ring-opening reaction in presence of OSs with increasing logP value from EtOAc to *n*-heptane are given in Fig. S3.

Water-immiscible solvents

For water-immiscible OSs (EtOAc, MTBE, DIPE, chloroform, toluene, cyclohexane, *n*-hexane, and *n*-heptane), correlation between solvent polarity (logP) and activity, represented as c_{50}, was discovered in PNSHH ring-closure reaction (Fig. 1a). Here, c_{50} is defined as the volume concentration of OS which reduces enzyme activity by half (assessed by PNSHH test). It incorporates the overall influence of the OS on the enzyme catalysis, including not only enzyme inhibition by the solvent but also deactivation due to rapid unfolding and substrate partitioning between the two phases. The parameter c_{50} is estimated from concentration-activity profiles obtained by the initial reaction rates method (Figs. S2 and Table S1). It was found that the increase in hydrophobicity of OSs is accompanied by greater specific enzyme activity. In the epoxide ring-opening reaction, OSs with higher logP values also display negative effect on enzyme activity to a lesser extent (Figs. S3 and Table S2); however, direct correlation was not established in this case (Fig. 1b).

Water-miscible solvents

From the activity profiles, it is evident that the water-miscible OSs (DMSO, DMF, MeOH, *i*-PrOH, acetone, MeCN, THF) have a more serious negative effect on enzyme activity (Fig. 2). HheC has fairly good tolerance for lower concentrations of MeCN and DMF, up to 15 and 20%, respectively (Fig. 2a). Other tested water-miscible OSs (THF, MeOH,

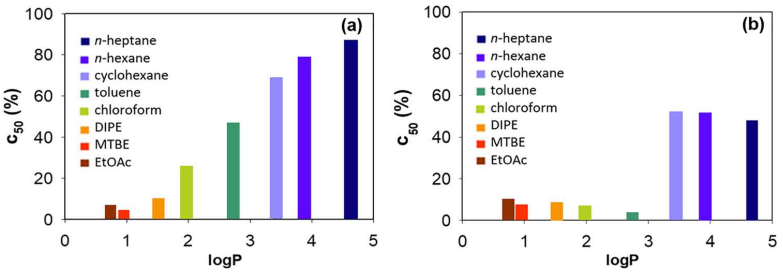

Fig. 1 Influence of the solvent polarity (logP) on the enzyme activity, expressed as c_{50} (volume concentration of OS that reduces enzyme activity by half) **a** in PNSHH ring-closure reaction; **b** in PNSO ring-opening reaction.

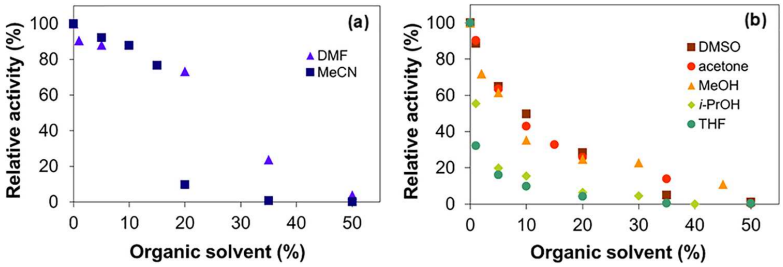

Fig. 2 Relative activity of wild-type HheC in the presence of water-miscible OSs at different volume ratios **a** DMF and acetonitrile; **b** DMSO, acetone, MeOH, *i*-PrOH, and THF.

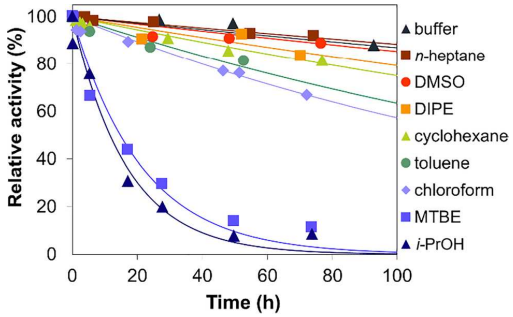

Fig. 3 Comparison of the wild-type HheC relative kinetic stability at 25 °C and 1000 rpm during incubation in buffer and in the presence of 30% (v/v) OSs.

i-PrOH, acetone, and DMSO) cause distinctive decrease in enzyme activity even when present in small amounts (c_{50} < 10%), with THF having the strongest negative effect (Fig. 2b). Although already 1% THF reduces enzyme activity to 30%, no structural changes were detected by dynamic light scattering (DLS) (Fig. S4).

Stability of wild-type HheC in water-organic solvent mixtures

Besides altering enzyme initial activity, OSs affect enzyme stability, i.e., activity over time. During 100 h, HheC remains considerably stable in buffer and 30% (v/v) hydrophobic OSs (*n*-heptane, toluene, DIPE, chloroform, cyclohexane) as well as DMSO (Figs. 3 and S5). Although DMSO noticeably lowers enzyme activity in the ring-closure reaction, the stability in this OS is high (Milčić et al. 2022). Except DMSO, other tested hydrophilic solvents (*i*-PrOH, DMF) are rather destructive towards HheC stability, which can be viewed from enzyme half-life times and residual activities (Table 1).

The stability of the enzyme during incubation was also assessed with selected OSs at different volume ratios and the activity decays were described by the first-order kinetics (Table 1). Increasing the concentration of DMSO and MTBE has a major negative impact on stability, while the half-lives in *n*-heptane or cyclohexane water mixtures are the same for all evaluated ratios.

Table 1 Effect of OSs on the stability of wild-type HheC during incubation at 25 °C

Solvent	v/v (%)	k_d (min^{-1})	$t_{1/2}$ (h)	Residual activity (%)[a]
None	0	$2.22 \cdot 10^{-5} \pm 1.44 \cdot 10^{-6}$	520	97
n-Heptane	30, 50, 80	$2.07 \cdot 10^{-5} \pm 2.04 \cdot 10^{-6}$	557	98
Cyclohexane	30, 50	$4.79 \cdot 10^{-5} \pm 3.03 \cdot 10^{-6}$	241	93
Toluene	30	$7.59 \cdot 10^{-5} \pm 6.53 \cdot 10^{-6}$	152	89
DIPE	30	$3.85 \cdot 10^{-5} \pm 3.59 \cdot 10^{-6}$	300	95
MTBE	10	$3.56 \cdot 10^{-5} \pm 3.30 \cdot 10^{-6}$	324	95
MTBE	30	$7.85 \cdot 10^{-4} \pm 8.04 \cdot 10^{-5}$	14.7	32
Chloroform	30	$8.55 \cdot 10^{-5} \pm 1.03 \cdot 10^{-5}$	135	80
i-PrOH	30	$7.85 \cdot 10^{-4} \pm 6.04 \cdot 10^{-5}$	11.6	24
DMF[b]	20	$1.11 \cdot 10^{-2} \pm 1.03 \cdot 10^{-3}$	1.0	0
DMF[b]	35	$2.00 \cdot 10^{-2} \pm 2.21 \cdot 10^{-3}$	0.6	0
DMF[b]	50	$2.26 \cdot 10^{-2} \pm 2.35 \cdot 10^{-3}$	0.5	0
DMSO[b]	30	$2.39 \cdot 10^{-5} \pm 5.21 \cdot 10^{-6}$	484	96
DMSO[b]	40	$2.81 \cdot 10^{-4} \pm 9.31 \cdot 10^{-6}$	41.2	67
DMSO[b]	50	$1.67 \cdot 10^{-2} \pm 2.53 \cdot 10^{-3}$	0.7	0

[a]After 24 h

[b]Data from (Milčić et al. 2022)

Properties of thermostable variant ISM-4 in the presence of organic solvents

The optimum temperature of wild-type HheC is 50 °C (Liao et al. 2018), while stability at the same temperature is very low, with no apparent differences between deactivation in OSs and buffer medium (Figs. S6 and S7, Table 2). Since enzyme resistance to high temperatures is often accompanied with enhanced activity and stability in OSs (Arabnejad et al. 2016), we have selected thermostable HheC variant ISM-4 to evaluate its biocatalytic properties in the presence of several OSs at 30% (v/v) (Figs. S8 and S9). We found that ISM-4 exhibits strong

Table 2 Comparison of wild-type HheC (WT) and ISM-4 half-lives at 25 and 50 °C with 30% (v/v) OSs

Solvent (v/v) (%)	$t_{1/2}$ WT (h)		$t_{1/2}$ ISM-4 (h)	
	25 °C	50 °C	25 °C	50 °C
buffer	520	0.51	803	538
n-Heptane	577	0.53	643	604
Toluene	152	0.39	236	179
DIPE	300	0.28	344	214
MTBE	14.7	0.27	292	281
i-PrOH	11.6	0.26	313	1.2
DMSO	483	0.39	342	183

tolerance to all tested OSs at 25 °C, with half-lives in MTBE and *i*-PrOH 20 and 30-fold higher than for the wild-type HheC, respectively (Fig. S8, Table 2). In contrast to the wild-type HheC (Fig. S7 and Table 2), ISM-4 demonstrates remarkably higher stability at 50 °C with all OSs except *i*-PrOH (Fig. S9). This implies that the mutations not only increased the thermostability of the enzyme but also ensured its longevity in buffer medium and in the presence of OSs.

Epoxide ring-opening reaction in the presence of OSs

Conversion of vicinal haloalcohols into epoxides is naturally occurring activity; however, HHDHs have the ability to catalyze the ring-opening of epoxides with different non-natural nucleophiles, such as azide ions, which is synthetically more useful compared to ring-closure reaction. To further explore HheC behavior in the epoxide ring-opening, in addition to PNSO ring-opening activity assay with bromide ions in presence of hydrophobic OSs, we chose azidolysis of 2-(benzyl) oxirane (BNO) as a model reaction, due to high activity and chemical stability of BNO (Scheme S4). The progress curves for the reactions performed in 30% (v/v) OSs are given in Figs. 4 and S10. The course of the reactions is comparable in buffer (Fig. 4a) and in the presence of DMSO, *n*-heptane, cyclohexane, and DIPE for both enzymes (Figs. 4b, d–f), whereas ISM-4 performs better in 30% MTBE, *i*-PrOH,

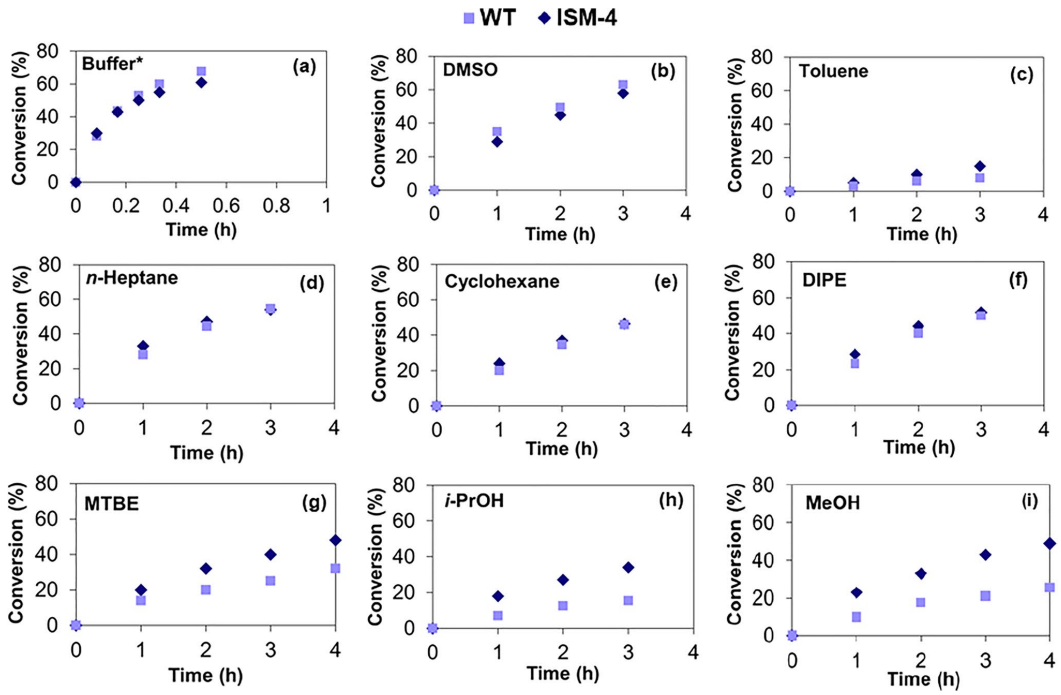

Fig. 4 Progress curves for ring-opening reactions catalyzed by wild-type HheC (WT) and ISM-4 in **a** buffer (*contains 1% (v/v) DMSO for substrate solubility); **b** 30% DMSO; **c** 30% toluene; **d** 30% *n*-heptane; **e** 30% cyclohexane; **f** 30% DIPE; **g** 30% MTBE; **h** 30% *i*-PrOH; **i** 30% MeOH. Reaction conditions: BNO (5 mM), NaN_3 (10 mM) and 200 µL of HheC (as CFE) in Tris-SO_4 buffer (50 mM, pH 7.5) at 25 °C and 1000 rpm (4 mL total volume of reaction mixture).

and MeOH (Figs. 4g–i), solvents that are detrimental to the stability of wild-type HheC. This indicates that higher tolerance towards those OSs is accompanied by higher activity of ISM-4 in their presence.

Influence of the organic solvents on the enantioselectivity

In addition to altering enzyme activity and stability, OSs can also enhance or reduce enantioselectivity of the reaction (Stepankova et al. 2013). Therefore, we evaluated the influence of the OSs on the enantioselectivity of the two enzymes in the epoxide ring-opening reaction (the azidolysis of BNO, Scheme S4). Due to low solubility of the substrate in purely aqueous media, the reaction conditions with 1% DMSO were selected as the benchmark for solvent comparison. As the hydrophilicity of the solvent increases (designated by the negative logP values), the enantioselectivity decreases for both enzymes (Table 3). The *E* values for 30% hydrophobic OSs (*n*-heptane, cyclohexane, toluene, DIPE) and buffer medium are almost the same, also indicating that these OSs are a better alternative. Compared to the wild-type HheC, ISM-4 displays not only higher stability but also higher enantioselectivity in the given reaction in all OSs (Table S3).

Table 3 Comparison of enantioselectivity (*E* value) of wild-type HheC (WT) and ISM-4 variant at 30% (v/v) of different OSs

Solvent	logP	E_{WT}	E_{ISM-4}
buffer[a]		6	12
n-Heptane	4.0	6	12
Cyclohexane	3.2	6	13
Toluene	2.5	5	12
DIPE	1.9	5	12
MTBE	0.94	4	10
MeOH	-0.76	3	9
DMSO	-1.3	5	7

[a]Referent reaction: buffer containing 1% DMSO for substrate solubility

Biocatalysis in biphasic solvent system at elevated temperature

The benefits that come along with biocatalysis at elevated temperatures are better solubility of substrates and higher reaction rates. Therefore, improved enzyme stability contributes to their application under realistic operating conditions and can meet the requirements of an industrial process. Thus, ISM-4 was further tested in 30% *n*-heptane at different temperatures, ranging from 30 to 90 °C, and compared with the wild-type HheC (Fig. 5a). In the presence of 30% *n*-heptane the half-life of ISM-4 is 46 h at 65 °C, compared to 0.53 h for wild-type HheC at 50 °C (enzyme's optimal temperature). The course and the enantioselectivity of the reactions performed at different temperatures reveal that ISM-4-catalyzed reaction is only slightly faster at room temperature, while the enantioselectivity is twice that of the wild-type HheC (Fig. 5b). As the temperature increases, the ISM-4-catalyzed reaction proceeds more rapidly, with the decrease in enantioselectivity. At 65 °C, the reaction proceeds 6-fold faster than with the wild-type HheC at room temperature, still with comparable enantioselectivity. In practice, this means that equivalent amount of product, with slightly higher *ee*, can be obtained a lot faster with ISM-4 at elevated temperatures. ISM-4 undoubtedly has shown to be superior to the wild-type enzyme in this reaction in presence of *n*-heptane, yet a broader range of substrates should be examined and enantioselectivity determined to identify the potential application of this biocatalyst.

Discussion

The application of enzymes in organic synthesis often requires the use of OSs in order to dissolve poorly soluble substrates and facilitate reactions. In case of HHDH-catalyzed reactions, OS presence would be beneficial for catalysis on a scale greater than millimolar not only due to low solubility but hydrolytic instability of many substrates as well. Recently, we have found that DMSO, the most commonly

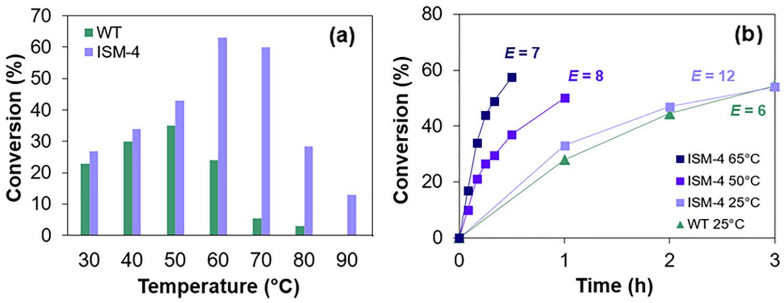

Fig. 5 **a** Conversions of BNO in 30% (v/v) *n*-heptane determined after 30 min at different temperatures; **b** Progress curves for ring-opening reactions in 30% (v/v) *n*-heptane catalyzed by wild-type HheC (WT) and ISM-4, at different temperatures with corresponding *E* values.

used cosolvent in the HHDH-catalyzed reactions, has strong inhibitory effect on wild-type HheC when present at low concentrations, while structure degradation starts occurring at concentrations over 30% (v/v) (Milčić et al. 2022). These findings aroused the need to study HHDH-catalysis in other OSs and explore the type and extent of the OSs influence on this enzyme group. Therefore, this study represents the first systematic analysis of the influence of different OSs on members of the HHDH family with the aim of analyzing their process suitability. One of the first steps to consider when setting-up biotransformation is the selection of the appropriate form of the biocatalyst. CFE containing HheC proved to be a more stable biocatalyst form than purified enzyme (Fig. S1). Better HheC stability, along with other advantages of CFE over purified enzyme in terms of economical aspect, favor the cell lysate as a viable biocatalyst form. It should be noted that the study was further performed with CFE, whereby the results for the CFE do not necessarily always reflect the behavior of the purified enzyme. As satisfactory activity in OS is a foremost condition for successful biocatalysis in alternative media, wild-type HheC was subjected to these measurements first. After analyzing the activity of HheC in the ring-closure reaction (PNSHH test, Scheme S2) with 15 different OSs at various ratios, we found clear correlation between activity and logP for water-immiscible solvents (EtOAc, MTBE, DIPE, chloroform, toluene, cyclohexane, *n*-hexane, and *n*-heptane) (Fig. 1). Such a correlation between OSs properties and HHDH performance is valuable result, and is of high importance since predictable enzyme behavior enables narrowing down the choices of OSs for biotransformations in the future. The increase in hydrophobicity of OSs is accompanied by greater specific enzyme activity, whereby the c_{50} values in *n*-hexane and *n*-heptane are as high as 78 and 87%, respectively (Table S1). Although the activity is still high at 90% (v/v) of these OSs, increasing the concentration to 98% results in an abrupt drop in activity to 8–12% of the maximum value (Fig. S2). These results clearly demonstrate that bulk water is not necessarily required in the hydrophobic OS-water reaction systems, while extremely low-water amount results in an inefficient catalysis. Our results are consistent with the ones presented by Jin et al. obtained with HHDH-expressing cells (Jin et al. 2013). Authors used cells co-expressing HheC and epoxide hydrolase for the cascade synthesis of (*R*)-epichlorohydrin in an aqueous-organic system. High yields were achieved with *n*-hexane, *n*-heptane, and cyclohexane, while poor results were obtained with acetone and MTBE. Since wild-type HheC retains higher activity in presence of hydrophobic OSs and a direct correlation between enzyme activity in PNSHH assay and OS hydrophobicity was discovered, we tested whole set of hydrophobic OSs in the PNSO ring-opening reaction with bromide ions. The overall effect of OSs in this reaction was found to be more severe, whereby hydrophobic alkanes (cyclohexane, *n*-hexane, *n*-heptane) demonstrated lesser negative effect on enzyme activity in comparison with other tested OSs (EtOAc, MTBE, chloroform, toluene). Although the most hydrophobic OSs again proved to be most suitable, no direct logP-c_{50} correlation was found, with toluene and chloroform deviating most from the trend observed in the ring-closure reaction (Fig. 1b). Such differences indicate probable enzyme inhibitions to different extent, which will be discussed more below.

As expected, water-miscible OSs (DMSO, DMF, MeOH, *i*-PrOH, acetone, MeCN, THF) have more serious negative effect on enzyme activity. This trend is not surprising, as numerous studies with various enzymes have shown that hydrophilic solvents can have a considerably stronger negative effect on enzyme activity compared to hydrophobic ones. Besides, no common correlation was found for the activity of wild-type HheC and OS hydrophilicity (Table S1). HheC has fairly good tolerance for lower concentrations of MeCN and DMF, retaining 70% of its initial activity at 15 and 20%, respectively (Fig. 2a). After an initial plateau where the activity decreases slightly with concentration rise, a steeper drop occurs. Such a drastic drop in activity, upon transitioning from 15 to 20% MeCN and 20 to 30% DMF, may be the result of the destruction of the hydration shell on the protein surface followed by structural changes of the protein (Klibanov 1997; Cui et al. 2020). The strongest negative influence was found for THF (Fig. 2b) that reduces the activity to 30% even when present in amount as low as 1% (v/v). Enzyme deactivation is often associated with structural deformation and aggregation (Wang et al. 2010). Monitoring changes in protein size by DLS can provide insight in deviation from the native structure of the enzyme (Sate et al. 2007), which was already shown for DMSO and HheC (Milčić et al. 2022). In 1% (v/v) THF, aggregation of wild-type HheC was not detected (Fig. S4), implying that structural changes are not the reason for abolition of enzyme activity. Rather, the cause could be derived from an inhibitory effect of THF.

Apart from analyzing the influences of the OSs on the activity, enzyme stability with OS should be addressed as well. Stability represents the essential property for enzyme commercial applicability and is often affected with the introduction of OSs into the reaction media. We have found that wild-type HheC is very stable in the presence of hydrophobic OSs, such as *n*-hexane, cyclohexane, toluene, DIPE, and up to 30% of polar DMSO, as it retains activity for days in a form of crude extract (Fig. 3). Arabnejad et al. reported previously that wild-type HheC is very stable in 25% DMSO, while in 50% activity rapidly decreases (Arabnejad et al. 2016). As confirmed later, the enzyme tolerates DMSO at ratios up to 30%, after which the stability decreases abruptly due to denaturation (Milčić et al. 2022). Except DMSO, other hydrophilic cosolvents tested (*i*-PrOH, DMF) are

rather destructive towards wild-type HheC (Table 1). As expected, hydrophobic OSs are better alternative in terms of protein stability. Alkane-protein interactions are known to be solely hydrophobic; hence, alkanes can preserve the intact protein structure and promote its rigidity, sometimes even leading to enhanced or prolonged stability of the enzyme (Wang et al. 2016). Besides, the half-lives in *n*-heptane or cyclohexane water mixtures are the same for all evaluated ratios, including 80% (Fig. S5, Table 1), which means that the water content does not play a decisive role in the examined range of OSs concentrations. Our findings are comparable to the previous study presenting that HheC (10 mg/mL) retained 90, 80, and 72% of the initial activity after incubation with 50% (v/v) *n*-heptane, *n*-hexane, and cyclohexane, respectively, for 5 h (Liao et al. 2018). Slightly lower stability is possible at higher enzyme loadings, as faster protein aggregation occurs due to the greater kinetic possibility of collision (Wang et al. 2010; Nikfarjam et al. 2020; March et al. 2021). In another work, *E. coli* cells expressing HHDH were employed in resolution of *rac*-2,3-dichloro-1-propanol after incubation in organic-aqueous biphasic system for 24 h. Authors have found that cells retained high specific activity after incubation with solvents in following order: *n*-heptane, toluene, and cyclohexane (Zou et al. 2014).

Another important property of the industrial biocatalysts is thermal resistance, which often correlates well with storage and operational stability. Thermostabilized proteins are also often accompanied with enhanced stability and activity in OSs (Arabnejad et al. 2016), and therefore, good candidates for screening towards improved OS resistance. So far, there are several thermostable HHDH mutants reported in the literature (Arabnejad et al. 2016; Wu et al. 2017; Solarczek et al. 2019; Wessel et al. 2021). A thermostable ISM-4 was designed by error-prone PCR with low mutagenesis frequency and four rounds of iterative saturation mutagenesis (Wu et al. 2017). This variant has 8 residues exchanged and exhibits an 18 °C increase in apparent T_m and 3400-fold improvement in $t_{1/2}$ at 65 °C. In this study, we examined the solvent tolerance of ISM-4 variant and found that mutations are beneficial not only to thermostability but also to OS resistance (Table 2, Fig. S8). This is especially apparent in the case of MTBE and *i*-PrOH at 25 °C, which have showed a detrimental effect on the stability of the wild-type HheC, while ISM-4 has half-life times around 300 h in their presence. The variant also exhibits superior stability in the case of combined action of OSs (*n*-heptane, toluene, DIPE, MTBE, and DMSO) and elevated temperature of 50 °C (Fig. S9, Table 2). Although this is not always the case, a linkage between thermostability and enhanced resistance to various denaturing agents, including OSs, has been reported previously for other enzymes (Doukyu and Ogino 2010; Koudelakova et al. 2013; Floor et al. 2014) and HHDH (Arabnejad et al. 2016). In addition to superior thermal stability, ISM-4 displays higher enantioselectivity in all OSs compared to the wild-type (Table 3).

In general, both enzymes perform better in the presence of hydrophobic than hydrophilic solvents. Such behavior has already been confirmed with other types of enzymes, and the common causes are dehydration, structural changes, and consequent deactivation (Wang et al. 2016; Stepankova et al. 2013). However, some discrepancy was observed in the ring-opening compared to the ring-closure reaction. The ring-opening of epoxides with different nucleophiles is synthetically useful process, since it generates versatile chiral building blocks and is therefore more interesting compared to dehalogenation of haloalcohols to epoxides. As expected, azidolysis of BNO is faster in biphasic systems with hydrophobic OSs (*n*-heptane, DIPE, cyclohexane, MTBE) and slower in hydrophilic ones (MeOH, *i*-PrOH). On the other hand, BNO ring-opening reaction in toluene proceeds much slower than with other hydrophobic OSs listed above (Fig. 4c). These results, together with the 10-fold lower c_{50} value in the ring-opening reaction compared to the ring-closure reaction (Fig. 1), suggest that the enzyme tolerates toluene well during incubation but inhibits the enzyme in individual reactions to different extent. The findings from Zou et al. also support this assumption, where *E. coli* expressing HheC showed very good activity in *rac*-2,3-dichloro-1-propanol resolution after incubation with toluene (Zou et al. 2014). Toluene could be involved in π–π interactions with aromatic amino acids in the active site, hindering the entry of the substrate and inhibiting its binding. For conducting enzymatic reactions, chloroform is by far the worst among immiscible OSs. Although wild-type HheC is relatively stable in its presence ($t_{1/2}$ = 135 h), after 24h in 30% chloroform, only 1% of product was formed, again implying inhibition by the solvent. This is consistent with the very low c_{50} value of 6.8% (v/v) obtained in the PNSO ring-opening assay. Since halogenated compounds are natural substrates of HHDH, occurring in small amounts during catalysis, it is not unlikely that chloroform, which contains multiple chlorinated groups, will have a serious inhibitory effect in the ring-opening reaction, especially when present in high concentrations, i.e. molar scale. In addition, lower c_{50} value in ring-opening compared to ring-closure reaction (6.8 and 25.2%, respectively) could be due to mass-transfer limitations, since these limitations could have a greater impact in epoxide ring-opening reactions where two substrates are involved instead of one. Among the tested OSs, *n*-heptane stands out as the most suitable for conducting reactions due to relatively high enzyme stability and activity in it.

Apart from being relatively unstable substrates that are poorly soluble in aqueous media, we have found that epoxides often act as HHDH inhibitors at higher concentrations (Milčić et al. 2022). Since OSs can serve as a pool for organic compounds in biphasic systems, this approach

could provide enzyme protection in terms of substrate/product inhibition along with easier product isolation. However, we anticipate that HheC is prone to OS inhibitions, particularly in the case of toluene, chloroform, and THF, where high kinetic stability is accompanied by low enzyme activity. Further experimental and computational studies would be required to verify this assumption. This study provides insights into the nature of HheC with different types of OSs, however, it is possible that some behaviors reported here, inhibitions in particular, may not be observed among other members of the HHDH family. At the end, it should be taken into account that every enzyme-OS combination represents a special case and generalizations are not recommended without being supported by experiments. Hence, the presented results may serve as an initial guide for the future selection of the most suitable solvent system for HHDH-catalyzed biotransformations.

Supplementary Information The online version contains supplementary material available at https://doi.org/10.1007/s00253-023-12450-2.

Author contribution NM, PŠ, and MME conducted experiments. NM, MS, and MME designed the research. MS, ZFB, and MME supervised the research. ZFB, LT, and MME acquired resources. MME acquired funding. All authors wrote, read, and approved the manuscript.

Funding This work was financially supported by the Croatian Science Foundation (HrZZ, IP-2018-01-4493). A part of the presented materials is the work supported by the Chinese-Croatian bilateral collaboration (2019-2021). N.M. is supported by a PhD scholarship from the Croatian Science Foundation through the Career Development Project for Young Researchers.

Data availability The data that supports the findings of this study are available in the supplementary material of this article.

Declarations

Ethical approval This article does not contain any studies with human participants or animals performed by any of the authors.

Conflict of interest The authors declare no competing interests.

References

Arabnejad H, Dal Lago M, Jekel PA, Floor RJ, Thunnissen A-MWH, Terwisscha van Scheltinga AC, Wijma HJ, Janssen DB (2016) A robust cosolvent-compatible halohydrin dehalogenase by computational library design. Protein Eng Des Sel 30:175–189. https://doi.org/10.1093/protein/gzw068

Bradford MM (1976) A rapid and sensitive method for the quantitation of microgram quantities of protein utilizing the principle of protein-dye binding. Anal Biochem 72:248–254. https://doi.org/10.1016/0003-2697(76)90527-3

Calderini E, Süss P, Hollmann F, Wardenga R, Schallmey A (2021) Two (chemo)-enzymatic cascades for the production of opposite enantiomers of chiral azidoalcohols. Catalysts 11:982. https://doi.org/10.3390/catal11080982

Cao C, Matsuda T (2016) Biocatalysis in organic solvents, supercritical fluids and ionic liquids. Organic Synthesis Using Biocatalysis. Elsevier, In, pp 67–97

Chen S-Y, Yang C-X, Wu J-P, Xu G, Yang L-R (2013) Multi-enzymatic biosynthesis of chiral β-hydroxy nitriles through co-expression of oxidoreductase and halohydrin dehalogenase. Adv Synth Catal 355:3179–3190. https://doi.org/10.1002/adsc.201300549

Cui H, Zhang L, Eltoukhy L, Jiang Q, Korkunç SK, Jaeger K-E, Schwaneberg U, Davari MD (2020) Enzyme hydration determines resistance in organic cosolvents. ACS Catal 10:14847–14856. https://doi.org/10.1021/acscatal.0c03233

Cui H-B, Xie L-Z, Wan N-W, He Q, Li Z, Chen Y-Z (2019) Cascade bio-hydroxylation and dehalogenation for one-pot enantioselective synthesis of optically active β-halohydrins from halohydrocarbons. Green Chem 21:4324–4328. https://doi.org/10.1039/C9GC01802F

de Jong RM (2003) Structure and mechanism of a bacterial haloalcohol dehalogenase: a new variation of the short-chain dehydrogenase/reductase fold without an NAD(P)H binding site. EMBO J 22:4933–4944. https://doi.org/10.1093/emboj/cdg479

Dong F, Chen H, Malapit CA, Prater MB, Li M, Yuan M, Lim K, Minteer SD (2020) Biphasic bioelectrocatalytic synthesis of chiral β-hydroxy nitriles. J Am Chem Soc 142:8374–8382. https://doi.org/10.1021/jacs.0c01890

Doukyu N, Ogino H (2010) Organic solvent-tolerant enzymes. Biochem Eng J 48:270–282. https://doi.org/10.1016/j.bej.2009.09.009

Findrik Blažević Z, Milčić N, Sudar M, Majerić Elenkov M (2021) Halohydrin dehalogenases and their potential in industrial application – a viewpoint of enzyme reaction engineering. Adv Synth Catal 363:388–410. https://doi.org/10.1002/adsc.202000984

Floor RJ, Wijma HJ, Colpa DI, Ramos-Silva A, Jekel PA, Szymański W, Feringa BL, Marrink SJ, Janssen DB (2014) Computational library design for increasing haloalkane dehalogenase stability. ChemBioChem 15:1660–1672. https://doi.org/10.1002/cbic.201402128

Haak RM, Berthiol F, Jerphagnon T, Gayet AJA, Tarabiono C, Postema CP, Ritleng V, Pfeffer M, Janssen DB, Minnaard AJ, Feringa BL, de Vries JG (2008) Dynamic kinetic resolution of racemic β-haloalcohols: direct access to enantioenriched epoxides. J Am Chem Soc 130:13508–13509. https://doi.org/10.1021/ja805128x

Hasnaoui-Dijoux G, Majerić Elenkov M, Lutje Spelberg JH, Hauer B, Janssen DB (2008) Catalytic promiscuity of halohydrin dehalogenase and its application in enantioselective epoxide ring opening. ChemBioChem 9:1048–1051. https://doi.org/10.1002/cbic.200700734

Jin H-X, Liu Z-Q, Hu Z-C, Zheng Y-G (2013) Production of (*R*)-epichlorohydrin from 1,3-dichloro-2-propanol by two-step biocatalysis using haloalcohol dehalogenase and epoxide hydrolase in two-phase system. Biochem Eng J 74:1–7. https://doi.org/10.1016/j.bej.2013.02.005

Klibanov AM (1997) Why are enzymes less active in organic solvents than in water? Trends Biotechnol 15:97–101. https://doi.org/10.1016/S0167-7799(97)01013-5

Koudelakova T, Chaloupkova R, Brezovsky J, Prokop Z, Sebestova E, Hesseler M, Khabiri M, Plevaka M, Kulik D, Kuta Smatanova I, Rezacova P, Ettrich R, Bornscheuer UT, Damborsky J (2013) Engineering enzyme stability and resistance to an organic cosolvent by modification of residues in the access tunnel. Angew Chem Int Ed 52:1959–1963. https://doi.org/10.1002/anie.201206708

Liao Q, Du X, Jiang W, Tong Y, Zhao Z, Fang R, Feng J, Tang L (2018) Cross-linked enzyme aggregates (CLEAs) of halohydrin dehalogenase from *Agrobacterium radiobacter* AD1: preparation, characterization and application as a biocatalyst. J Biotechnol 272–273:48–55. https://doi.org/10.1016/j.jbiotec.2017.12.014

Lutje Spelberg JH, Tang L, Kellogg RM, Janssen DB (2004) Enzymatic dynamic kinetic resolution of epihalohydrins. Tetrahedron Asymmetry 15:1095–1102. https://doi.org/10.1016/j.tetasy.2004.02.009

Lutje Spelberg JH, Tang L, van Gelder M, Kellogg RM, Janssen DB (2002) Exploration of the biocatalytic potential of a halohydrin dehalogenase using chromogenic substrates. Tetrahedron Asymmetry 13:1083–1089. https://doi.org/10.1016/S0957-4166(02)00222-7

Ma SK, Gruber J, Davis C, Newman L, Gray D, Wang A, Grate J, Huisman GW, Sheldon RA (2010) A green-by-design biocatalytic process for atorvastatin intermediate. Green Chem 12:81–86. https://doi.org/10.1039/B919115C

March D, Bianco V, Franzese G (2021) Protein unfolding and aggregation near a hydrophobic interface. Polymers 13:156. https://doi.org/10.3390/polym13010156

Mikleušević A, Hameršak Z, Salopek-Sondi B, Tang L, Janssen DB, Majerić Elenkov M (2015) Oxazolidinone synthesis through halohydrin dehalogenase- catalyzed dynamic kinetic resolution. Adv Synth Catal 357:1709–1714. https://doi.org/10.1002/adsc.201500111

Milčić N, Stepanić V, Crnolatac I, Findrik Blažević Z, Brkljača Z, Majerić Elenkov M (2022) Experimental and computational insights on the influence of organic co-solvent on structural and catalytic properties of a biocatalyst: inhibitory effect of DMSO on halohydrin dehalogenase. Chem Euro J 28:e202201923. https://doi.org/10.1002/chem.202201923

Nikfarjam S, Jouravleva EV, Anisimov MA, Woehl TJ (2020) Effects of protein unfolding on aggregation and gelation in lysozyme solutions. Biomolecules 10:1262. https://doi.org/10.3390/biom10091262

Roiban G-D, Sutton PW, Splain R, Morgan C, Fosberry A, Honicker K, Homes P, Boudet C, Dann A, Guo J, Brown KK, Ihnken LAF, Fuerst D (2017) Development of an enzymatic process for the production of (*R*)-2-butyl-2-ethyloxirane. Org Process Res Dev 21:1302–1310. https://doi.org/10.1021/acs.oprd.7b00179

Sate D, Janssen MHA, Stephens G, Sheldon RA, Seddon KR, Lu JR (2007) Enzyme aggregation in ionic liquids studied by dynamic light scattering and small angle neutron scattering. Green Chem 9:859–886. https://doi.org/10.1039/b700437k

Schneider C (2006) Synthesis of 1,2-difunctionalized fine chemicals through catalytic, enantioselective ring-opening reactions of epoxides. Synthesis 23:3919–3944. https://doi.org/10.1055/s-2006-950348

Schrittwieser JH, Lavandera I, Seisser B, Mautner B, Kroutil W (2009) Biocatalytic cascade for the synthesis of enantiopure β-azidoalcohols and β-hydroxynitriles. Eur J Org Chem 2009:2293–2298. https://doi.org/10.1002/ejoc.200900091

SCIENTIST handbook (1986–1995) Micromath. City, Salt Lake

Seisser B, Lavandera I, Faber K, Lutje Spelberg JH, Kroutil W (2007) Stereo-complementary two-step cascades using a two-enzyme system leading to enantiopure epoxides. Adv Synth Catal 349:1399–1404. https://doi.org/10.1002/adsc.200700027

Solarczek J, Klünemann T, Brandt F, Schrepfer P, Wolter M, Jacob CR, Blankenfeldt W, Schallmey A (2019) Position 123 of halohydrin dehalogenase HheG plays an important role in stability, activity, and enantioselectivity. Sci Rep 9:5106. https://doi.org/10.1038/s41598-019-41498-2

Staar M, Henke S, Blankenfeldt W, Schallmey A (2022) Biocatalytically active and stable cross-linked enzyme crystals of halohydrin dehalogenase HheG by protein engineering. ChemCatChem 14:e202200145. https://doi.org/10.1002/cctc.202200145

Stepankova V, Bidmanova S, Koudelakova T, Prokop Z, Chaloupkova R, Damborsky J (2013) Strategies for stabilization of enzymes in organic solvents. ACS Catal 3:2823–2836. https://doi.org/10.1021/cs400684x

Szymanski W, Postema CP, Tarabiono C, Berthiol F, Campbell-Verduyn L, de Wildeman S, de Vries JG, Feringa BL, Janssen DB (2010) Combining designer cells and click chemistry for a one-pot four-step preparation of enantiopure β-hydroxytriazoles. Adv Synth Catal 352:2111–2115. https://doi.org/10.1002/adsc.201000502

Tang L, van Hylckama Vlieg JET, Lutje Spelberg JH, Fraaije MW, Janssen DB (2002) Improved stability of halohydrin dehalogenase from *Agrobacterium radiobacter* AD1 by replacement of cysteine residues. Enzyme Microb Technol 30:251–258. https://doi.org/10.1016/S0141-0229(01)00488-4

van Schie MMCH, Spöring J-D, Bocola M, Domínguez de María P, Rother D (2021) Applied biocatalysis beyond just buffers – from aqueous to unconventional media. Options Guidel. Green Chem 23:3191–3206. https://doi.org/10.1039/D1GC00561H

Wang S, Meng X, Zhou H, Liu Y, Secundo F, Liu Y (2016) Enzyme stability and activity in non-aqueous reaction systems: a mini review. Catalysts 6:32. https://doi.org/10.3390/catal6020032

Wang W, Nema S, Teagarden D (2010) Protein aggregation—pathways and influencing factors. Int J Pharm 390:89–99. https://doi.org/10.1016/j.ijpharm.2010.02.025

Wessel J, Petrillo G, Estevez-Gay M, Bosch S, Seeger M, Dijkman WP, Iglesias-Fernández J, Hidalgo A, Uson I, Osuna S, Schallmey A (2021) Insights into the molecular determinants of thermal stability in halohydrin dehalogenase HheD2. FEBS J 288:4683–4701. https://doi.org/10.1111/febs.15777

Wu Z, Deng W, Tong Y, Liao Q, Xin D, Yu H, Feng J, Tang L (2017) Exploring the thermostable properties of halohydrin dehalogenase from *Agrobacterium radiobacter* AD1 by a combinatorial directed evolution strategy. Appl Microbiol Biotechnol 101:3201–3211. https://doi.org/10.1007/s00253-017-8090-2

Zhang X-J, Shi P-X, Deng H-Z, Wang X-X, Liu Z-Q, Zheng Y-G (2018) Biosynthesis of chiral epichlorohydrin using an immobilized halohydrin dehalogenase in aqueous and non-aqueous phase. Bioresour Technol 263:483–490. https://doi.org/10.1016/j.biortech.2018.05.027

Zou S-P, Zheng Y-G, Du E-H, Hu Z-C (2014) Enhancement of (*S*)-2,3-dichloro-1-propanol production by recombinant whole-cell biocatalyst in n-heptane–aqueous biphasic system. J Biotechnol 188:42–47. https://doi.org/10.1016/j.jbiotec.2014.08.014

Supplementary Information

Impact of organic solvents on the catalytic performance of halohydrin dehalogenase

Nevena Milčić,[1] Petra Švaco,[2] Martina Sudar,[1] Lixia Tang,[3] Zvjezdana Findrik Blažević[1] and Maja Majerić Elenkov[2*]

[1] Faculty of Chemical Engineering and Technology, University of Zagreb, Savska c. 16, 10000 Zagreb, Croatia

[2] Ruđer Bošković Institute, Bijenička c. 54, 10000 Zagreb, Croatia
Phone: +38514560965; fax: +38514680108; e-mail: majeric@irb.hr

[3] University of Electronic Science and Technology, No. 4, Section 2, North Jianshe Road, Chengdu, China

Contents

Reactions catalyzed by halohydrin dehalogenases

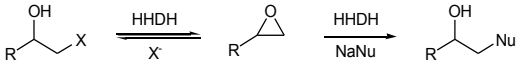

X = Cl, Br, I Nu = N_3, NO_2, CN, OCN, SCN, HCOO

Scheme S1. Scope of halohydrin dehalogenase-catalyzed reactions.

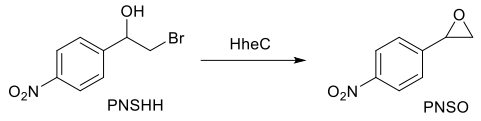

Scheme S2. PNSHH-test: ring-closure reaction of PNSHH to PNSO catalyzed by HheC.

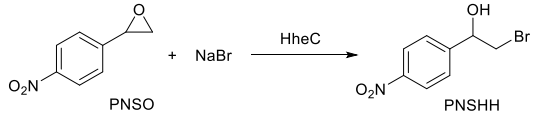

Scheme S3. Ring-opening reaction of PNSO to PNSHH catalyzed by HheC.

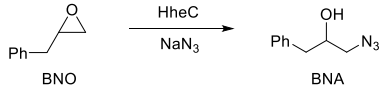

Scheme S4. HheC-catalyzed azidolysis of BNO yielding BNA.

The impact of the enzyme formulation on wild-type HheC stability

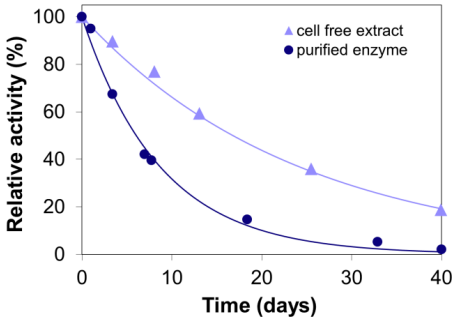

Figure S1. Comparison of the stability of 0.1 mg/mL wild-type HheC at 1000 rpm in Tris-SO_4 (500 mM, pH 7.5) of different biocatalyst form at 25 °C.

Specific activity of wild-type HheC in the organic solvent-water mixtures

Ring-closure reaction

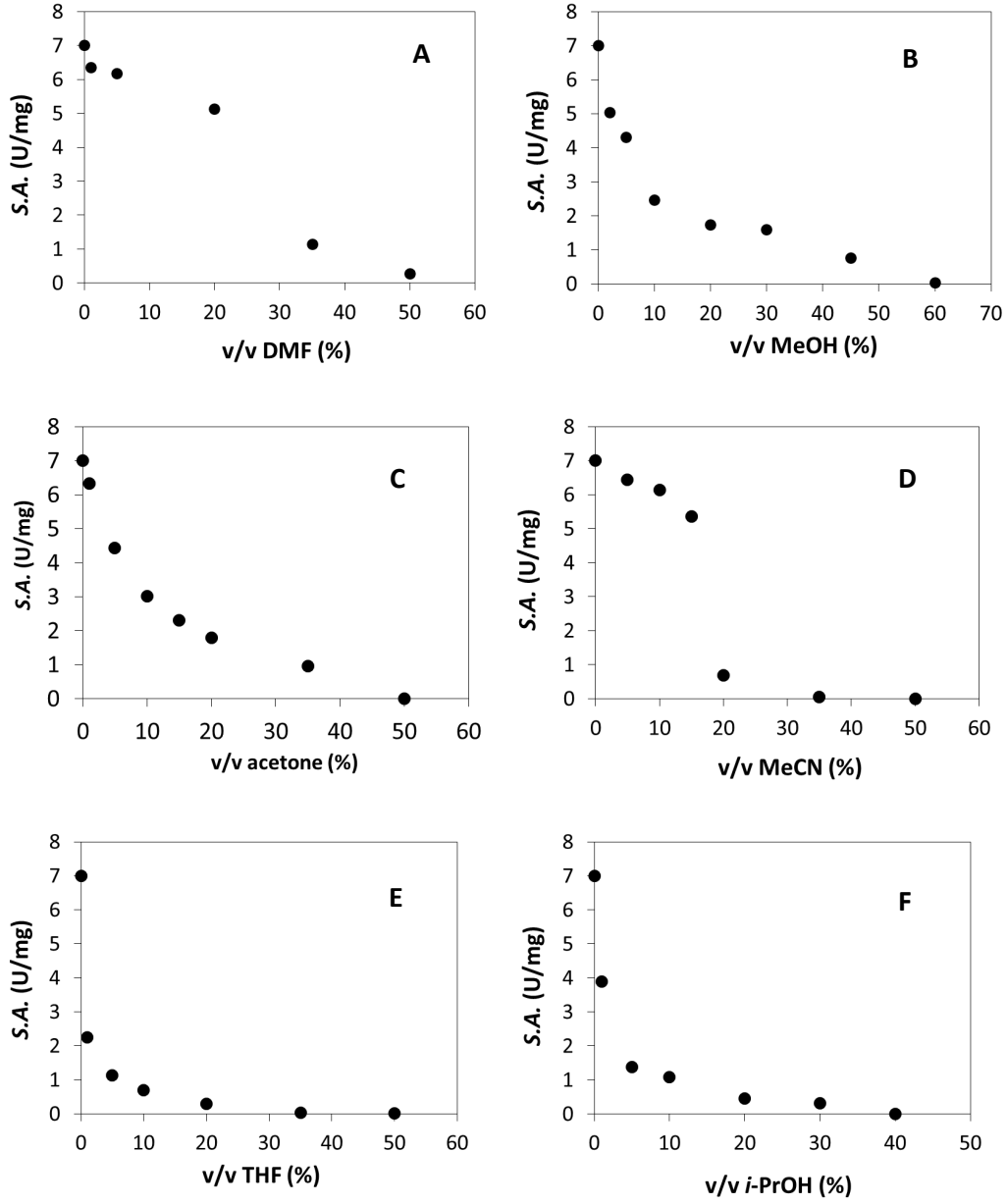

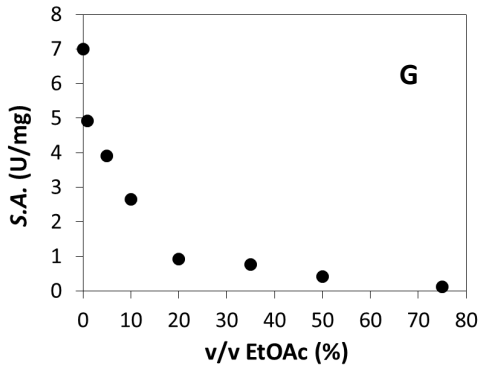
G
S.A. (U/mg)
v/v EtOAc (%)

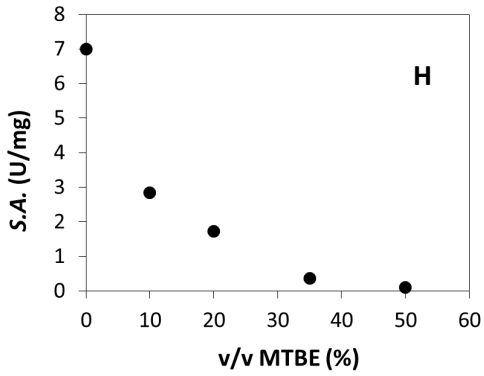
H
S.A. (U/mg)
v/v MTBE (%)

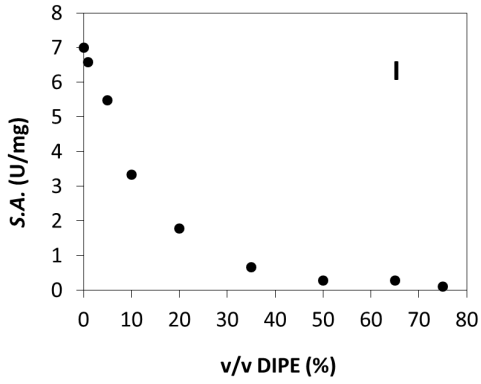
I
S.A. (U/mg)
v/v DIPE (%)

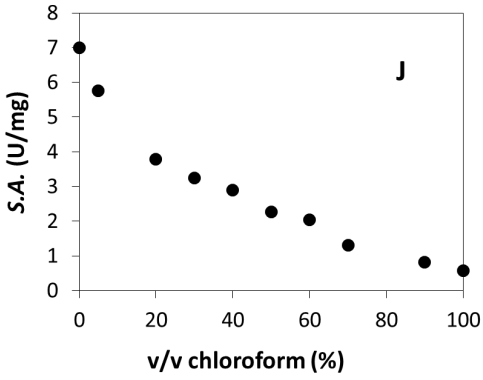
J
S.A. (U/mg)
v/v chloroform (%)

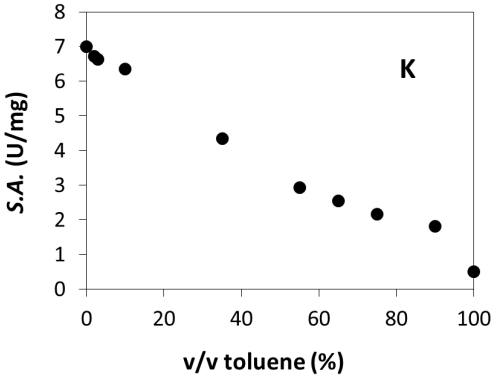
K
S.A. (U/mg)
v/v toluene (%)

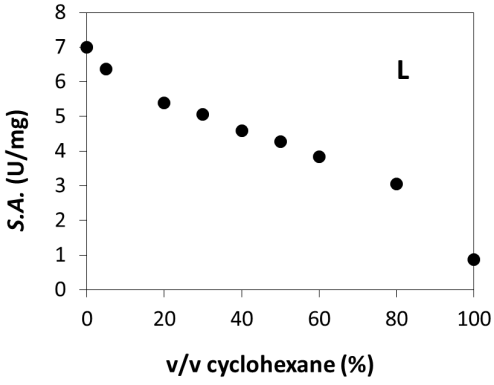
L
S.A. (U/mg)
v/v cyclohexane (%)

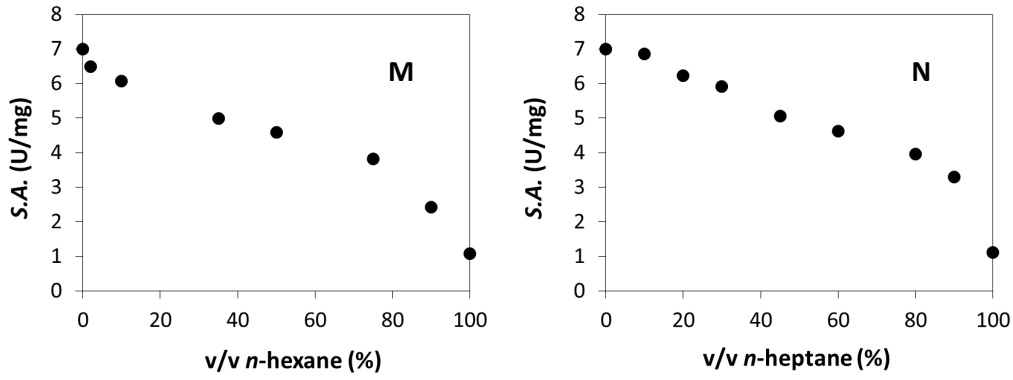

Figure S2. Specific activity of HheC enzyme in PNSHH ring-closure reaction in the presence of different water-solvent ratios; **A.** dimethylformamide (DMF); **B.** methanol (MeOH); **C.** acetone; **D.** acetonitrile (MeCN); **E.** tetrahydrofuran (THF); **F.** isopropyl alcohol (*i*-PrOH); **G.** ethyl acetate (EtOAc); **H.** methyl *tert*-butyl ether (MTBE); **I.** diisopropyl ether (DIPE); **J.** chloroform; **K.** toluene; **L.** cyclohexane; **M.** *n*-hexane; **N.** *n*-heptane. Results for dimethyl sulfoxide (DMSO) are previously reported (Milčić et al. 2022).

Table S1. Comparison of half maximum effective concentration (c_{50}) and partition coefficient between octanol and water (log P) for different organic solvents for wild-type HheC in PNSHH ring-closure reaction.

Solvent	**logP**	**c_{50} / %**
DMSO	-1.35	9.8
DMF	-1.01	27.0
MeOH	-0.77	7.2
acetone	-0.34	8.3
MeCN	-0.24	17.0
i-PrOH	0.05	8.0
THF	0.46	0.7
EtOAc	0.73	6.6
MTBE	0.94	4.1
DIPE	1.52	9.6
chloroform	1.97	25.2
toluene	2.73	47.0
cyclohexane	3.44	68.8
n-hexane	3.9	78.4
n-heptane	4.66	86.9

Ring-opening reaction

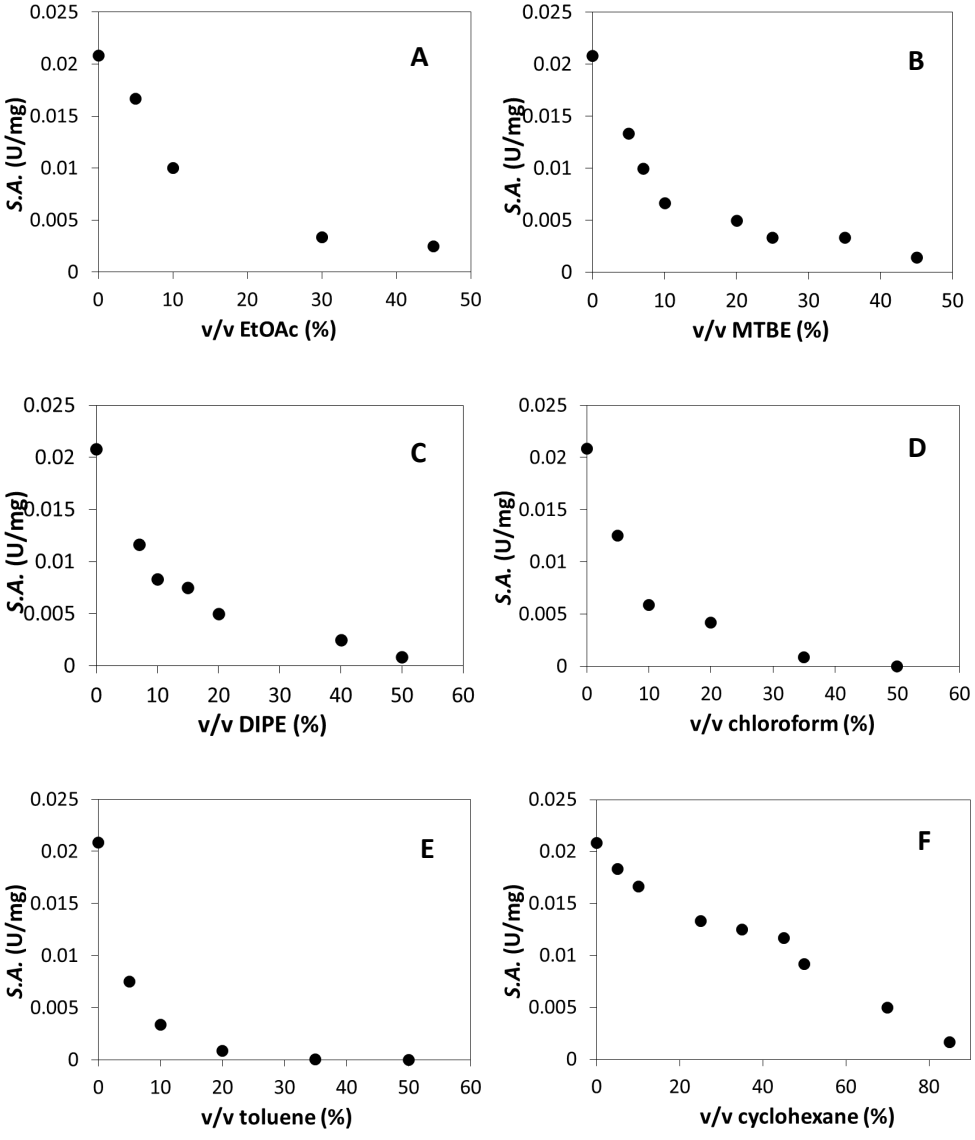

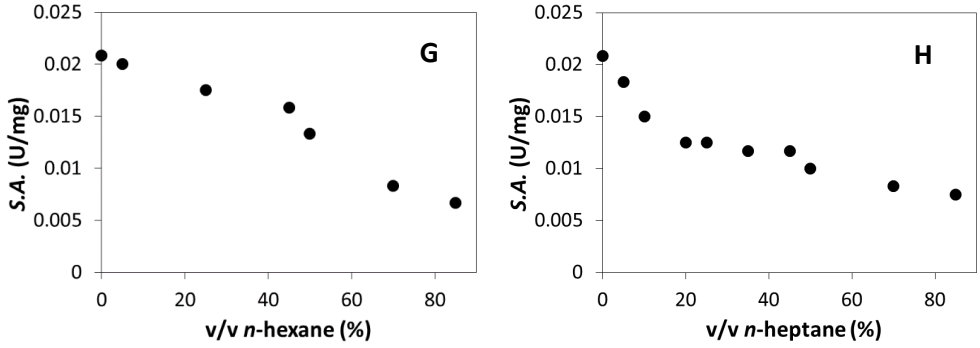

Figure S3. Specific activity of HheC enzyme in PNSO ring-opening reaction in the presence of different water-solvent ratios; **A.** ethyl acetate (EtOAc); **B.** methyl *tert*-butyl ether (MTBE); **C.** DIPE; **D.** chloroform; **E.** toluene; **F.** cyclohexane; **G.** *n*-hexane; **H.** *n*-heptane.

Table S2. Comparison of half maximum effective concentration (c_{50}) and partition coefficient between octanol and water (log P) for different hydrophobic organic solvents for wild-type HheC in PNSO ring-opening reaction.

Solvent	**logP**	**c_{50} / %**
EtOAc	0.73	9.9
MTBE	0.94	7.4
DIPE	1.52	8.2
chloroform	1.97	6.8
toluene	2.73	3.8
cyclohexane	3.44	51.9
n-hexane	3.9	51.3
n-heptane	4.66	47.3

Protein size distribution

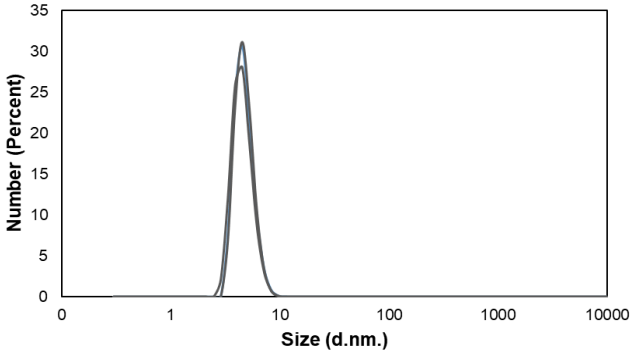

Figure S4. Number size distribution of wild-type HheC obtained by dynamic light scattering (DLS) in presence of 1% (v/v) THF during 5 min.

Stability of wild-type HheC and ISM-4 variant

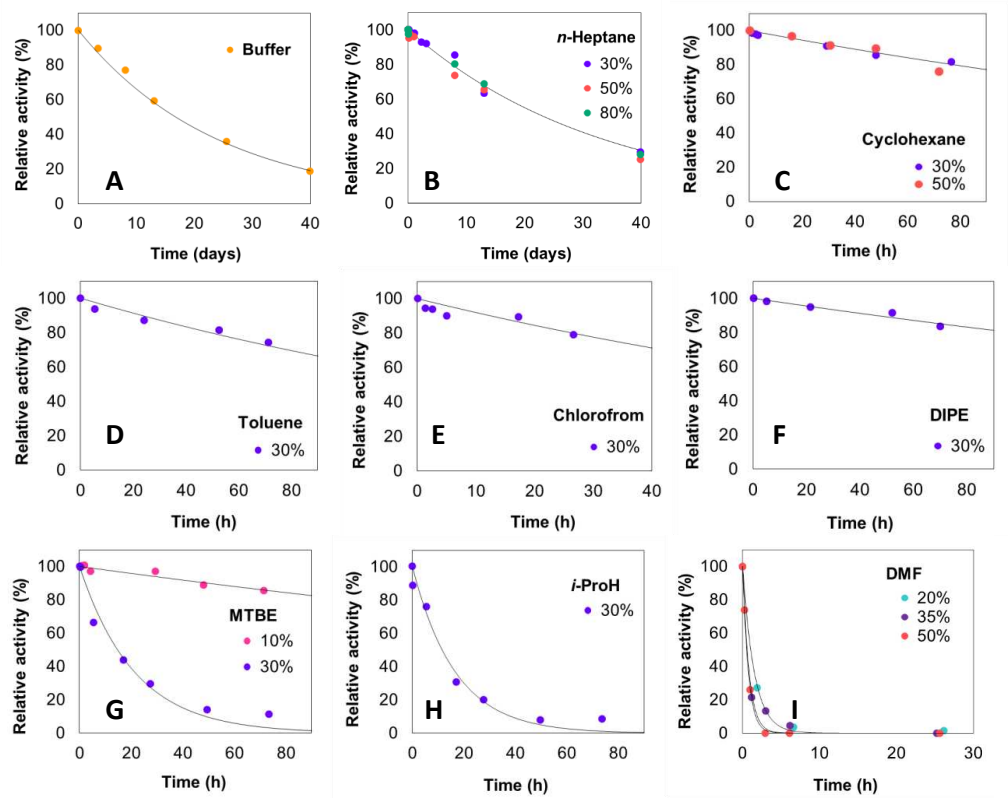

Figure S5. Stability of wild-type HheC during incubation at 25 °C (1000 rpm, V_R = 2 mL, 500 mM Tris-SO_4 pH 7.5, γ_{HheC} = 0.1 mg/mL): **A.** buffer medium; **B.** *n*-heptane (30, 50, 80%); **C.** cyclohexane (30, 50%); **D.** toluene (30%); **E.** chloroform (30%); **F.** DIPE (30%); **G.** MTBE (10, 30%); **H.** *i*-PrOH (30%); **I.** DMF (20, 35, 50%).

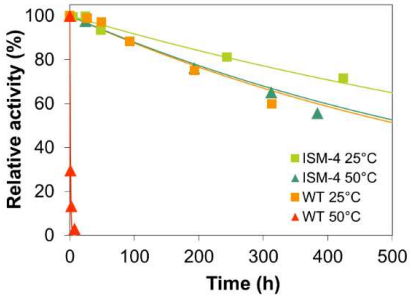

Figure S6. Comparison of stability of wild-type HheC and ISM-4 variant at 25 and 50 °C in buffer medium.

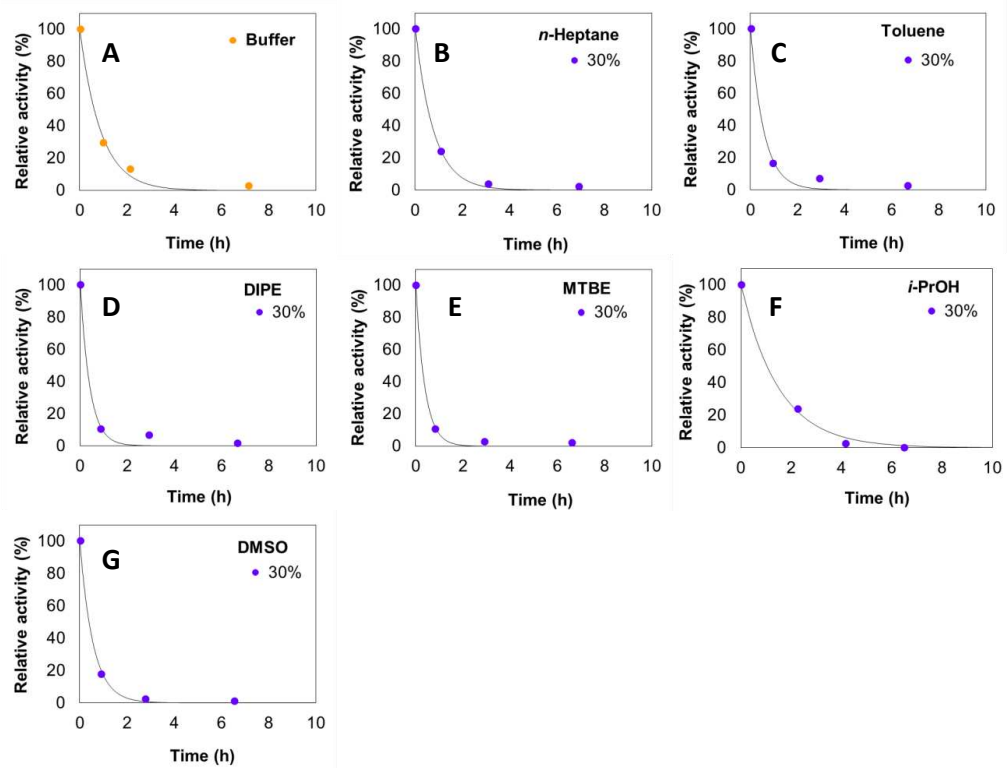

Figure S7. Stability of wild-type HheC during incubation at 50 °C (1000 rpm, V_R = 2 mL, 500 mM Tris-SO_4 pH 7.5, γ_{HheC} = 0.1 mg/mL) with: **A.** buffer medium, and 30% (v/v) of solvents: **B.** *n*-heptane; **C.** toluene; **D.** DIPE; **E.** MTBE; **F.** *i*-PrOH; **G.** DMSO.

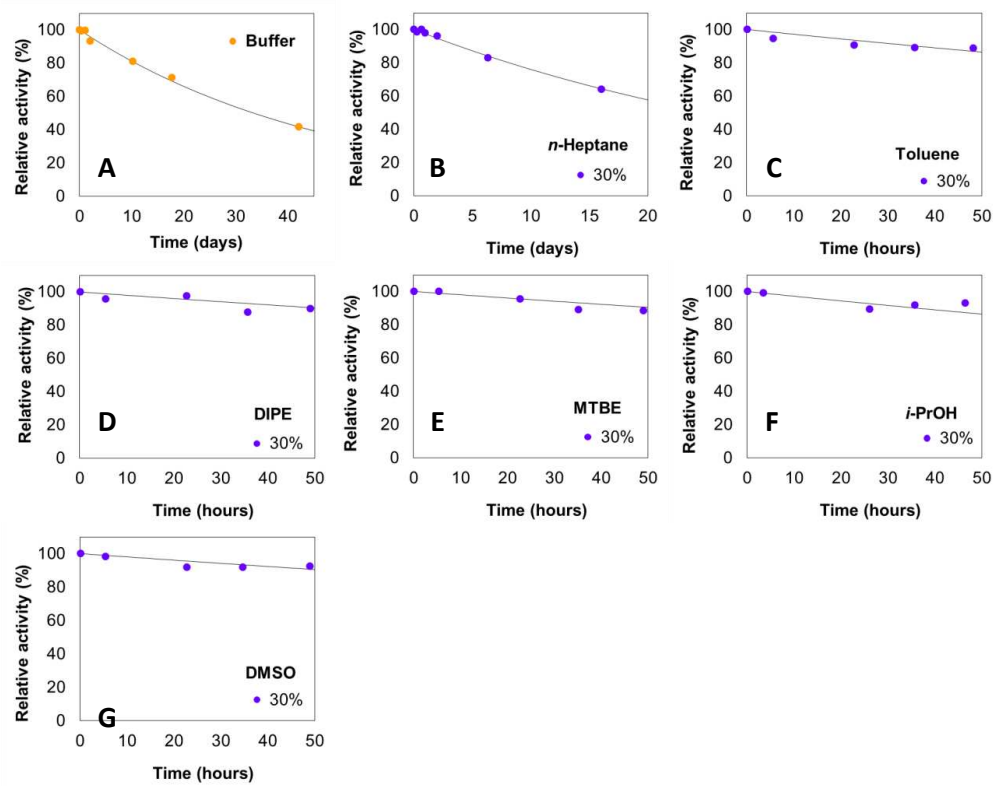

Figure S8. Stability of ISM-4 variant during incubation at 25 °C (1000 rpm, V_R = 2 mL, 500 mM Tris-SO_4 pH 7.5, γ_{HheC} = 0.1 mg/mL) with: **A.** buffer medium, and 30% (v/v) of solvents: **B.** *n*-heptane; **C.** toluene; **D.** DIPE; **E.** MTBE; **F.** *i*-PrOH; **G.** DMSO.

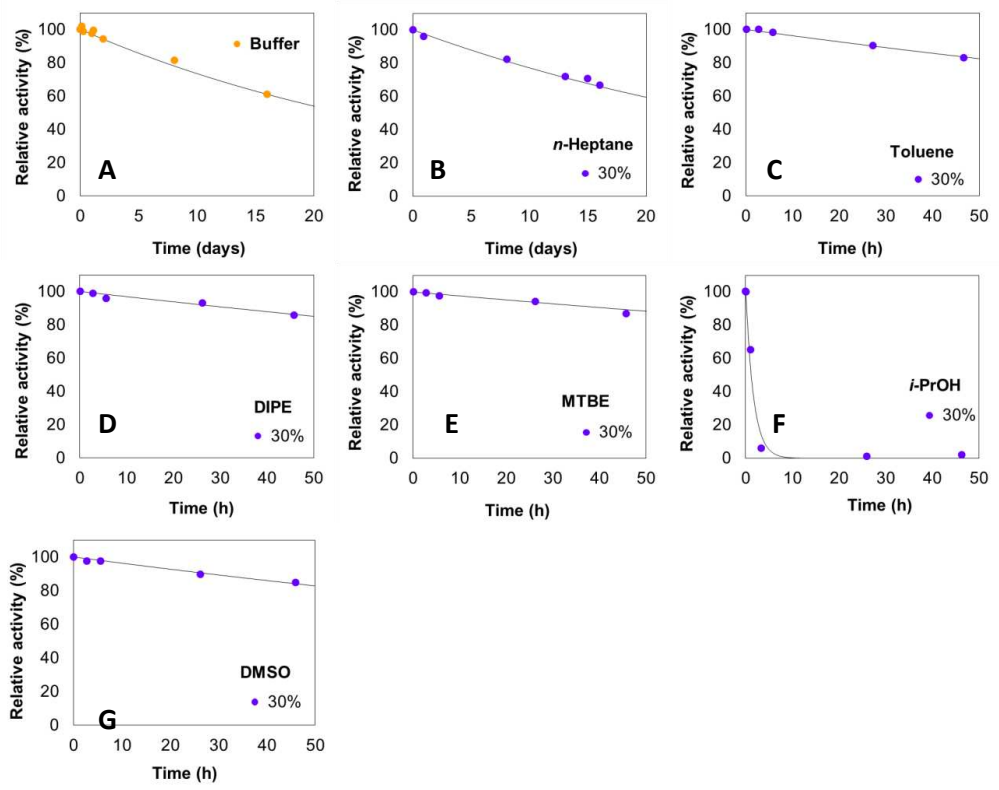

Figure S9. Stability of ISM-4 variant during incubation at 50 °C (1000 rpm, V_R = 2 mL, 500 mM Tris-SO_4 pH 7.5, γ_{HheC} = 0.1 mg/mL) with: **A.** buffer medium, and 30% (v/v) of solvents: **B.** *n*-heptane; **C.** toluene; **D.** DIPE; **E.** MTBE; **F.** *i*-PrOH; **G.** DMSO.

Epoxide ring-opening reaction in the presence of organic solvents

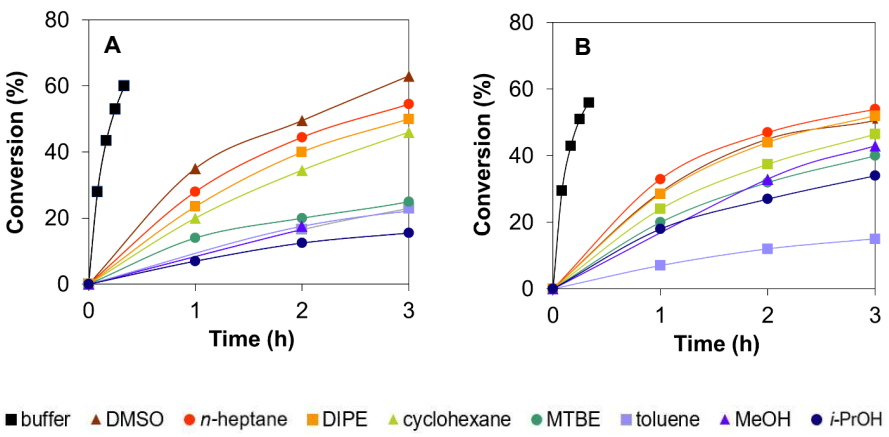

Figure S10. Progress curves for ring-opening reactions of BNO in buffer (containing 1% DMSO) and 30% (v/v) OSs catalyzed by: **A.** wild-type HheC; **B.** ISM-4 variant. Reaction conditions: BNO (5 mM), NaN_3 (10 mM) and 200 μL of HheC (as CFE) in Tris-SO_4 buffer (50 mM, pH 7.5) at 25 °C and 1000 rpm (4 mL total volume of reaction mixture).

Influence of the organic solvents on the enantioselectivity

Table S3. Results on the evaluation of the enantioselectivity of wild-type HheC (WT) and ISM-4 variant in different media on model substrate (azidolysis of benzyloxirane).

Solvent	%	T (°C)	HheC	t (h)	Conv. (%)	ee_s (%)	ee_p (%)	*E*
DMSO	1	rt	WT	5min	28	26	67	6
				10min	43.5	47	60.5	6
				15min	53	62.5	55	6
				20min	60	75	50	6
				30min	67.5	88	42	7
		rt	ISM-4	5min	29.5	33	79	12
				10min	43	56.5	74	12
				15min	51	72.5	69	12
				20min	56	83	65	12
	5	rt	WT	0.25	38	38	61	6
				0.5	53	61	53	6
				0.75	64.5	80.5	44.5	6
		rt	ISM-4	0.25	41	53	75	12
				0.5	54	79	68	12
				0.75	61	92	59.5	12
	30	rt	WT	1	35	30.5	57.5	5
				2	49.5	50	51	5
				3	63	71	42	5
		rt	ISM-4	1	29	29	70	7
				2	45	51	62	7
				3	50.6	61.5	60	7
				4	59	77	53.5	7
n-heptane	30	rt	WT	1	28	25	63.5	6
				2	44.5	45.5	56.5	6
				3	54.5	60	50	5
		rt	ISM-4	1	33	38.5	79	12
				2	47	65.5	73	12
				3	54	80	68	13
		50	ISM-4	5min	10	9	78	9
				10min	21	21	77	9
				15min	26.5	27	75	9
				20min	29.5	31	74	9
				30min	37	42	71	9
		65	ISM-4	5min	17	15	71.5	7
				10min	34	35	68.5	7
				15min	44	51	64	7
				20min	49	59	61.5	7
				30min	57.5	76	56	8
cyclohexane	30	rt	WT	1	20	17	68	6
				2	34.5	33	63	6
				3	46	48	57	6
		rt	ISM-4	1	24	26	82	13
				2	37.5	47	78	13
				3	46.5	64.5	73.5	13
toluene	30	rt	WT	2	16.5	13	66	6

				3	23	19.5	65	6
				4	30	26	61	5
		rt	ISM-4	3	15	16	85	14
				6	25	26.5	80	12
				24	46	64	74	13
MTBE	30	rt	WT	1	14	10	62	5
				2	20	15	58	4
				3	25	19	56	4
				4	32.5	25.5	53	4
		rt	ISM-4	1	20	20	77.5	10
				2	32	35	75	10
				3	40	49	72	10
				4	48	63	68	10
DIPE	30	rt	WT	1	23.5	20	65	6
				2	40	38	57	5
				3	50	52.5	52	5
		rt	ISM-4	1	28.5	31.5	79	12
				2	44	57	74	12
				3	52	73.5	68	11
MeOH	30	rt	WT	2	17.5	10.5	50	3
				4	25.5	16	46.5	3
		rt	ISM-4	2	33	36	72	9
				3	43	52	68	9
				4	49	62	65	9
		50	ISM-4	1	44	50	65	7
				2	60	77.5	53	7
				3	67	88.5	46	7
i-PrOH	30	rt	WT	1	7	4.5	60.5	4
				2	12.5	8	56.5	4
				3	15.5	10	55	4
				4	18	11.5	53	4
		rt	ISM-4	1	18	16	74.5	8
				2	27	26	71	8
				3	34	35	69	8
EtOAc		rt	ISM-4	3	7	6	84.5	13
				5.5	11	10	79.5	10
				22	33	36	73	9
THF	30	rt	ISM-4	6	14.5	10	60	4
$CHCl_3$	30	rt	WT	24	1.5	1	70	4

Reference

Milčić N, Stepanić V, Crnolatac I, Findrik Blažević Z, Brkljača Z, Majerić Elenkov M (2022) Inhibitory Effect of DMSO on Halohydrin Dehalogenase: Experimental and Computational Insights on the Influence of Organic Co-solvent on Structural and Catalytic Properties of a Biocatalyst. Chem Euro J 28:e202201923. https://doi.org/10.1002/chem.202201923

7. List of symbols

1,3-DCP	1,3-dichloro-2-propanol
1k	2-[4-(trifluoromethyl)phenyl]oxirane
2k	2-azido-1-[4-(trifluoromethyl)phenyl]ethanol
3k	2-azido-2-[4-(trifluoromethyl)phenyl]ethanol
4k	2-[4-(trifluoromethyl)phenyl]-1,2-ethanediol
API	active pharmaceutical ingredient
BNO	2-(benzyl)oxirane
c	molar concentration, mmol dm^{-3} (mM)
c_{50}	volume ratio of organic solvent which reduces enzyme activity by half, %
COBE	ethyl 4-chloroacetoacetate
CPME	cyclopentyl-methyl ether
DCM	dichloromethane
DIPE	diisopropyl ether
DLS	dynamic light scattering
DMF	dimethylformamide
DMSO	dimethyl sulfoxide
DSC	differential scanning calorimetry
ECH	epichlorohydrin
ee	enantiomeric excess
EtOAc	ethyl acetate
FDA	Food and Drug Administration
GC	gas chromatography
HHDH	halohydrin dehalogenase
HheC	C-type halohydrin dehalogenase
HPLC	high-performance liquid chromatography
i-PrOH	isopropyl alcohol
ISM-4	thermostable HheC variant obtained by error-prone PCR with low frequency of mutation and subsequent 4 rounds of iterative saturation mutagenesis

k_d	operational stability decay rate constant, min^{-1}
DLS	dynamic light scattering
DSC	differential scanning calorimetry
k_h	kinetic constant of the pseudo-first order in the hydrolysis reaction, min^{-1}
K_i	inhibition constant, mmol dm^{-3} (mM)
K_m	Michaelis constant, mmol dm^{-3} (mM)
logP	partition coefficient between octanol and water, /
m	mass, g
MD	molecular dynamics
MeCN	acetonitrile
MetOH	methanol
MTBE	methyl *tert*-butyl ether
NSD	number size distribution
OS	organic solvent
PCR	polymerase chain reaction
Phe, F	phenylalanine
PNSHH	*para*-nitro-2-bromo-1-phenylethanol
PNSO	*para*-nitro styrene oxide
Pro, P	proline
Q	volume flow rate, $cm^3\ h^{-1}$
r	reaction rate, mmol $dm^{-3}\ min^{-1}$
S	reaction selectivity, /
S.A.	specific activity, U mg^{-1}
SDR	short-chain dehydrogenases/reductase
t	reaction time, min
$t_{1/2}$	half-life time, h
THF	tetrahydrofuran
T_m	protein melting temperature, °C
Tris	tris(hydroxymethyl)aminomethane
Tris-SO_4	tris(hydroxymethyl)aminomethane sulfate buffer
Trp, W	tryptophan
V.A.	volumetric activity, U cm^{-3}
v/*v*	volume ratio, /

V_E	enzyme volume, cm^3
V_m	maximum reaction rate, U mg^{-1}
V_r	reactor volume, cm^3
VSD	volume size distribution
W249P	HheC variant with exchanged Trp and Pro amino acids on position 249
X	substrate conversion, %
Y	reaction yield, %
γ	mass concentration, mg cm^{-3}
ΔH	process enthalpy, kJ mol^{-1} K^{-1}
ΔT @ ½ h	thermogram peak width at the half of its height, °C

8. Curriculum vitae

Nevena Milčić [redacted] She studied Environmental Engineering at the Faculty of Chemical Engineering and Technology, University of Zagreb, and finished her Bachelors Studies (2013/2014 – 2015/2016) with *cum laude* diploma. As a graduate student, she was awarded with University of Zagreb scholarship for excellence (2016/2017) and the City of Zagreb scholarship for excellence (2017/2018). She was awarded with the Rector's Award (2016/2017) for the scientific work *Recovery of rendering plant wastewater for irrigation by the hybrid process of coagulation, sand filtration and ultrafiltration* and participated in the preparation of a scientific paper on that topic. In 2019, she received a scholarship for an Erasmus+ internship and spent 5 months on Catalan Institute for Water Research (Girona, Spain). She graduated from Masters Studies (2016/2017 – 2017/2018) with *cum laude* diploma and gained academic title Master Engineer of Environmental Engineering.

After graduation, she started working at the Department of Reaction Engineering and Technology of the Faculty of Chemical Engineering and Technology, University of Zagreb, as a research assistant (01/2019 – 04/2019) on the project *Sustainable industrial processes based on a C-C bond-forming enzyme platform* – CARBAZYMES (Horizon 2020, project leader Prof. Zvjezdana Findrik Blažević, Ph.D.). After the completion of the project, she was employed as a research assistant through the Young researchers' career development project funded by Croatian Science Foundation on the project *Enzymatic synthesis of fluorinated chiral building blocks* – EnzyFluor (Croatian Science Foundation, project leader Maja Majerić Elenkov, Ph.D.). At the same time, she enrolled in postgraduate doctoral study Chemical Engineering and Applied Chemistry at the Faculty of Chemical Engineering and Technology, University of Zagreb, under the dual mentorship of Prof. Zvjezdana Findrik Blažević, Ph.D. and Maja Majerić Elenkov, Ph.D. During her PhD studies, she participated in the preparation of four review papers and four original experimental papers, on six of which she was the first author. She was a visitor researcher at the Faculty of Chemistry and Chemical Engineering, University of Maribor (Slovenia) within bilateral project *Stabilization of halohydrin dehalogenases for use in non-conventional media* (27^{th} June – 24^{th} July 2022) and two times at Institute for Molecular Biotechnology, Graz University of Technology (Austria) within the bilateral project *Enzyme engineering and process engineering for the synthesis of fragrance compounds from renewable*

resources (1st – 31st October 2022; 11th February – 11th March 2023). She was awarded a COST scholarship as part of the GREENERING action to participate in the *Enzyme Engineering XXVI* conference (Dallas, Texas, 2022) and Academic mobility funds for participation in the conference 10th International Congress on Biocatalysis (Hamburg, Germany, 2022).

Publications

Scientific papers

N. Milčić, P. Švaco, M. Sudar, L. Tang, Z. Findrik Blažević, M. Majerić Elenkov, Impact of organic solvents on the catalytic performance of halohydrin dehalogenase, Appl. Microbiol. Biotechnol. (2023), JRC/SRJ = Q2/Q1.

N. Milčić, M. Sudar, I. Dokli, M. Majerić Elenkov, Z. Findrik Blažević, Halohydrin dehalogenase-catalysed synthesis of enantiopure fluorinated building blocks: bottlenecks found and explained by applying a reaction engineering approach, React. Chem. Eng. 8, 673 (2023) 673-686, JRC/SRJ = Q2/Q1

N. Milčić, V. Stepanić, I. Crnolatac, Z. Findrik Blažević, Z. Brkljača, M. Majerić Elenkov, Inhibitory Effect of DMSO on Halohydrin Dehalogenase: Experimental and Computational Insights into the Influence of an Organic Co-solvent on the Structural and Catalytic Properties of a Biocatalyst, Chem. Eur. J. 28 (2022), JRC/SRJ = Q2/Q1.

I. Dokli, **N. Milčić**, P. Marin, M. Svetec Miklenić, M. Sudar, L. Tang, Z. Findrik Blažević, M. Majerić Elenkov, Halohydrin dehalogenase-catalysed synthesis of fluorinated aromatic chiral building blocks, Catal. Commun. 152, 5 (2021), 106285, JRC/SRJ = Q3/Q2.

M. Racar, D. Dolar, M. Farkaš, **N. Milčić**, A. Špehar, K. Košutić, Rendering plant wastewater reclamation by coagulation, sand filtration, and ultrafiltration, Chemosphere 227 (2019) 207-215, JRC/SRJ = Q1/Q1.

Reviews

N. Milčić, I. Ćevid, M. M. Çakar, M. Sudar, Z. Findrik Blažević, Enzyme reaction engineering as a tool in investigation of the application potential of enzyme reaction systems, Hung. J. Ind. Chem. (2021).

Z. Findrik Blažević, **N. Milčić**, M. Sudar, M. Majerić Elenkov, Halohydrin Dehalogenases and Their Potential in Industrial Application – A Viewpoint of Enzyme Reaction Engineering, Adv. Synth. Catal. 363 (2021), 388-410, JRC/SRJ = Q1/Q1.

N. Milčić, Z. Findrik Blažević, M. Vuković Domanovac, Fitoremedijacija - pregled stanja i perspektiva, Kem. Ind. 68 (2019), 417-426.

N. Milčić, M. Česnik, M. Sudar, Z. Findrik Blažević, Primjena matematičkog modeliranja u razvoju enzimskih kaskadnih reakcija, Kem. Ind. 68 (2019) 397-406.